AUTOMATION OF RAILWAY SWITCH AND CROSSING INSPECTION

by

MARIUS FLORIN RUSU

A thesis submitted to the University of Birmingham for the degree of DOCTOR OF PHILOSOPHY

School of Electronic,
Electrical and Systems
Engineering
University of Birmingham
December 2015

Abstract

In recent years, there has been an increase in railway usage. This increase has led to the problem of congested railways and, as a result, increased pressure in the allocation of passenger traffic, freight traffic and rail maintenance. In response to this pressure, infrastructure owners are trying to increase the availability of the network by improving maintenance practises. The drive is to reduce maintenance time, maintenance frequency and increase reliability at the same time. Railway switches and crossings (S&C) are an important asset of any complex railway network and they typically account for 30% of the total budget spent on maintenance.

The first part of this work researches the feasibility of automatically inspecting S&Cs in accordance with Network Rail inspection requirements and the likely necessary advancements. Current S&C inspection requirements, as well as current and developing inspection solutions, were analysed and categorised. This revealed the required technological advances and likely changes that the railway will have to adopt. As many S&Cs components are safety critical assets (their failure can lead to derailments), their inspection solutions, when used as a primary tool and not a complementary one, require a high Safety Integrity Level (SIL), therefore the inspection techniques require a high degree of accuracy, precision and reliability. Thus, some condition monitoring techniques were not explored as they were unable to meet this condition.

The second part of the work researches the weakness of conventional S&C profile inspection practices used in industry. Analysis of recent derailments showed that current inspection practices to identify derailment hazards at switches can be affected by human error. Furthermore, the management of crossing profile was considered by senior personnel to be negatively affected by the variable crossing inspection practices currently used which are prone to human error. The work identified the main reasons that led to poor inspection of the S&C profile, developed a novel, automatic method to carry out the profile measurements which eliminated human error and identified possible improvements in the area of S&C profile inspection. During this research, an inspection trolley was prototyped, field trials were carried out, and good results were obtained.

The increased inspection reliability can also improve repairs carried out at S&C, thus reducing their frequency. As a result, reliability could increase and overall maintenance time decrease.

Acknowledgements

The author would like to thank the following people/parties for their help and support:

Clive Roberts, for his continuous support, friendship and supervision throughout the course of this PhD.

Paul Weston, Stephen Kent and Hamed Rowshandel, for their help and invaluable knowledge in mechanical design and railway inspection trolleys.

Edward Stewart, Gemma Nicholson, Felix Schmid and Andreas Hoffrichter, for their help and support.

Adnan Zentani, for help and support in manufacturing the S&C inspection trolley.

Philip Winship and Paul Richards of Network Rail, for their experienced guidance in S&Cs.

Anthony Jones and Philip Neep of Network Rail, for their help and advice on S&Cs and inspection standards as well as providing S&C inspection equipment.

Hume Alexander, Alan Gurley and Grant Headington of Network Rail, for their practical experience in S&C inspections.

Richard Oliver of Network Rail, for arranging data collection at Whitemoor Rail Recycling Centre.

Simon Groom, Glenn Powell, Sean Massaiah, Glyn Bann and Andy Ellis all of Alstom, for arranging and helping with data collection at Alstom Wolverhampton Traincare Centre.

Steve Dunmore and Colin Flack, for arranging access at the Long Marston facility for data collection.

Ali Keyvanpazhouh and again Stephen Kent, for their help and assistance with data collections.

Katherine Slater, for her help in achieving a good command of English in all my written materials.

The participants of the EU-funded project “Augmented Usage of Track by Optimisation of Maintenance, Allocation and Inspection of railway Networks” (AUTOMAIN), for networking, support and provision of funds.

Finally, I would like to thank my partner, Andrada Radu, for her continuous love and encouragement throughout the entire course of the PhD.

Table of Contents

List of Figures

List of Tables

Glossary of Terms / List of Abbreviations

Term	Meaning
ASIV	Automatic Switch Inspection Vehicle
AUTOMAIN	Augmented Usage of Track by Optimisation of Maintenance, Allocation and Inspection of railway Networks
CM	Condition Monitoring
DB	Deutsche Bahn
DfT	Department for Transport
FP7	7th Framework Programme for Research and Technological Development
GB	Great Britain
NR	Network Rail
ORR	Office of Rail and Road (previously Office of Rail Regulation)
RAIB	Railway Accident Investigation Branch
RAMS	Reliability, Availability, Maintainability and Safety
RCM	Reliability-centred Maintenance
SIM	Switch Inspection and Measurement (train)
S&C	Switch and Crossing
TRL	Technology Readiness Level
UIC	International Union of Railways
UK	United Kingdom (Great Britain and Northern Ireland)

1 INTRODUCTION

1.1 Background

In recent years, there has been an increase in railway usage in Great Britain. As described in a report commissioned by the Department for Transport (DfT), the railway accommodated an increase of 57% in passenger journeys and 26% in freight moved between 1996/97 and 2009/10 [1]. If the period up to recession is instead taken (1996/97 to 2006/07), then the increase in freight moved would be 45% [1]. Furthermore, in 2014 the DfT forecasted that by 2030 rail journeys will increase by a further 40% and that rail freight traffic has the potential to nearly double during the same period [2]

In order to assure its availability to meet rail traffic demand, the railway infrastructure is maintained periodically. The availability of the railway is shared between passenger transportation, freight transportation and, not least, maintenance and renewal. With the increase in both passenger and freight traffic, the allocation of time for maintenance has become increasingly challenging.

Current practice in Great Britain includes “working on a line open to traffic”, commonly known as working in a red zone, in order to carry out short maintenance operations (e.g. inspections). However, due to safety concerns, this practice is being discouraged leading to a further possible reduction of access to the infrastructure assets [3].

1.2 Railway vision towards 2040

As described in the infrastructure section of the Industry’s Rail Technical Strategy 2012, the vision for the upcoming period to 2040 supports the use of automated inspection systems as trainborne inspection systems which can provide accurate and timely information [4]. Network Rail (NR), as an infrastructure owner, has also expressed interest in the use of automatic track inspection techniques in order to maintain their infrastructure [5]. The use of automatic inspection can provide more timely and precise information in part due to frequent automatic measurements being carried out without human intervention.

The ability to know the state of the infrastructure can be used to identify and monitor failing assets and therefore schedule on-condition maintenance tasks. The scheduling of on-

condition maintenance tasks is a widely accepted maintenance plan and in the second edition of "Reliability Centred Maintenance", Moubray describes it as the preferred option in the context of a reliability-centred maintenance plan [6].

The use of automatic inspection techniques to support on-condition maintenance tasks has the potential to:

- decrease or eliminate inspection time;
- reduce or eliminate safety risks faced by railway workers;
- increase inspection accuracy, precision and reliability;
- increase the safety of rail operations;
- decrease maintenance time by adopting a condition based maintenance approach;
- decrease the need for human resources and consequently money spent on wages and other administrative costs, and;
- provide up to date information on the state of the infrastructure.

Thus, such advancements have the potential to deliver various advantages including increased availability which can reduce the pressure on traffic allocation and help meet forecasted freight traffic demands and overall operational demands [4].

1.3 Consideration of switches and crossings (S&C)

Railway S&Cs (i.e. turnouts or switches) are a common mechanical installation found in railway systems that are used to safely guide trains from one track to another; they are commonly found in complex railway networks. In comparison to plain line S&C design is more complex and they are exposed to higher forces which make them more susceptible to damage, despite the continuous efforts to improve their design and reliability. Thus, as stated by the International Union of Railways (UIC) in a report concerning S&Cs, their maintenance takes up a considerable amount of money from the total maintenance budget: "Switches and crossings (S&C) are a serious cost driver and take up about 25% to 30% of the total maintenance and renewal budget each year" [7]. Thus, S&Cs are an important asset in any complex railway network and their management is important towards achieving the goals and vision as described in the previous section.

Another important aspect of S&Cs is their safety level. The maintenance of S&Cs is very important in the context of a safe railway infrastructure. In 2002 seven people were killed and many others were injured when a train derailed while it was approaching Potters Bar train

station [8]. The Health and Safety Executive (HSE) concluded that the main cause of the accident was "the failure of the support system within points 2182A to retain the right-hand switch rail in the open position during the passage of the train over the points" [8]. Just five years later a similar accident occurred at Grayrigg, where eighty percent of the passengers that were travelling were injured to some extent [9]. The cause of the accident was the poor condition of the switch at the moment of the accident [9]. During the last 10 years NR have experienced a number of derailments due to poor switches [10–14], all of which had less serious consequences than the Potters Bar and Grayrigg derailments. Thus, S&Cs are safety-critical assets and must be well maintained in order to assure the safe operation of railways and avoid damage and injuries. Figure 1-1 shows a diagram of a common S&C design (movable parts are in red). The S&C has a straight path and a diverging (curved) path.

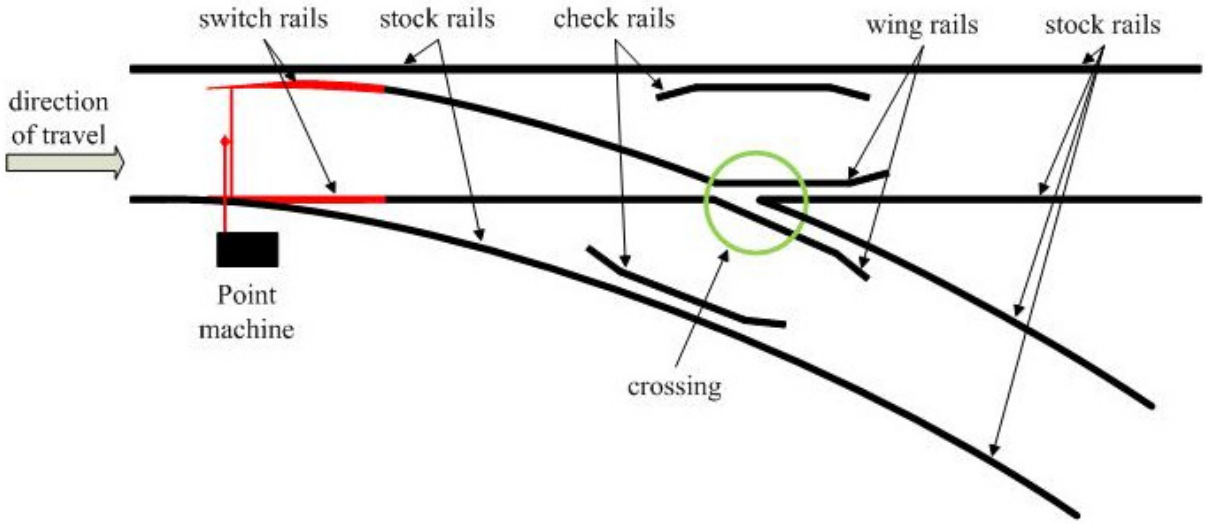

Figure 1-1 Diagram of a common S&C design

The main components of an S&C are:

- the "switch", which comprises of switch rails, stock rails, and other parts (not shown on the diagram) and is responsible for safely changing the path of the train;
- the "crossing", which includes the wing rail and provides support for the train wheel where two rails intersect paths, and;
- the "points" which are used to move and lock the switch rails in place.

The “points” are comprised of:

- point machine, which generates the force that moves the switch rails and locks them in place;
- point fittings, the mechanical parts that connect the point machine to the switch rails (stretcher bars, lock stretcher bar, drive rod, lock rods and associated bolts, nuts and brackets)
- mechanical supplementary drive (optional), which are similar with the point fittings but drive the rear end of the switch rails, and;
- switch rollers (optional).

It should be noted that certain point machines are designed to be installed in the four-foot (i.e. the area between the two stock rails).

1.4 Research aim and objectives

This research project has two aims and thus the work was carried out in two stages. The first research aim was led by the increasing difficulty in allocating maintenance time for S&C in GB. The hypothesis of the aim is to identify whether or not current technologies can be used to automatically fully inspect S&Cs in GB by eliminating the need for human inspection. In the case that fully automatic inspection of S&Cs is not possible using current S&C inspection technologies, the research then identifies the likely necessary technology advances that are required to achieve automatic inspection of S&Cs in GB.

The objectives associated with this aim are:

1. to identify and categorize the NR S&C inspection requirements (sections 2.1 and 2.2);
2. to identify commercial and research level solutions for the automatic inspection of S&Cs (sections 2.3 and 2.4);
3. to identify whether or not S&Cs could be automatically inspected using current technologies (section 2.5), and;
4. if applicable, to identify the main challenges and required advances in order to achieve a “self-inspecting” S&C, as well as any changes that would be vital to the achievement (section 2.5).

As S&Cs are safety-critical components and the research evaluates the feasibility of replacing manual inspection with automatic and/or remote inspection, in section 2.3 an important comparison between condition monitoring and automatic inspection is discussed.

During the first part of this research it became evident that railways have a history of S&C failures, some of which had led to derailments. In Britain, certain derailments were caused by a failure to accurately inspect the S&C in accordance with the NR/L2/TRK/0053 [15] inspection standard. Furthermore, during a meeting with senior NR personnel (January, 2012) it was asserted that NR was seeking to have better management over the profile of crossings, as current crossing profile inspection, as defined in the NR/L2/RK/1054 [16] inspection standard, is affected by human error and this reduces the effectiveness of the whole maintenance process. Thus, the second aim of this research is to improve a weakness in the current S&C inspection regime practised in GB.

The aim is best expressed as a set of 3 individual objectives:

- to identify whether or not the use of current S&C profile inspection methods, as defined by the NR/L2/TRK/0053 and NR/L2/TRK/1054 inspection standards, can lead to considerable measurement errors and the source of those errors;
- to identify if possible and to develop alternative automatic inspection methods can be used to replicate the current S&C profile inspection tasks as defined by the NR/L2/TRK/0053 and NR/L2/TRK/1054 inspection standards whilst eliminating human errors;
- to identify whether or not improvements on the developed S&C profile inspection methods could reduce the systematic errors of inspecting S&Cs.

Due to compatibility, integration and safety issues, the system must replicate the manual measurements as they are. The system should work on all standard right-hand and left-hand S&Cs for which the NR/L2/TRK/0053 inspection standard is applicable. For safety reasons, the system should also be transparent in the way in which the results are calculated.

1.5 Scope

The research is primarily focused on inspection standards and maintenance practices in Great Britain.

However, due to the following reasons, inspection requirements and maintenance practices from other countries have also been consulted:

- to gain an overview of the inspection tasks that are common across different European countries and those that are different;
- to learn from other countries practices;
- novel inspection solutions are more valuable when they address an issue experienced across Europe rather than only country wide, and;
- standardization between countries can bring beneficial effects.

Because of the poor availability of information relating other countries, inspection requirements and maintenance practices from other countries have been considered to a lesser extent.

1.6 Methodology

The first stage of this research is described in Chapter 2 can be summarised as three main steps, as shown in Figure 1-2.

The first step consisted of the identification, categorization and recording of S&C inspection requirements. Railway inspection standards and relevant documents applicable to S&Cs in Great Britain, Germany and Netherlands were consulted. The relevant S&C inspection tasks have been classified and recorded in an Excel® spreadsheet file. The first step is described in sections 2.1 and 2.2.

During the second step an effort was made to identify inspection solutions that can or have the potential to automatically and/or remotely inspect S&Cs in accordance with the inspection standards. Inspection solutions practiced in the current GB railway industry, other railway industries, commercially available products and solutions at low and medium Technology Readiness Levels (TRL) were considered. The work was not meant to provide an index of every possible solution, but at least one from each promising technology. The second step is described in sections 2.3 and 2.4.

During the third step, gaps in the S&C inspection solutions and some of the most promising technologies that need to be (re)developed had become evident. The third step is described in section 2.5.

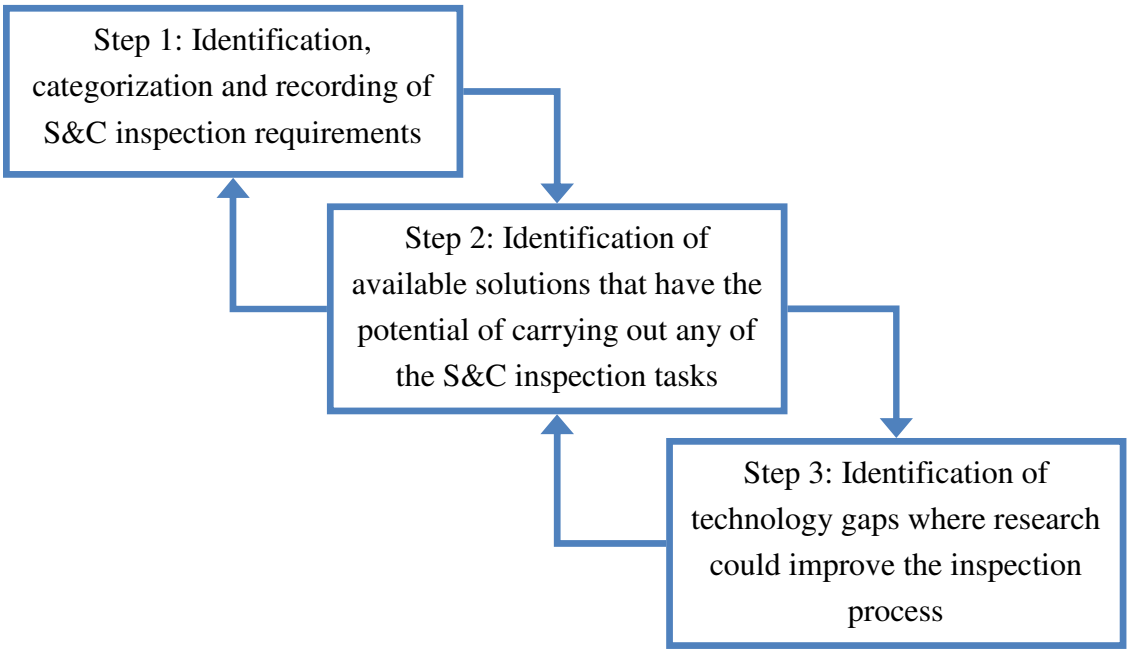

Figure 1-2 Methodological summary of first stage

As the above diagram suggests, the process was executed working up and down between the steps, while continuously revising towards the end goal.

The second stage of this research considers the issue of derailments at S&Cs due to failure to comply with the NR/L2/TRK/0053 [15] inspection standard as well as the issue of accurately inspecting crossing profiles as per NR/L2/TRK/1054 [16] inspection standard.

In Chapter 3 the problem is defined and a set of system level requirements was established, further refined by lower level requirements.

In order to achieve the second objective of this stage, a laser-based profile inspection trolley was developed to accurately measure the profile of rails in S&Cs. The development process is described in Chapter 4.

The methodology to achieving the second objective of this stage is summarised in Figure 1-3 as three steps.

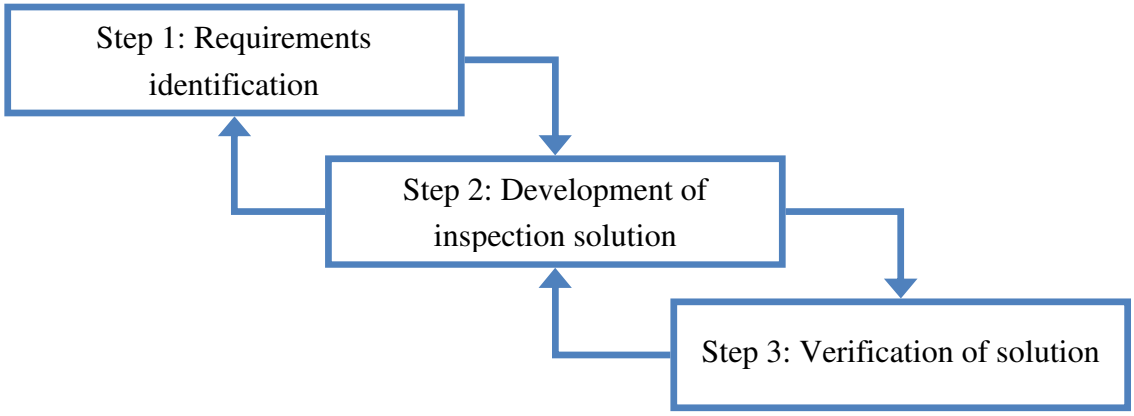

Figure 1-3 Methodological summary of second objective of the second stage

As the inspection process of switches differs significantly in comparison to the inspection process of crossings, the two are discussed in separate chapters. Chapter 5 researches the issues related to the inspection of switches and Chapter 6 the issues related to the inspection of crossings. However, each of the two chapters individually accomplishes, step by step, all three objectives of the second stage of the research as defined in section 1.4.

Chapter 7 compares the advantages and disadvantages of using a laser-based S&C inspection system in various inspection solutions ranging from dedicated measurements trains to hand gauges.

In Chapter 8 a range of conclusions are drawn.

1.7 Extracurricular work

The work and findings of this research have also fed into Work Package 3 of the European FP7 project AUTOMAIN (Augmented Usage of Track by Optimisation of Maintenance, Allocation and Inspection of railway Networks, http://www.automain.eu/).

2 RESEARCH ON STATE OF THE ART SWITCH INSPECTION STANDARDS, MAINTENANCE PRACTICES AND INSPECTION SOLUTIONS

The objective of this chapter is to identify the main challenges and areas of research that are necessary in order to develop and support a maintenance strategy that does not require the scheduling of manual inspection of S&Cs in Britain. This is achieved through a step-by-step process which as described in Figure 1-2. Although the scope is limited to the inspection of S&Cs within Britain, the investigation also considered overseas practices and inspection solutions.

2.1 Current standards for switch inspection

The railway infrastructure is commonly maintained through the use of inspection standards which help infrastructure managers to adequately assess their infrastructure against wear and damage and identify the required actions. In Network Rail these standards are classified as Level 2 standards, standards which "outline business processes, assurance systems and controls" [17].

Commonly, inspection standards contain, but are not limited to, the following:

- a name/description of the inspected asset;
- a description of the tools required for inspection;
- a inspection procedure;
- a method for interpreting the inspection results, and;
- a list of post-inspection required actions.

The NR switch inspection standards have been identified and then by focusing on a "key standard" and exploring all the standards that are referred to by the "key standard". These standards refer to other standards, which were also inspected, and this process was repeated while assigning each standard a letter (or group of letters) as follows:

- L, for live standard in which case all references from that standard were inspected;
- NA, for not applicable in which case the standard was irrelevant and it was not inspected;

- D, for dead standard in which case it was not inspected, and;
- R, for repeated standard for standards that have already been inspected.

The methodology of inspecting standards was adopted from Roberts et al. [18]. The most important leads tables are shown in APPENDIX B: LEADS TABLES.

2.1.1 Great Britain railway standards

The main railway infrastructure owner in Great Britain is Network Rail. Whilst a key standard issued for the inspection of S&Cs (i.e. complete turnout) was not identified, the "NR/L2/TRK/001" was identified as a key group standard for the inspection of switches, crossings and related track components and "NR/L3/SIG/10663" for the inspection of points. Figure 2-1 shows the NR S&C inspection standards tree (live and applicable standards only).

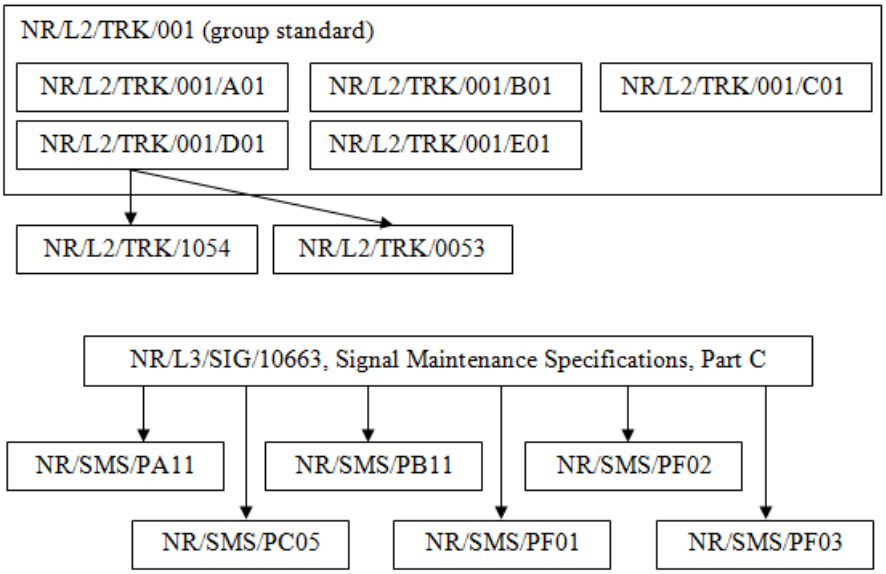

Figure 2-1 NR S&C inspection standards (tree)

Table 1 shows the titles of all NR S&C inspection standards that have been found relevant towards this work.

Table 1 NR S&C inspection standards (listed)

NR/L2/TRK/001	Inspection and Maintenance of Permanent Way [19]
NR/L2/TRK/001/A01	Inspection and maintenance of permanent way – Inspection [20]
NR/L2/TRK/001/B01	Inspection and maintenance of permanent way – Rail management [21]

NR/L2/TRK/001/C01	Inspection and maintenance of permanent way – Geometry and gauge clearance [22]
NR/L2/TRK/001/D01	Inspection and maintenance of permanent way – Specific requirements for switches and crossings [23]
NR/L2/TRK/001/E01	Inspection and maintenance of permanent way – Installation requirements, maintenance limits and intervention limits [24]
NR/L2/TRK/1054	Inspection, Maintenance and Repair Procedures for Cast, Welded and Fabricated Crossings in the Track [16]
NR/L2/TRK/0053	Inspection and Repair to Reduce the Risk of Derailment at Switches [15]
NR/SIG/10663	Signal Maintenance Specifications (SMS) [25]
NR/SMS/PA11	Point Inspection [26]
NR/SMS/PB11	Clamp Lock Hydraulic Points [27]
NR/SMS/PC05	Point Machine HW Style [28]
NR/SMS/PF01	Point Fittings [29]
NR/SMS/PF02	Mechanical Supplementary Drives [30]
NR/SMS/PF03	Point Fittings: Switch Rollers [31]

Network Rail maintenance standards include a section titled “reference documentation” which contains a list of all referenced documents within the standard. The section was found to be beneficial towards assuring completeness of the results.

2.1.2 European railway standards

In the case of European standards, the work provides an overview of European inspections (and practices) that supplements the British inspection requirements and is not meant to achieve perfect completeness and accuracy of recorded information. Thus, the adopted procedure of inspecting standards was not carried out in the case of European standards.

The following three documents were used to collect information about inspection requirements and practices around Europe:

1. *Regelwerk Oberbau, Richtlinienfamilie 821 „Oberbau inspizieren“* [32], which defines inspection requirements and procedures within DB Netz, the main infrastructure owner in Germany;

2. *UIC Working Group Switch & Crossings, Questionnaire – Maintenance Specifications S&C* [33], a questionnaire about the maintenance specification of S&C within Prorail, the main infrastructure owner in Netherlands, and;
3. *UIC Project Switches & Crossings, Inspection of Switches & Crossings, State of the Art Report* [7], which, among other content, reports on the maintenance requirements and practises of several European countries.

In the case of European inspection standards, the author made use of the best information that was available at the time of carrying out the work and the completeness and accuracy of the gathered inspection tasks is therefore limited.

2.2 Overview of railway inspection requirements

In order to facilitate the entire process (inspection tasks identification, solution identification and technology gap identification), the gathered inspection tasks were collated and organised in an .xlsx inspection template. Each identified inspection task was categorized along with the following information (whenever possible): country of application, source of information, inspection frequency, current inspection method(s) and other remarks.

During the collation and categorization of the inspection requirements it was found that the diversity of the gathered data was great as switches are complex parts of the infrastructure (with dozens if not hundreds of failure modes); there are variances between them (within the same country as well as between different countries) and variances between how they are maintained across different countries.

Thus, an effort was made to maintain a balance between gathering detailed information and working with a manageable amount of information.

During this process, it was decided that the optimum classification method was a combination of classification by current/potential inspection method and classification by inspected part. The first adopted level of classification is based on the broad type of the inspection: visual inspection or measured inspection. The second level of classification is based on the type of the inspected part.

Throughout this work, visual inspection tasks refer to those tasks where physical contact with the infrastructure is generally not required. As an example, the inspection of a stretcher bar through the application of a small force using a crow bar (to check its rigidity) is not considered a visual inspection task. However, all tasks where contact is made with the

inspected part solely due to cleaning purposes, are still considered visual inspection tasks. Where contact is required for a different reason, the task is classified as a measured inspection task no matter the purpose of the contact.

It has become clear that there are several broad S&C inspection topics which are addressed by current technology and which can be further researched and redeveloped. These topics can together tackle three quarters (or even more) of the total inspection requirements and they are as follows:

1. Visual inspection tasks;
2. Inspection of shape, size and position of switch rails, stock rails, crossing, wing rails and check rails;
3. Geometry measurements (gauge, cant, twist, alignment and levelling);
4. Measurement of cracks in rails and crossing;
5. Tightness checks; and
6. Point machine inspections.

The classification can be seen in Figure 2-2.

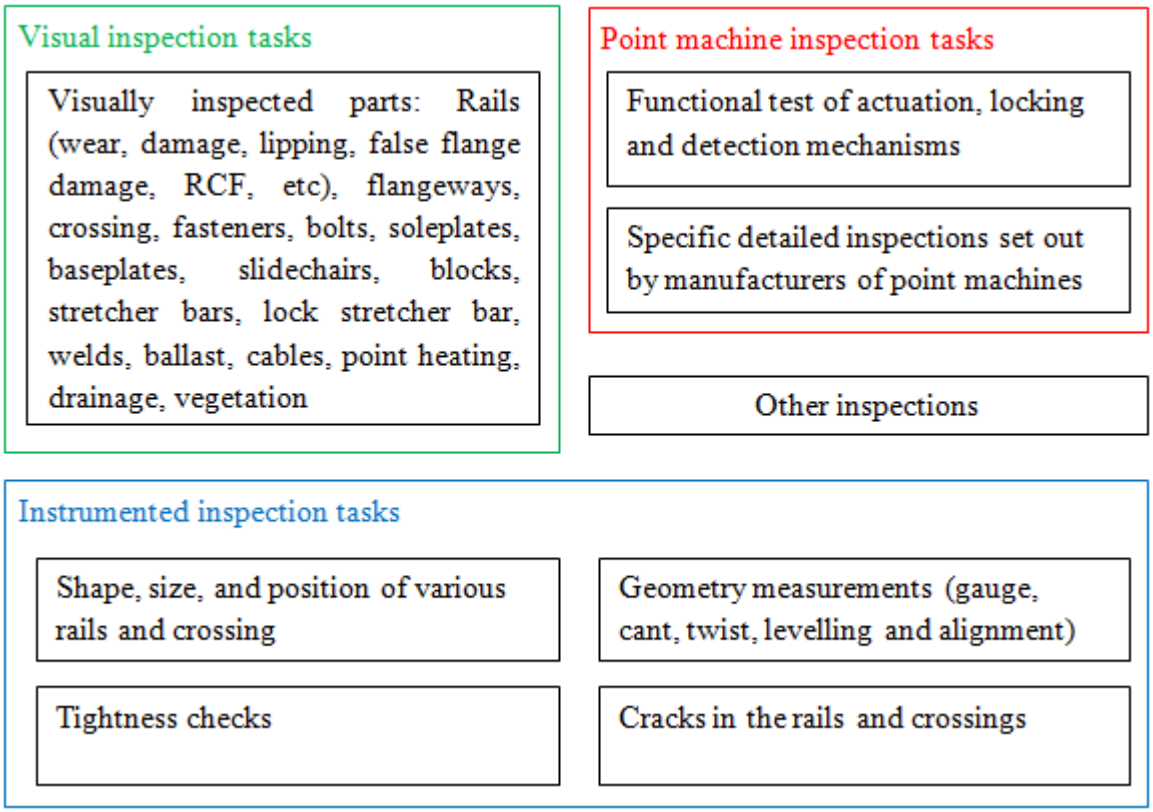

Figure 2-2 Overview of inspection requirements

Because of the following reasons, the point machine (not to be confused with "points") inspection tasks have been classified separately instead of being considered a part of either visual inspection or instrumented inspection:

- inspection of point machines can require their cover to be removed prior to carrying out the inspection tasks;
- the inspection tasks are highly dependent on the type of the point machine;
- some inspection tasks includes maintenance tasks such as adding grease or oil, and;
- the inspection of some point machines require a functional test to throw the point machine in both the extended and retracted state.

The "other inspections" category contains inspection tasks that could not be included in any of the other categories. Examples of such tasks include checking rail isolation and the inspection of vegetation along the walking path.

It was concluded that, due to the railway infrastructure having similar designs across different European countries and generally the assets suffer from similar failure mechanisms, similar measurement and inspection techniques are used. However, the method of inspection (including the equipment used), intervention limits and maintenance strategies vary between different railway industries.

The .xlsx sheet containing the collated inspection tasks and related information is available in

APPENDIX C: SWITCH INSPETION REQUIREMENTS.

It was also concluded that failure to correctly inspect S&C components within any of the mentioned categories, excluding the "visual inspection tasks" category and "other inspection" category, can lead to significant damage and/or injuries. Failure to inspect the switch rail fittings and their fastenings and joints can lead to catastrophic accidents, Grayrigg [9]. Both the shape and position of switch rails are a safety concern as several rail accidents have demonstrated [9–12]. Continuous growing cracks within the rails and crossing can lead to abrupt rail breaks [14]. Track twist can be a major contributor to train derailments in both S&Cs and plain line, as happened in one of the most recent derailments in the north-west of London [34]. Malfunctions in the point machine can undoubtedly leave it in an unsafe state, which again can cause a derailment.

Agreeing with Whalen, in that the incorrect operation of a safety-critical asset "could lead to loss of life, substantial material or environmental damage, or large monetary losses" [35], S&Cs have safety-critical components within almost all mentioned inspection categories. Therefore, when considering new methods for S&C inspection, inspection accuracy, precision and reliability have a key role in assuring railway safety. Due to this, inspection systems and condition monitoring systems that are not able to meet this requirement are considered unsuitable for the purpose of this chapter.

2.3 Difference between condition monitoring and automatic inspection

2.3.1 Introduction

Recently there have been many technological advances in the area of railway inspection and condition monitoring. Many researchers, as well as companies, are now trying to develop innovative methods that are able to inspect and monitor the railway infrastructure rapidly, automatically, remotely and with a reduced number of staff. Many of these advancements have been in the area of condition monitoring techniques. Condition monitoring can greatly improve the maintenance of assets and it is the solution that many researchers choose to take forward. This section aims to detail the differences and similarities between condition monitoring and inspection. As Groom [36] mentioned in a paper, it is difficult to fully define what condition monitoring is; it is no different here, but the best effort at a description was made.

2.3.2 Comparison between condition monitoring and inspection

Objectives of condition monitoring

Condition monitoring techniques can be used as a tool to achieve in the broadest sense what it promises (i.e. to monitor the condition of assets). However, when publications are consulted from the speciality literature, despite the large volume of information and diverse techniques presented [37–40], it is clear that the scope of condition monitoring is focused on faults wtih the aim of preventing impending failure. Thus, the scope of condition monitoring techniques can be summarized by a set of three objectives as follows:

1. Fault detection, which is the ability of a system to detect if a fault is present in an asset;
2. Fault isolation and identification, which is the ability of a system to tie a fault to a certain part of the monitored asset and/or determine the nature of the fault, and;

3. Fault prediction, which is the ability of a system to predict future faults in the monitored asset.

The latter two objectives are also commonly referred to as fault diagnosis and prognosis, which represent the main aims of condition monitoring systems. Most often, the research and development of condition monitoring systems is also driven by other aims which make them efficient in the context of real applications:

- Low production cost of the monitoring system;
- Easy to retro-fit on existing assets;
- Low operating and maintenance cost;
- High reliability (avoiding false negatives and false positives); and
- Minimal or no influence over the monitored system.

Measured parameters of condition monitoring

In general, condition monitoring techniques do not measure the parameters that define the fault(s). Instead, most condition monitoring systems rely on the dependence between the fault and one or several effects that they produce. Thus, many condition monitoring systems measure one or several of the following broad categories of effects: dynamic, particle, chemical, physical, temperature, and electrical [6].

As an example, most bearing condition monitoring techniques are based on dynamic effects, in particular vibration or acoustic analysis. The fault itself which could be, for example, a deformed shape or cracks in the bearing components is not measured directly [41]. In some cases, including this example, accurate measurement of the fault itself (deformed shape or cracks) is not even of interest; instead a quantization of the extent of the fault(s) is desired. As a second example, Asada [42] developed a condition monitoring algorithm which was tested on railway AC point machine actuators. By measuring the active power used by the actuator (AC motor), he successfully identified different severity levels of overdriving and underdriving faults which are millimetric misalignments in the mechanical assemblies.

Thus, in general, condition monitoring systems usually measure parameter(s) which:

- Can be measured using inexpensive sensors;
- Can be easily accessed, and (as a consequence);
- Are not the fault itself but are influenced by the fault.

Measurement accuracy and reliability of condition monitoring

The accuracy of condition monitoring techniques varies greatly depending on their performance. For example, fault detection monitoring systems can provide as little as a pass or fail indication. At the other end of the range, fault prediction monitoring systems generally have good accuracy. Even so, many condition monitoring techniques are not able to measure the actual fault at high accuracy (for example in the case of faulty bearings, accurate measurement of deformation and cracks of the individual faults in the bearings). In the case of point machine condition monitoring, the mentioned algorithm is not able to accurately measure the millimetric misalignment.

Measurement reliability is still a limitation of current condition monitoring systems. In particular, reliable measurements independent of the variations in the monitored assets and while operating in a real environment are more difficult to achieve than reliable measurements from a single system running in a laboratory environment.

Inspection systems

Generally, the purpose of inspection systems is to measure or assess certain properties (e.g. mechanical, electrical, chemical, etc) of the inspected asset. Most often, the measurements of inspection systems are within certain accuracy and precision limits which are set by the manufacturer. Thus, to achieve this, most inspection systems measure the parameter of interest directly whenever possible. Due to the direct measurement, their reliability seldom requires improvement. However, for the same reason the use of such systems can be more expensive and invasive, as they need access to the measured parameters unlike many condition monitoring systems, which measure affected parameters and not the parameter itself.

Conclusion

Due to their relatively low cost, ease of installation and continuous measurements, condition monitoring systems can be used to maintain assets in a cost effective way (most often using a condition based maintenance strategy). However, their limited accuracy, precision and reliability can be insufficient to replace more traditional inspection processes, especially when the asset is a safety-critical component and an inspection failure can lead to a substantial loss of assets and/or injuries.

Thus, in this chapter condition monitoring techniques are considered, but, where their reliability is limited, they are not considered for inspection of safety-critical assets.

2.4 Commercially available and potential turnout inspection solutions

After the inspection of relevant standards, the research continued with the investigation of available and potential S&C inspection solutions. Therefore, the market for inspection technologies for switches and crossings was researched and relevant available technologies were mapped in the spreadsheet file in a separate column.

The following section describes off-the-shelf and research-level solutions that have the potential to replace manual inspections on S&C components.

2.4.1 Train borne inspection solutions including rail vehicles and robots

1. Switch Inspection & Measurement (SIM) wagon from Eurailscout

In 2005, Eurailscout, a German-Dutch joint venture, developed their own solution to S&C inspection, "Switch Inspection & Measurement" (SIM), which was a vehicle based S&C inspection system. This was later redeveloped to become what is today the SIM11 and SIM12 [43]. While the predecessor was a locomotive with inspection systems, the later SIM11 and SIM12 are wagons that can be pushed or pulled by a locomotive. These have a "switch inspection system" and a "switch measurement system".

The **switch inspection system** has 8 CCD cameras which are used to synchronously record video footage of the S&C at different angles. The footage can be manually inspected offline from a desk in an office and it is claimed that certain faults can be automatically identified through image processing such as missing fastening devices depending on the type, crumbling of concrete rail sleepers affecting safety, cracks in the concrete rail sleepers affecting safety, which can be detected with 0.5 mm accuracy, and ballast deficit/surplus.

The **switch measurement system** includes a **laser measurement system** which uses the triangulation principle [44] and an **inertial measurement unit** (IMU). The lasers measure the profile of the rail every 20 mm while the wagon is pushed or pulled at 40 km/h. The following can be calculated: track gauge, flangeway gap, and horizontal and vertical wear.

An **IMU**, optimised for short and medium wavelengths, is mounted on the switch measurement system and allows for geometry measurements to be taken. It is advertised that

the following parameters can be delivered: track width, shift, height, transverse gradient, and all derived parameters.

The SIM needs to be scheduled in the train timetable in order to carry out the necessary inspections. However, once this is achieved, no possessions are required (unless detailed inspection needs to be arranged), which increases asset availability as well as safety and eliminates time spent travelling between sites and office.

Figure 2-3 Switch Inspection & Measurement (SIM) wagon
Courtesy and Copyright Eurailscout

Currently, this technology is proven on the Dutch rail network. It is advertised that in Amsterdam, the SIM is capable of inspecting 100 S&Cs (both paths) in less than 6 hours [43]. In 2013 the SIM was trialled in Germany and the results were favourable towards its use there [45].

2. RILA-system, Fugro

The RILA-system, initially developed by Raildata, is a compact measurement system that can be easily attached to the end of passenger trains and is able to measure the absolute track geometry even when running over S&Cs. The system uses a combination of sensors including GPS, accelerometers and line lasers and it is claimed that all required geometry parameters can be made available at reasonably high accuracy. The system was first operated in 2009 in Netherlands and in 2013 it had been successfully trialled on the railway in Britain [46].

Figure 2-4 RILA-system mounted on a passenger train
Courtesy and Copyright Fugro

It is worth mentioning that there are known limitations of the RILA system such as: inability to work in bright daylight (due to the limitations of the lasers used) and limitations surveying certain parts within S&Cs (due to the geometry), however these issues could be overcome.

3. Automatic Switch Inspection Vehicle (ASIV) from ZETA-TECH

ZETA-TECH, a US based rail consultancy firm, have developed a rail vehicle (ASIV) [47] which is able to survey the physical dimensions of a switch in a similar manner to the SIM wagon manufactured by Eurailscout.

Figure 2-5 Automatic Switch Inspection Vehicle (ASIV)
Courtesy and Copyright ZETA-TECH

The ASIV is equipped with a pair of Optical Rail Inspection and Analysis (ORIAN™) units [48], a laser-based system produced by KLD Labs. It is claimed that the system is able to measure various S&C parameters as described in Table 2.

Table 2 Summary of potential measurements using the ASIV vehicle

Rail Type	Measurement
Stock rail opposite a switch rail:	Vertical wear
	Gauge side wear
	Field side wear
	Gauge face angle
	Gauge corner radius
Switch rail:	Gauge face angle
	Breaking or chipping
	Gauge corner radius
Stock and switch rail:	Vertical height difference
	Lateral gap width
	Wheel contact point through switch point
Closure rails:	Vertical wear
	Side wear
Frog:	Frog flangeway gap width
Frog nose and wing rail:	Relative height of nose and wing rail
	Wear/batter on wing rail
	Batter/damage to frog
	Surface damage: batter, chipping
	Wheel contact through frog
	Wing rail profile (within field of view)

It must be noted that although the word batter does not have a well defined scientific definition, it is widely used to express a type of damage to S&Cs and thus, is also used in this thesis as well. Rail batter is a type of wear which generally occurs due to impact forces, around an area of wheel transfer. The result is a flattening of the crossing nose and wing rails at crossings and rail ends at rail joints. Sometimes it can be accompanied by metal breakage. The damage is generally higher on heavy haul railways.

ZETA-TECH reported successful switch inspection trials in both British and US railways. Although the profile measurements have been claimed to have better accuracy (due to the presence of acute angles in the rail profile) when compared with the industry's leading rail

profile measurement system MiniProf [47], no information was found regarding the accuracy and precision of the specific rail measurements (as defined in Table 2) or their reliability.

4. Loccioni's FELIX robot

Loccioni, an Italian-based company founded in 1968, have developed an S&C inspection robot named FELIX [49]. The robot is capable of measuring the profile of rails (and crossing) as well as the geometry of the switch. The robot weights around 150 kg when assembled and the heaviest part when disassembled is 47 kg. Thus, it is brought to the railway site in parts and assembled there. The robot can be controlled remotely from a short distance and its autonomy is 6 hours. The measurements are taken at around 5 km/h.

Figure 2-6 Felix robot
Courtesy and Copyright Loccioni

The robot was initially designed for the Italian railway and is further developed for usage on various European railways. It is claimed that the robot can measure most rail parameters including rail wear, flangeway gap and track gauge with good accuracy. The manufacturer states a resolution of 0.1 mm.

2.4.2 Line-side monitoring and inspection solutions

1. POSS monitoring system, Strukton

Strukton is a Dutch rail company which produced a number of technical solutions for the railway industry, including S&C inspection and monitoring systems. In 2012 they expressed their vision of a switch inspection system [50]. They believe a switch is best inspected using

a combination of a wagon based inspection system (SIM, or similar) and a condition monitoring system for the point machine.

They developed a condition monitoring system called Preventive Maintenance and Fault Diagnosis System (abbreviated POSS) which can monitor several railway assets including point machines. The monitoring of the point machine is non-intrusive as it uses current transducers which are installed in the proximity of the point machine. The analogue signal is fed to a box through a DB9 connector, as shown in Figure 2-7, where it is digitised and transmitted wirelessly over GPRS or Ethernet to the POSS cloud from which it can be accessed using an internet browser.

The monitoring system can generate alerts if the current consumption of the point machine falls outside predefined limits during any of the point machine phases (e.g. locking, unlocking, throwing, etc). It is relatively easy to obtain installation approval as there is no electrical connection between it and the monitored switch. Thus there are a limited number of wires to be installed as the data can be sent wirelessly.

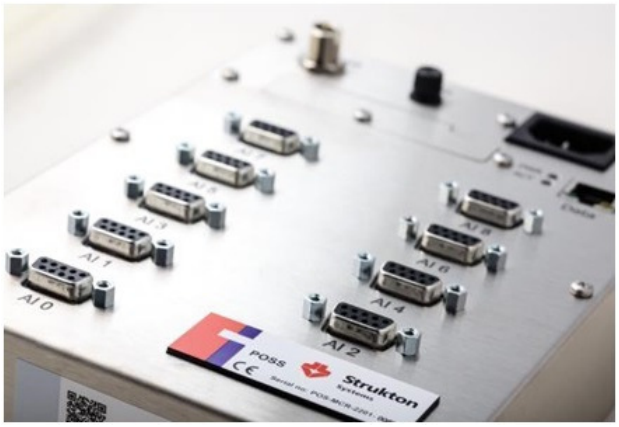

Figure 2-7 POSS monitoring unit
Courtesy and Copyright Strukton

However, Strukton does not claim to be able to identify and diagnose subtle changes in the current. Subtle changes in the current can provide early signs of incipient point machine failure but fairly complex algorithms are required, as simple thresholding techniques are not sufficient [51].

The POSS monitoring system has been successfully installed on many railway networks across Europe and Australia.

2. Current research in point machine condition monitoring

Recently, much research has been carried out on condition monitoring of various mechanical systems including Single-Throw Mechanical Equipments (STME), such as railway point machines. Condition monitoring of Britain point machines is generally aimed towards prediction of adjustment faults (i.e. misalignment within various rods connecting the point machine to the switch rails) [42,51]. Although considerable progress had been achieved in this area, there are still challenges to be addressed, such as assuring a high level of confidence for a large number of point machines (>10.000) and in various weather conditions.

3. Fixed asset monitoring system, Voestalpine

Voestalpine is a steel-based technology group operating on all five continents which developed an asset monitoring system called VAE ROADMASTER 2000. The system comes in three versions: light, advanced and pro. The pro system is able to monitor the condition of S&Cs through the installation of a wide range of sensors as shown in Figure 2-8.

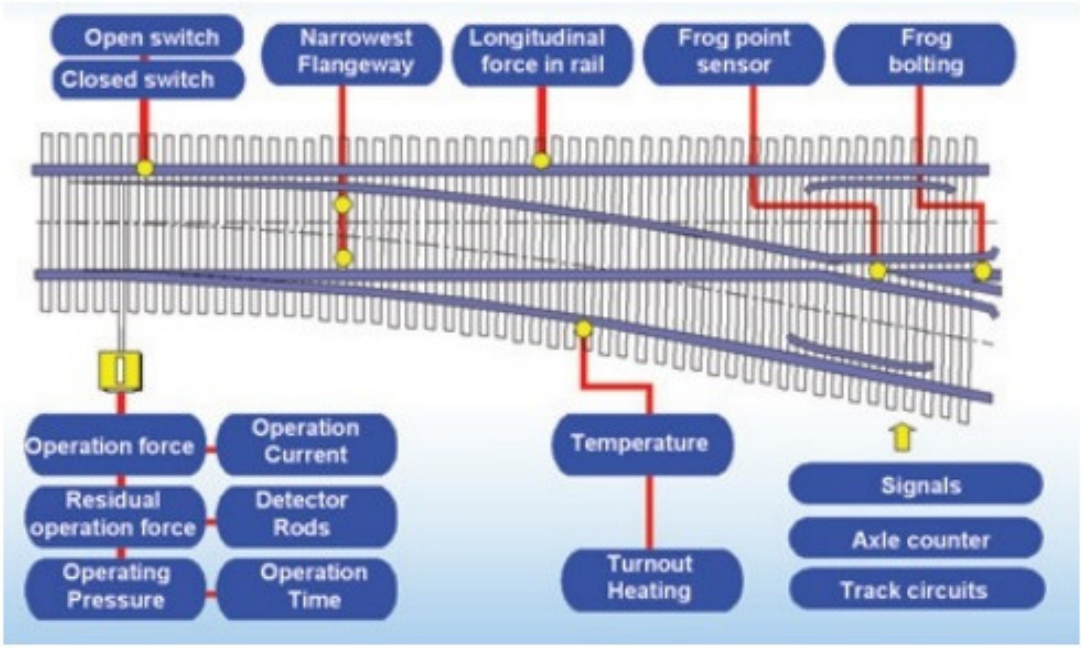

Figure 2-8 Voestalpine's switch monitoring capabilities
Courtesy and Copyright Voestalpine

It is advertised that the evaluation of the measured data will be done using intelligent algorithms which take into account the variation of weather related parameters in order to accurately decide whether or not to generate an alarm. The system is also advertised to "recognize all initiating errors".

4. Vossloh's sensory capabilities

Vossloh, a German company supplying infrastructure and rolling stock assets to the rail industry, has over 10 years of S&C monitoring experience. Table 3 shows Vossloh's sensory capabilities in S&C inspection and condition monitoring and has been reproduced from a unpublished report in 2008 [52].

Table 3 Vossloh's sensor capability in S&C monitoring

Sensory solution / S&C inspection or condition	PM.PEL - active power sensor	PM.RKA - current in detection circuit	PM.F - force to move the switch	PM.ACM - vibration sensor on point machine	PM.ACC - shock sensor on the frog	PM.C - displacement of throwing rod	PM.2P - distance between stock and switch rail (at point)	PM.2T - distance between stock and switch rail(at fwg)	PM.MET - rail and air temperature and air humidity
Distance between stock rail and switch blade at the point							X		
Distance between stock rail and switch blade at the flangeway								X	
Distance between the frog and the check rail					X				
Maximum throwing force (for switch and movable frog)			X						
Throwing rod out of adjustment			X			X			
Problem in locking device	X		X			X			
Obstruction	X	X	X			X	X	X	
Problem in the detection circuit		X				X	X	X	
Level of tamping				X					
Weather conditions									X

The "X" in the table implies that there is dependence between the inspection tasks or condition and the reading from the sensor. However, it is unlikely that with the use of a sensor (e.g. PM.F or PM.C), the nature of the fault can be established.

Prior to installation of such systems, various issues have to be considered such as: installation time & requirements, compliance with railway standards (PM.F uses a load pin which can render the machine unusable if it breaks, EMC, tamping clearance, etc), maintenance requirements and reliability in a railway environment.

5. SmartBolts, Stress Indicators

Stress Indicators Inc., a US-based company, specialises in the design and manufacture of stress visual indicating devices in the form of bolts and studs. As pictured below, their SmartBolts give a red visual indication when a bolt is loose.

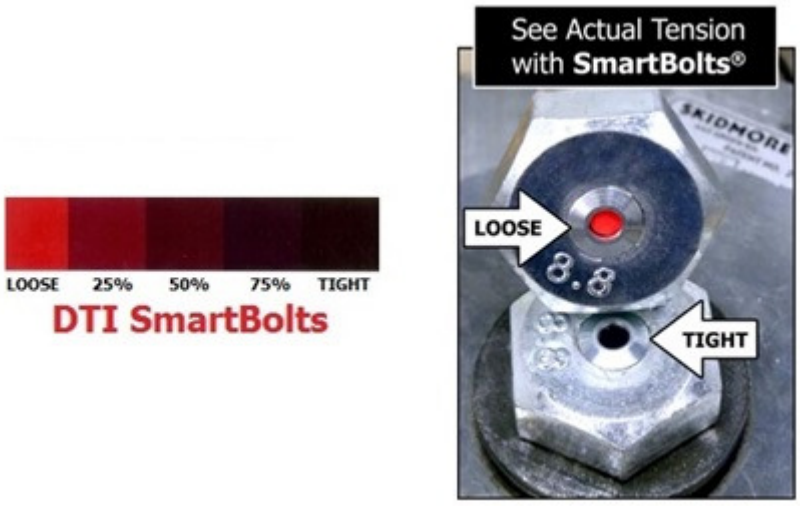

Figure 2-9 The SmartBolt
Courtesy and Copyright Stress Indicators

The colour of the indicator changes linearly with the amount of stress in the bolt which allows easy identification when stress in the bolt has been significantly reduced. The company manufactures bolts in various steel grades ranging between 5 and 10.9.

6. Smart Washer, Smart Component Technologies Limited

A smart washer is a self instrumented washer that is able to wirelessly transmit information regarding current stress, and therefore the condition of bolted joints. Smart Component Technologies Limited, is a recent spin-out company from the University of Huddersfield that has continued to redevelop a smart washer concept. Their devices currently rely on near field wireless recharging technology and long life batteries. However, the company recently received a Technology Strategy Board (TSB) fund to research the feasibility of adding a vibration energy harvester to their smart washer giving the possibility of developing a true fit-and-forget device [53].

7. RotaBolt-TD, James Walker RotaBolt Ltd

The RotaBolt-TD bolt is a join monitoring device similar to the smart washer. The sensor and transmitter are embedded in a bolt together with a battery which is claimed to provide 5 years of continuous unattended operation [54].

8. Tracksure locking mechanism, Wheelsure Holdings

Wheelsure Holdings is a UK based limited company which supplies an innovative mechanical device for securing bolts. The device is based on the use of a reverse thread preceded by a normal one. Two nuts are fitted on the bolt and a cover forces them to rotate synchronously (i.e. in the same direction and same amount). The loosening of the nuts is achievable only when they rotate in opposite directions. For this to happen, significant damage has to occur (e.g. on the thread, cover, etc) making the mechanical device very resistant to loosening.

Figure 2-10 Tracksure locking mechanism
Courtesy and Copyright Wheelsure Holdings

The Tracksure locking device, an award winning (2007 and 2008) innovation, is already in use in several industries including the rail industry.

9. Multi-sensor, Vortok

Vortok is a rail company that supplies many technical solutions to the railway industry.

They produced a multi-sensor which can be installed in the web of the rail as a 10 mm diameter bolt as shown in Figure 2-11. The multi-sensor is able to measure force (in the vertical or horizontal plane), acceleration (both vertically and laterally) and core temperature.

Figure 2-11 The multi-sensor
Courtesy and Copyright Vortok

The sensor is described as compact, rugged and easy to install. Using the data provided by the multi-sensor, various information relating to the running of trains over the piece of rail can be calculated.

10. Overhead line mounted CCD camera developed by Luleå University of Technology and Swedish Transport Administration (Trafikverket)

As a response to the need for S&C inspection, Asplund [55] considered the inspection of railway S&Cs using a fixed CCD camera mounted on the overhead line. He concluded that zoom and tilt capabilities are desirable in order to record good resolution footage of various parts of the S&C. The types of inspection tasks carried out by such a system are mostly visual, while measured inspection tasks are also possible depending on the performance of the camera. Measured tasks may include track gauge, flangeway gap, switch toe opening and residual switch opening.

Figure 2-12 Overhead line mounted CCD camera prototype (left) and sample image (right) Courtesy and Copyright Matthias Asplund

The system is intended for turnouts which are heavily used, are susceptible to high failure rates or which would cause high disturbance to the railway timetable due to their important location within the railway network. In such conditions the camera has the advantage of facilitating the inspection more frequently than other inspection methods (e.g. trains, robots, trolleys, patrolling).

2.5 Identification of gaps and research opportunities in technologies for switch inspection

The last step was the identification of technology gaps where the current technology is not able to provide a solution. This step revealed areas of research where new innovation may improve the way in which inspection is carried out.

The aim of this research is to investigate the feasibility of eliminating the need for human inspection of S&Cs. Thus, the scope is limited to researching alternative ways of carrying out the S&C inspections as required by the inspection standards, therefore, any optional inspection or condition monitoring solution that is not able to replace any inspection tasks as required by the inspection requirements is considered unhelpful towards achieving the goal of this chapter. Other related analysis, such as cost saving calculations are also outside the scope of this chapter.

2.5.1 Inspection tasks carried out by visual inspection

Visual inspection is one of the oldest and simplest types of inspection carried out in the railway industry. The visual inspection of S&Cs is usually carried out on a fortnightly to monthly basis. During the inspection, most parts that make up the turnout are visually examined to some extent to assess whether or not they are in a good condition. Thus, many

developing problems can be identified at an early stage by carrying out this type of inspection. If a problem is then identified but the extent and severity cannot be accurately quantified, a measured inspection can be scheduled out which will accurately determine the severity.

As defined in this work, this category covers only those inspection tasks which do not imply the use of any measurement or inspection devices.

The required S&C visual inspection tasks are shown in

APPENDIX C: SWITCH INSPETION REQUIREMENTS and can be summarized as follows:

- condition of switch/stock rails for wear, damage, lipping, RCF, false flange damage and residual switch opening;
- condition of switch rail fittings: stretcher bars, lock stretcher bars, driving rod and their fastenings for bent, damage, dents, missing and cracks;
- condition of crossing, wing rails, check rails and flangeways for wear, batter, lipping and cracks;
- condition of rail fastenings, soleplates, baseplates, blocks, welds, ballast, rail joints, and;
- condition of vegetation, drainage and other visual inspection tasks.

State-of-the-art solutions

Currently, all alternative solutions are based on the CCD camera and this is unlikely to change.

The CCD cameras can be used in two ways: as line-side equipment and train-borne, both of which are currently under use and further development.

Another concept of a CCD S&C inspection camera (author's work) is the use of two fixed, wireless, self-powered CCD cameras in the four-foot of a switch aimed towards the tip of the switch rails, as shown in Figure 2-13.

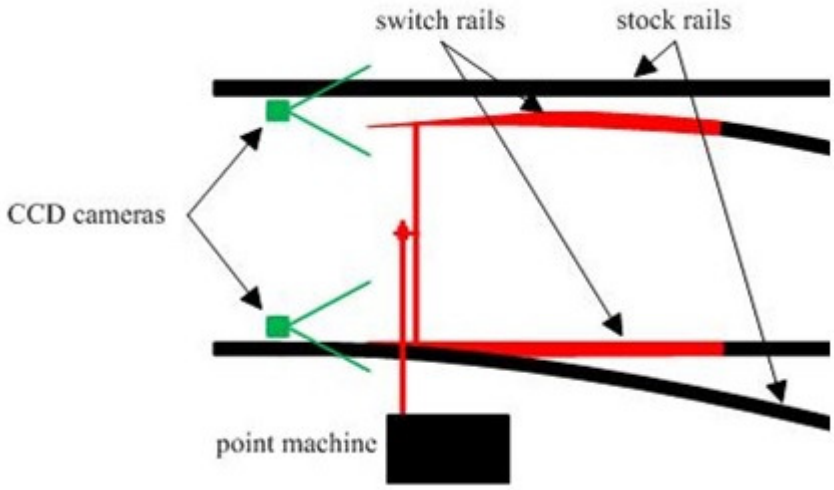

Figure 2-13 Possible use of CCD cameras for turnout inspection (concept)

The main drawbacks of such a system are: the challenge of maintaining the cleanliness of the CCD cameras, the ability of the cameras to function in such a harsh environment (due to high vibration forces and dust/debris), the difficulty in assuring a fixed gauge between the cameras and the small coverage of required visual inspection tasks. The latter drawback does not necessary apply in the context of condition monitoring of S&Cs. It is also noted that lineside equipment has to comply with a series of standards, including the railway group standard GC/RT5212 which defines requirements for defining and maintaining clearances.

In Table 4, a comparison is drawn based on the inspection task coverage of the two broad inspection methods, vehicle-based and line-side.

Table 4 Comparison between vehicle-borne and line-side CCD camera inspection techniques

	Vehicle-borne	Line-side
Percentage of visual inspection tasks that can be replaced using the CCD camera inspection technique	Vehicle-borne CCD inspection systems can make use of multiple cameras installed at various angles taking close-up pictures. Due to this, it is possible to remotely carry out a high	Line-side CCD cameras include any cameras that are permanently fixed on or near the vicinity of the S&C. Two such examples are CCTV cameras and the over-head line camera [55]. The percentage cannot be reasonably estimated as it depends on many factors such as the number and position of CCD

	number of inspection tasks using the captured footage. The author estimates this to be in the range of 80 to 95% depending on the standards of the railway infrastructure owner.	cameras as well as their resolution, zoom and tilt abilities. However, due to the fact that the CCD cameras are in a fixed position relative to the S&C, the percentage of inspection tasks that can be covered is appreciated to be less than in the case of vehicle-borne CCD cameras.

Although vehicle-borne CCD cameras have a greater inspection coverage, line-side CCD cameras have other advantages over the vehicle-borne CCD cameras (e.g. ability to inspect on-demand) which can make them more suitable in some specific use cases (e.g. for heavily used key turnouts) [55]. However, vehicle-borne cameras have better potential for achieving the highest inspection coverage.

It has been concluded that the following visual inspection tasks cannot be carried out using vehicle-borne CCD inspection systems:

- visual identification of cracks around the goose-neck stretcher bar bracket commonly used in Britain railways; certain cracks can build up on the bottom of the bracket which are therefore not visible unless a mirror is placed underneath; a similar limitation applies to the visual inspection of cracks at the bottom of crossings as this also requires the use of a small mirror that is placed between the ballast and the foot of the crossing where cracks can initiate;
- inspection of any parts of the turnout which are covered by dirt and which require cleaning before a visual inspection can be carried out;
- inspection of drainage systems, walking path;
- difficulty in quantifying lipping on the inner faces of the stock and switch rail pair (i.e. the faces which meet when the switch is in the closed position);
- difficulty inspecting the back of the switch rail for scar signs from flange contact or signs that it has been strike by wheel flanges, and;
- difficulty in checking if the closure rail baseplates are pushed down into sleepers and if the crossing is sinking.

Line-side CCD cameras are also unable to carry out the above mentioned inspection tasks (unless CCD cameras specially designed for a specific purpose are to be used). In the case of the CCD camera the following adds to the list of uncovered inspection tasks:

- difficulty in identifying small rail and crossing surface defects (e.g. wear, RCF, head-checks, wheel burns, lipping, deformed crossing nose, weld defects, etc);
- difficulty in identifying slide chairs, baseplates, blocks and fishplates if they are bent, squashed or cracked;
- difficulty in assessing if stretcher bars, soleplates and wing rails are bent, distorted, squashed or cracked, and;
- difficulty in inspecting certain bolts (e.g. horizontal bolts in fabricated crossings).

Conclusion

Currently, the use of CCD cameras does not offer full inspection coverage against the visual inspection tasks as identified in

APPENDIX C: SWITCH INSPETION REQUIREMENTS. Vehicle-borne CCD cameras offer the highest inspection coverage; their limitations in visual inspection can be linked back to three main limitations as follows:

1. the system can not accurately inspect any object which is far from the immediate field of view of the cameras (around the four-foot);
2. the system cannot replace any visual inspection requirement which requires the use of mirrors, and;
3. the system cannot inspect any parts which require cleaning prior to inspection.

The first limitation is of less importance as the condition of assets and the environment sounding the S&C change at a relatively slow rate and thus frequent inspection is not required.

The second limitation can be mitigated through the use of better S&C components. In fact, a new type of stretcher bar has recently been developed, the tubular stretcher bar [56], and has already been installed on some S&Cs within the NR infrastructure. Due to its complete new design, it is expected that it will not suffer from the same failure modes. Similarly, research has been carried out to improve crossings design and Hsu reported a recommendation for the mitigation of cracks in the foot of crossings [57].

The build up of dirt on S&Cs in GB is related, in part, to the application of grease on switch rails. Other sources of dirt include oil from trains, filings from wheel-rail interaction, natural debris or even human waste from trains. During a meeting with senior NR personnel (January, 2012) it was understood that NR is looking at using better lubricants which have, among other properties, a lower viscosity thereby reducing the amount of dirt which builds up in and around the rails.

With the mentioned continuous improvements it is expected that train-borne CCD cameras could be able to provide a means of reliable remote inspection for NR's S&Cs without the development of new, innovative inspection solutions.

Machine vision for automatic inspection of track and turnout components is another field of research which has the ability to remove the need for a human to manually inspect the footage. Although this it is outside the scope of this research, it is worth mentioning that it is gaining interest in the context of vehicle-borne CCD cameras [58].

2.5.2 Shape, size, gauge and position of rails and crossing shape

This inspection category applies to most inspection tasks that require or relate to dimensional measurements of the inspected components. The tasks are grouped into two main categories:

1. eight inspection tasks, position related: track gauge, check gauge, free wheel passage, flangeway gap, switch toe opening, residual switch opening, position of switch toes and switch rail hogging, and;
2. five and four inspection tasks for switches, respectively crossings, profile related: TGP8 gauge, Gauge 1, Gauge 2, NR4, Switch Rail Radius Gauge, side wear at the crossing nose, batter at the rail knuckle, relative top wear between crossing nose and wing rail and top wear along the crossing nose.

Most measurement solutions can be classified into two groups: contact-based solutions and contactless solutions. Contact-based solutions (e.g. MiniProf®, manual gauges) are generally slow to use and are carried out manually on site. Optical measurement solutions are used where speed is an important factor (e.g. SIM, RILA). However, there are two issues that need to be addressed.

The first one, which has already been mentioned, is the build-up of grease and dirt. It is estimated that dirt and grease can compromise the accuracy of up to a third of the required measurements. The role of lubricants on curved rails has been long proven and research

continues to look at how to further reduce wear rates using lubricants [59,60]. It is also known that lubrication of the switch rail can mitigate the risk of derailment especially on recently ground switch rails [11]. Thus, it is very unlikely that NR will cease to lubricate their switches. However, as already mentioned NR is looking at improving S&C lubricants. Thus the improvement of lubricants could have a significant role in the remote inspection of physical dimensions and position of rails and crossings.

It is also worth mentioning that during a meeting with senior Strukton personnel (September, 2012), it was been understood that ProRail does not use lubricants on their S&Cs despite the proven benefits of switch rail lubrication.

The second issue is the measurement of switch rail hogging. This measurement is manually carried out by inserting a stepped gauge between the foot of the switch rail and the slide chair. Currently there is no contactless solution for the measurement of this dimension, although it is very important, as 3 out the 5 profile switch inspections cannot be accurately carried out without the correct measurement of switch rail hogging. Furthermore, the three tasks (TGP8 gauge, Gauge 1 and Gauge 2) are part of the inspection standard for assessing the derailment risk at S&Cs [15].

Although the ASIV vehicle is advertised to be able to carry out certain measurements as specified in the NR/L2/TRK/0053 there is no mention of it being able to measure the mandatory switch rail hogging [47,61].

Optical measurement systems cannot be used to measure switch rail hogging where the slide chair is heavily greased.

Figure 2-14 Voestalpine switch rollers (left); a heavy lubricated slidechair (right) left picture Courtesy and Copyright Voestalpine

As shown in Figure 2-14, the optical measurement would be affected by the build-up of dirt and grease on the slide chair. Furthermore, such lubricants can reflect the laser beam of triangulation lasers making it impossible to achieve any measurements at all. However, the solution can come from improved S&C components as certain S&Cs use switch rollers reducing the need for lubricants and maintenance while still maintaining low friction (left image in Figure 2-14). In such cases it is possible to measure switch rail hogging using optical measurements by measuring the height difference between the top surface of the slide chair and the top surface of the switch rail. Certainly, any tolerance within the thickness of the rail foot equally affects the measurement (in GB switch rail hogging is currently measured with a resolution of 1 mm).

Conclusion

In order to move towards an inspection free S&C, it is important that switch rail lubricants are reviewed in order to implement lubricants that do not adhere to dirt and dust and have negligible thickness. Furthermore, due to the difficulty in automatically measuring switch rail hogging, slide chair lubricants should also be reviewed. A possible alternative could be interflon products, which are advertised as being effective on switch rail slide chairs [62]. In the long term, it is expected that NR will also use improved S&C components such as the switch rail roller and thus the automatic measurement of switch rail hogging under difficult conditions would not be necessary.

2.5.3 Tightness checks

Current NR inspection standards require that certain torque prevailing nuts and hardlock nuts, as shown in Figure 2-15, within S&C assemblies are periodically checked to ensure they are tightened to the correct torque. This is achieved by using a calibrated 200 Nm wrench. The importance of this inspection has already been proven by the consequences of at least two fatal rail accidents [8,9] in which the loosening of bolts in turnouts played a significant role. This inspection topic had also been recently considered in the context of point machine condition monitoring, where certain parameters (current and voltage actuator, driving rod force and driving rod displacement) are used to collect data and diagnose the condition of the S&C [42,51].

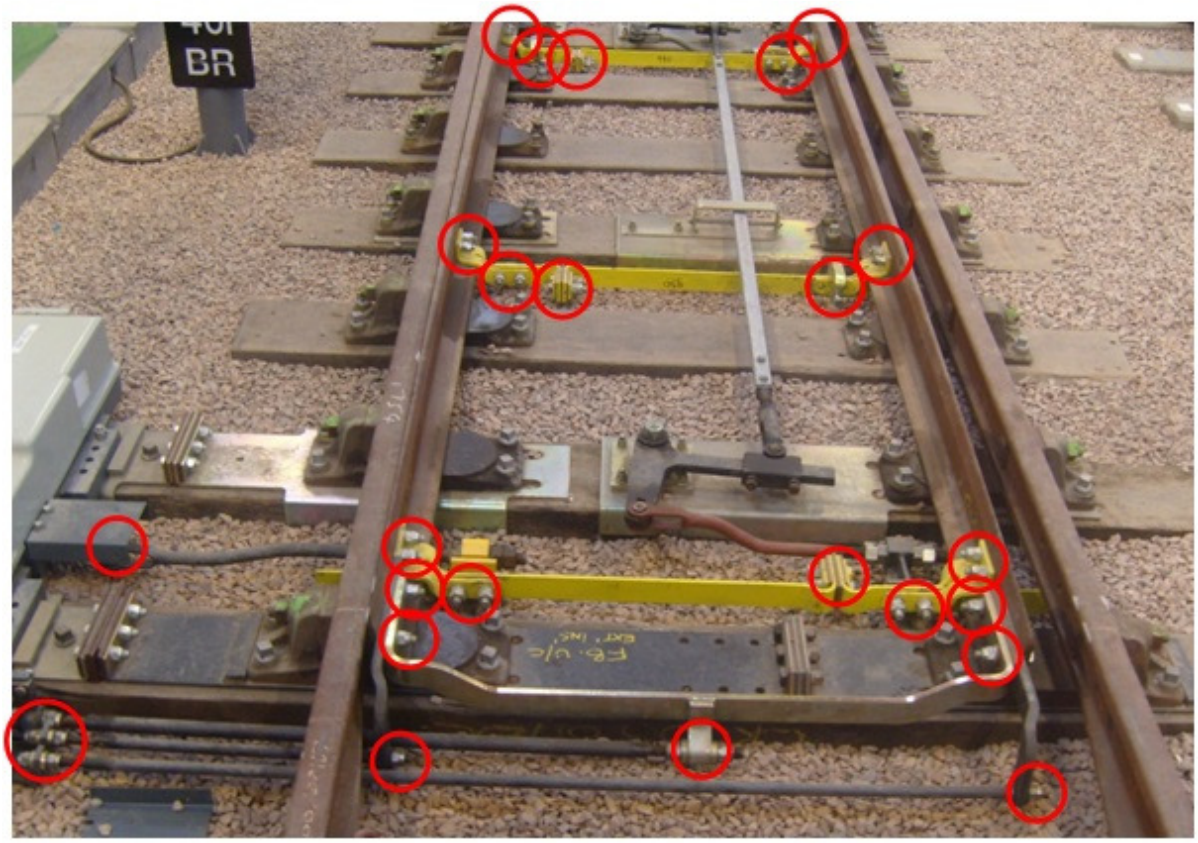

Figure 2-15 Inspected nuts on a GB NR turnout

With the use of train-borne CCD cameras, the tension of Smartbolts® bolts can be remotely inspected without the need for physical access to S&Cs. However, there are three drawbacks to using these bolts on a railway S&C:

1. certain components within the turnout require the installation of bolts in specific ways that do not permit the torque indicator to be visible (e.g. bolts in the switch rail) and therefore the torque's bolt cannot be inspected; this issue may be resolved if the manufacturer could produce bolts with the indicator on the thread end;
2. railway S&C are exposed to the build-up of dirt; therefore there is a significant risk of the tension indicator being covered by dirt and therefore not allowing proper remote inspection; this condition is particularly dangerous due to the bolt generating a false negative situation if image processing is used to automatically identify the red sports, and;
3. the partial loss of torque may not be identifiable, as the indicator changes colour proportionally to torque and not abruptly.

The Tracksure® locking mechanism provides an alternative which has had been proven within various industries including the railway industry. However, in the context of a self-inspection S&C, the question of liability arises. As the bolts would not be manually inspected on a periodic basis, it must be establish whether or not Tracksure® would take liability for losses and injuries caused as a result of loosening bolts. If Tracksure® cannot accept such a liability then their solution is not a true fit-and-forget solution and thus manual inspection would still be required.

Smart Component Technologies Limited could provide the railway industry a true fit-and-forget bolt monitoring device if an energy harvester could be fitted to their smart washers. The liability issue does not stand up here as the device can be designed to never fail in a false negative situation.

The RotaBolt-TD can also provide a solution for railway S&Cs, however due to the expected life of S&Cs it is expected that its battery should be at least 10 years. Thus, as S&Cs components are redesigned for greater reliability and a longer life it is expected that the life of S&Cs could extend further.

Conclusion

Electronic joint monitoring devices have a distinct advantage in comparison to mechanical joints (e.g. Tracksure®) and that is the ability to eliminate any on-site inspection while assuring that no false negatives will be experienced. Thus, as technology advances at such a fast rate, it is expected that an increasing number of safety-critical mechanical joints will be monitored electronically in the railway industry, as well as in other industries (e.g. aerospace, gas, etc).

2.5.4 Cracks in rails and the crossing

Cracks in the rails are a common problem to all railways and much research has been done to improve detection and sizing methods. Rail cracks develop under various failure modes such as rolling contact fatigue, head check, fish-bolt hole cracking, etc. Thus, they can appear in various locations of the rail and can develop into different shapes and sizes, all of which have to be reliably detected to assure safety. Furthermore, rail turnout components have non-standard shapes (shapes which are considerably different compared to a rail profile) which make them more difficult to inspect. S&Cs manufactured from austenitic manganese steel (AMS) pose an even greater challenge as many non destructive testing (NDT) techniques do

not work, at least not reliably enough, on this type of material. Currently, accurate NDT testing of S&Cs is achieved in most European countries by using hand held equipment [7].

In a review paper on state-of-the-art and future developments in NDT, Papaelias et al. [63] concluded that significant research is needed to achieve high-speed rail inspection (without even considering the specific challenges posed by S&Cs nor AMS components) and it is possible that this will come about by the integration of different techniques which can complement their deficiencies. Thus, even though NDT techniques have come a long way, it is needless to say that extensive research is required to improve current techniques and/or develop new ones in order to reliably inspect S&C using rail vehicles. The inspection of cracks within S&Cs without the use of manual equipment or trolleys currently seems unachievable, not now and not within the next few decades.

2.5.5 Geometry measurements

The main track geometry parameters which are used to assess its condition are: gauge, cant, twist, levelling (for each rail) and alignment (for each rail). Measurement devices are generally in the form of manual gauges, trolleys, robots and measurement cars (or wagons). Manual gauges have the advantage that they are generally quick to use on S&Cs whilst trolleys and robots provide better data in terms of accuracy and measurement frequency. However, measurement trains are the single solution which can provide geometry measurements without requiring a maintenance team to visit the S&C. Measurement train cars have various complexities. The inferior end of the range can use inertial measurement units (IMU) mounted on in-service passenger trains to measure acceleration and jerk values and generate an alert if they are too high [7]. Thus, they are instrumented trains rather than measurement trains as they do not provide accurate measurements of any of the five mentioned geometry parameters. At the other end of the range the rail industry makes use of dedicated measurement trains which travel at line speeds and accurately measure track geometry together with other parameters (e.g. catenary related). However, these trains are expensive to run, difficult to schedule and generally measure important mainlines leaving out the majority of S&Cs in stations.

Measurement systems such as the SIM can be used to successfully measure S&C geometry around large stations. Thus, the use of RILA systems and other similar measurement equipment mounted on in-service trains can provide an efficient means of measuring the geometry of S&Cs which are located at various locations within the railway network.

With the exception of dirt and grease on the gauge face of switch rails, which can slightly influence the measurements, there is no real challenge to geometry inspection of S&Cs using in-service trains/wagons.

2.5.6 Point machine inspection

Point machine inspections generally require cover removal/dismounting to allow access to various components such as the actuator and sensors and are classified separately for two main reasons. Firstly, the inspection requirements of point machines are highly dependent on the manufacturer and show a great diversity of tasks (e.g., visual inspection, measured inspection and even maintenance tasks such as adding grease/oil are documented as being part of the inspection process). Thus, the challenges of automating point machine inspection tasks are far greater than the benefit that could be gained. Secondly, many point machines require a functional test to be carried out. This is neither a visual or instrumented inspection as it requires the point machine to be thrown in its two possible states, extended and retracted.

Depending on the manufacturer and the type of machine, the design of railway point machines varies greatly, generally due to the various types of actuators, different sensors used and the overall mechanical design. The equipment manufacturer sets out the maintenance regime of the point machine, which includes periodic inspection tasks. Currently, there are no real alternatives to manually carrying out the required inspection tasks and for the following reasons, the development and implementation of remote inspection is most likely to be counter-productive:

- diversity is great, therefore, an inspection solution for one point machine will most likely not work on a different point machine as they require bespoke inspection tasks to be carried out;
- generally point machine inspection requires a large variety of inspection tasks; some of them are difficult to automate (e.g. checking if a pin is still in a shaft; checking the length of the carbon brushes in electrical motors) and others even require proactive maintenance actions (e.g. periodic lubrication);
- newer point machines are being built for reliability with minimum maintenance requirements at the heart of design specifications.

Therefore the author believes that the single solution feasible towards a "self-inspecting" turnout is the development and use of point machines with no or minimal inspection requirements.

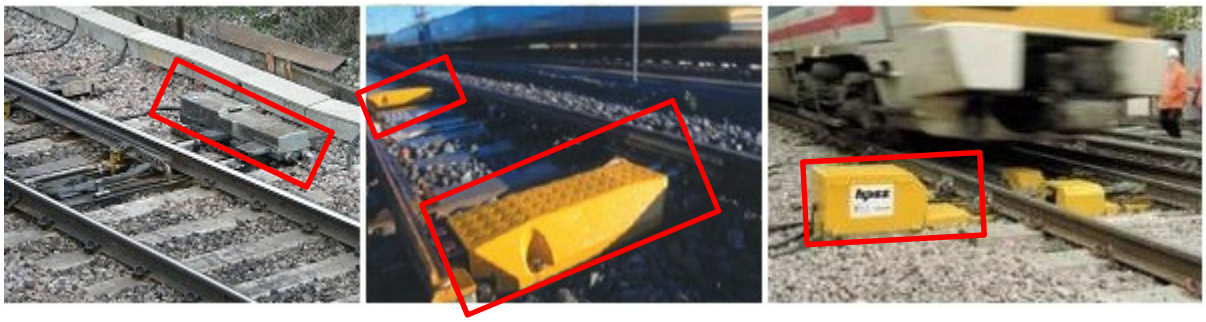

Figure 2-16 HW2000 point machine (left); Bombardier EBI point machine (centre); HPSS point machine (right)
left: Courtesy and Creative Commons Copyright McKenna; centre: Courtesy and Copyright Bombardier; right: Courtesy and Copyright Claverham

The most commonly used point machine in UK is the HW 2000 and it requires various types of periodic inspections. The most often periodic inspection is carried out on a fortnightly to monthly basis and it is known as a face point lock test.

The Bombardier EBI is a built in sleeper point machine that is widely used throughout the Netherlands. This machine does not require a periodic face point lock test and, as stated in its user manual [64] and also confirmed by senior Strukton personnel (September, 2012), the most frequent inspection is on a yearly basis. However, it must be mentioned that due to the location of the point machine, it is generally not possible to carry out any inspection or maintenance during the normal running of trains (unlike line-side point machines).

The High Performance Switch System (HPSS) [65] was designed for reliability. As its brochure states "Designed for 25 year service life, with zero scheduled maintenance", it was designed with the aim of eliminating both point machine maintenance and timetable disruptions. However, during a discussion with Philip Neep, NR (June, 2012), it was asserted that there are various failure modes affecting the HPSS machine. One such example is the failure of LVDT sensors.

Conclusion

In conclusion, with the development of newer point machines it is possible to move towards an inspection-free switch and this is more likely to provide an effective and efficient maintenance regime. Condition monitoring of point machines can help to increase the

efficiency of S&C maintenance but it cannot replace any required S&C inspection as stated in the GB railway inspection standards.

Final conclusions

The improvement of lubricants used for both the switch rail and slide chair should in future allow the use of optical systems for automatic inspection. As other S&C parts such as slide chair rollers, tubular stretcher bars, new crossing design, point machine, instrumented bolts, etc are further improved and introduced to the British railway industry the automatic/remote inspection of S&C becomes feasible, other than the inspection of cracks within the rails and crossing which is unlikely to be solved in the next few decades.

Various condition monitoring systems such as the VAE Roadmaster, POSS and other condition monitoring research carried out on point machines was found to not cover any inspection requirement as specified in the NR S&C inspection standards. Therefore, although these systems can be beneficial, they cannot be used to replace current inspection tasks.

It is possible that the reason for this is the fact that the S&C inspection standards were written and improved before the development of modern condition monitoring equipment and thus they were not written with the use of condition monitoring in mind. Furthermore, even if the S&C inspection standards are rewritten (this would be very costly partly due to the development of safety cases that need to support the replacement of old inspection tasks with condition monitoring techniques that can provide at least the same level of safety) it is clear that the current S&C inspection tasks have the ability of providing more detailed information regarding the health of S&C through the use of visual and measured inspection when compared with various CM techniques.

3 PROBLEM DEFINITION

3.1 Problem introduction

Network Rail, the infrastructure manager for most of Great Britain's railways, uses a set of two inspection standards to assess the profile condition of S&C. The main standards which set out procedures for assessing the profile of the S&C are: NR/L2/TRK/0053 – Inspection and repair to reduce the risk of derailment at switches [15] and NR/L2/TRK/1054 – Inspection, maintenance and repair procedures for cast, welded and fabricated crossings in the track [16].

NR/L2/TRK/0053 inspection standard

The purpose of the NR/L2/TRK/0053 standard is to provide an inspection method for identifying S&Cs that present a derailment hazard. According to Silmon and Roberts, a hazard is anything that can cause harm [66]. The NR/L2/TRK/0053 inspection standard defines five derailment hazards. S&Cs are inspected against each derailment hazard which is applicable to the inspected S&C (not all derailment hazards are applicable to all S&Cs). The inspection against each derailment hazard is carried out using one or several manual gauges. The standard specifies a total of six manual gauges which are used to inspect S&Cs: Gauge 1, Gauge 2, TGP8, Switch rail radius gauge, NR4 sidewear gauge, and stepped gauge. If no derailment hazards are identified, the S&C is deemed safe for rail traffic. The stepped gauge is used to measure the switch rail hogging. The amount of hogging is used to compensate for the measurement of TGP8, Gauge 1 and Gauge 2. The picture below shows one of the five manual gauges used to inspect the switch rails for derailment hazards, the TGP8 gauge.

In a railway accident report published by RAIB it was documented that, after the accident, most workers who had been interviewed had an adverse opinion regarding the use of the TGP8 gauge [12]. Workers found it difficult to use and some of them adopted their own method of using the gauge [12]. There are derailments which are known to have occurred as a result of incorrect usage of the TGP8 gauge [11,12]. Both the RAIB and Office of Rail Regulation (ORR) recommended that NR should improve the inspection method for measuring the contact angle (currently being carried out using the TGP8 gauge) [12,67].

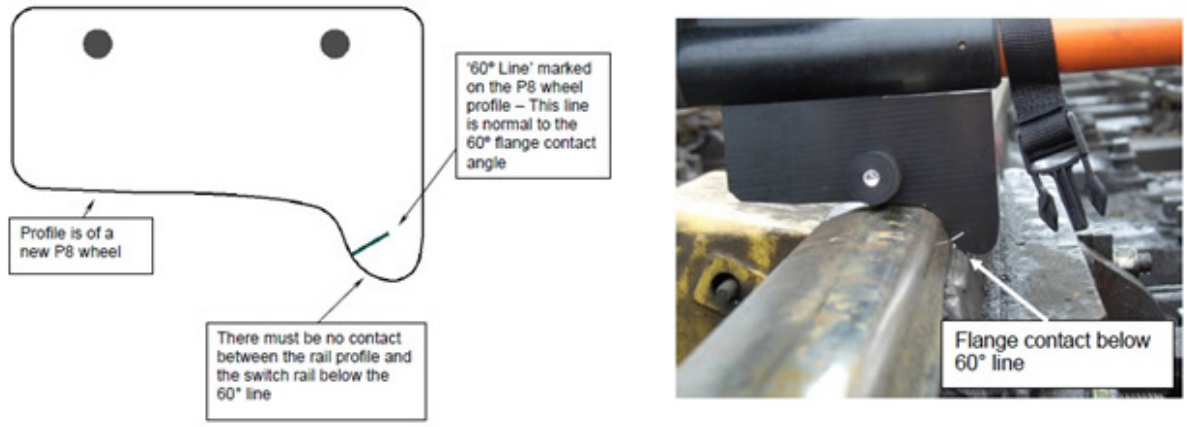

Figure 3-1 NR TGP8 manual gauge applied on a switch
Courtesy and Copyright Network Rail

In the last 10 years there have been a number of situations where S&Cs failed to comply with the NR/L2/TRK/0053 inspection standard, which has led to a derailment. These inspections are grouped into five chapters, each of them titled "derailment hazard 1" to "derailment hazard 5". The procedure of checking whether or not a derailment hazard exists can have one or several inspection tasks. Table 5 shows four derailment events and the derailment hazards (abbreviated DH1 to DH5) that were identified after the derailment had occurred. Each derailment hazard is discussed in detail in sections 5.1.3 to 5.1.7.

Table 5 S&C faults leading to a derailment

Location and date of derailment / Identified derailment hazard	London 11 September 2006 [10]	London 24 October 2006 [10]	Glasgow 3 September 2007 [11]	Edinburgh 27 July 2011 [12]
DH1	X	X		X
DH2	X	X	X	X
DH3				
DH4				
DH5		X		

The RAIB's investigation into the derailment in Edinburgh concluded that the train could have derailed on a section where the switch was compliant with the NR/L2/TRK/0053 standard [12]. This is because the switch passed the TGP8 profile, which simulates a new P8 profile, but failed when tested against a compliant worn P8 profile [12]. The same report

mentioned that “There is an apparent risk of a ramp being created where a switch rail that is failing gauge 2 in the first metre increases in height and is introduced between the stock rail and wheel flange from below (...)” [12]. Both these limitations can be overcome by introducing new inspection techniques.

During a meeting with senior NR personnel (January, 2012) it was reinforced that the S&C inspection procedure to protect against derailment hazards is susceptible to human errors and thus a new or improved inspection method should be developed. Moreover, it was stated that the lack of advice and information received by the S&C maintenance team decreases the effectiveness of the weld and grind repair on switch rails and that due to this switch rails can be left in a worse condition after repair. This is indeed what happened in 2007 [11] when workers introduced a “derailment hazard 2” while repairing “derailment hazard 1”. After the derailment in Edinburgh, 2011, RAIB concluded that the repair attempt on the S&C was unfeasible as the switch was beyond repair. A new or improved inspection method can help workers to better scope the work and thus improve the effectiveness and quality of the repair process.

NR/L2/TRK/1054 inspection standard

The purpose of the NR/L2/TRK/1054 standard is to identify and quantify the wear and batter on the profile of railway crossings. The standard specifies the use of a one-metre (or two-metre for high speed crossings) straight edge used in conjunction with a stepped gauge. The inspection is carried out by placing the straight edge in seven different locations on the crossing while using a stepped gauge to measure the gap between the two.

The measurement resolution is generally 1 mm. Figure 3-2 shows a representation of such a measurement in which two straight edges are used. The geometry of the profile is not considered to be a safety-critical issue as it is unlikely to derail a train on its own. However, the shape of the crossing has a direct influence over the dynamic forces that occur in the crossing due to the passage of trains. Crossings with poor profile are more susceptible to damage caused by running trains. This is supported by recent research that looks at optimizing the crossing profile [68]. Thus, the profile of railway crossings is important for the reduction of their life cycle cost (LCC).

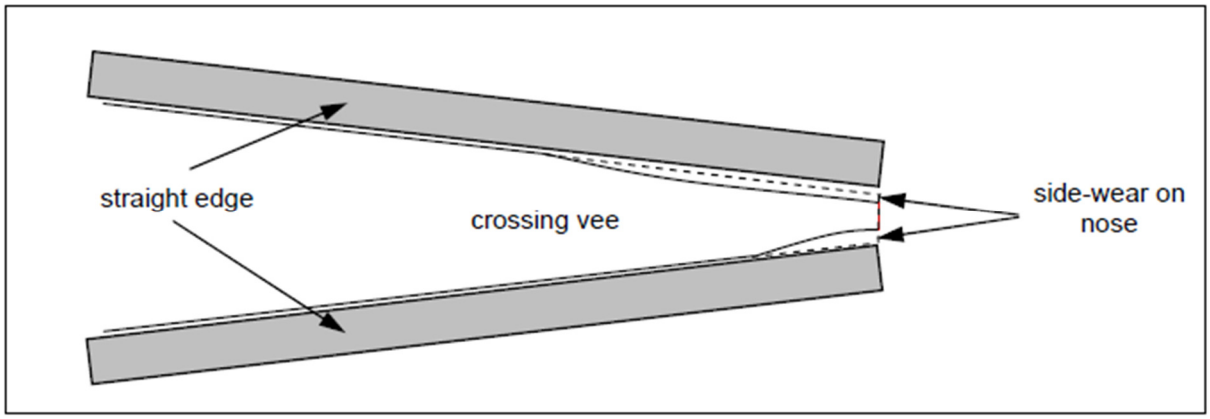

Figure 3-2 Representation of a crossing inspection task as defined in NR/L2/TRK/1054 Courtesy and Copyright Network Rail

During a meeting with senior NR personnel (January, 2012) it was asserted that NR was seeking to have better management over the profile of crossings as current crossing profile inspection is affected by human errors and this reduces the effectiveness of the whole maintenance process.

In a meeting with senior Deutsche Bahn (DB) personnel (June, 2012), it was stated that the reduced performance of some crossings within the DB railway network had been due to more than half of the newly installed crossings not complying with design profile specifications.

3.2 Requirements analysis

This section sets the requirements for a system which can address the above mentioned maintenance issues. The requirements are largely dictated by NR, which was actively involved in this step of the research.

The top-level requirement is defined as follows: A system shall be able to inspect the switch against the NR/L2/TRK/0053 inspection standard and the crossing profile against the NR/L2/TRK/1054 inspection standard. This requirement is further refined through several additional requirements:

1. Replication of inspection requirements: The system must be able to replicate the required inspection tasks just as if they would be carried out manually but without any human error. This will help the validation process for use on NR infrastructure.
2. No black box approach: The system must be transparent in the inspection method and the way it arrives at the final result. This will help the validation process for use on NR infrastructure.

3. Improved accuracy: The accuracy of the system must be better than the current accuracy of the manual inspection methods. For most inspection tasks the accuracy of the current inspection it is very difficult to establish. Because (1) the current inspection standard and gauge specifications (e.g. TGP8 gauge, Gauge 1, Gauge 2, Switch rail radius gauge and straight edge for crossing inspection) do not specify any inspection accuracy and (2) the loss of accuracy due to human errors is also undocumented, it is very difficult to accurately and objectively define the accuracy of current manual inspection. However, efforts have been made to identify the accuracy limitations of current manual inspections and research an improved alternative.
4. Acceptable price: The solution should not be overly expensive (<£100,000).
5. Availability: The solution should be available and ready to use with minimal/no overhead preparations (e.g. no scheduling of measurement trains).
6. Easy to use and immediate results: The solution should not require more than one or two personnel and should not need significant time to carry out an inspection (< 10 min).

By defining a set of clear system requirements at an early stage, the direction of the research is steered towards a well defined target instead of an ambiguous and changing target making the research process more effective and efficient. This is also a key aspect of systems engineering [69].

3.3 Inspection of S&Cs

The idea of surveying plain rail in order to measure and monitor its parameters is not new and there are many commercially available laser-based systems some of which are installed on dedicated measurement trains (e.g. NMT), others on passenger trains, some on rail robots (e.g. FELIX) and trolleys and others on hand held devices (e.g. Calipri). While much research and development has been focused on plain line measurements, little has been done on S&Cs.

The SIM measurement wagon manufactured by Eurailscout [43] was developed mainly with the aim of measuring the geometry of S&Cs and for off-line visual inspections. The system currently does not carry out a comprehensive set of measurements as defined in section 2.5.2. The RILA system has similar capabilities as the Eurailscout system, excluding visual inspection.

The ASIV system, which is a vehicle based system, was developed by Zarembski et al. [47,61,70] and focuses on the measurement of wear on the switch rail and stock rail as well as potential derailment hazards. The system has been developed to automatically inspect S&Cs against certain derailment hazards, but does not carry out a complete S&C inspection against derailment hazards as specified in the NR/L2/TRK/0053 standard. Little is available in the public domain regarding the methods used by the ASIV system or the system's accuracy and precision.

The FELIX S&C inspection robot [49] was designed to carry out many important S&C inspections within the area of geometry measurements and rail shape and position measurements. However, the system does not currently assess S&Cs in accordance with the NR/L2/TRK/0053 inspection standard. As the system weighs approximately 150 kg, it can only be considered to be semi-portable. The system is designed so that it can be carried in pieces (the heaviest part is 47 kg), and then assembled on site.

The CALIPRI measurement system from NextSense is a portable device that can acquire the profile of rails and crossings within S&Cs and carry out various measurements. The fact that the system is a hand-held device constrains the type of inspections that can be achieved. Inspections requiring the opposite rail as reference (such as the TGP8 gauge) cannot be carried out with the same accuracy as trolley-based or vehicle-based solutions. Measurements over a large longitudinal area (such as the one-metre edge measurement on crossings) can not be carried out.

3.4 Optical displacement measurement systems

The automatic assessment of S&C in accordance with the NR/L2/TRK/0053 and NR/L2/TRK/1054 standards requires the measurement of the physical shape and size of rails and crossings in at least two dimensions. There are a vast number of technological methods that can be used to survey objects; these can be classified into contact and non-contact methods.

Contact methods are generally slow to use, especially when high point density is required. Non-contact methods can be used to rapidly survey an object and some of the most important optical methods are: optical triangulation, time of flight and modulated light, structured light and conoscopic holography.

Survey techniques generally differ in accuracy and measurement range. The optical triangulation method is generally used to acquire data at accuracies between 5 µm and 1000 µm and measurement ranges between 5 mm and 1000 mm. This makes it a preferred method for many railway inspection and condition monitoring applications as most other methods have either poorer accuracy or a smaller measurement range.

Ji et al. present the principle of optical triangulation in displacement measurement devices [44]. The acquired data from triangulation laser scanners consists of point clouds. A point cloud is a collection of geometric points which represent samples taken from the surface of the surveyed object. These points can be extrapolated to reconstruct an approximate shape of the surveyed object.

3.5 Data registration and geometry measurements

Triangulation laser scanners can emit a single spot of light (point lasers), in which case a single distance measurement is achieved between the laser and a point on the target surface (one dimensional measurement). When a stripe of light is emitted (line lasers), multiple coplanar measurements can be achieved (two dimensional measurements). Many approaches have been developed to achieve three dimensional measurements using a single triangulation laser (e.g. using mirrors to direct the radiance in different directions or by generating multiple stripes) [71], however, they cannot be used to survey large areas (> 1 m) as this would exceed the maximum measurement range and furthermore certain areas would not be measurable due to shadowing of the laser light.

As the measurements obtained from line lasers are referenced to an internal coordinate system (i.e. relative to the laser), any changes in the position or orientation of the laser (i.e. pose in computer vision and robotics) become measurement errors unless they are correctly managed. The process of identifying and applying the required linear translation to each dataset in order to compensate for the pose of the laser scanner is known as data registration [71].

Common methods for data registration of 2D point clouds retrieved from triangulation lasers include: constraining the pose of the laser to a known value, measuring the pose using various sensors, and measuring overlapping areas of the surveyed object.

When a line laser is used on a rail trolley, then the task of pose estimation of the laser is very similar to the task of measuring track geometry. Track geometry measurement trolleys

commonly use various sensors such as: global navigation satellite systems (GNSS), inertial navigation systems (INS), inclination sensors, odometers, chord lasers, high-speed cameras (CCD, CMOS), prisms (subsidiary to optical total stations) and optical total stations in order to measure the geometry of railway tracks [72].

In this research, data registration has been accomplished using the following methods: constrained translation using wheel clamp, measurement of distance using an odometer, scanning overlapping datasets and inertial measurement from a gyroscope; this is further discussed in section 4.3.

3.6 Point cloud filtering

Due to laser measurement errors, the acquired point cloud data is rarely perfect and it can be expressed as the sum of ideal data and measurement errors. As a result the accuracy of any calculations executed on the measured point cloud data is affected. Measurement errors generally result in noisy point cloud data, and thus smoothing algorithms are used to improve their quality. Although the intent is to completely remove the measurement errors whilst not affecting the ideal data, this is rarely achievable and most often the errors will be either undercompensated or overcompensated resulting in a final data which is different from the ideal data.

Certain smoothing algorithms can be run directly in various software packages or by using the open-source PCL library [73] available for both commercial and research use. The PCL library contains various algorithms such as the Fast Bilateral Filter or Mesh Smoothing Laplacian VTK which can be used to smooth point cloud data.

Smoothing algorithms are often unable to eliminate all measurement errors and they can undesirably smooth out features of the surveyed object. As a result, much research has been undertaken to overcome undesirable smoothing by developing feature preserving smoothing algorithms. The goal of these algorithms is to smooth out the point cloud data while preserving the inherent features of the surveyed object (e.g. sharp corners). However, feature preserving algorithms generally work when a priori assumptions can be drawn upon the surveyed object. As an example, Volodine [74] proposed several variants of a point cloud feature preserving smoothing algorithm, namely $L^{(n)}, L^{(k)}$ and $L^{(f)}$. The $L^{(f)}$variant works well for objects with straight edges and sharp corners and $L^{(n)}$ works well for objects which do not have well defined edges and corners. Depending on the surveyed object, the

appropriate method should be used. As two different (although very similar) objects, when surveyed can lead to the same point cloud data, the problem of point cloud smoothing without any a priori knowledge becomes apparent.

In order to achieve the best results, information regarding the surveyed object and information regarding the measurement errors can be used optimise the smoothing algorithm. As a simple example, if the surveyed object is known to be a straight and smooth surface and the measurement errors are known to follow a normal distribution with a null average error, then the use of a linear regression technique such as linear least squares fitting is expected to provide better results than general purpose smoothing algorithms. If new or different information regarding the surveyed object or measurement errors are available (e.g. surveyed object is non-linear, the point cloud has many outliers, the mean error is -1, etc) then the filtering technique can be refined or even completely replaced by a different one in order to achieve better results. Thus, often in point could filtering, there is no one-size-fits-all technique that can be used to achieve the best results.

As convex hull is an important geometrical calculation that is often used in Chapter 5, it is briefly introduced here. There are endless definitions for convex hull and the following was chosen as it is more easily understood: "The convex hull of a finite set of points *S* in the plane is the enclosing convex polygon *P* with smallest area" [75].

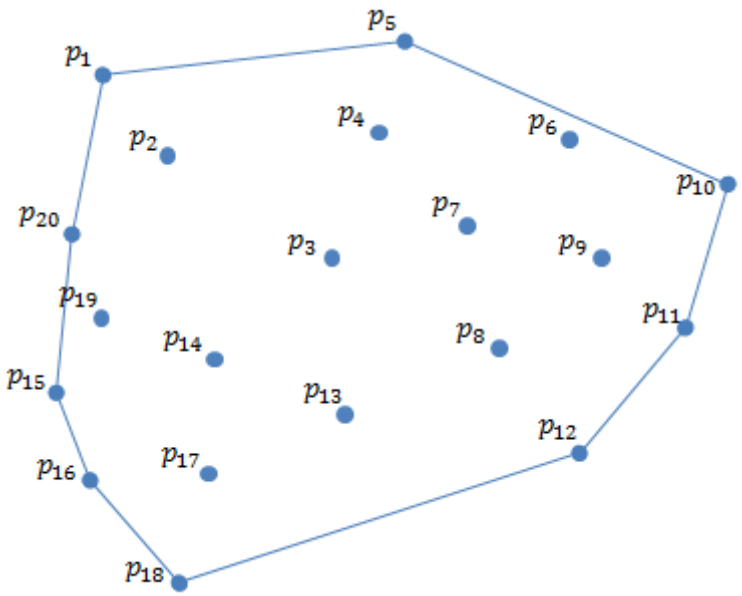

Figure 3-3 The convex hull of a set of random points

Applying the definition on a set of 20 random points in a 2D space, as shown in Figure 3-3, the convex hull is the polygon defined by the following set of points: $\{p_1, p_5, p_{10}, p_{11}, p_{12}, p_{18}, p_{16}, p_{15}, p_{20}\}$.

4 DEVELOPMENT OF A LASER BASED TROLLEY FOR THE MEASUREMENT OF RAIL PROFILES IN S&Cs

In order to achieve the objectives of the second stage of the research as set out in section 1.4, a laser based trolley was developed to measure the profile of the rails through S&Cs. The rail profile of several S&Cs was measured and the data was then used in Chapter 5 and Chapter 6.

Section 4.1 explains the notations used throughout this and the following chapters. Section 4.2 identifies the required accuracy of the measured rail profiles. Section 4.3 describes the adopted design and how the accuracy requirements are being met. Finally, section 4.4 briefly describes the process of acquiring the rail profiles.

4.1 Notations

For clarity, this section describes a number of notations that are often used in chapters 4, 5, and 6. Figure 4-1 shows most notations that refers to rails or parts of a rail.

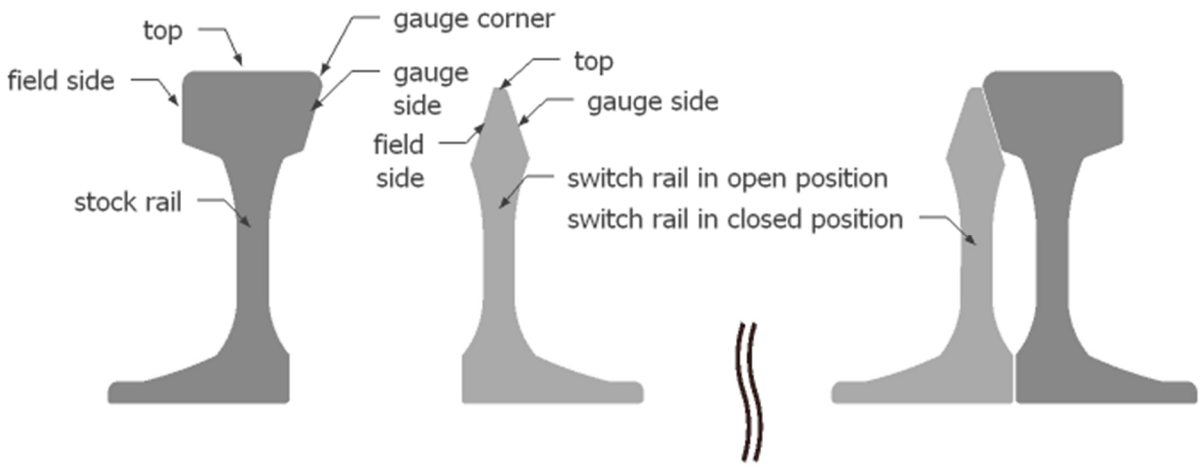

Figure 4-1 Rail notations

Opposite rail always refers to the rail opposite the one being inspected. *Gauge points* and *field points* are points on the gauge side and field side of the rails and crossing at a height of 14 mm below the *top* of the rail or crossing (or as close as possible). *Top* is the highest point in a 2D rail or crossing profile. *Switch toe* refers to the very beginning of the switch rail (visible in Figure 4-2).

The inspection of switches against derailment hazards generally requires the inspection of two dimensional, transversal sections of the rails. When considering the transversal sections of the rail, a preference was given to use a XOY notation for the coordinate system (most common notation used to describe a plane in a two dimensional space) instead of a XOZ coordinate system. For this reason the Z axis became along the length of the rail instead of being the vertical axis. The adopted coordinate system is shown in Figure 4-2. The X and Y axes are also referred to as the horizontal axis, and vertical axis respectively.

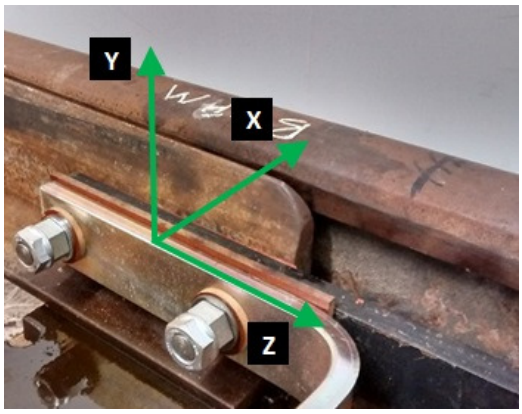

Figure 4-2 Naming of Cartesian axis used throughout this work

Translations are expressed as a column vector: $\begin{pmatrix} a_X \\ a_Y \\ a_Z \end{pmatrix}$, where a_X, a_Y and a_Z expresses the translation, in millimetres, along each of the three axes shown in Figure 4-2. Where two dimensional translations are expressed, a_Z is omitted from the vector.

Unless otherwise specified, all angles are referenced to the horizontal axis (X axis).

4.2 Accuracy requirements for point cloud data

4.2.1 Introduction

This section aims to identify the necessary accuracy of the point cloud data.

The NR/L2/TRK/0053 inspection standard requires the inspection of switch rails and stock rails in various locations along the length of the switch. Each inspection is carried out on the transversal profile of one or both of the two rails. Figure 4-1 shows an example of transversal profile within a switch. In order to carry out a complete inspection in a given location along the switch, the following areas must be measured: field side, top area and gauge corner of the stock rail, and top area and gauge side of the switch rail.

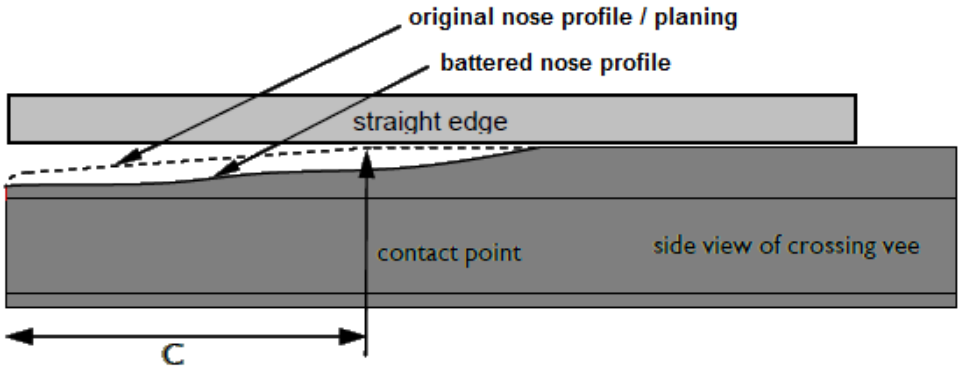

Figure 4-3 Crossing profile inspection along the centre of the crossing as defined in NR/L2/TRK/1054
Courtesy and Copyright Network Rail

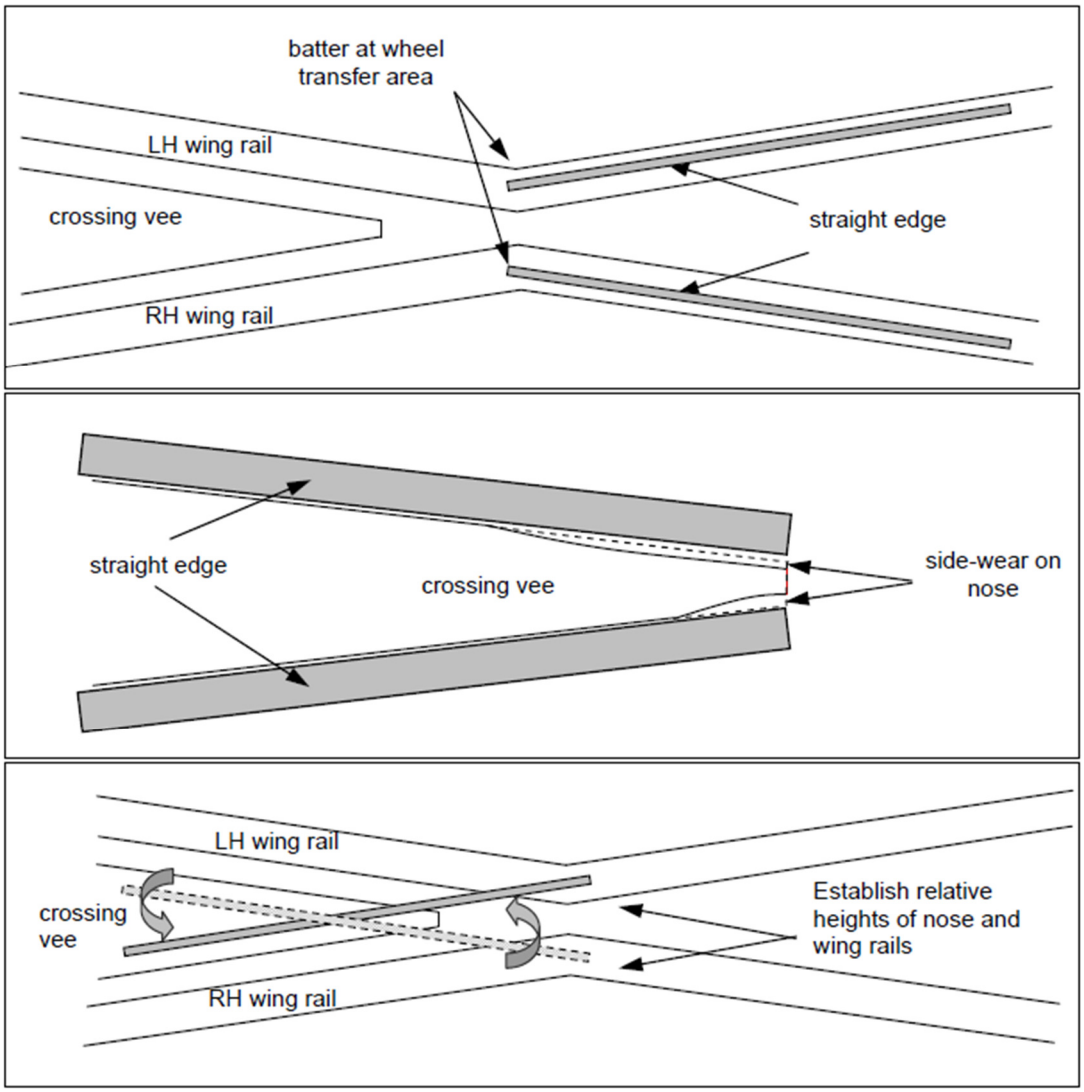

Figure 4-4 The six longitudinal paths of crossing inspection as defined in NR/L2/TRK1054
Courtesy and Copyright Network Rail

The NR/L2/TRK/1054 inspection standard requires the inspection of rails and crossings along seven paths, one central to the crossing and six longitudinal to the rails, as shown in Figure 4-3, and Figure 4-4 respectively. As a conclusion, both transversal profiles (for inspection of switches) and longitudinal profiles (for inspection of crossings) must be acquired. In this work, transversal profiles (XOY) were acquired by using a two 2D laser scanners positioned as shown in Figure 4-5. Longitudinal profiles were achieved by scanning consecutive 2D transversal profiles, combining them to create a 3D model of the inspected S&C, and then extracting the required 2D longitudinal profile from the 3D model. The measurement of consecutive 2D transversal profile (to obtain a 3D model) was achieved by designing an S&C inspection trolley which moved the lasers along the length of the S&C.

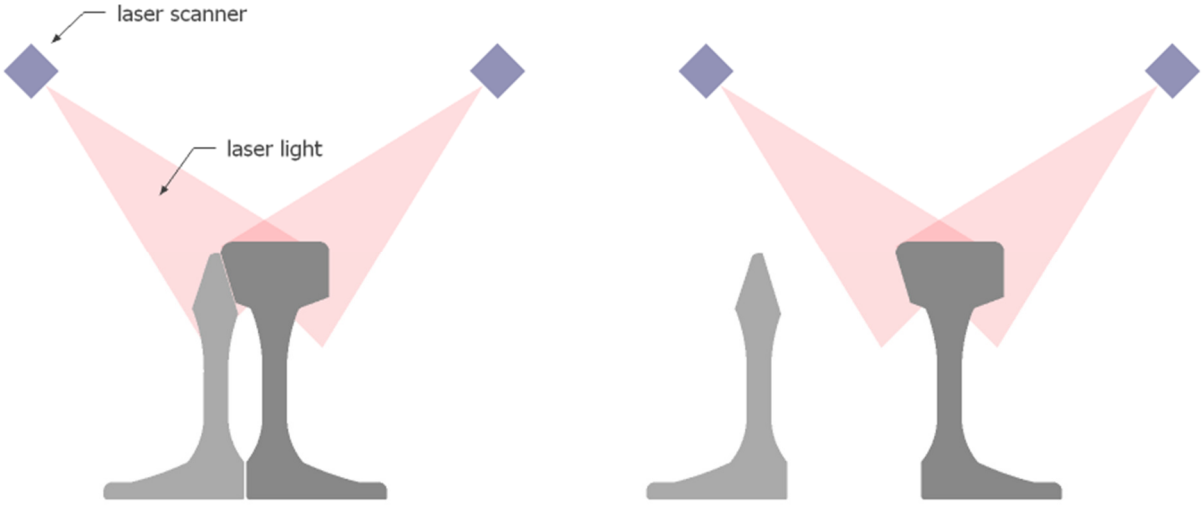

Figure 4-5 Laser scanners setup for the inspection of a pair of switch rail and stock rail

As the accuracy of 3D model is highly dependent on the accuracy of the individual 2D profiles, the accuracy requirements of the 2D profiles was calculated first. Then, the accuracy requirements of the 3D model was calculated which is dependent on the accuracy of the 2D profiles and other accuracies.

4.2.2 Accuracy requirements for inspection of 2D profiles within switches and crossings

The NR/L2/TRK/0053 inspection standard specifies the use of six manual gauges: Gauge 1, Gauge 2, TGP8, NR4, Switch rail radius gauge and Stepped gauge. Their use is briefly explained below, where necessary. Issues relating to correct usage of the gauges and their possible limitations are discussed in sections 5.1.3 to 5.1.7. The accuracy requirements were analysed for each inspection gauge.

Gauge 1 and Gauge 2 inspection

The inspections using Gauge 1 and Gauge 2 assess whether or not the relative height difference between the top of the stock rail and the top of the switch rail is less than 15 mm or more than 19 mm respectively. As the measurement depends on the visual acuity of the inspector it has been considered that a measurement error of up to 0.5 mm is acceptable.

TGP8 gauge inspection

The TGP8 gauge is used to identify whether or not the lowest contact point between the train wheel and the switch rail is above 60 degrees (measured to the horizontal). Figure 4-6 shows an example of a TGP8 inspection. For the inspection to pass there must not be any contact between the TGP8 gauge and the rail below the white line.

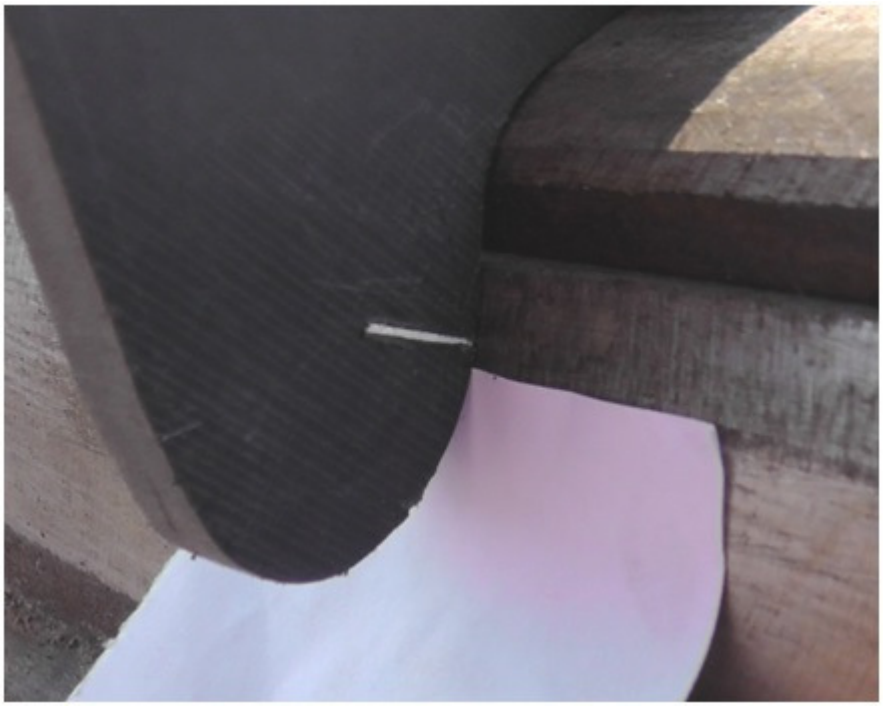

Figure 4-6 Example of TGP8 measurement using a white paper

Because it can be very difficult to determine if there is any contact below the white line, some personal use a white piece of paper which they push between the rail and the TGP8 gauge. This is also the practice that has been used for all TGP8 inspections throughout this work. Figure 4-7 shows two computerized TGP8 measurements in the form of images.

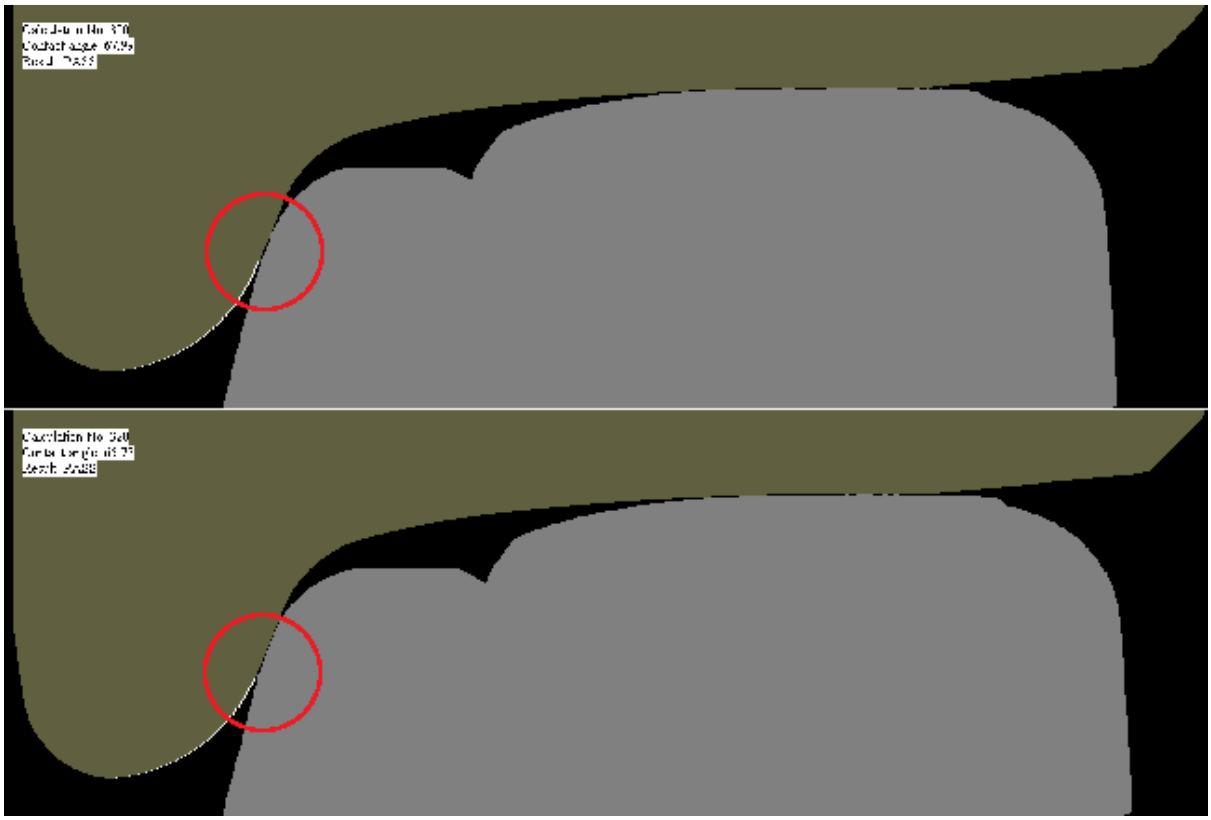

Figure 4-7 Two TGP8 measurements; top: 67.99 degrees, bottom: 65.72 degrees (to scale)

The measurements were carried out with the following considerations: a) the point cloud data was converted to an image with a resolution of 0.1 mm per pixel, and b) a contact condition was considered if the horizontal distance between the two parts was no more than a pixel (equivalent to 0.1 mm, to account for the thickness of the white paper).

Although the images are very similar, the lowest contact points are made at slightly different angles: 67.99 degrees and 65.75 degrees.

The errors involved in measuring the TGP8 contact angle are: laser measurement error, quantization error of the rail profile, quantization error of the TGP8 gauge and errors in the transformation matrix that converts the axis of origin of the laser into the axis of origin of the track. The latter two types of errors are considered constant throughout the process of acquiring the two measurements. Thus, the difference between the two results is attributed to the former two types of errors. The maximum quantization error is +/-50 µm on each of the two axes. The maximum laser measurement errors have been estimated at +/-150 µm by consulting the sensor acceptance report and taking into account the average distance at which

the measurements were taken (errors increase as distance to target increases). Thus the maximum measurement errors have been estimated at +/-200 µm.

In conclusion, small measurement and quantization errors of up to +/-200 µm lead to an error of 2.25 degrees when measuring the lowest contact angle between the TGP8 gauge and rail.

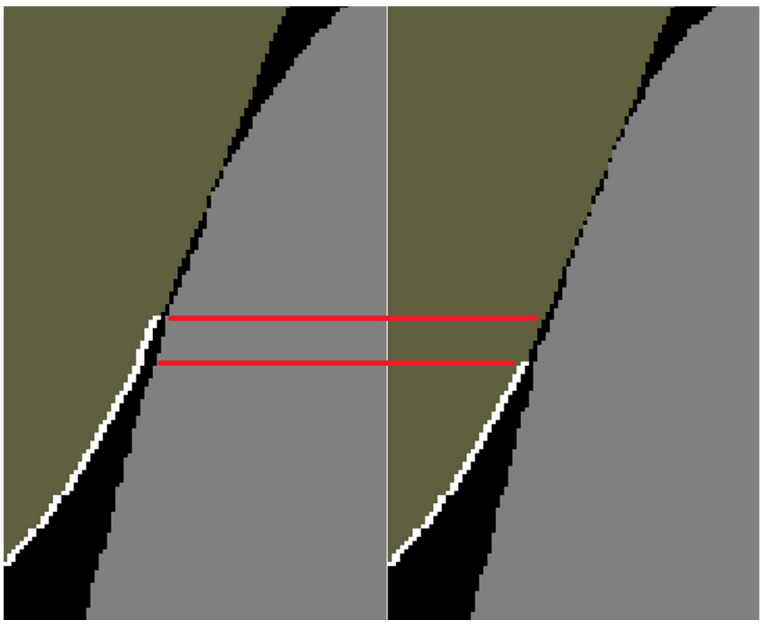

Figure 4-8 Close-up of the two TGP8 measurements; left: 67.99 degrees, right: 65.75 degrees (equal scale on both axes)

Figure 4-8 shows a close up of the two images. Random measurement errors can decrease the conformity between the two shapes which in turn leads to smaller contact areas. Smaller contact areas generally lead to the measurement of higher TGP8 contact angles. It is concluded that the result of this measurement is highly dependable on the conformity between the TGP8 gauge and stock and switch rail pair. This is particularly important as the measurement system could generate a false negative (e.g. a pass measurement of 61 degrees when the result should be a fail of 59 degrees).

As a result, it was concluded that the measurement error for the calculation of the TGP8 contact angle should ideally be no more than ±0.1 mm.

NR4 sidewear inspection

The NR4 gauge was designed to measure the sidewear on stock rails. As shown in Figure 4-9, the measurement process requires that the gauge is in contact with the rail in three locations: field side, for alignment, and the gauge corner and top, for measurement. If accidentally

reversed (i.e. using the gauge side for alignment), the gauge would lead to erroneous measurements. The gauge has two parts, one for measuring rail heads of 72 mm, which can be identified by the presence of two small holes, and one for rail heads of 70 mm, which can be identified by the absence of the two holes. Hence, the picture shows the measurement of a rail head with a width of 70 mm. In essence, the gauge measures the sidewear by comparing the height loss of the gauge corner relative to the top of the rail. The difference is measured using a stepped gauge with increments of 0.78 mm. The stepped gauge is marked with numbers from 0, where its thickness is 10 mm (for highest sidewear), to 18, where its thickness is 24.04 mm (for brand new rail).

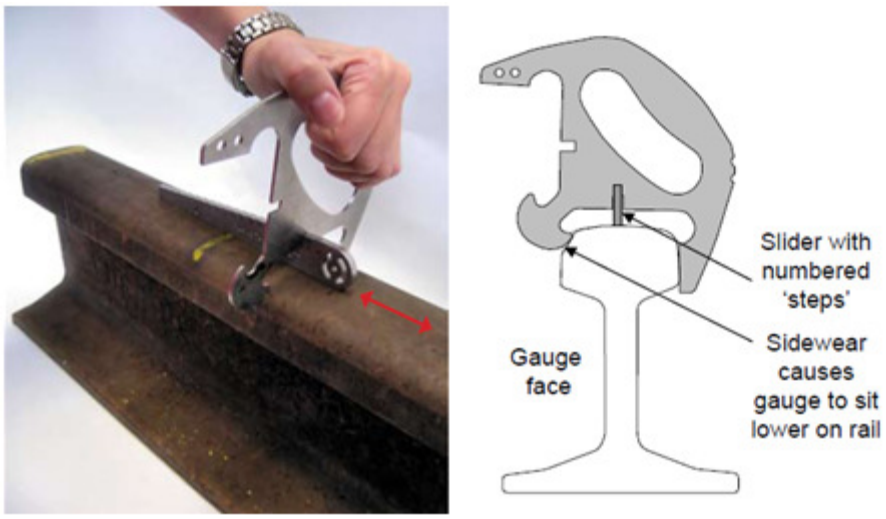

Figure 4-9 Application of NR4 sidewear measurement gauge
Courtesy and Crown Copyright RAIB

To understand how measurement errors can affect the NR4 sidewear measurements, a UIC60 rail profile was modelled and then artificially worn by a new P8 train wheel (most common wheel profile in GB). In Figure 4-10 shows the modelled rail and the important parts of a NR4 sidewear measurement gauge. The contact angle on the gauge corner is approximately 45 degrees.

The errors affecting the NR4 measurement were both calculated and then verified using the model. The calculation and the model produced very similar results (difference of less than 1%). The small difference is due to considering the contact angle fixed at 45 degrees in the calculations (to reduce calculation complexity) whereas in reality it often changes when measurement errors are introduced in the point cloud data.

The distance between the top of the rail and the middle of the gauge is 18.7 mm, resulting in a sidewear reading on the stepped gauge of number 12. Considering a horizontal measurement error of -0.1 mm on both the gauge corner and field side and a vertical measurement error of +0.1 mm on the top of the rail (the rail becomes slightly thinner and taller), the rail to gauge distance becomes 18.4 mm and the sidewear reading on the stepped gauge becomes number 11.

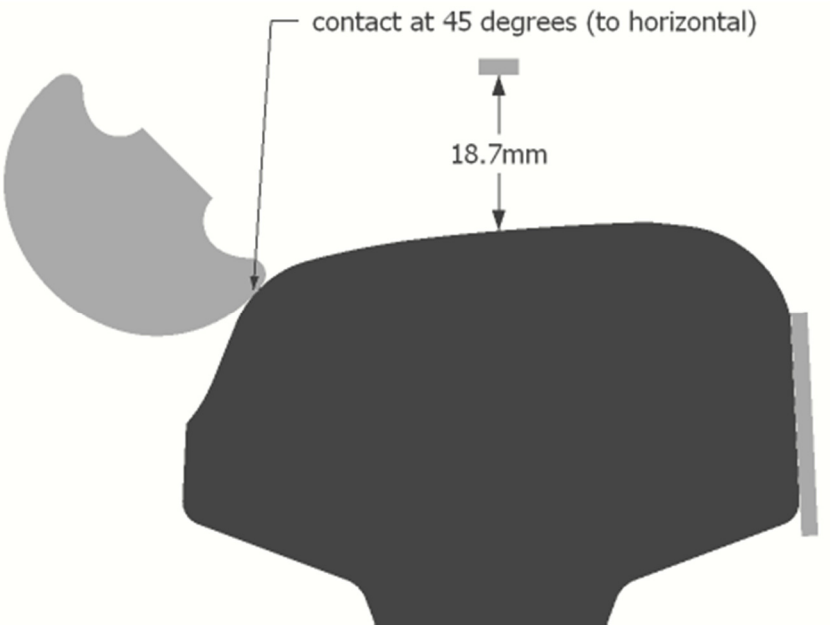

Figure 4-10 A model of the NR4 gauge placed over a heavily worn UIC60 rail

As the measurement errors change the reading by 0.3 mm (from 18.7 mm to 18.4 mm) and the sidewear is measured in increments of 0.78 mm, the measurement error is 0.38 units on the sidewear scale.

It must be noted that, for heavily worn stock rails where the gauge contacts the gauge corner (or gauge side) at a steep angle such as 60 degrees (to the horizontal), the measurement error on the gauge corner (or gauge side) can almost double its impact on the measurement: $0.2 \times \tan(60) = 0.34\ mm$ (instead of $0.2 \times \tan(45) = 0.2\ mm$). If the top measurement error is considered as well, the total error becomes $0.34 + 0.1 = 0.44\ mm$ (instead of $0.3\ mm$).

A similar case is considered where the field side of the rail is affected by measurement errors, such that the lowest point and the highest point within the field side of the rail that comes in contact with the NR4 gauge have measurement errors of 0.1 mm and -0.1 mm respectively on the horizontal axis. In this case, the measurement errors lead to a counter clockwise rotation

of the gauge by $\arctan(0.2/23) = 0.5\ degrees$. This results in a final measurement error of 0.4 mm, which equates to 0.51 units on the stepped gauge.

Considering another (worst) case where the rail measurements are affected by 0.1 mm errors, a maximum error of 0.67 mm can occur where 0.4 mm is due to the errors in the field side causing gauge rotation, 0.1 mm is due to top measurement error and 0.17 mm is due to gauge side measurement error (considering a worst case 60 degrees contact condition).

Although this error is significant, the probability of the point cloud data being affected by such errors is extremely small. This is mostly because every point in the field side of the rail which comes in contact with the gauge should have a specific error in order to rotate the gauge by 0.5 degrees. Thus, as the errors affecting the acquired point cloud data can generally be considered to follow a normal distribution and show a random component, it was concluded that measurement errors of up to ±0.1 mm are acceptable. It was also considered that measurement errors of up to ±0.2 mm could be acceptable if filtering is used to improve the point cloud data.

Switch rail radius gauge inspection

The inspection using the Switch rail radius gauge (widely known as pac man) is used to establish whether or not the switch rail gauge face has a sharp or pronounced edge. Due to the design of the gauge and the method of use, the evaluation of sharp corners is carried out over an area of the switch blade and not locally at each potential sharp edge. This means that the measurement error can be as high as 0.5 mm. However, the inspection standard states that any tactile or visual sign of a sharp edge fails the switch. Thus an alternative algorithm for the inspection of sharp switch rails is proposed in this work. As the algorithm individually assesses every potential sharp edge, the measurement error should not exceed ±0.3 mm.

Stepped gauge inspection

The stepped gauge is used to measure the amount of hogging present at the foot of the switch rail. This is achieved by inserting a stepped gauge between the foot of the switch rail and the slide chair. The measurement resolution is 1 mm. As the slide chair and switch blades can become very dirty and greasy, optical techniques cannot be used to automatically measure the switch rail hogging. No techniques have been found to automatically measure the switch rail hogging from a safe distance (>20 cm) and thus this measurement has not been automated. As one of the requirements for this research was to eliminate human error, the implications of

hogging not being measured automatically are significant. Many of the switch inspection tasks for checking against derailment hazards cannot be carried out accurately if this measurement is inaccurate. The automatic measurement of switch rail hogging over a percentage of switches could be beneficial as long as the measurements would be guaranteed to be accurate.

Visual switch inspection

The NR/L2/TRK/0053 requires the visual inspection of the switch rail for damage. The types of defects which this inspection standard aims to find are generally well sized (>1 mm) and thus the measurement accuracy can be as poor as ±0.5 mm.

Crossing profile inspection

The profile of railway crossings is currently inspected with a resolution of 1 mm. Thus, the measurement error should be no more than ±0.5 mm. However, as the height of the crossing is compared along its length, the error applies to a 3D crossing profile with a length of 1 metre (the length of the straight edge used to inspect the crossing) and not a 2D profile. Thus, in order to achieve this error limit, the maximum error within a 2D profile should not exceed ±0.2 mm.

Conclusion

Considering that the laser measurement errors follow a normal distribution (with a relatively null average error) and show a random component, it was concluded that the errors for measuring 2D point cloud data should be no greater than ±0.2 mm, although ±0.1 mm is recommended for the TGP8 measurement.

4.2.3 Accuracy requirements for 3D inspection of switches

A physically unconstrained object (i.e. an S&C inspection trolley) has six degrees of freedom: heave, sway, surge, pitch, yaw and roll. The first three describe translation motions along the three axis of the tri-dimensional Cartesian coordinate system (up/down, left/right and forward/backward) and the latter three describe the three possible rotations around the axes of the coordinate system. The six degrees of freedom are shown in Figure 4-11. Ideally, a 3D survey of the switch is carried out by moving the laser scanner along the red axis (surge) while constraining the other five degrees of movement. However, in practice, this is difficult

to achieve and thus, the impact of unaccounted movement (translational and rotational) over the measurement process is considered here.

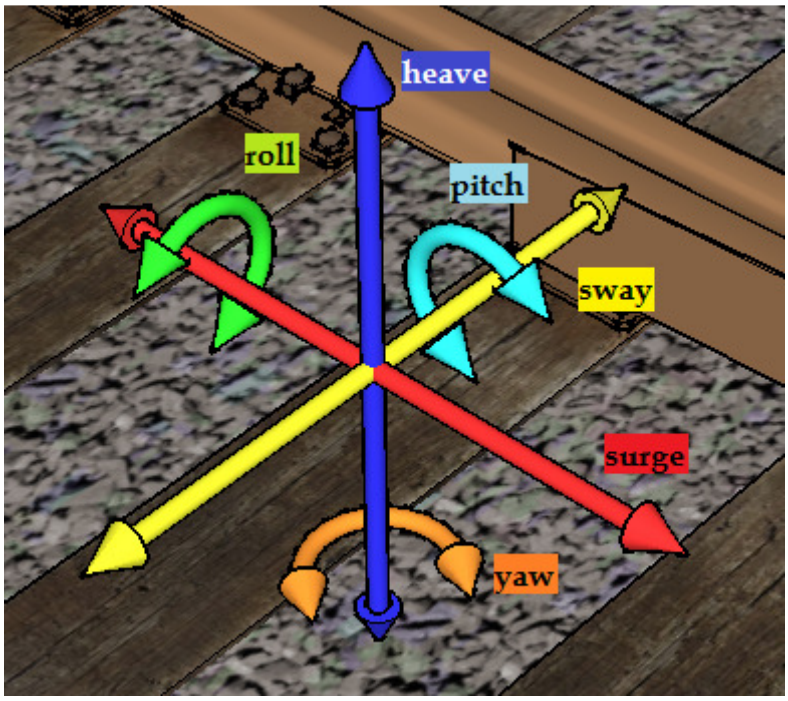

Figure 4-11 The six degrees of freedom in a 3D environment

Because the effect of rotational movement is dependent on the rotation origin (which at this stage is unknown), the rotation origin for all rotational movements is considered in the geometrical centre of the acquired data.

A distinction is made between two types of errors, absolute errors and constant relative errors. Considering a tridimensional Cartesian coordinate system in a tridimensional space, the difference between the measured coordinates and the true coordinates of a point, $p_m - p_t$, is considered an absolute error. An absolute error divided by the true value, $(p_m - p_t)/p_t$, is considered a relative error. A relative error that does not change (or change very slightly) during a complete set of measurements is considered a constant relative error. To exemplify, the measurement errors generated by the distance measurement wheel as a result having a different diameter is a constant relative error (i.e. if a true distance of 1000 mm, is measured at 1010 mm, then, considering the error to be constant relative, at 2000 mm, the expected measured distance is 2020 mm).

1) **Heave** (up/down)

All inspections involving the use of manual gauges are not influenced by heave errors. For the inspection of switch rail damage, random errors should not exceed ±0.5 mm, but errors of up to 0.2 mm per 1 mm of surge have been considered acceptable.

2) **Sway** (left/right)

The acceptable errors for sway have been considered to be the same as for heave.

3) **Surge** (forward/backward)

Due to the requirements of positioning the gauges on the switch, it has been considered that constant relative surge errors of up to ±10% are acceptable.

4) Pitch

Pitch errors of up to ±3 degrees lead to acceptable measurement errors (i.e. 4% of a unit for the NR4 gauge, 20 µm for Gauge 1 and 26 µm Gauge 2 and unquantified but considered acceptable TGP8 errors).

5) Yaw

Yaw errors of up to ±3 degrees lead to acceptable measurement errors (i.e. 10% of a unit for the NR4 gauge and unquantified but considered acceptable TGP8 errors). Gauge 1 and Gauge 2 are not affected by yaw.

6) Roll

Roll errors of up to ±3 degrees can lead to measurement errors in excess of 1 mm in the case of Gauge 1 and Gauge 2. Although unquantified, it was also concluded that roll errors of up to 3 degrees can significantly change the TGP8 contact angle and thus impact on the inspection accuracy. As a result, roll errors should not exceed ±0.5 degrees. The NR4 gauge is not influenced by roll errors as their effect is mitigated in the required fitting process of the gauge.

Note: The TGP8 gauge, Gauge 1 and Gauge 2 are mechanically designed to rest on the opposite stock rail in order to minimize roll errors to within acceptable values.

4.2.4 Accuracy requirements for 3D inspection of crossings

1) **Heave** (up/down)

Current manual measurement method has a resolution of 1 mm. However, the accuracy is also affected by systematic errors and human errors. This error can be as high a several millimetres and are discussed in more detail in sections 6.1.3 to 6.1.6. Thus it was concluded that random errors of up to 0.5 mm are acceptable. Errors which are proportional with surge do not decrease the accuracy of measurements as defined by the NR/L2/TRK/1054 inspection standard.

2) **Sway** (left/right)

Similar to heave, random sway errors should not exceed 0.5 mm and sway errors which are proportional with surge errors do not affect the measurements.

3) **Surge** (forward/backward)

Due to the requirements of using a straight edge with a certain length, constant relative surge errors should not exceed ±10%.

4) Pitch, yaw and roll

It was concluded that small (±5 degrees) pitch, yaw and roll errors have little influence over the measurements (the rotational origin was considered in the geometrical centre of the rail crossing profile). Thus, rotational errors of up to ±5 degrees were considered acceptable.

4.3 Mechanical design, sensory setup and management of accuracy

4.3.1 Management of measurement errors of 2D point cloud data

Measurement errors of 2D point cloud data are mainly attributed to the performance of the triangulation laser scanners. The chosen laser scanners are scanCONTROL 2700-100(500) produced by MICRO-EPSILON. The measurement errors of the laser are dependent on the measurement depth and are up to ±0.2 mm. Detailed information regarding the laser sensors' performance can be found in APPENDIX D: LASER SCANNER “SENSOR ACCEPTANCE REPORT”.

To minimize the errors of the transformation matrix that converts the axis origin of the laser into the axis origin of the trolley, the position and orientation of the lasers were calibrated.

The calibration process was as follows:

1. A rectangle calibration object with a precisely known width (70.15 mm) was placed in the field of view of the two lasers where the stock rail would normally be expected to be; the top surface of the calibration object was set up parallel with the transversal line that goes through the top of the two stock rails on which the trolley was sitting;
2. The corner of the calibration object was measured and the X axis of the laser was adjusted so that the corner measured exactly 90 degrees; this calibration step was needed as the manufacturer of the lasers confirmed independent laboratory experiments which found that the X axis of the laser was suffering from a systematic error;
3. The rotational component of the transformation matrices was calculated so that the faces of the calibration object became vertical and horizontal when referenced to the trolley's coordinate system;
4. The horizontal translation of the transformation matrices was calculated so that the width of the measured profile was the same as the width of the calibration object (70.15 mm) and the horizontal value of the gauge point of the measured profile (referenced to the trolley's coordinate system) reflected the correct track gauge;
5. The vertical translation of the transformation matrices was calculated so that the top area of the measured profile was at the same height between the two lasers and the vertical value of the top of the measured profile reflected the height of the calibration object in relation to the trolley wheel.

During the calibration process, the combined measurement errors have been constrained to ±0.1 mm.

4.3.2 Mechanical design and sensory setup

Based on inspection requirements (as described in NR/L2/TRK/0053 and NR/L2/TRK/1054), S&C dimensions (both design and actual dimensions), specifications of triangulation laser scanners (e.g. measurement ranges) and required inspection accuracies, a mechanical design, sensory setup and post processing algorithms were developed. These factors are highly interdependent and thus a holistic view and analysis was needed. Based on a holistic view of the factors shown in Figure 4-12, an S&C inspection trolley prototype was designed. The trolley weighs less than 20 kg. Figure 4-13 shows the 3D model designed in Google Sketch-up® and Figure 4-14 shows the physical trolley.

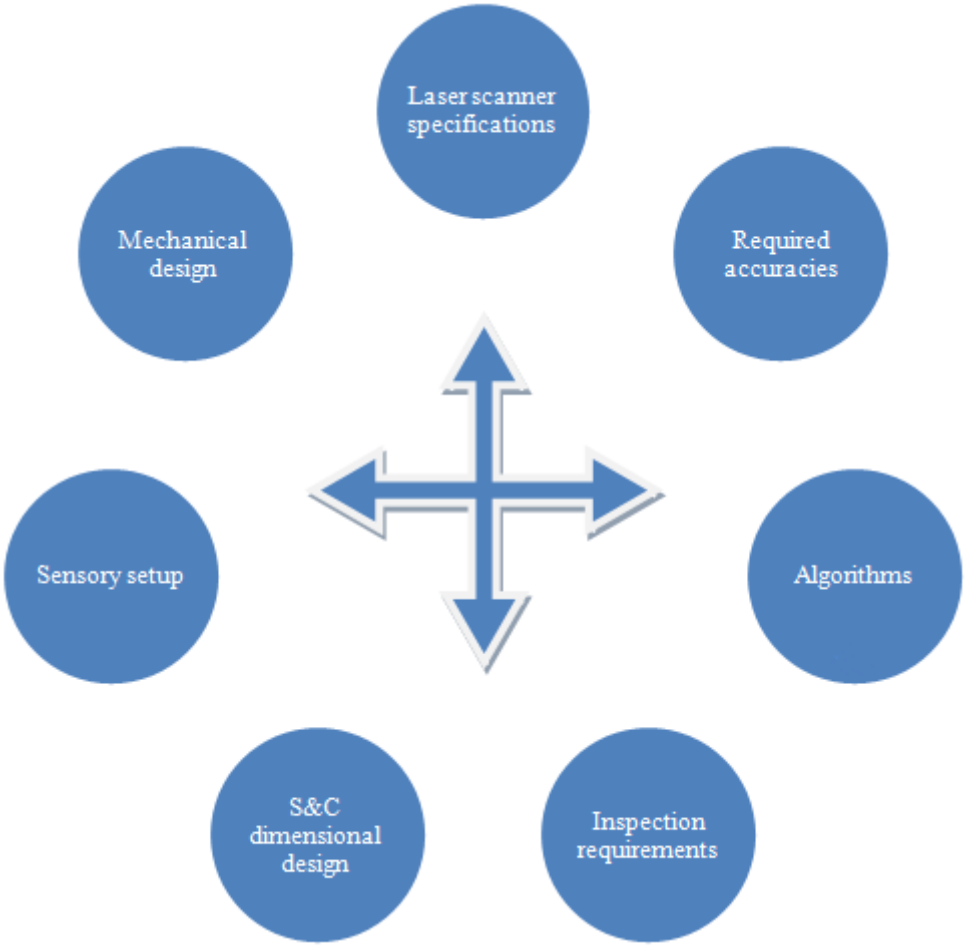

Figure 4-12 Interdependable factors affecting the design process

The following section shows how a change in the design process has immediate effects on other design decisions, thus supporting a holistic view.

The use of a wheel clamping mechanism which constrains the trolley motion to "follow" the gauge side of the opposite stock rail instead of the field side of the opposite stock rail is a mechanical design feature which, due to the S&C dimensions (curved switch rail), would make the trolley follow the measurement rail more closely (i.e. less unwanted sway) and thus allow the change of laser scanner specifications to a lower measurement range with higher measurement accuracy. This can help to meet the required accuracies. However, poor surfaces of the switch rail gauge side (S&C dimensions) can lead to unwanted trolley roll, which introduces surge errors in the measured data which must not exceed the required accuracies. Even if the surge errors are within acceptable limits, due to the inspection requirements, the switch rail has to be scanned twice, including once with the opposite switch

rail in the open position. Thus, the use of laser scanners with relatively high measurement ranges is still required.

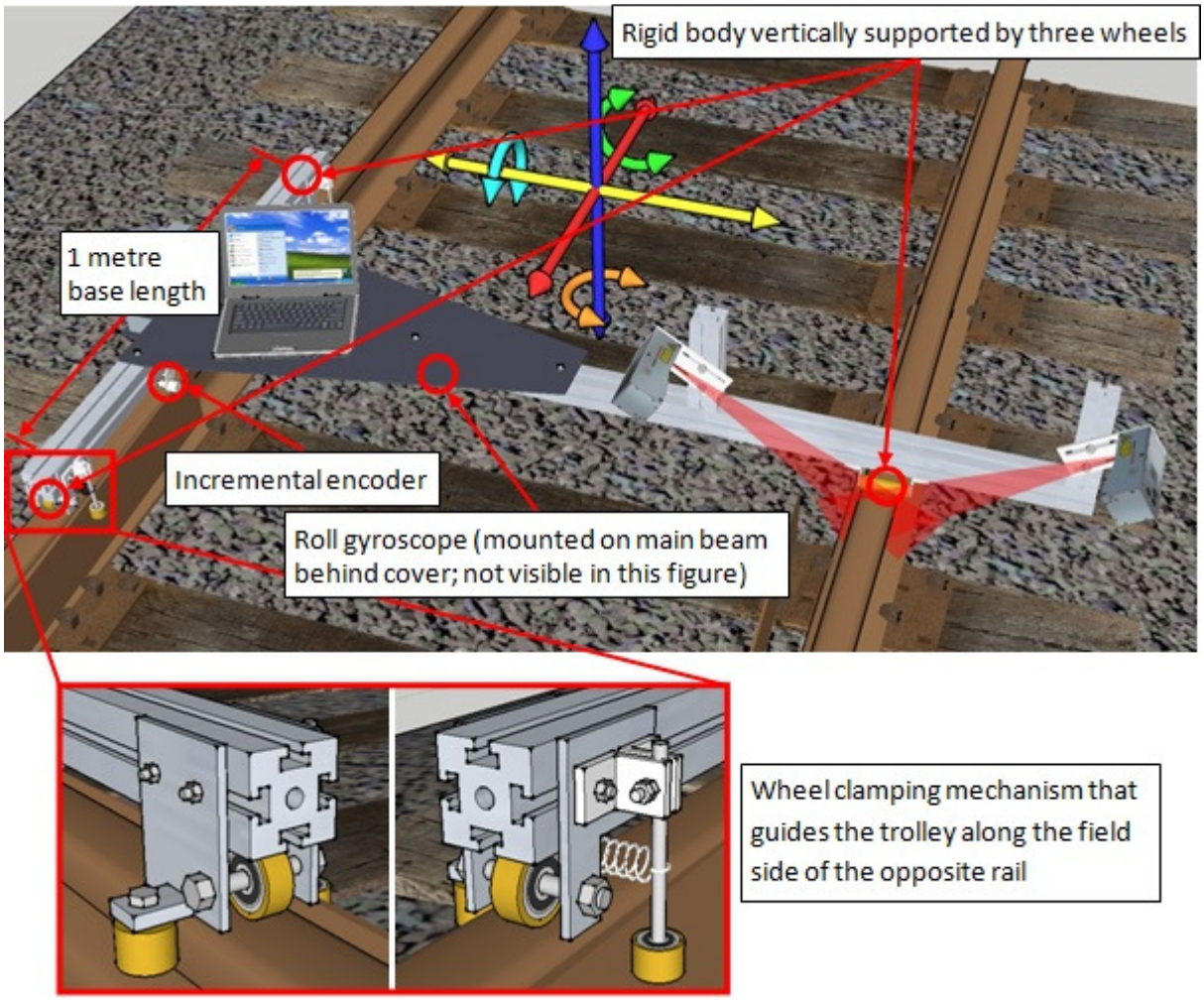

Figure 4-13 3D model of the S&C inspection trolley

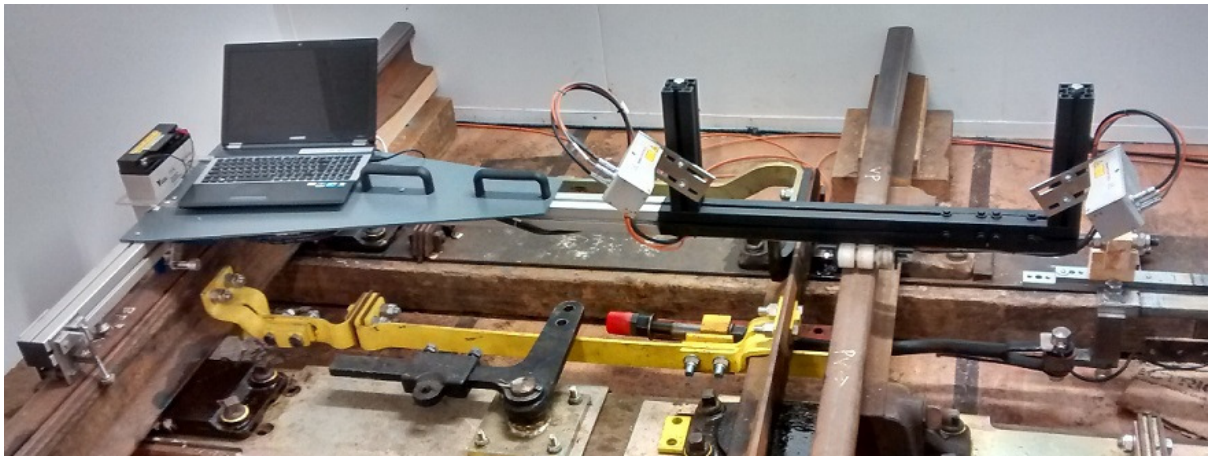

Figure 4-14 S&C inspection trolley

The design features of the S&C inspection trolley are as follows:

- rigid body vertically supported by three wheels;
- two wheel clamping mechanisms mounted on the opposite rail, guiding the trolley along the field side of the opposite rail;
- 1 metre distance between the two clamping mechanisms;
- a Kubler incremental encoder (05.2400.1122.0500), which is used to measure trolley surge, and;
- a Silicon Sensing gyroscope (CRS-09), which is used to measure the rate of roll.

All the above design features are important to achieving the desired accuracy.

4.3.3 Management of measurement errors of 3D point cloud data

The 3D measurement errors are attributed in part to the 2D measurement errors and in part to the mechanical design of the trolley together with the accuracy limitation of the algorithms used to inspect S&Cs.

The management of errors in 3D measurements was achieved as follows:

- the use of a three wheel rigid body assured that position and orientation was well defined (unlike four wheel rigid body);
- two clamping mechanisms 1 metre apart assured negligible pitch and yaw values during measurement; the clamping mechanisms guided the trolley along the field side of the opposite rail, which is considered free of wear;
- an algorithm was developed to accurately measure the roll of the trolley using the data provided by the CRS-09 gyroscope, and;
- based on matching overlapping point cloud data, an algorithm was used to register the two sets of 2D point cloud data (with the switch rail in the open and closed position) and calculate switch rail data by “subtracting” them.

The following sources of errors affect the 3D point cloud data but were estimated to be sufficiently below the maximum acceptable errors (as calculated in sections 4.2.3 and 4.2.4) and thus have been considered acceptable for the inspection of S&Cs in accordance with the inspection standards:

- errors affecting 2D point cloud data (as listed in section 4.3.1, laser scanner measurement errors and laser calibration errors);

- irregularities (from one millimetre to one metre wavelengths) on the field side of the opposite stock rail which can generate yaw, surge and sway errors in the rail profile point cloud data;
- irregularities (from one millimetre to one metre wavelengths) on top of the opposite stock rail which can generate pitch, surge and heave errors, as well as roll and heave errors in the rail profile point cloud data;
- the effects of wheel out of roundness and light dirt on the surface of wheels;
- the effects of considering the opposite stock rail vertically and horizontally straight for both switch and crossing inspection, and;
- the effects of laser scanner vibration due to movement of the trolley.

The algorithm used to calculate the roll of the trolley is discussed in section 6.1.1.

4.4 Data acquisition

A total of 11 datasets comprising half-set switches and half crossings (as detailed in Table 6) were inspected both manually and automatically at Whitemoor Rail Recycling Centre, UK. Additionally, two half-set switches were inspected at the Birmingham Centre for Railway Research and Education, UK. The switches were of curved chamfered CEN56 type (113A metric equivalent) which is the most common type of switch used within NR.

Table 6 List of inspected switches and crossings

S&C name / Inspected parts	13 PTS	16 PTS	61 PTS	far end 1	far end 2	BCRRE lab
Right half-set switch	x		x	x	x	x
Left half-set switch		x		x		x
Crossing – straight		x		x		
Crossing – diverging	x	x		x		

Accurate optical inspection is possible only when the inspected parts are clean. Thus, all S&Cs were cleaned prior to inspection. This is also standard practice when carrying out manual S&C measurements on NR infrastructure.

An automated solution for measuring switch rail hogging was not identified and thus any hogging measurements were carried out manually.

The distance between two consecutive 2D profile measurements was 4 mm. The location along the switch was calculated by considering the switch toe at 0 mm.

When a complete set of manual switch inspections are carried out in accordance with the NR/L2/TRK/0053 inspection standard, the switch has to be thrown in both positions. Although it may be possible for an automatic inspection system to carry out all inspections while the switch is kept in a single position (either open or closed), this has not been researched in this work and thus the inspection system requires the switch to be thrown in both positions.

A complete acquisition of a half switch set was accomplished through the following steps:

1. Switch is thrown in the closed position (if necessary);
2. Trolley is positioned anywhere in front of the switch toe;
3. Trolley is pushed at least 2 meters along the switch;
4. Trolley is pushed back in front of the switch toe;
5. Switch is thrown in the open position, and;
6. Trolley is pushed a second time at least 2 meters along the switch;

A total of 2*500 profiles were acquired along the length of the switch during two scans (500 profiles per scan).

A complete acquisition of a crossing was accomplished through the following steps:

1. Trolley is positioned at one of the crossing ends, on one of the two train paths;
2. Trolley is stationary for at least 10 seconds during which gyroscope data is acquired;
3. Trolley is pushed at least 4 meters over the crossing;
4. Trolley is pushed back to its initial position;
5. Trolley is stationary for another 10 seconds during which gyroscope data is acquired, and;
6. Steps 1-5 are carried out again with the trolley on the other train path.

A total of 2*1000 profiles were acquired along the length of the crossing during two scans (1000 profiles per scan).

5 INSPECTION OF RAILWAY SWITCH PROFILE

Throughout the period of maintaining their railway infrastructure, NR identified five derailment hazards which can cause a train to derail. These derailment hazards are described in the NR/L2/TRK/0053 inspection standard. The standard also specifies the use of six manual gauges, together with visual inspections in some cases to determine whether or not the inspected switch presents any of the five derailment hazards.

Each of the five derailment hazards are discussed in detail in separate sections from 5.1.3 to 5.1.7. The objectives of each of the mentioned sections are, as set out in section 1.4:

- to identify whether or not the use of current switch profile inspection methods, as defined by the NR/L2/TRK/0053 inspection standard, can lead to considerable measurement errors and the source of those errors;
- to identify if possible and to develop alternative automatic inspection methods can be used to replicate the current switch profile inspection tasks as defined by the NR/L2/TRK/0053 inspection standard whilst eliminating human errors;
- to identify whether or not improvements on the developed switch profile inspection methods could reduce the systematic errors of inspecting switches.

Section 5.1.8 discusses improvements which are modifications to the current inspection standard or completely new inspections and processes. Thus, section 5.1.8 lies outside the aims and objectives of this research work; however, as it is highly relevant it is included in this thesis.

5.1.1 Point cloud data preparation

Prior to the calculation of derailment hazards, the acquired point cloud data was prepared using simple point cloud processing techniques such as outlier removal, and elimination of unnecessary data.

As the switch point cloud data is formed out of two data acquisitions, one of both the stock rail and switch rail and one just with the stock rail, the sole shape of the switch rail was not available. Loosely speaking, the shape of the switch rail was identified by comparing the two

acquisitions (pair by pair, 500 times) and identifying the points that were present in the first scan, but not in the second.

The process is described below as two steps:

1. Data registration of the two data acquisitions through matching overlapped areas

Although, due to the constrained movement of the trolley, the point cloud data should already be registered along the X and Y axes, misalignments can occur. Lateral misalignment was caused mostly because the side rollers had been compressed with different forces during the two data acquisitions. Vertical misalignment was caused by severely hogged switch rails, which forced the trolley to climb on them instead of running on the stock rail. The data registration was achieved by aligning the data in two locations.

For the purpose of aligning the two datasets, two reference points were used, a vertical one calculated at a height of 20 mm below the top of the rail (on the field side) and a horizontal one at a horizontal distance of 30 mm from the vertical reference point. The calculation of the point was done by averaging 5 points.

```
for profileNumber=1 to 500 do
    for scanNumber=1 to 2 do
        Calculate the maximum height of profile profileNumber in scanNumber;
        Identify the field point, FP20, which is 20 mm below (or closest) the
            maximum height of the profile;
        Calculate the average X coordinate of the four closest points to FP20 point,
            including the FP20 point;
        Identify the top point, TP30, which is 30 mm to the right (or closest) of
            FP20 point;
        Calculate the average Y coordinate of the four closest points to TP30 point,
            including the TP30 point;
    end
    //calculate registration values for each 2D profile
    Calculate the X registration value by subtracting the averaged X coordinate of the
        first scan from the second scan;
    Calculate the Y registration value by subtracting the averaged Y coordinate of the
        first scan from the second scan;
    //apply registration
    Add the X registration value to the X coordinate of every point in the profile
        profileNumber of the first scan;
    Add the Y registration value to the Y coordinate of every point in the profile
```

profileNumber of the first scan;
end

Algorithm 5-1 Registration of switch rail profiles

Several [76,77] Iterative Closest Point (ICP) algorithms were also used to align the data, but all with worse results when compared with the final method. The reason for this could have been the fact that a-priori information regarding the data was available and its use allowed the writing of a bespoke and more efficient algorithm.

2. Calculation of the minimum distance between each point in the first acquisition (stock rail and switch rail) and the polygon formed by all points in the second acquisition (stock rail only) and selection of points where the distance is greater than 1 mm

The process is exemplified in Figure 5-1.

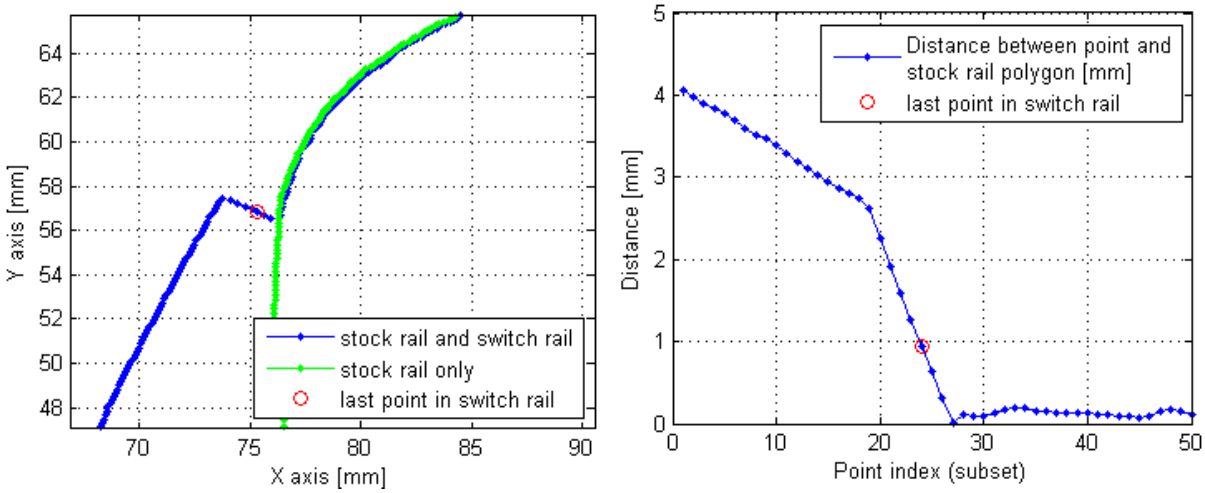

Figure 5-1 Exemplification for the process of identifying the switch rail (left plots to scale)

The left plot in Figure 5-1 shows a sample of acquired data and the right plot shows a subset of the minimum distance. All data points whose distance is at least 1 mm are considered part of the switch rail. Where the distance becomes less than 1 mm it is considered to be the last point of the switch rail (red circle in Figure 5-1).

5.1.2 A feature preserving point cloud filtering approach for convex point cloud data

Smoothing algorithms are often unable to eliminate all measurement errors and they can undesirably smooth out features of the surveyed object. As a result, much research has been undertaken to overcome undesirable smoothing by developing feature preserving smoothing

algorithms. The goal of these algorithms is to smooth out the point cloud data while preserving the inherent features of the surveyed object (e.g. sharp corners).

Often, the evaluation of feature preserving algorithms used to smooth out point cloud data is based on a visual, subjective evaluation of performance and on a limited set of point cloud datasets. However, in the context of inspection of safety-critical components, it is important to assure that the point cloud data is altered within understandable limits which do not allow the deformation of important shape features and cannot increase the error in the point cloud data. However, with most feature preserving smoothing algorithms this is difficult to assure.

Another important issue regarding feature preserving smoothing algorithms is that they generally require setting up one or several smoothing parameters (or the user must choose a variant of the algorithm). The parameters (or variants) are generally selected based on information regarding the data which is to be filtered. However, in the case switch rail profiles there is very little that can be safely inferred.

Several algorithms were used to filter 2D transversal profiles of switch rails, two of these being the Savitzky–Golay smoothing filter and the Mesh Smoothing Laplacian VTK found in the PCL library. The above two issues were common amongst most used algorithms.

Thus, a point cloud filtering algorithm was developed specifically for the presented inspection system. The algorithm was developed only for convex point cloud data. Thus, it is used to filter only point cloud data representing stock rails (excluding switch rails).

The approach

The measurement errors of scanCONTROL 2700-100(500) laser scanners, as shown in the sensor acceptance reports available in APPENDIX D: LASER SCANNER “SENSOR ACCEPTANCE REPORT”, can be mostly attributed to errors in the measured distance between the laser and the object, commonly named the Z axis by many laser scanner producers. Figure 5-2 is extracted from one of the two sensor acceptance reports.

The algorithm was demonstrated using artificially created convex data that contains both close to straight segments and round corners with a small radius of 2 mm (representing the far ends of the range of shapes found in stock rails). The noise was generated in MATLAB® as a vector of 100 elements that follow a normal distribution with an average of 0 and a standard deviation of 0.1. A histogram of the noise is shown in Figure 5-3. Although the graph seems

to have a break, in reality none of the 100 elements were inside the range of the penultimate bin.

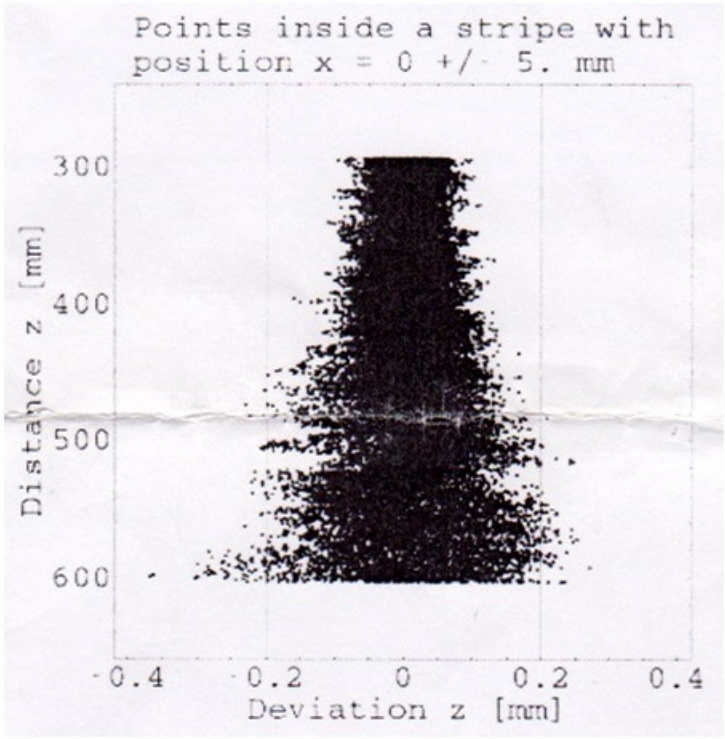

Figure 5-2 Z axis linearity errors of a scanCONTROL 2700-100(500) laser scanner

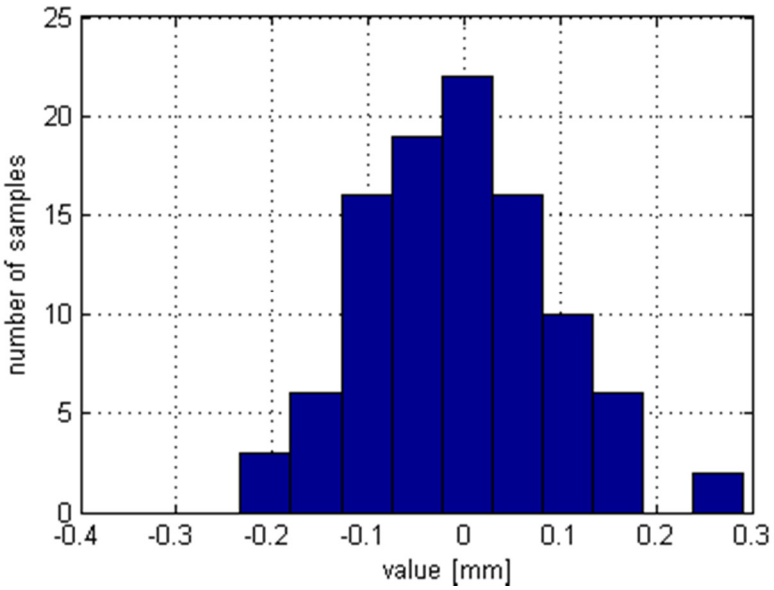

Figure 5-3 Histogram of generated values following a normal distribution

Figure 5-4 shows, in green, the noise free data and, in red, the noisy data. The noise was added perpendicular to the shape of the object to mimic the effects of the laser scanner errors (often described as Z axis errors by laser scanner manufacturers). In other words, the noise was added along the normals of the noise free data.

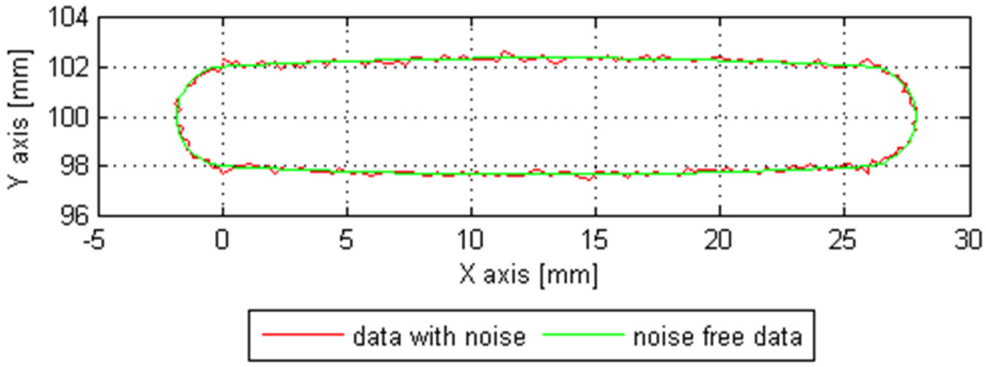

Figure 5-4 Generated data with and without noise (to scale)

The steps of the algorithm are as follows:

1. Generation of convex hull

A convex hull of the point cloud data was generated.

2. Elimination of points

As positive errors increase in the area of the measured object, it increases the area of the convex hull. Thus the majority of the points forming the convex hull are affected by high positive errors, as shown in the top plot of Figure 5-6. The points forming the convex hull (generally points with high positive errors) were successively eliminated as long as the following two rules were met: 1) there are never more than two consecutive eliminated points, and 2) there are never two consecutive groups, each having two eliminated points.

Figure 5-5 Graphical representation of the elimination rules

The rules are expressed graphically in Figure 5-5, where red squares represent eliminated points and green squares represent points which cannot be further eliminated.

3. Iteration of steps 1 and 2

The previous two steps are iterated until no points forming the convex hull can be further eliminated. Figure 5-6 shows the result of the first, fifth and tenth iteration of steps 1 and 2.

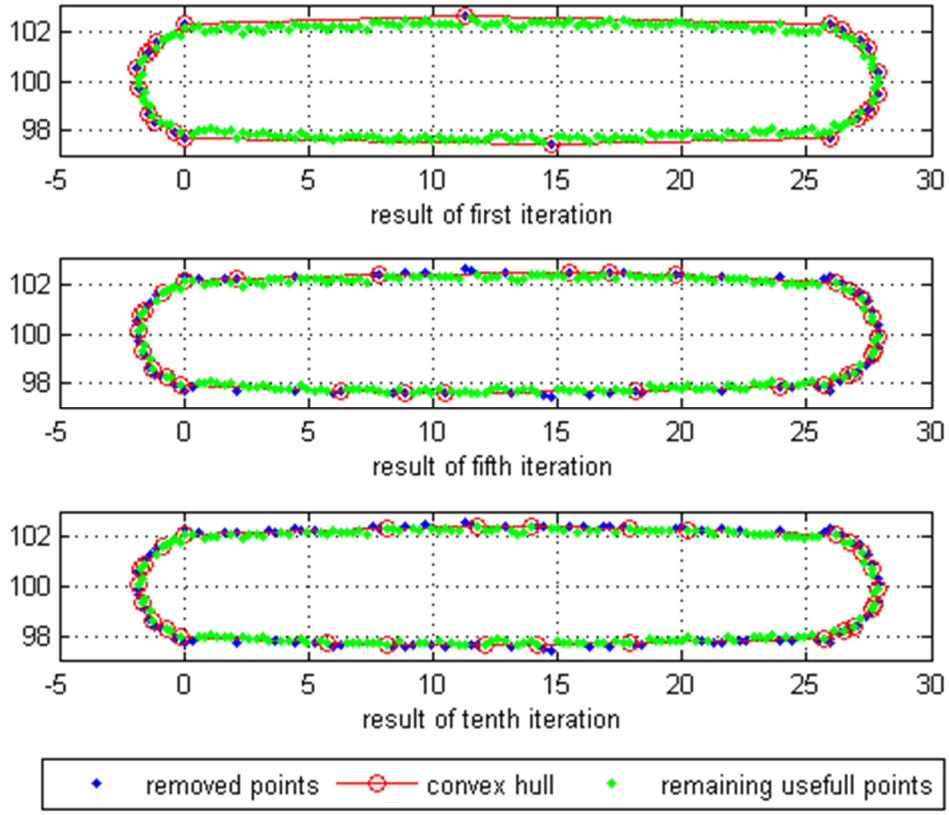

Figure 5-6 Iterative results of steps 1 and 2 of point cloud filter algorithm (to scale)

In this example, during the first iteration 22 points were eliminated; 20 from the small corners and 2 from the almost straight areas of the shape (Figure 5-6, first plot, blue dots in red circles). During the fifth iteration 10 points were eliminated from almost straight areas of the shape and none from the corners (Figure 5-6, second plot, blue dots in red circles). During the tenth iteration no points could be further eliminated (Figure 5-6, third plot, all circled dots are now green) and the algorithm finished execution.

Discussion of results

In principle, the algorithm improves the smoothness of the data through elimination of points that are more likely to be affected by large positive errors. Most positive errors are eliminated in the iterative process described in step 3. Most negative errors are eliminated at the end when the final convex hull is calculated. The overall results of the filter algorithm on a convex surface are shown in Figure 5-7.

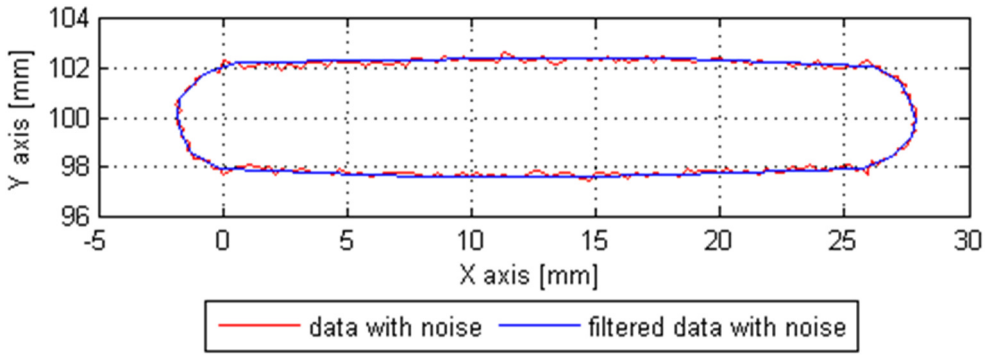

Figure 5-7 Filter result on the convex point cloud data (to scale)

Figure 5-8 shows one of the best results, where the filtered noisy data is very smooth and the average difference between the noise free data and the filtered noisy data is less than 20 µm.

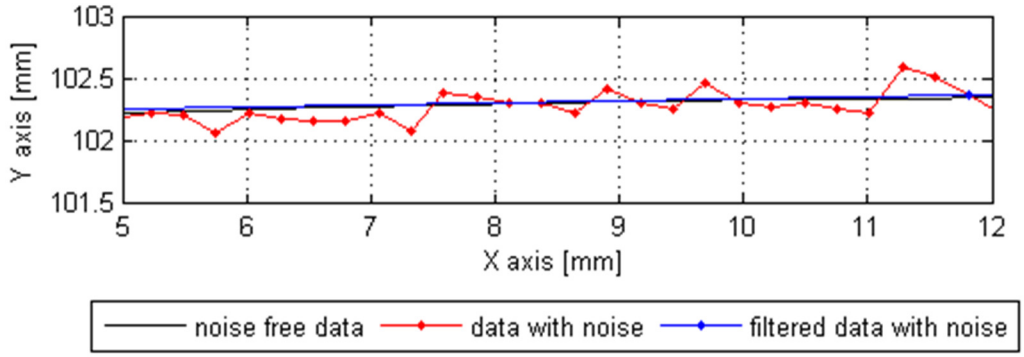

Figure 5-8 Example of good filter result (to scale)

Figure 5-9 shows one of the poorest filter results. The arc circle is poorly reproduced with a highest error of approximately 130 µm. The main reason for this is that the point cloud data contains 10 consecutive points all with errors of the same sign. The precision of the algorithm decreases where large groups of consecutive points have errors with the same sign. A shape (e.g. circle, rectangle or even a random shape) if scanned using a laser scanner which is consistently affected by errors of same sign will appear as being either enlarged or compressed (depending on the sign of the error). It is reasonable to say that such errors cannot be compensated using any method unless some additional information is available regarding the errors and/or the shape.

However, point cloud data collected from the laser scanners do not show such poor randomness. Groups of consecutive points with errors of the same sign are generally limited to three or four.

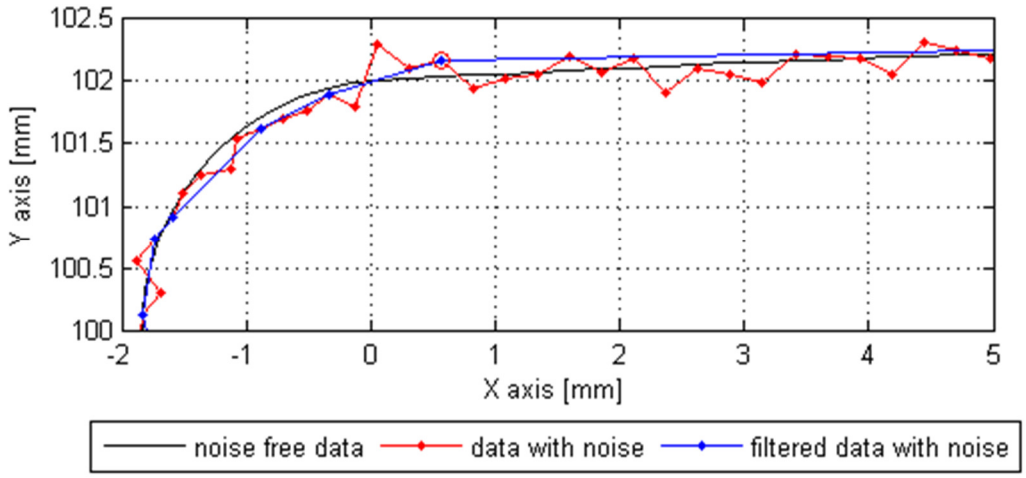

Figure 5-9 Example of poor filter result (to scale)

Another poor result in Figure 5-9 is the blue point in a red circle which has not been eliminated. The result would have been better if the preceding point had been eliminated instead. The algorithm does not evaluate the order in which points should be deleted. It is expected that a rule to establish the order of elimination could improve the algorithm, such as: points which lead to a greater reduction of convex hull area are eliminated first. In the case of Figure 5-9 the above rule would keep the preceding point instead of the circled one, and thus improve the results.

Final comments

The filtering algorithm is recommended where: (1) the point cloud data is convex, (2) the errors follow a normal distribution with a mean error close to zero and the sign of the error is reasonably random, and (3) the smallest features within the data are defined by at least 6-8 points.

The point cloud data collected from the laser scanners showed significantly better accuracy. This helped to achieve good results when using unfiltered switch rail point cloud data.

5.1.3 Derailment hazard 1

This hazard can appear on switches where the stock rail is heavily worn and the switch rail has very little wear. As the stock rail develops a sidewear scar, the height of the lowest part of the sidewear scar moves down the gauge face eventually reaching the top of the switch rail (e.g. Figure 5-10, diagram 3b). Under such conditions, the constant passage of wheel sets bends the tip inside the stock rail sidewear scar, as shown in diagram 3c.

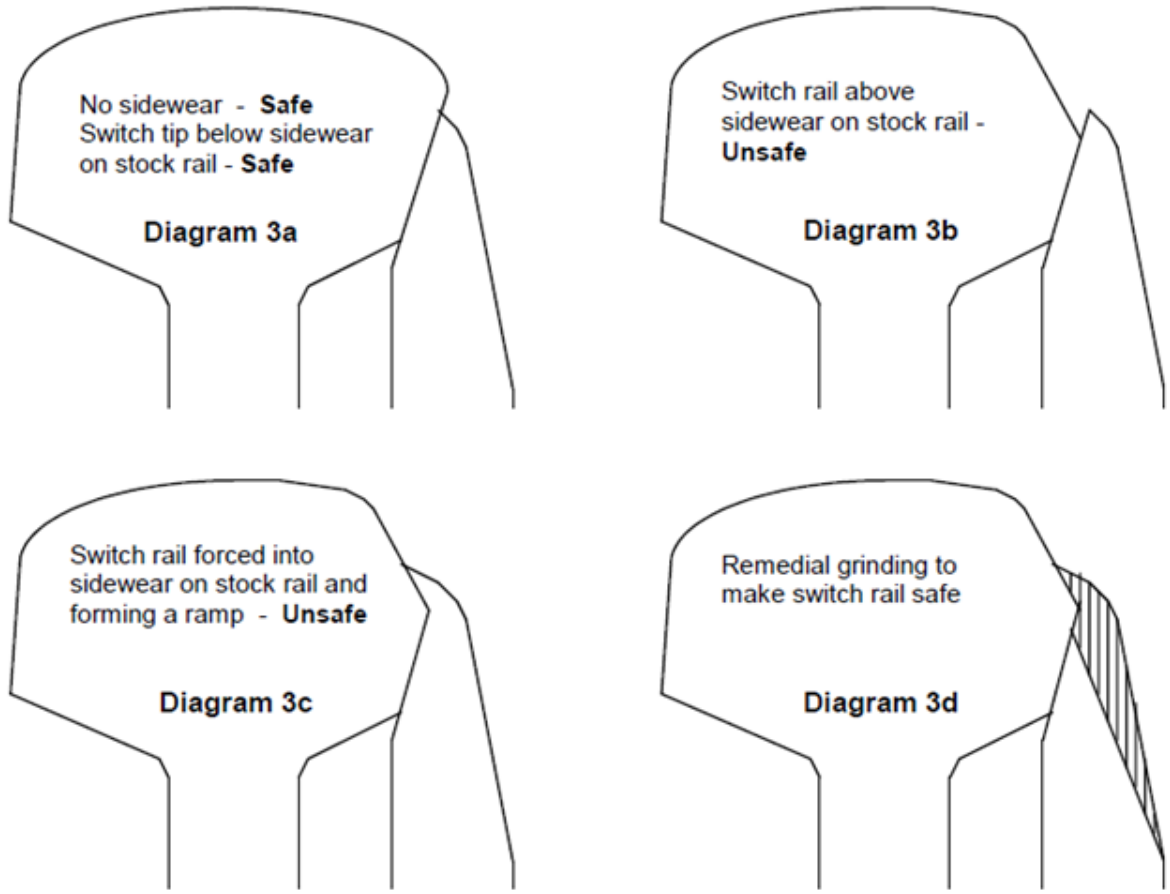

Figure 5-10 Description of derailment hazard 1
Courtesy and Copyright Network Rail

Derailment mechanism

Such deformation of the switch rail can change the interaction between the switch rail and the wheel to such an extent that the switch rail can provide a ramp on which the wheel flange can climb up.

Note: During the normal life cycle, a switch gradually wears out changing its shape from diagram 3a to diagram 3c without passing through diagram 3b (i.e. as the switch tip rises below the sidewear scar it is immediately bent towards the stock rail). However, it is not impossible for a switch to be in the condition of diagram 3b. This would be possible if inadequate repairs are carried out. If so, this could create a different hazard: train wheel striking the top of the switch rail. This hazard is also known to have caused derailments in some situations [78].

Method of inspection

Inspection for this derailment hazard is carried out using (1) a NR4 sidewear measurement gauge, and (2) by visually checking to see whether or not the top of the switch rail is above the lowest part of the stock rail sidewear scar.

Measurement principle of NR4 gauge

In order to achieve accurate measurements the straight edge of the gauge must be fitted flush to the field side of the rail head. The gauge must also be pushed down and the sidewear is measured by sliding in a specific stepped gauge between it and the rail head.

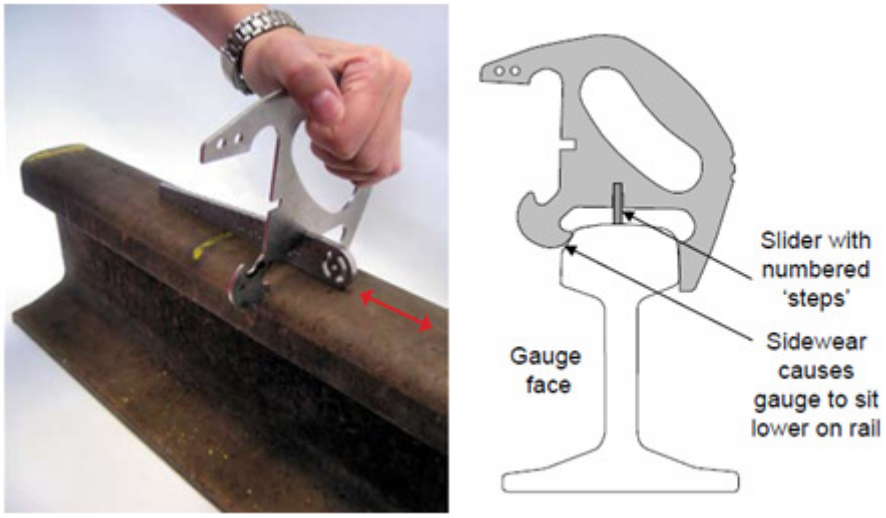

Figure 5-11 Application of NR4 sidewear measurement gauge
Courtesy and Crown Copyright RAIB

In principle, the NR4 gauge measures the height difference between two parts of the rail: the middle and close to the flange side. The straight edge of the gauge is inclined at 1:20 from vertical as commonly used rail head profiles have a 1:20 inclination on the field side.

Inherent reliability limitations of NR4 gauge

During measurement trials, it was concluded that a considerable source of error results from the failure to properly fit the straight part of the gauge to the field side of the rail (this supported the analysis for accuracy requirements discussed in section 4.2.2).

Rails which has developed rust, or rails where the field side of the stock rail was not straight and smooth for environmental reasons, were difficult to measure with a high repeatability. In such conditions the accuracy of the measurement was reduced. Furthermore, under some

conditions, the uneven surface led to rocking of the gauge, which reduced the precision of the measurements.

Thus, two sources of errors have been identified: (1) instrumental errors due to the limitation of the measurement device measuring rails with an uneven field side (systematic error), and (2) operator errors due to failing to place the gauge in the best possible position and failing to keep the gauge stationary during the whole duration of the measurement (random error).

Although, systematic errors can often be corrected, in the case of the NR4 measurement, the error is variable, and dependent on the shape of the rail head and thus is not easy to correct.

Proposed automatic NR4 measurement algorithm

The main challenge within this measurement comes from the inherent measurement reliability previously discussed. An automatic solution must choose the best possible fit based on the features of the rail. This was achieved in steps 3-5 and the performance of these steps determine, in large, the accuracy of the measurement. The rest of the steps did not pose challenges nor add any significant errors to the measurement process.

The steps which are undertaken to measure the sidewear are explained below:

1. Modelling of the NR4 gauge as point cloud data (one time only)

A point cloud model of the NR4 gauge was created using the official drawings of the gauge. An average distance of $0.2\ mm$ between two consecutive points was used.

2. Preparation of point cloud data as described in section 5.1.1 and application of point cloud filtering algorithm on the stock rail point cloud data as described in section 5.1.2
3. Generation of stock rail head convex hull

As a laser based inspection is expected to closely reproduce the manual measurement, the algorithm was designed to replicate the manual inspection as much as possible. Thus, the convex hull of the rail is calculated as it identifies all the sides of the rail against which the gauge could be fitted, as well as the relative inclination between the rail and the gauge.

4. Selection of convex hull segments whose angles are within 92.86 ±1.6 degrees

The main rail profiles which are used within Network Rail infrastructure are designed with a field side inclined at 1:20 (this equates to an inclination of 2.86 degrees from vertical). Due to the tolerances of the rail and the installation, a designed inclination of 1:20 can in practice

have any values between 1:40 and 1:13 and still be within design limits [79]. This equates to a tolerance of -1.43 and +1.54 degrees respectively.

There are situations where the field side of the rail may not allow an accurate measurement due to all segment angles being far from 92.86 degrees (note: this is a limitation of the NR4 gauge). Thus, in the case of such a rail head profile, if no angles are found to be within the normal range of 92.86 ±1.6 degrees, the measurement is aborted as a high accuracy measurement is unlikely to be achieved.

All segments outside these tolerances are omitted from the next steps.

5. Weighting calculation for each segment based on the following formula: $w = w_1 * w_2 * w_3$where:

- w_1 is inversely proportional to the minimum y value of the points forming the segment
- w_2 is proportional with the length of the segment
- w_3 is highest when the segment angle is 92.86 degrees and reduces as the segment angle becomes far from 92.86 degrees

This is the most important step, as within this step the best fit between the gauge and the rail is decided by choosing just one of the available field side segments. In order to achieve this, the best segment is chosen based on the set of three criteria mentioned above. Each of the three weightings, w_i, help to establish which segment within the field side should be chosen to fit the gauge against. The better the segment, the bigger the individual weights for that segment.

The first criterion advantages lower segments on the vertical axis. Upper areas of the field side tend to suffer more from metal migration and lipping than lower areas and as such lower areas of the field side are more reliable. As segments can have lengths of up to 20 mm, the lowest point in each segment is considered.

The second criterion advantages long segments. The length of the segment is generally inversely proportional to the curvature. Thus, the longer a segment is, the more likely it is to be located in a flat area of the field side.

The third criterion advantages segments whose angle is closer to 92.86 degrees. This is due to the expectation that the field side would have an inclination of 1:20 and that track cant is 0. If the inclination and cant differ from this expectation, the new values should be accounted for.

6. Rotation of the rail head so that the angle of the chosen segment is 92.8 degrees

Once the segment has been selected, the rail is rotated to match the angle of the straight edge of the NR4 gauge.

7. NR4 gauge translation along both axes so that the gauge is vertically above the rail and its straight edge is collinear with the segment that has the highest weighting

8. Repetitive NR4 gauge translations of $\begin{pmatrix} 1/400 \\ -1/20 \end{pmatrix}$ until any one point of the gauge is on or inside the rail head

During this step, the gauge is repeatedly translated on the vertical axis by $-50\ \mu m$, making the gauge ultimately intersect the rail. As the straight part of the gauge is inclined at 1:20, the gauge is also horizontally translated $2.5\ \mu m$ at every iteration. The repetitive process ends when any point of the gauge is on or within the rail head.

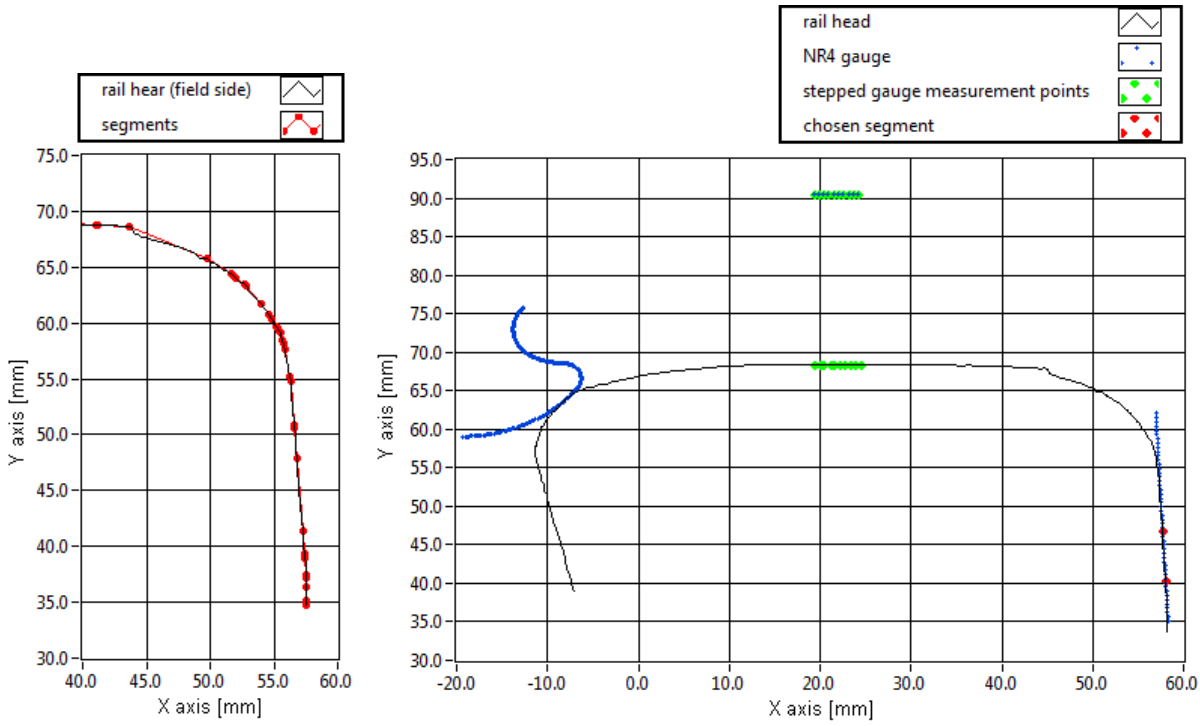

Figure 5-12 NR4 fitting process; left: available segments; right: NR4 fitting based on a the chosen segment (both not to scale)

9. Measurement of the minimal vertical distance, d, between the middle of the gauge and the rail head

In practice, this step is carried out by using a stepped gauge that is placed between the gauge and the rail. The top surface of the rail (rail measurement area) may not be parallel with the top gap in the gauge (gauge measurement area).

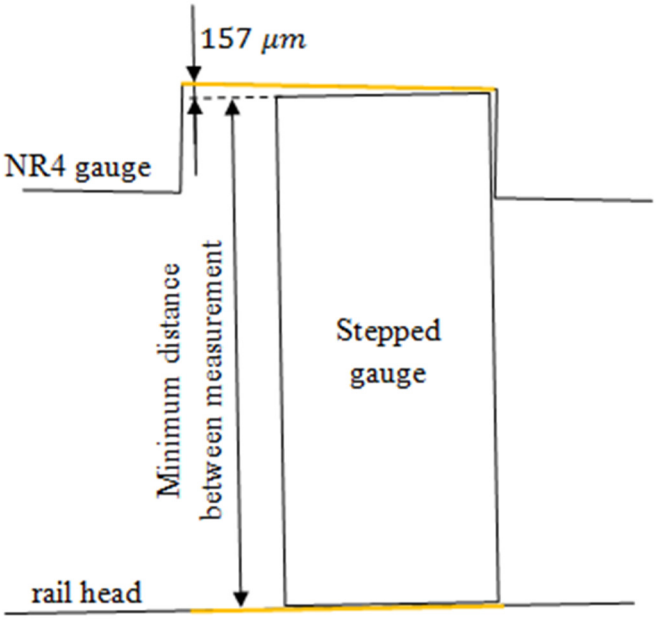

Figure 5-13 Fitting of stepped gauge

An angle difference of 1.5 degrees would make the distance vary by $\sin(1.5^{\circ}) * 6 = 157\mu$m across the measurement area. The stepped gauge has a thickness of 5 mm and the gap in the NR4 gauge is 6 mm. This limits the lateral play to just 1 mm. Thus, the maximum measurement error due to the possibility of placing the stepped gauge in various positions is just $157\mu m * \frac{6-5}{6} = 26\mu m$ and was considered negligible (a maximum inclination of the rail's top area of 1.5 degrees was considered). The measurement is taken as the minimum distance between the two measurement areas (marked in orange in Figure 5-13).

10. Calculation of sidewear using the following formula: $s = \lceil (d - 10)/0.78 \rceil$

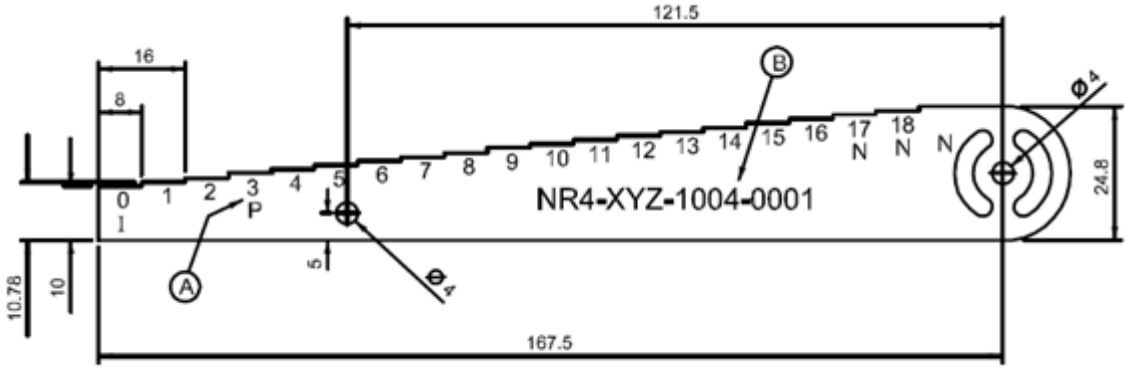

Figure 5-14 Drawing of stepped gauge used in conjunction with the NR4 gauge Courtesy and Copyright Network Rail

The calculation of the sidewear, s, is accomplished by using the above formula, which was derived by analyzing the official drawing of the stepped gauge. The gauge has a starting thickness of 10 mm and each step is 0.78 mm thick. The round up operator reflects the behaviour of the stepped gauge not fitting unless d has a minimum distance.

Discussion of the accuracy of automatic NR4 measurement algorithm

The gauge is modelled to such accuracy that the error contribution to the final measurement is considered negligible.

The 2nd step improves the point cloud precision and is considered to have only positive effects towards the final result.

In the 3rd step, the convex hull is calculated. The calculation of convex hulls is an error free process.

The 4th step eliminates segments that do not allow an accurate measurement.

The 5th step is the most important step, as it decides how the gauge will be fitted against the field side of the rail. As explained, this step takes into account three rail features which lead to accurate measurements.

In the 6th step a rotation is executed. As a double-precision floating-point format is used; all rotations are considered to produce negligible errors.

The 7th step introduces no errors.

The 8th step introduces an error of up to $50\ \mu m$, which is considered negligible and can easily be improved if necessary.

The 9th step introduces an error of up to $26\ \mu m$, which is due to the design of the gauge and is considered negligible.

Finally, the 10th step does not introduce any errors.

With the exception of the 4th step, all the steps undertaken to measure the NR4 sidewear are error free or negligible. The error involved here is difficult to quantify as it is dependent on the shape of the rail head. In many situations the identification of an error free fit is impossible due to the absence of a clear definition of best fit. Although it is concluded that it is not possible to calculate the best fit (which means that it is also not possible to calculate the measurement error), the sidewear can still be measured with good accuracy.

The collected point cloud data from the scanCONTROL lasers had significantly better accuracy than the accuracy stated in the sensor acceptance report. Using the presented methodology, 68% of the automatic NR4 measurements matched the manual measurements while the remaining 32% were off by one sidewear unit. This equates to an average error of 0.32 units on the sidewear gauge, or 0.25 mm on the vertical axis.

It must be noted that part of the difference may be attributed to operator errors.

Switch tip height inspection

A visual check is carried out to identify whether or not the tip of the switch rail is above the lowest part of the stock rail sidewear scar. This will be simply referred to as the switch tip inspection. The figure below shows two sketched examples of this check, a PASS example on the left side and FAIL example on the right side. The green arrows show the lowest point of the stock rail sidewear scar. If the green arrow is vertically below or levelled with the blue arrow then the switch fails the inspection. In practice this inspection is carried out visually without the use of any tools or devices.

The derailment mechanism in this case is that as the sidewear of the stock rail progresses, the wheel flange can start to strike the switch rail. This situation is hazardous as (1) the wheel can start to climb on the switch rail and (2) the switch rail can be bent into the void forming between the two rails changing the wheel-rail contact angle (low wheel-rail contact angle is a derailment hazard, discussed in more detail in section 5.1.4).

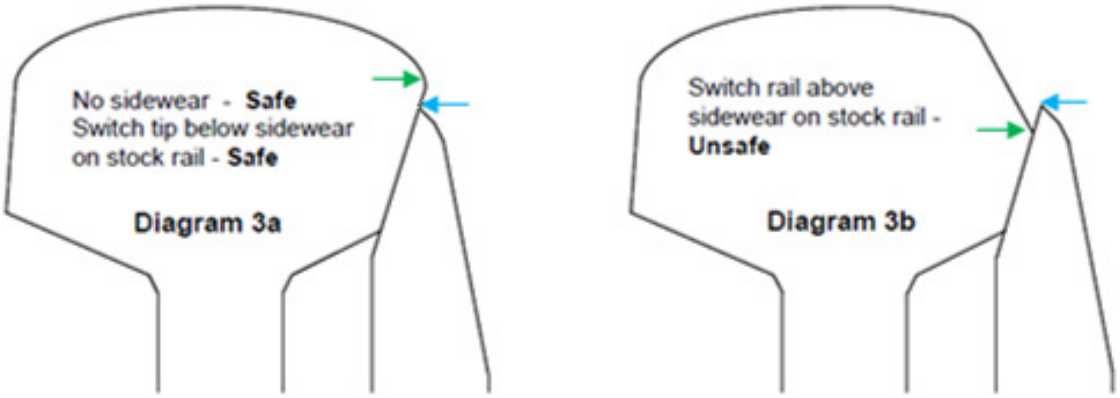

Figure 5-15 Two examples of switch tip height check; PASS (left), FAIL (right) adapted from NR/L2/TRK/0053; Courtesy and Copyright Network Rail

Four hypothetical cases are considered and are shown in Figure 5-16. All four plots have the same stock rail. Two types of switch rail are shown, one type in plot (a) and (b) and another type in plot (c) and (d).

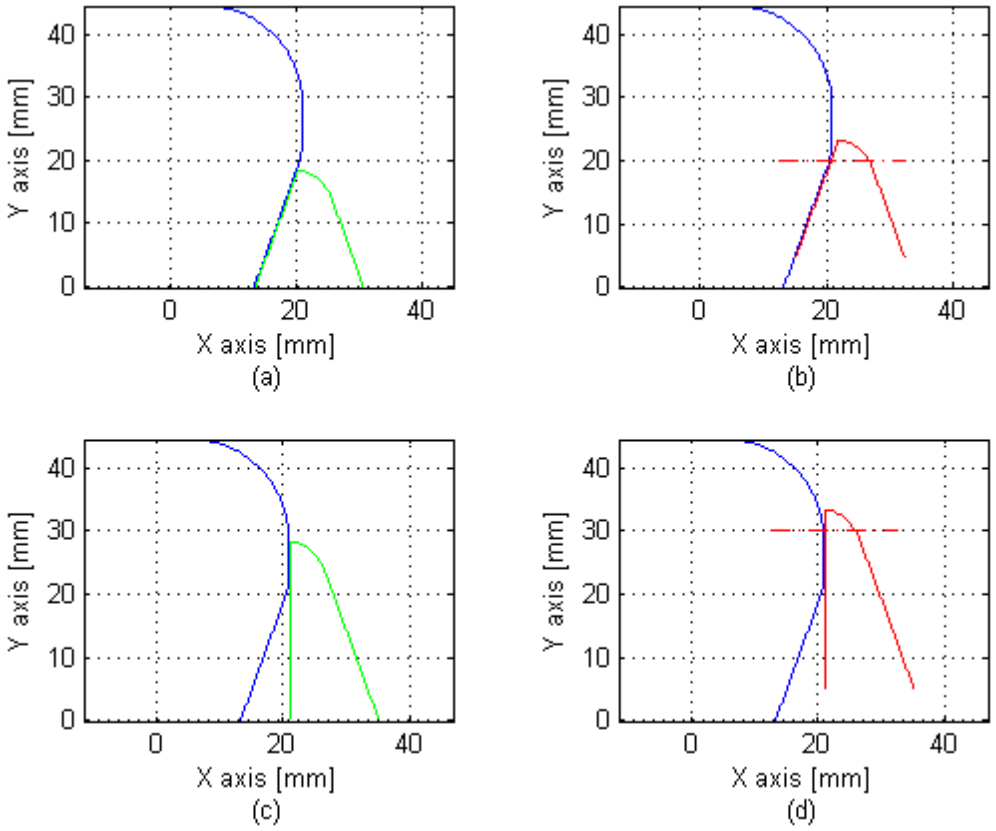

Figure 5-16 Switch tip height case study (to scale)

As the stock rail shows a fairly round gauge corner it is difficult to identify the exact location of the sidewear scar and thus to carry out a correct inspection. However, plots (b) and (d)

should be positively identified, as due to the small gap between the two rails, there is a risk that the switch rail could be bent out of shape, whereas plots (a) and (c) should not be considered to show a derailment hazard, as the stock rail does not have any sidewear that would allow the train switch rail to be bent out of shape or the wheel flange to strike it.

It must be observed that in the case of plots (a) and (b) the hazard is present if the switch rail is above the 20 mm mark, while in plots (c) and (d) the hazard is present only if the switch rail is above the 30 mm mark. As all four plots have identical stock rails but different heights for determining the presence of the derailment hazard, it was concluded that the sidewear scar of the switch rail may be an unreliable source of information. As a result, it was considered that the best method for determining the derailment hazard is to identify the location on the stock rail at which it no longer provides lateral support to its switch rail.

It is true that the shapes shown in Figure 5-16 are not of any standard. The reason for experimenting with non-standard rail types is because it is difficult to understand the limits under which the rails can change their shape, due to the high number of existing rail types and high number of wearing mechanisms such as abrasion, metal flow, other rail damage and not the least repairs (NR switch repair procedures do not define the shape of rail that must be achieved after the repair is complete). Thus, a robust method was needed to cope with rail shapes which may be very different than expected.

Although colour information can be used to help identify the location of the stock rail sidewear scar, this method was not researched due to the following disadvantages: (1) dimensional measurement accuracy is generally poor, and (2) for the purpose of this work, the use of vision techniques is very unlikely to produce reliable results.

In this work two approaches are presented for switch tip height inspection.

First approach of automatic switch tip inspection: rule based

This approach is explained on three of the switch planing designs used by NR (Figure 5-17), but can be adapted for other types. All three switch rail designs show the field side at an angle of -15 degrees from vertical. Although the top and gauge area of the switch rail can change to any shape, the field side of the switch rail remains the same. It can only be affected by lipping.

Figure 5-17 Switch planing used throughout NR railway infrastructure (left: 113 curved chamfered; centre: UIC60 shallow depth; right: 113A/UIC54B shallow depth)

The corner of the worst case flange worn train wheels shows an angle no steeper than 10 degrees from vertical. Due to this wear, the stock rail cannot develop a sidewear at an angle steeper than 10 degrees.

Figure 5-18 shows a wheel-rail example where the stock rail is marked at -15 degrees and 10 degrees.

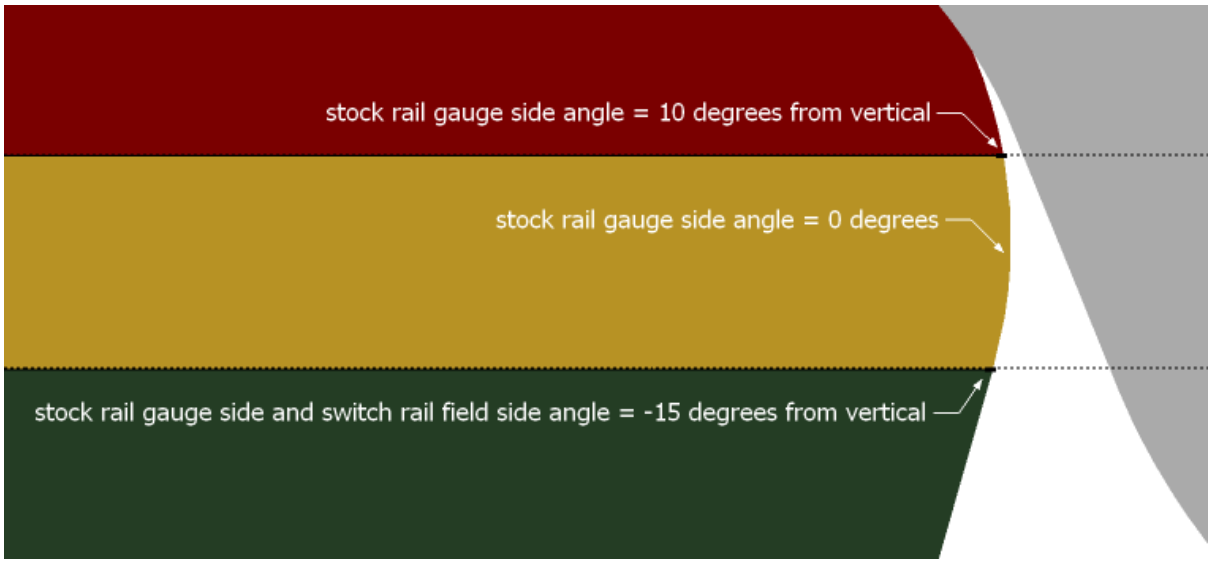

Figure 5-18 Important angles in the evaluation of Derailment hazard 1 grey: P8 wheel; red, orange and green: rail (to scale)

If the top of the switch rail is below the -15 degrees mark (in the green area), it is in an area where stock rail sidewear cannot develop (a stock rail sidewear scar cannot develop below the 10 degrees mark shown in Figure 5-18), and thus it is considered hazard free. Moreover, the stock rail provides full support to the field side of the rail.

If the top of the switch rail is above the -15 degrees mark (in the yellow area), it is below the stock rail sidewear, and thus it is considered hazard free. However, the flange of the wheel can slightly bend the switch rail into the shape of the stock rail.

If the top of the switch rail is above the 10 degrees mark, it is in an area where stock rail sidewear can develop, and thus it is considered a hazard. Moreover, train wheels with a flange angle of 10 degrees (worst case) are likely to strike the top of the switch when approaching under flange contact conditions.

Proposed automatic switch tip inspection algorithm

The switch tip inspection is carried out on each acquired set of profiles (the switch rail in both the open and closed positions) for the first 250 mm of the switch rail and the steps are as follows:

1. Preparation of point cloud data as described in section 5.1.1 and application of point cloud filtering algorithm on the stock rail point cloud data (as described in section 5.1.2)
2. Generation of stock rail convex hull
3. Calculation of vertically lowest point of the convex hull where the upper segment forming the convex hull has an angle of 10 degrees or more from vertical

Various rail defects such as rolling contact fatigue (RCF) cracking and gauge corner breaking can create small (millimetre and sub-millimetre) concave areas on the rail surface, most commonly on the gauge corner. These types of defects can lead to catastrophic failures such as rail breaks; however, they are managed by other inspection standards which are outside the scope of this work. However, these defects are relevant in the sense that they can alter the profile of the rail by introducing concave areas. As concave areas in the rail profile do not contact the train wheel, their angles are not of interest. Thus, in addition to filtering the data, the convex hull is further used to improve the measurement of angles within the point cloud data by filtering the concave areas of the rail profile.

4. Calculation of vertically highest point in the switch rail
5. Calculation of vertical difference between the two identified points in steps 3 and 4

Results

One surveyed switch was affected by derailment hazard 1 and was used to evaluate the algorithm. The switch is pictured in Figure 5-19 and Figure 5-20. Figure 5-19 shows the bent tip of the rail as well as the stock rail sidewear scar.

Figure 5-19 A switch that failed Derailment Hazard 1 (photo 1)

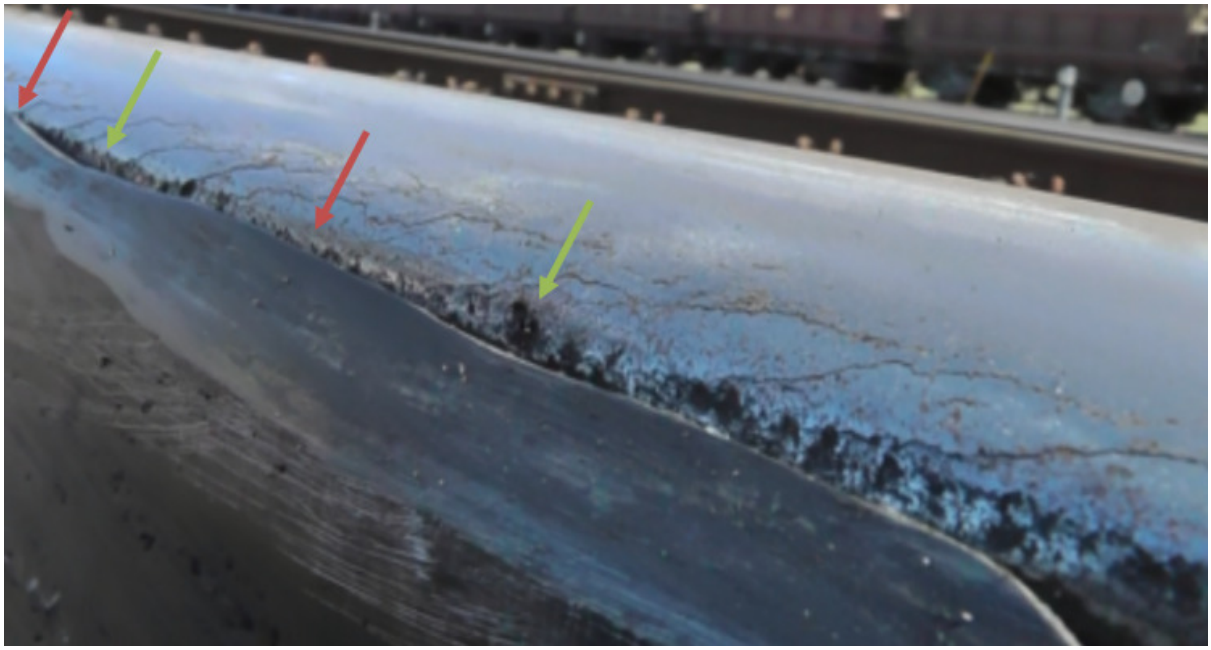

Figure 5-20 A switch that failed Derailment Hazard 1 (photo 2)

In Figure 5-21 the result of the algorithm is shown. The results match the extent of the damage as shown in Figure 5-19 and Figure 5-20:

- At the beginning of the switch the tip of the switch rail is just a millimetre above the stock rail sidewear scar
- Five centimetres along the switch (first green arrow counted from the switch toe) the bottom end of the stock rail sidewear scar is clearly visible. The algorithm marginally fails the switch at this location

- Seven to eleven centimetres along the switch (first red arrow), the switch rail covers part of the sidewear scar and is visibly bent in Figure 5-19. The algorithm fails it with 2 to 3 mm
- Twelve to fifteen centimetres along the switch rail (second green arrow), the switch rail has a low height but Figure 5-19 shows that its tip is slightly bent. The algorithm fails it with 1 to 2 mm
- Seventeen centimetres along the switch (second red arrow), the switch shows one of the most pronounced failures. The algorithm fails the area with almost 5 mm of excessive height difference.

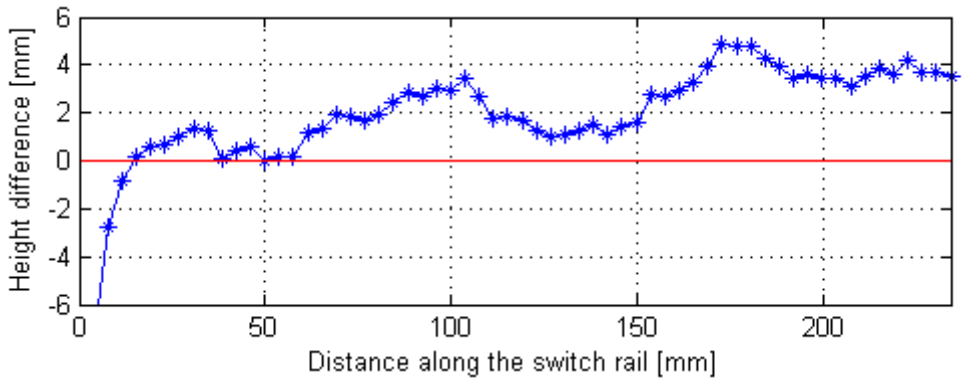

Figure 5-21 Result of switch tip algorithm on a failed switch

Advantages of presented method

The method is simple, efficient (a relatively low number of calculation are required). The sidewear of the stock rail is reliably identified irrespective of the shape of the stock rail (i.e. the algorithm is reliable even if the stock rail is shaped as a circle)

Disadvantages of presented method

The method was researched and tested only for the commonly used rail types in NR. Older switch rails are designed with a vertical field side. Although the 10 degree limit for failing the switch relates to the worst case flange worn train wheels, meaning that no change to the algorithm is required, this was not the subject of this research and thus its performance on these rails was not researched.

Instead of measuring the stock rail sidewear, the algorithm considers the worst case for the stock rail sidewear. This means that in some cases the algorithm may be slightly conservative (e.g. the algorithm identified a marginal fail condition at 5 cm along the switch rail, while the

visual inspection was a marginal pass; however, this results in a measurement difference of less than a millimetre between the manual and automatic inspection and it is on the safe side).

Second approach of automatic switch tip inspection: wheel-rail interaction based

The stock rail sidewear scar is a result of contact (abrasion) between the wheel and rail. As a result, the location of the sidewear is the same as the location of the wheel-rail contact. Thus, this approach fits a new P8 train wheel to the stock rail (the fitting process is explained in section 5.1.4) and identifies the lowest contact point on the gauge corner of the stock rail. The identified point is considered to be the lowest point of the stock rail sidewear and is then compared with the top of the switch rail. The results (shown in Figure 5-22) are poor, as they underrate the severity of the fault and also show low precision (the results are noisy).

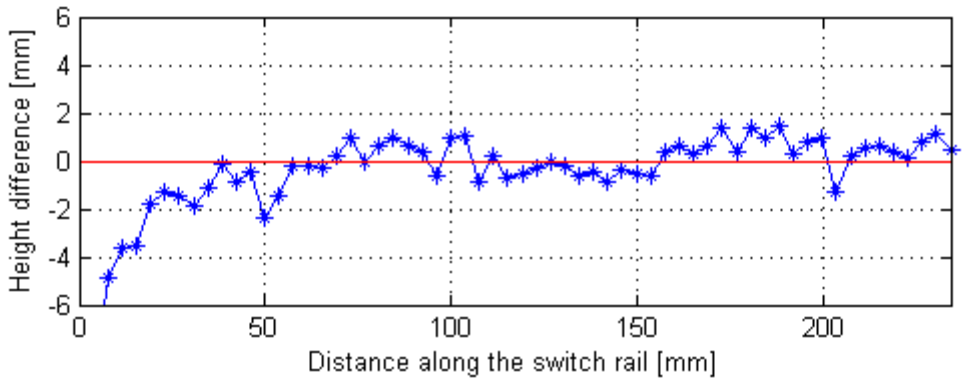

Figure 5-22 Result of switch tip algorithm on a failed switch

The conformity between a new P8 profile and the worn rail is poor and as a result a two-point contact (in reality, the contact points are two small patches the size of a coin) is formed which is dependent on both the shape of the rail and the shape of the wheel. Thus, in order to identify the correct location of the sidewear, a certain train wheel profile must be used which closely conforms to the profile of the stock rail. Moreover, the rail profile generally changes slightly along the length of the switch.

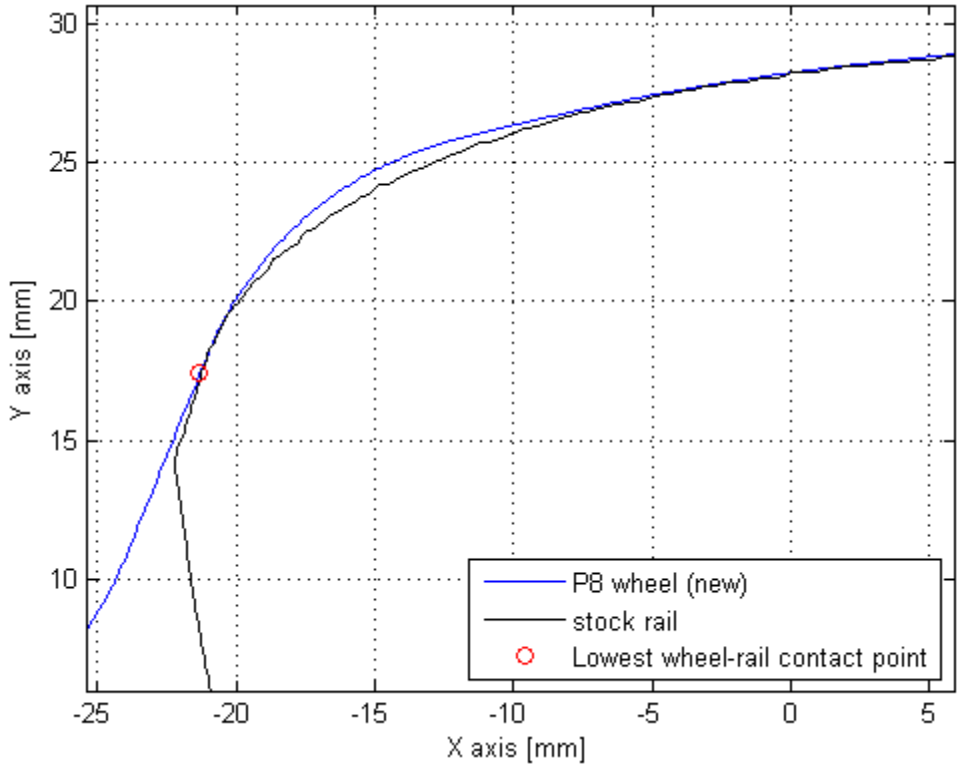

Figure 5-23 Wheel-rail fitting using a P8 profile (new) (to scale)

In Figure 5-23 the lowest contact point was at a height of 17.3 mm but the stock rail sidewear was below 15 mm. The steeper the wheel flange is, the lower the contact point is. Thus, it is concluded that the identification of the sidewear location is better achieved using the first approach where the 10 degree limit can be used to set the worst case wheel flange angle that is expected to occur on the railway network.

5.1.4 Derailment hazard 2

According to the NR/L2/TRK/0053 inspection standard, a derailment hazard can occur if the sidewear angle of the switch rail is flatter than the sidewear angle of the stock rail. This hazard generally occurs at switches that have a sideworn stock rail and switch rail. This hazard can also occur when the switch rail has suffered damage and rail traffic has smoothed it out.

The figure below shows two situations, one in which the switch rail sidewear angle is flatter than the stock rail sidewear angle (left diagram; fail) and one in which the sidewear angle is steeper (right diagram; pass). The hatched area in the right diagram shows remedial grinding work that would normally be carried out in order to repair the switch rail profile.

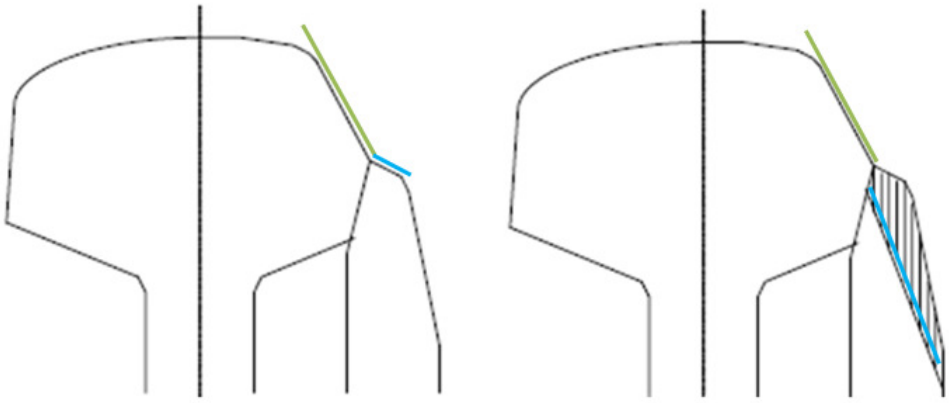

Figure 5-24 Two examples of rail sidewear; fail (left), pass (right)
Courtesy and Copyright Network Rail

Before 2005, the NR/L2/TRK/0053 inspection standard required a visual comparison of the sidewear angles on the two rails. Mathematically, the sidewear angle is a tangent line to a point within the rail profile and hence is dependent on the point at which it is being calculated. Although, in the above example, the tangent is easy to identify as the rail has a large area of flat surface where the tangent is constant, this is not always the case. Figure 5-25 shows an example with possible sidewear angle readings (marked as *t*).

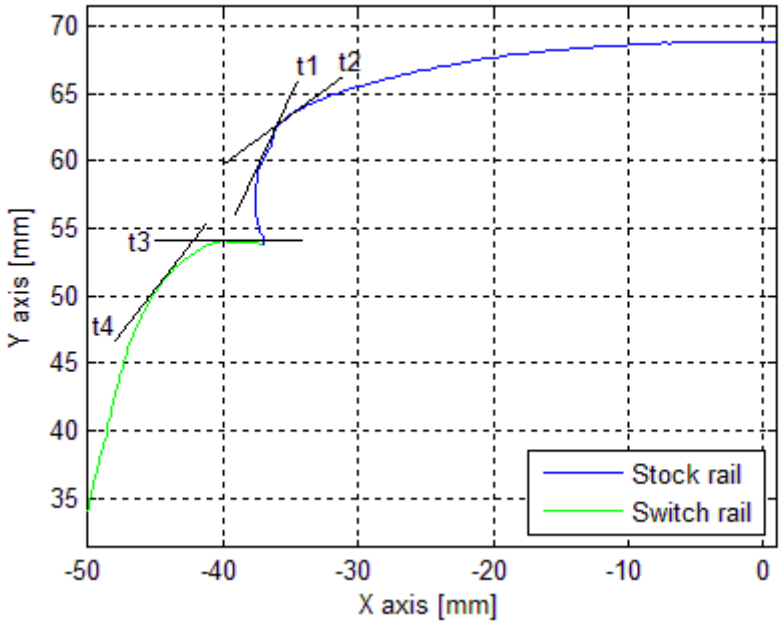

Figure 5-25 Possible sidewear angles on a measured stock rail and switch rail (to scale)

A reading of $t1$ and $t3$ would fail the inspection while a reading of $t2$ and $t4$ would pass it. In 2005, the TGP8 (Track Gauge P8) was introduced to replace the visual comparison of sidewear, which allowed a more accurate identification of this hazard [10].

Method of inspection: The current NR/L2/TRK/0053 standard describes the use of three gauges:

1. TGP8 (also known as P8 gauge) is used to identify the presence of the derailment hazard by analysing the contact angle between a new P8 wheel and the rail
2. Gauge 2 is used to determine the relative height between the two rails
3. NR4, in conjunction with a stepped gauge, is used to measure the amount of sidewear on the stock rail

Gauge 2 is used purely for the identification of areas where the top of the switch rail is at least 19 mm below the top of the stock rail. This does not pose any technical challenges and is not further discussed.

The measurement of NR4 sidewear is accomplished as described in section 5.1.3.

Flange climb derailment mechanism and the TGP8 contact angle

A flange climb can occur at switches where a lateral force is acting upon the wheel pushing it towards the rail and the wheel has a positive angle of attack (AoA) [79], as shown in Figure 5-26. As the wheel rolls over the rail the wheel flange continuously slides down along the gauge side of the rail [80]. If the friction or lateral force is too high a derailment can occur. This is described by Nadal's well known formula:

$$\frac{L}{V} = \frac{tan(\delta) - \mu}{1 + \mu * tan(\delta)}$$

Where:

- L is the lateral force acting on the wheel
- V is the vertical force acting on the wheel
- δ is the flange angle relative to horizontal
- μ is the friction coefficient between the wheel and the rail

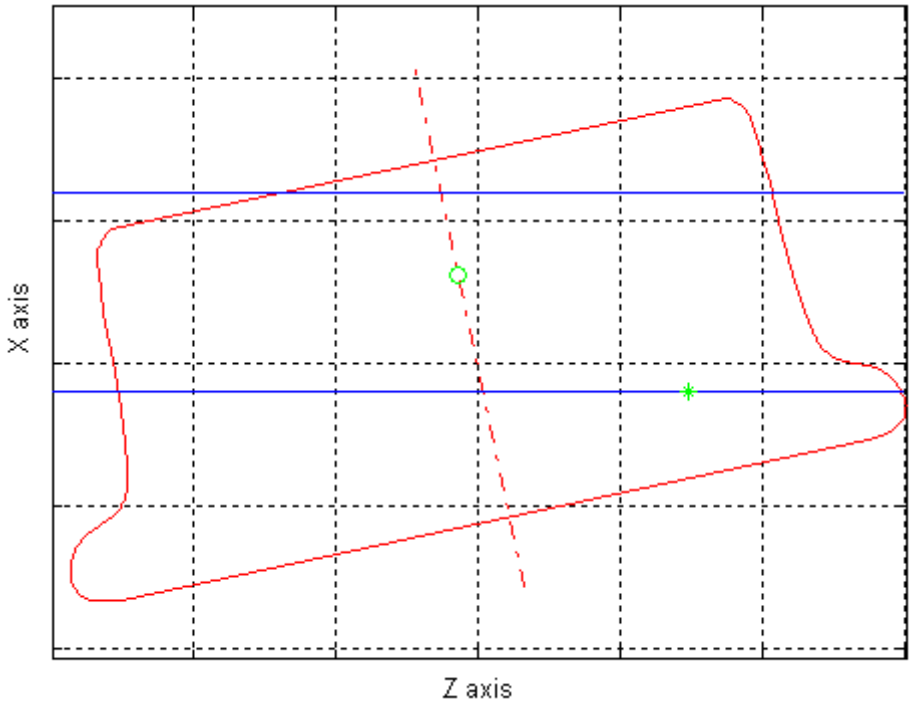

Figure 5-26 Diagram showing a two point contact for a positive AoA (top view; not to scale)

For NR, the flange climb derailment hazard is partially managed by limiting the flange contact angle δ to 60 degrees. Often, the flange contact takes place under a range of angles. The TGP8 contact angle refers to the flattest (worst case) flange angle between the P8 wheel and the rail.

The use of TGP8 gauge

The gauge has a small line which identifies the 60 degree mark.

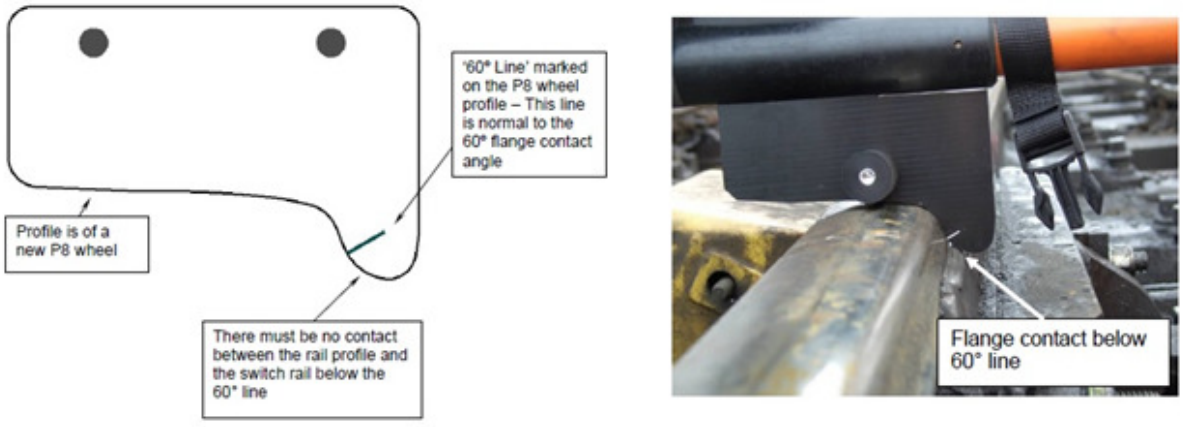

Figure 5-27 Drawing of TGP8 gauge (left); example of failed TGP8 inspection (right)
Courtesy and Copyright Network Rail

The correct use of the TGP8 can be seen as a two-step process: (1) correct application of gauge over rails and (2) correct reading of the TGP8 angle. The author considers the second step to be fully defined, as irrespective of the shape of the rails, it can always (limited to visual acuity) be identified whether or not any part of the two rails is in contact with the lower part of the gauge (below the white line). However, there is no clear and complete definition of what is a correct fitting of the TGP8 gauge. In most cases, due to the shape of the rails, such a definition is not necessary. However, in the context of automatic inspection of safety-critical assets, a clear definition of the inspection task is very important in achieving accurate, precise and reliable results irrespective of any factors such as the shape of the inspected rail.

In order to understand and refine the definition of a correct TGP8 fitting, a challenging TGP8 fitting is considered. Considering a square shaped rail profile as shown in Figure 5-28, most TGP8 users would fit the TGP8 gauge in different positions. Without a clear definition for a correct TGP8 fitting, an automatic fitting algorithm is also likely to produce less predictable and satisfactory results in such a case. However, if the definition of TGP8 fitting is well defined, considering no human errors, all users and all automatic fitting algorithms should produce the same and predictable fitting.

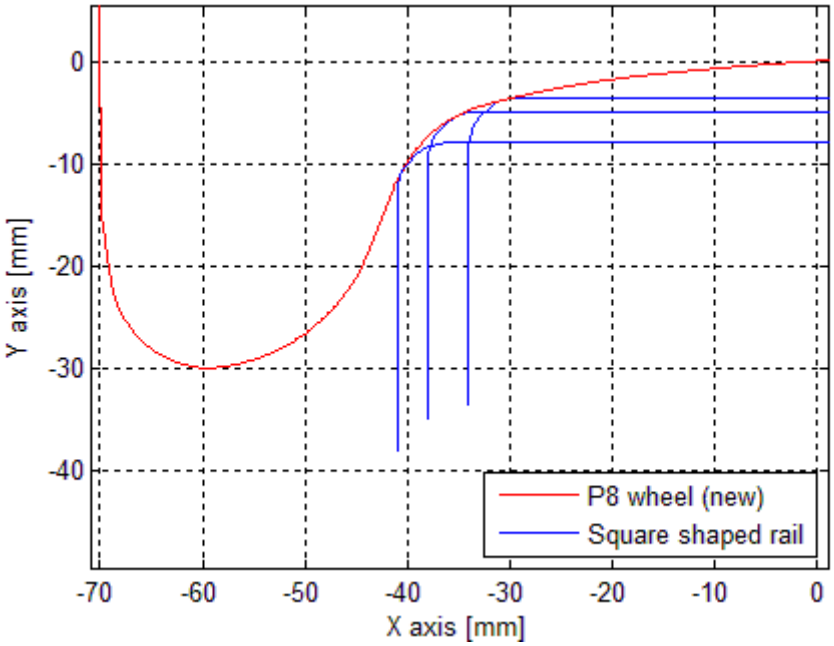

Figure 5-28 P8 wheel with three different possible fittings over a theoretical squared shaped piece of rail (to scale)

For this reason the square rail has been considered and a definition for TGP8 fitting was elaborated. Figure 5-28 shows possible TGP8 fittings over a hypothetical square rail. The inspection standard alone is not sufficient to identify the correct TGP8 fitting in this particular and more challenging scenario.

Measurement reliability of TGP8 gauge

In 2007 a train derailed near the Exhibition Centre station in Glasgow and four years later another train derailed at Princes Street Gardens in Edinburgh, both derailments taking place at poorly maintained switches. In both cases incorrect inspection using the TGP8 gauge had a causal role in the derailment [11,12]. During the investigation of the Edinburgh accident, RAIB found that most personnel questioned found the TGP8 gauge difficult to use [12].

The RAIB investigation also discovered that a section of the switch which was compliant with the TGP8 gauge had a contact angle of less than 60 degrees when a worn P8 wheel was used.

Figure 5-29 shows a switch rail which passed the TGP8 gauge inspection.

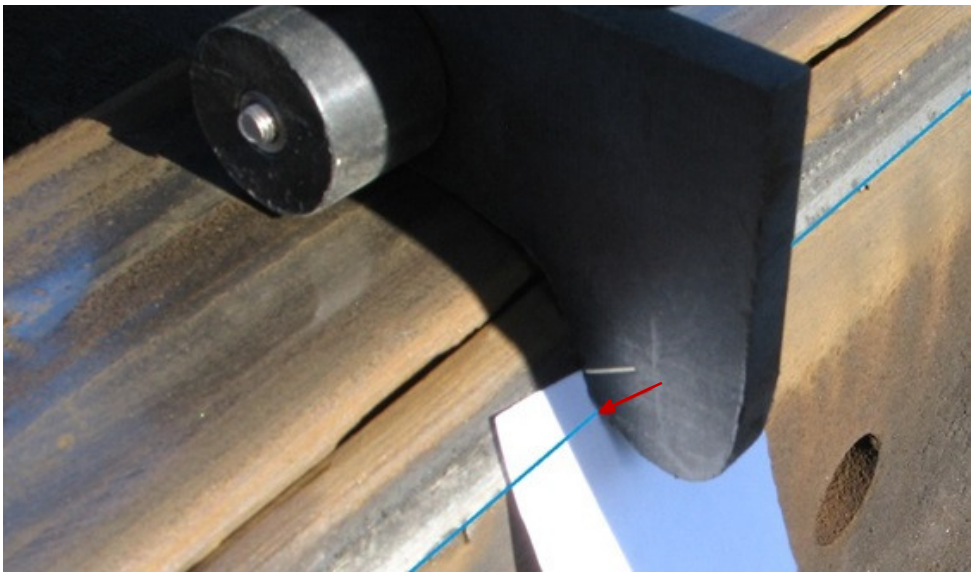

Figure 5-29 A second example of a switch rail which passes the TGP8 gauge but has signs of contact well below the pass mark

The measurement was carried out by continuously pushing the TGP8 gauge against the two rails after which the piece of white paper was pushed into the remaining gap between the switch rail and the gauge. The lowest worn part of the switch rail (blue line and red arrow) was significantly below the 60 degree limit. Thus, unless the switch rail has a much higher

vertical position with respect to the stock rail when trains are passing over it (a situation which could not be explained), the actual contact angle can be significantly below the contact angle measured using a TGP8 gauge. Any switch rail hogging cannot account for this situation as the compensation only makes matters worse.

As a conclusion, measurement reliability is limited due to both human error and the inability to check the contact angle against different wheel profiles. However, the use of a laser based inspection system could improve the TGP8 measurements with respect to both these limitations.

The 20 degree criterion for TGP8 fitting

Under a square shaped rail head the correct fit of the TGP8 gauge is not obvious. A clear and precise method for the application of the TGP8 gauge was sought and the adopted one is presented here.

Considering two objects which are pushed against each other (with rotational restrictions) the fitting between the two is dependent on the forces that are applied to the objects. Thus, the fitting was considered as a physics problem where two solid objects are fitted together under the presence of a force, with zero rotational movement and zero friction conditions.

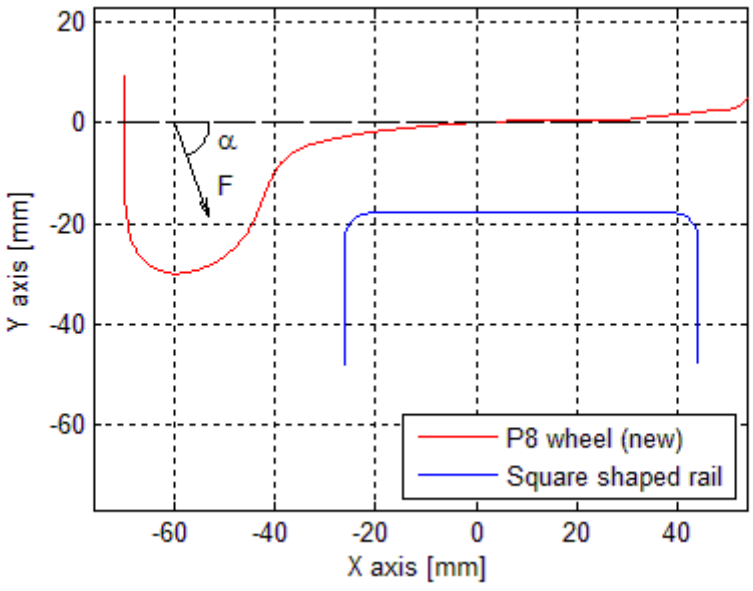

Figure 5-30 Description of the chosen TGP8 fitting criterion (to scale)

A force angle of 70 degrees was found to well replicate the manual procedure of fitting the TGP8 gauge on a piece of rail and was adopted as a physical constrain for the calculation of

TGP8-rail contact angle. The process always produces a unique solution for any given TGP8-rail fitting.

The TGP8-rail fitting can be carried out using a physics engine (a program or software that can simulate the physical interaction between multiple bodies) and adding the mentioned constrains, namely zero rotational movement, zero friction conditions and the presence of a force acting on the TGP8 gauge at 70 degrees from horizontal. However, in order to reduce complexity, the fitting was carried out without the help of a physics solver.

When the fitting is carried out with the mentioned constrains in place, the fit always results in a 20 degree contact between the TGP8 gauge and rail or a range of contacts which includes 20 degrees. Thus, an iterative algorithm was written that calculates the TGP8-rail fitting and stops when the contact between the TGP8 and rail is 20 degrees or the range of contacts includes 20 degree. The algorithm delivers the same results as using a physics solver and setting the mentioned constraints.

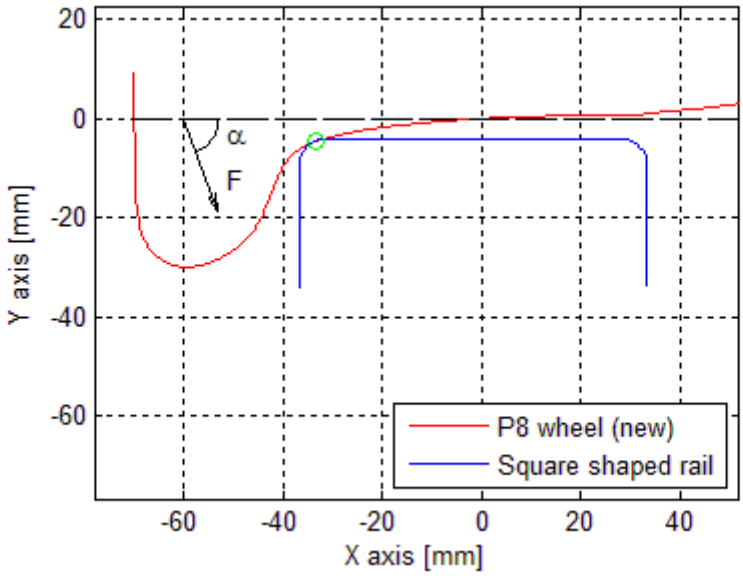

Figure 5-31 Fitting example for a square shaped rail using the 20 degrees criterion (to scale)

Figure 5-31 shows the result of a fitting against a square shaped rail when the 20 degrees criterion is used. The green circle marks the contact point between the TGP8 and rail.

Proposed automatic TGP8 measurement algorithm

For simplicity, the TGP8 gauge and rail point cloud data will be referred to as simply TGP8 and rail. The steps are as follows:

1. Modelling of TGP8 as point cloud data

The distance between two consecutive 2D points and the resolution were chosen to have unnoticeable effects on the accuracy of the measurement process.

2. Preparation of rail point cloud data as described in section 5.1.1

After the data is prepared, the rail is automatically positioned in the vicinity of the TGP8.

3. Fitting of TGP8 on rail according to the "20 degrees" criterion

The fitting is carried out by changing the position of the rail instead of the TGP8, but this does not affect the final result. The rail's position is calculated using successive approximations which gradually decrease the fitting error at every iteration. Successive approximation is a well known mechanism that is used in Successive Approximation Analogue to Digital Convertors. The application of this mechanism in ADCs is described in numerous books, one example being [81].

The successive approximation operations are carried out in a nested loop to account for both X and Y axes. After every iteration, if the range of TGP8-rail contact angles includes 20 degrees, the rail is moved to the left, otherwise to the right. The algorithm stops after 12 iterations when the fitting error is < 12.2 µm on each axis.

```
Position the rail below the wheel and to the left of the wheel flange
dx=25; //mm
dy=25; //mm
for i=1 to 12 do
Move rail left by dx;
    for i=1 to 12 do
        Move rail up by dy;
        if Rail and TGP8 overlaps then
            Revert last vertical move;
        end
        dy=dy/2;
    end
    if range of TGP8-rail contact angles > 20 degrees then
        Revert last horizontal move;
    End
    Vertically reposition the rail below the wheel
```

```
        dx=dx/2;
end
```

Algorithm 5-2 TGP8 fitting algorithm

Figure 5-32 shows a TGP8 fitting result.

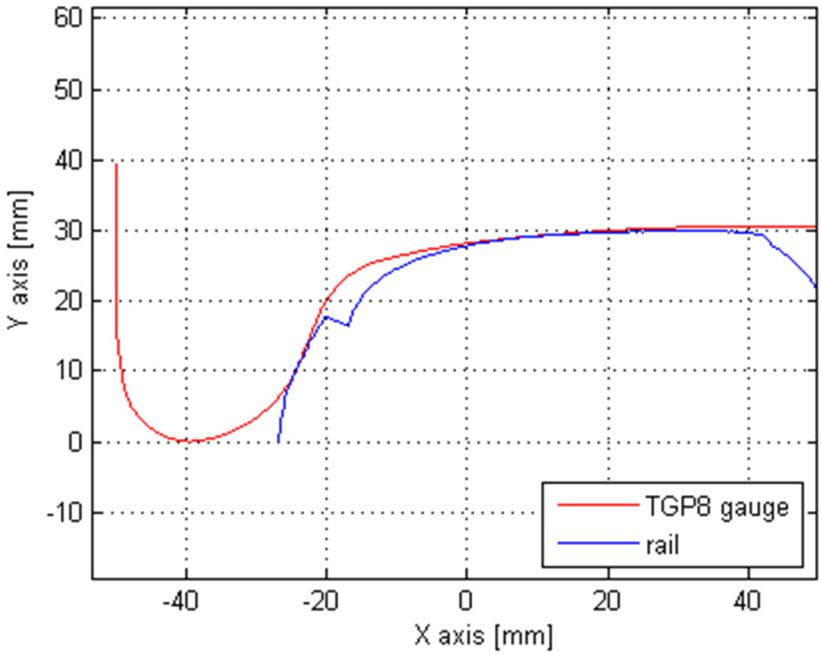

Figure 5-32 TGP8 fitting result on a measured switch (to scale)

4. Calculation of TGP8-rail contact angle

The TGP8-rail contact angle is measured by calculating the distance between the TGP8 points and the polygon formed by the rail points. As the manual measurements were carried out using a piece of white paper to aid visibility (a practice also used by some NR personnel), where the distance between the TGP8 and the rail is less than 0.1 mm (approximate paper thickness) the TGP8 was considered to be in contact with the rail. Figure 5-33 shows a close-up of a TGP8 fitting. The black circle marks the lowest point of the TGP8 that is considered to be in contact with the rail.

In Figure 5-33 the tangent at the black circled point is 59.86 degrees (to horizontal).

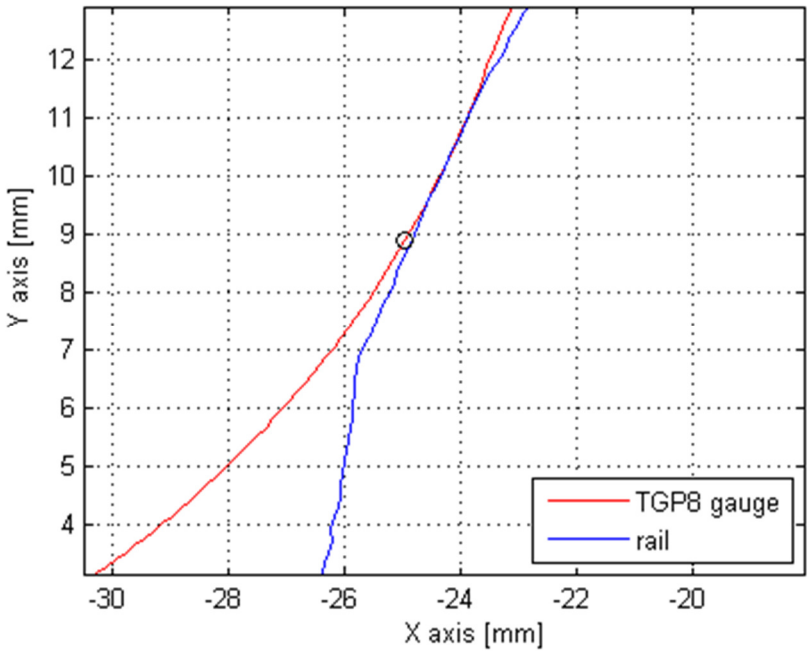

Figure 5-33 Close-up of TGP8 fitting example on a measured switch (to scale)

Discussion of proposed TGP8 algorithm

Due to the repetitive calculation of the time-consuming operation to check if a point is inside a polygon during the fitting stage, a TGP8 calculation in MATLAB® takes 8 to 9 seconds to complete on an Inter® Core™ 2 Duo @ 2.8 GHz processor. For a fitting accuracy of 50 µm (on each axis), the calculation takes 6 seconds to complete.

A different method was developed where the TGP8 gauge and rail are handled as images. The main advantage is that the previously mentioned time-consuming operation is not needed. For a resolution of 10 pixels per mm using LabVIEW® the calculation time was less than a second. However, this method introduces quantization errors. For a higher resolution of 100 pixels per mm the processing time was over a minute.

The calculation process is influenced by three sources of error:

1. Laser measurement errors

The first source of error acts as noise over the measured rail surface and it can never be completely eliminated. The noise is specific to the laser scanner and the scanCONTROL used in this work generally showed a normal distribution whereby small errors in the range of ±20 µm are more likely than larger errors in the range of ±100 µm. As one of the two contact points that usually form (thread and flange contact points) generally shows a concave shape,

the filtering algorithm presented in section 5.1.2 was not used. Due to the risk of shape deformation the rail data was used unfiltered.

As the noise increases the roughness of the rail, the increased roughness decreases the conformity between the two surfaces, which can decrease the area of contact and therefore can slightly increase the measured contact angle.

2. Laser sensor axis origin errors

In order to achieve accurate measurements it is important that the P8 wheel profile is placed over the rail at the same roll angle as the manual TGP8 gauge (which in turn is designed to replicate the roll angle of the train wheel set). During a wheel-rail contact stress analysis, Todd Euston, el al., [82] modelled a wheel set and used one wheel-rail contact point as a pivot point to rotate the wheel set until the other wheel would contact the rail, therefore calculating the correct roll angle of the wheel set. This solution is useful for a variety of wheel-rail fitting analysis; however, it can only be applied when both rails are recorded. In this work, the roll angle is calculated by knowing the transformation matrix between the trolley wheel-rail contacts and axis origin of the laser sensors. The error of the transformation matrix as well as the deformation of the trolley frame and vibration of the laser scanners has been considered negligible.

The change in roll due to TGP8 having wheel profiles at both ends was not accounted for. As the TGP8 is fitted under flange contact conditions, the other P8 profile which is placed on the opposite rail experiences a tread contact. As a result, any track gauge variations lead to very small roll angles, which have been considered negligible in the computerised TGP8 measurements (a change in height of 1 mm of the P8 profile sitting on the opposite rail leads to a roll error of just 0.036 degrees).

3. TGP8-rail fitting measurement errors

The fitting errors of 12.2 μm (for each axis) are considered negligible.

4. Measurement of TGP8 contact angle

For the identification of the lowest contact point a spacing allowance of 0.1 mm was adopted in order to simulate manual inspection methods. This is believed to introduce negligible errors. The contact angle was measured by calculating the tangent in the TGP8 profile. The high number of points forming the TGP8 point cloud data ensured a high resolution in measuring the tangent.

Overall, the highest source of errors is considered to come from the laser scanner. The difference between the manual measurements and the automatic ones is very small, but due to the nature of the measurement (shape fitting and lowest contact measurement), an overall measurement accuracy was not calculated.

Differences between TGP8 contact angle and the contact angle as experienced by train wheels

1. Under the weight of the train, point contacts deform to patches the size of small coins. This increases the conformity between the wheel and rail and thus the area of contact. This decreases the wheel-rail contact angle. In conclusion, the real wheel-rail contact angle can be slightly lower than the measured one. However, the difference is unlikely to be significant and if necessary can be partially compensated in the fitting process.
2. Under the passage of train wheels with various wheel profiles, the rails wear out to various shapes. The lowest wheel-rail contact depends on the profile of both the wheel and the rail. Where the wheel profile is similar to the rail profile, a low contact can generally be achieved. Where the wheel-rail conformity is poorer, the lowest contact angle can become higher.

For example, Figure 5-34 shows how the unworn flange of the TGP8 gauge can disallow contact to be made at a lower height and thus the TGP8 measurements can show a higher contact angle.

In Figure 5-34 the black circle shows the location where the contact angle was automatically measured and the blue circle shows where contact could be made if the flange of the TGP8 is worn.

In the case of Figure 5-35 it is the unworn gauge corner of the TGP8 which disallows contact to be made at a lower height along its flange.

Although the difference is large, such situations appear further along the switch where the derailment hazard is very unlikely to appear and thus is not even checked. This measurement was taken at 1.2 m from the switch toe whilst the TGP8 measurements are required just for the first 1 metre in the case of this switch.

There is at least one documented occurrence where the inspection of a switch passed the TGP8 gauge but failed when tested against a compliant worn P8 profile [12]. The use of the laser based system allows the measurement of the P8 contact angle using various P8 profiles (worn, part-worn, thread wear, flange wear, etc) assuring greater safety.

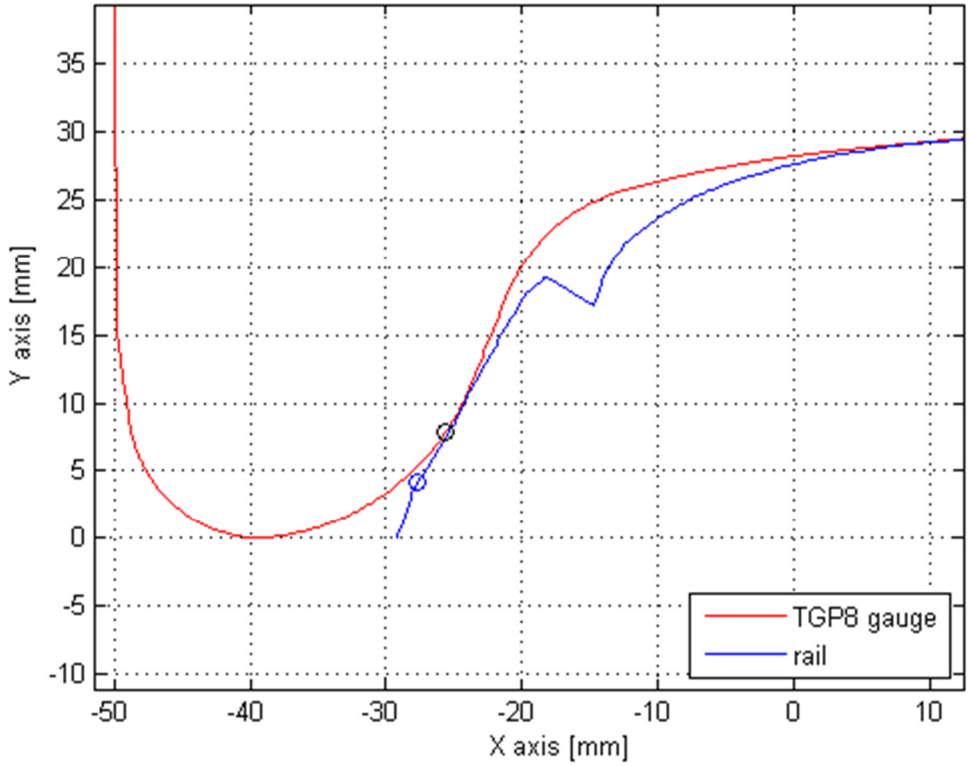

Figure 5-34 Example of TGP8 unworn flange now allowing contact at a lower height

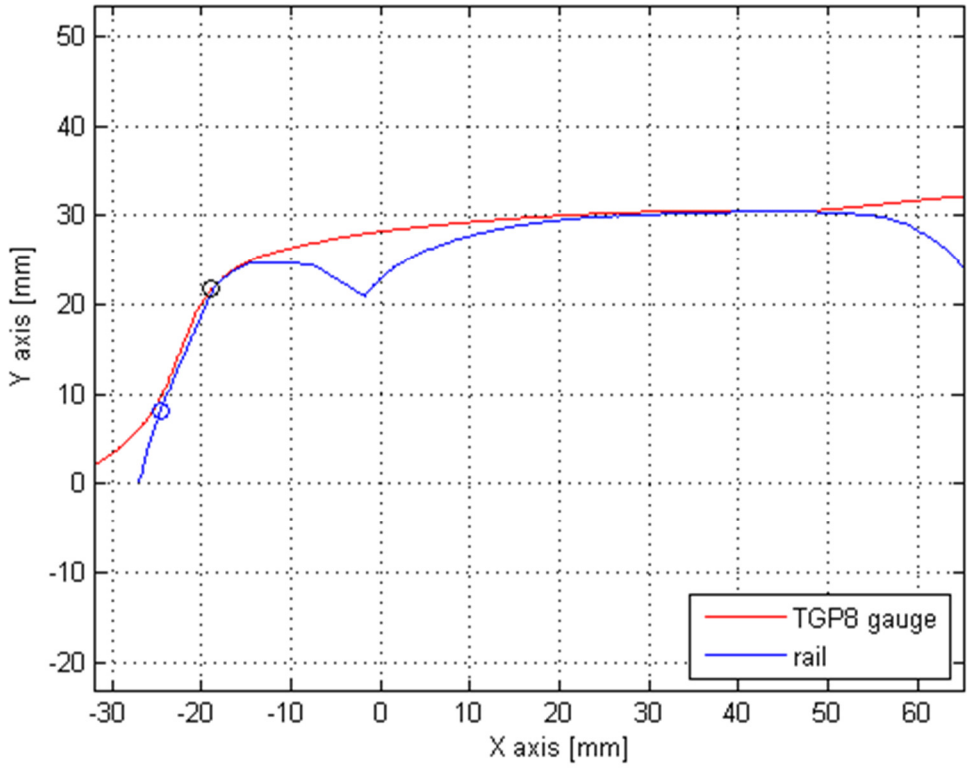

Figure 5-35 Example of TGP8 unworn gauge corner now allowing contact at a lower height

3. The TGP8 gauge measures the contact angle between the rail and a new P8 wheel when the wheel is fitted flush to the rail at a neutral angle of attack. In practice, the flange of a real P8 wheel may come in contact at a positive angle of attack, as shown in Figure 5-26. Thus, in this situation the wheel-rail contact angle can differ from the measured TGP8 contact angle. The actual contact angle depends on: wheel profile, rail profile and relative position between the two. The relative position between the two is difficult to know as it depends, among other factors, on the track geometry and vehicle suspension and dynamics. Hence, the use of a laser based system alone cannot compensate for this error unless approximations are used, which would inevitably reduce the measurement accuracy.

Although all of the above situations have the potential of generating a false-negative inspection result, which is dangerous for a safety-critical asset, the amount of error generated when using the TGP8 is relatively bounded. The author believes that the current maintenance limit of 60 degrees for a TGP8 measurement is a conservative one which can accommodate for errors in the measurements. For example, three trains managed to safely pass over a switch rail which measured a contact angle of just 46 degrees [11].

5.1.5 Derailment hazard 3

The third derailment hazard inspection is carried out, depending on the switch type, by using either Gauge 1 or a TGP8 gauge.

Gauge 1 is used to measure the height difference between the top of the stock rail and the top of the switch rail. This does not raise any challenges. The measurement of the TGP8 contact angle has already been discussed in section 5.1.4.

Any hogging of the switch rail must be measured and used in order to compensate both measurements.

5.1.6 Derailment hazard 4

As explained in the NR/L2/TRK/0053 standard, the buildup of lipping on the inner faces of the two rails slowly prevents the switch rail from fully closing. Thus, the lipping provides a pivot point against which force develops and breaks off parts of the switch rail. The aim of this inspection task is the identification of such switch rail damage as it can pose a derailment hazard.

Provided the switch rail is cleared of grease and dirt, the manual inspection can be considered to have a good immunity against human errors. In 2012 at Shrewsbury station in the UK, the failure to correctly inspect a switch rail against damage was mostly due to inadequate cleaning of the switch rail [13], which if done improperly can cause any visual inspection method to fail. However, the aim of this chapter is to replicate all inspection tasks defined in the NR/L2/TRK/0053 standard while reducing, if not eliminating, human errors.

The manual inspection starts by identifying the areas of damage. The depth of the identified damage is evaluated using Gauge 2 and the switch fails inspection if: (1) the depth of any damage renders the remaining top of the switch rail below Gauge 2 (more than 19 mm below the top of stock rail), (2) the length of the damage is more than 200 mm along the length of the switch rail, (3) if damage is present in two or more separate locations along the length of the switch rail, or (4) if the damage is associated with the switch toe. Thus, the inspection system must be able to identify damages and establish:

1. their location along the switch;
2. their length, and;
3. their depth relative to the top of the stock rail.

Methodology

The methodology for automatically identifying damaged switch rails according to the NR/L2/TRK/0053 inspection standard is composed of three steps. The first one was to first develop an understanding of what the switch rail damage is. Secondly, this understanding was then disseminated in order to identify a set of characteristics that characterise damaged switch rails and can be expressed in a mathematical context. Lastly, an algorithm was written to assess switch rails based on the identified characteristics of switch rail damage in accordance with NR/L2/TRK/0053.

Step 1: Understanding switch rail damage in accordance with NR/L2/TRK/0053

There has been little information published relating to the understanding of how the switch rail breaks and the shapes under which damage can occur. Due to the fact that switches are immediately replaced or repaired once it has been identified that they have sustained damage, it is very difficult to have access to damaged switches on the railway network. Thus, the switches that were assessed for the presence of derailment hazard 4 were either from old rail yards or in pictures obtained by the author from various sources.

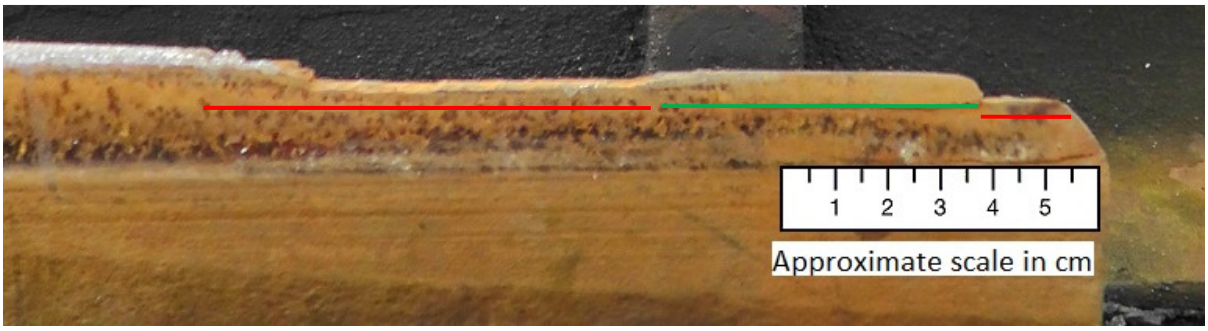

Figure 5-36 Example of damaged switch rail (photo 1)

In Figure 5-36 as well as the following figures, the red lines mark the damaged areas of the switch rail and the green lines mark the undamaged areas in accordance with NR/L2/TRK/0053.

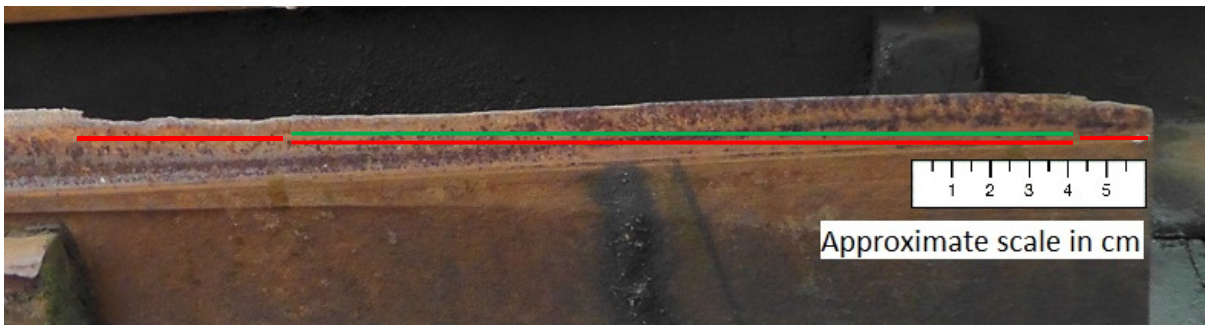

Figure 5-37 Example of damaged switch rail (photo 2)

In Figure 5-37 the switch rail has damage in both the left and the right areas. When the middle part is individually assessed it shows no signs of switch rail damage. However, given the context (how it blends with the two damaged areas) it is possible that it had also suffered damage, but for one reason or another it is in a better condition. One such reason is that rail traffic may have smoothed out the damage. As the NR/L2/TRK0053 inspection standard does not provide any guidance on this matter, the clasification is considered open for debate. In practice, such situations may require a judgement call as the application of the NR/L2/TRK/0053 standard may be insuficient.

Figure 5-38 Example of damaged switch rail (photos 3 and 4)
right: Courtesy and Copyright Joss Apps

The switch rail in the left photo of Figure 5-38 has small damage along its length (including both red and green areas). The author believes that because the damage indicated by the green line does not extend across the whole thickness of the switch rail all the way to the gauge side (along the X axis), it does not provide a rough surface on which a flange climb can occur. Thus, although vaguely specified in NR/L2/TRK/0053, the author believes that the green area in left photo of Figure 5-38 does not represent a derailment hazard.

The tip and the end of the switch rail in the right photo of Figure 5-38 are free of damage; however the middle part had sustained some damage on its field face. As in the case of the

left photo in Figure 5-38, this damage also does not extend to the gauge side of the switch rail and thus is not considered by the author to be a derailment hazard.

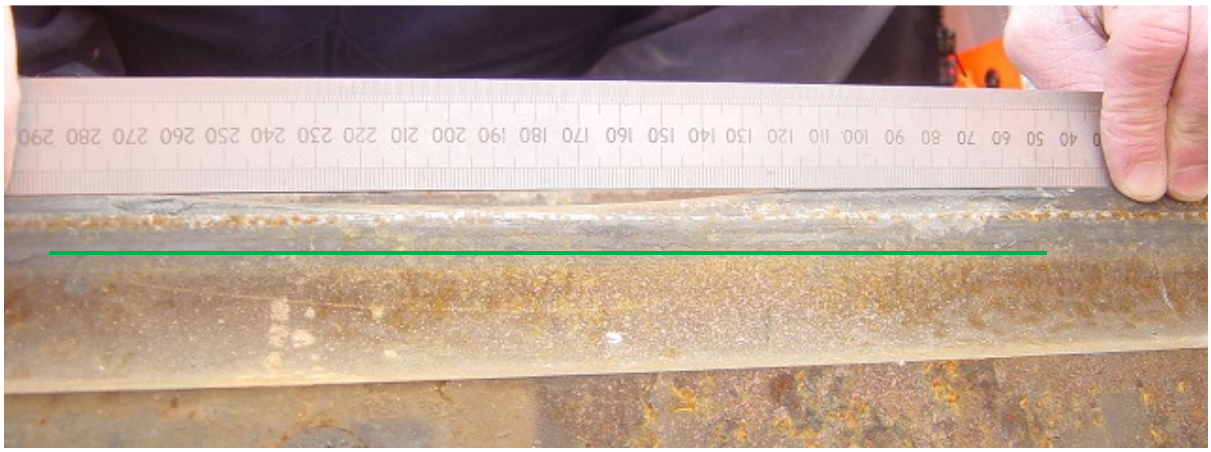

Figure 5-39 Example of damaged switch rail (photo 5)
Courtesy and Copyright Joss Apps

Although the damage pictured in Figure 5-39 is across the whole thickness of the switch rail, the damage is smooth and does not present any signs of breaking which may provoke flange climb. Thus, under NR/L2/TRK/0053 it is not considered a derailment hazard.

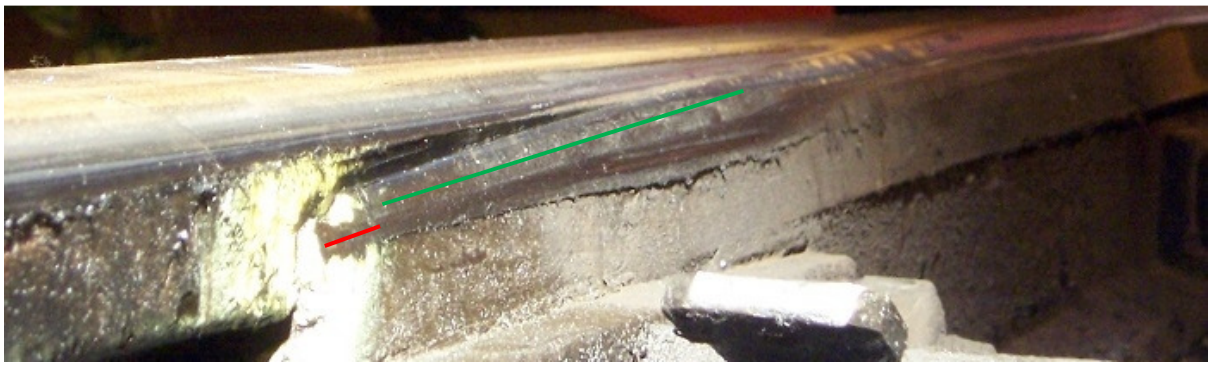

Figure 5-40 Example of damaged switch rail (photo 6)
Courtesy and Copyright Joss Apps

Similar judgement applies to the switch rail shown in Figure 5-40. With the exception of the switch tip, the switch rail does not present a derailment hazard as described in NR/L2/TRK/0053 (even though the switch rail presents a steep ramp which could help a train wheel to climb up).

Figure 5-41 Example of damaged switch rail (photo 7)

In Figure 5-41, the damage is similar to that shown in Figure 5-39 and Figure 5-40, but in comparison it is much more irregular in height. Although difficult to assess, the author believes that it does not show derailment hazard 4 as there are no signs of breaking at the top of the switch rail as described by the NR/L2/TRK/0053 inspection standard.

Step 2: Identification of switch rail damage characteristics in accordance to NR/L2/TRK/0053

Based on the developed understanding, a set of characteristics were established that define damage in accordance with the NR/L2/TRK/0053 inspection standard. These characteristics are as follows:

1. Damage is present extending across the whole thickness of the switch rail (along X axis);
2. The top of the switch rail has an irregular height along the length of the switch (along Z axis), and;
3. Parts of the switch rail which present the first characteristic but not the second may be classified as damaged if other parts of the switch present both the first and second characteristics (open to interpretation).

Step 3: Automatic inspection of switch rail damage in accordance with NR/L2/TRK/0053 inspection standard

As stated in section 3.2, one of the requirements of this research is to not use black box techniques. Thus, the algorithms must be easy to understand. The use of signal processing techniques is less transparent to the user and is not used in this work for the identification of switch rail damage.

Based on the three characteristics of switch rail damage, it is clear that the maximum height of the switch rail along its length contains enough information to be solely used for the identification of damage. Thus, it will be referred to as the *height profile*. The *height profile* is used to create a *defect free height profile* which has similar features to the *height profile* but it does not show any defects. The difference between the two is calculated and called *potential damage*. The *potential damage* is then classified as *gradient defect* (not a derailment hazard 4 damage) and *damage defect* (a derailment hazard 4 damage). The process is shown in Figure 5-42.

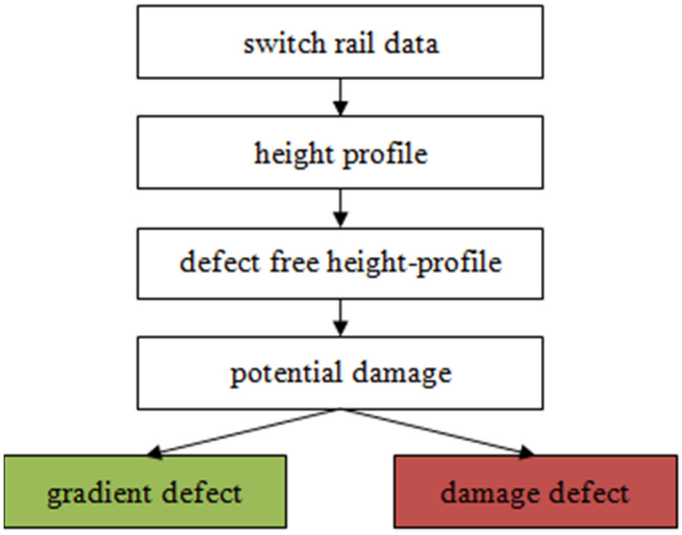

Figure 5-42 Damage identification process

The *height profile* of in-service switches can be very different from the manufacturer specifications and still be considered to be in a good condition, therefore the *defect free height profile* is derived from the *height profile* and not S&C design specifications.

Figure 5-43 shows the correct *defect free height profile* for four hypothetical switch rail *height profiles*. For the sake of clarity the figure is shown at a scale of 1:1 and the *defect free height profile* is shown slightly above the *height profile*.

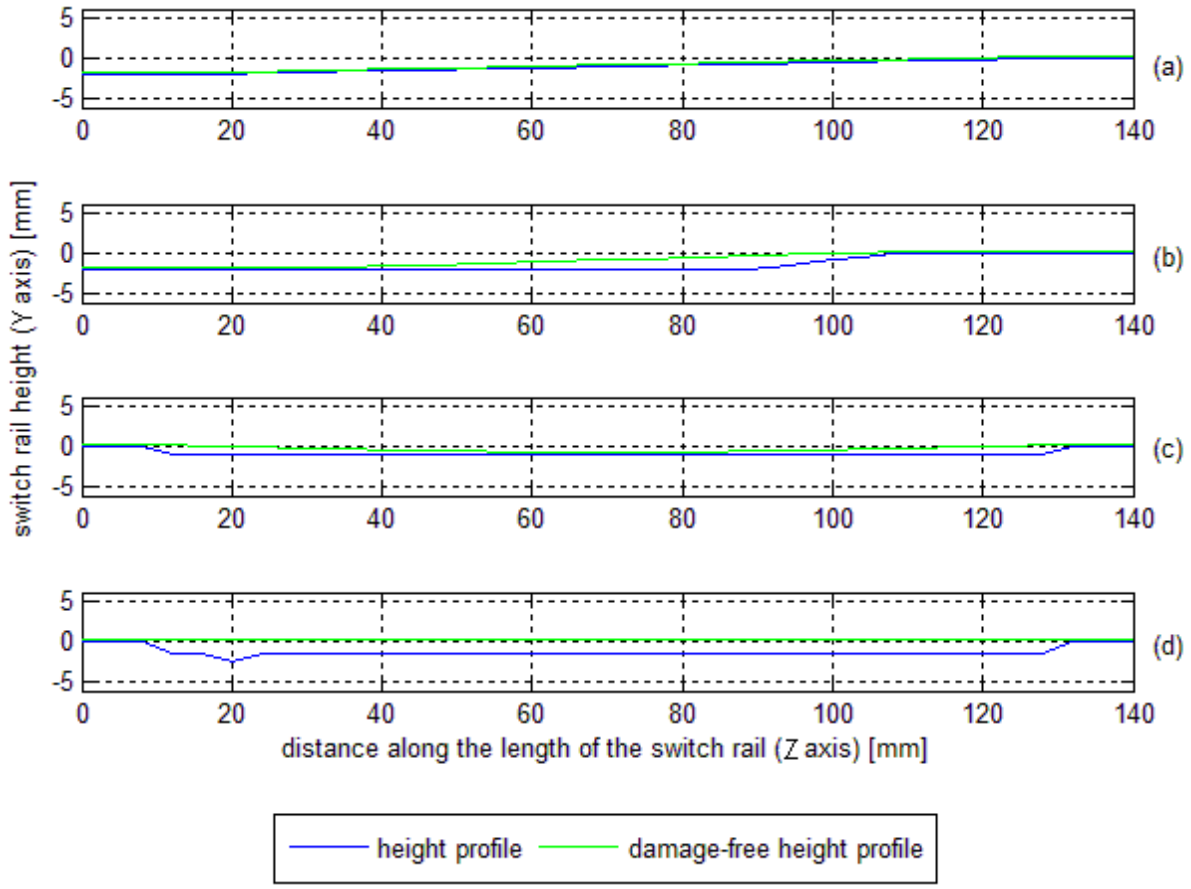

Figure 5-43 Defect-free height profiles for four theoretical height profiles (1:1 scale)

A distinctive feature that the *defect-free height profile* must have is that it should have a holistic view of the switch. For example, in Figure 5-43 plot (c), the *defect-free height profile* identifies two separate possible defect areas whereas in Figure 5-43 plot (d), due to the higher defect depth, the two defects are treated as just one.

The calculation of the convex hull of the *height profile* partially satisfies the requirements for the generation of *defect-free height profile*. However, as it is not sufficient, an extra step has been introduced. Prior to the calculation of the convex hull, the *height profile* is deformed. The amount of deformation is proportional to the severity of height variations, which are still considered defect-free. The process is graphically shown in Figure 5-44, where the blue plot represents an *height profile* 2 metres long and the green plot represents the *deformed height profile* using a radius of 1.5 meters.

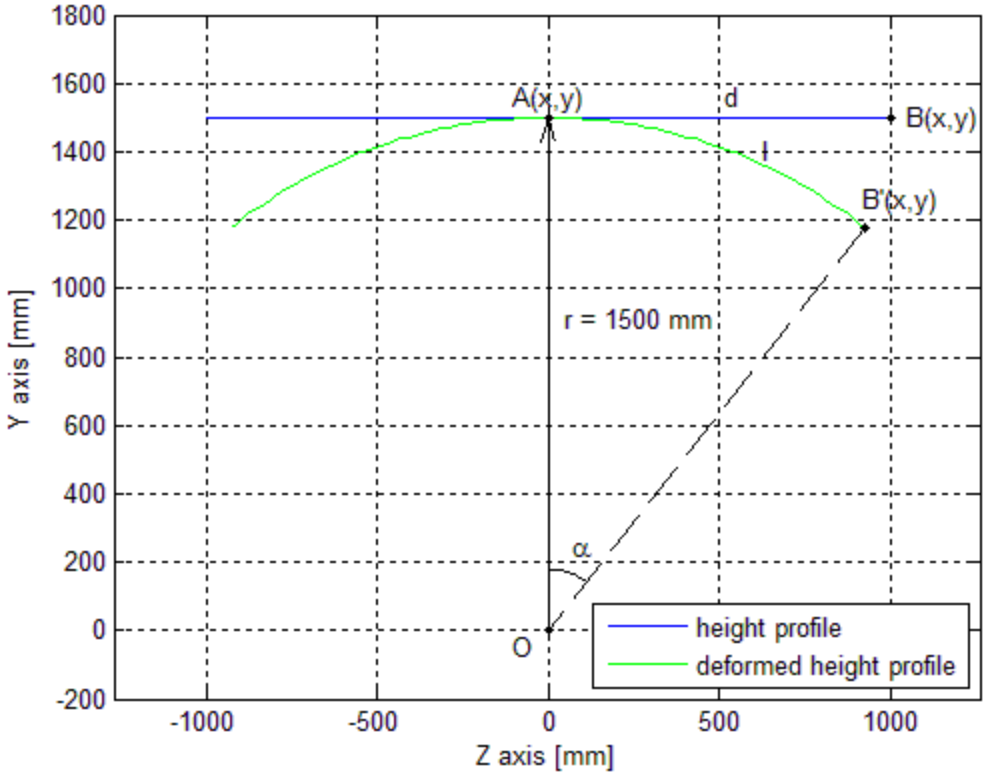

Figure 5-44 Deformation of height profile before calculation of convex hull (to scale)

Considering point B(x,y) part of a perfectly horizontal *height profile*, B'(x,y) is calculated using the following formulas:

$$\propto [rad] = \frac{l}{r}$$

$$B'(\mathrm{x}) = \mathrm{r} \cdot \sin(\alpha)$$

$$B'(\mathrm{y}) = \mathrm{r} \cdot \cos(\alpha)$$

Where $l = d$ and $d = B(x) - A(x)$.

Now considering a *height profile* which is not perfectly horizontal, then any height variations are added to the deformed height profile along OB' and thus the last two formulas become:

$$B'(x) = r \cdot sin(\alpha) + \big(B(y) - A(y)\big) \cdot sin(\alpha)$$

$$B'(y) = r \cdot cos(\alpha) + \big(B(y) - A(y)\big) \cdot cos(\alpha)$$

The convex hull of the deformed *height profile* is then calculated. The indexes of the points that define the convex hull are then used to identify the shape of the *defect free height profile* based on the original *height profile.*

The last step is defect classification. In Figure 5-45, plot (a) shows a relatively good *height profile*, plot (b) one with a *damage defect*, plot (c) one with a *gradient defect* and plot (d) one with a *damage defect* and high gradients (i.e. a combination of plot (b) and (c)). For clarity they are shown at a scale of 1:1.

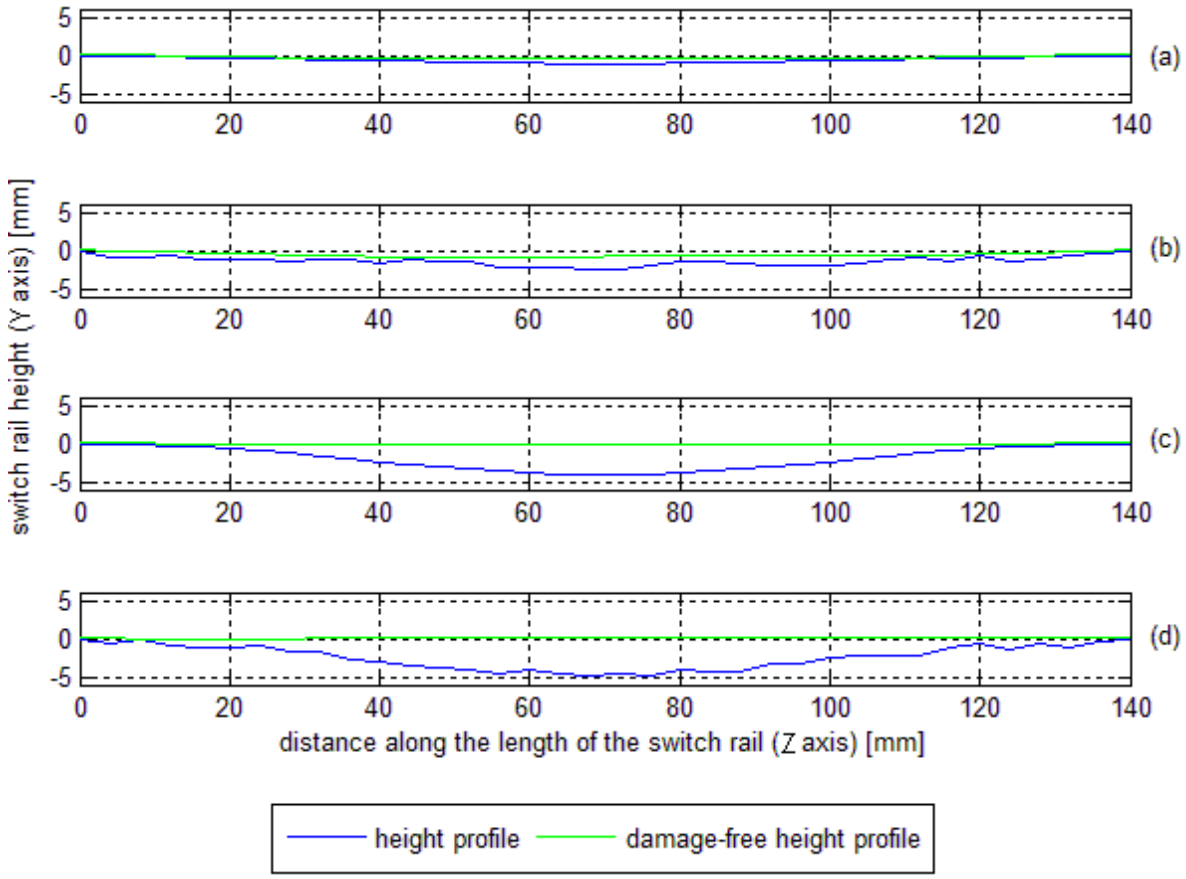

Figure 5-45 Switch rail height profile examples (1:1 scale)

According to the identified characteristics of a damaged switch rail, the second derivative of *potential damage* can be used to identify *damage defects*. Thus, a simple threshold technique can be used to identify the damage defects. The results are shown in Figure 5-46.

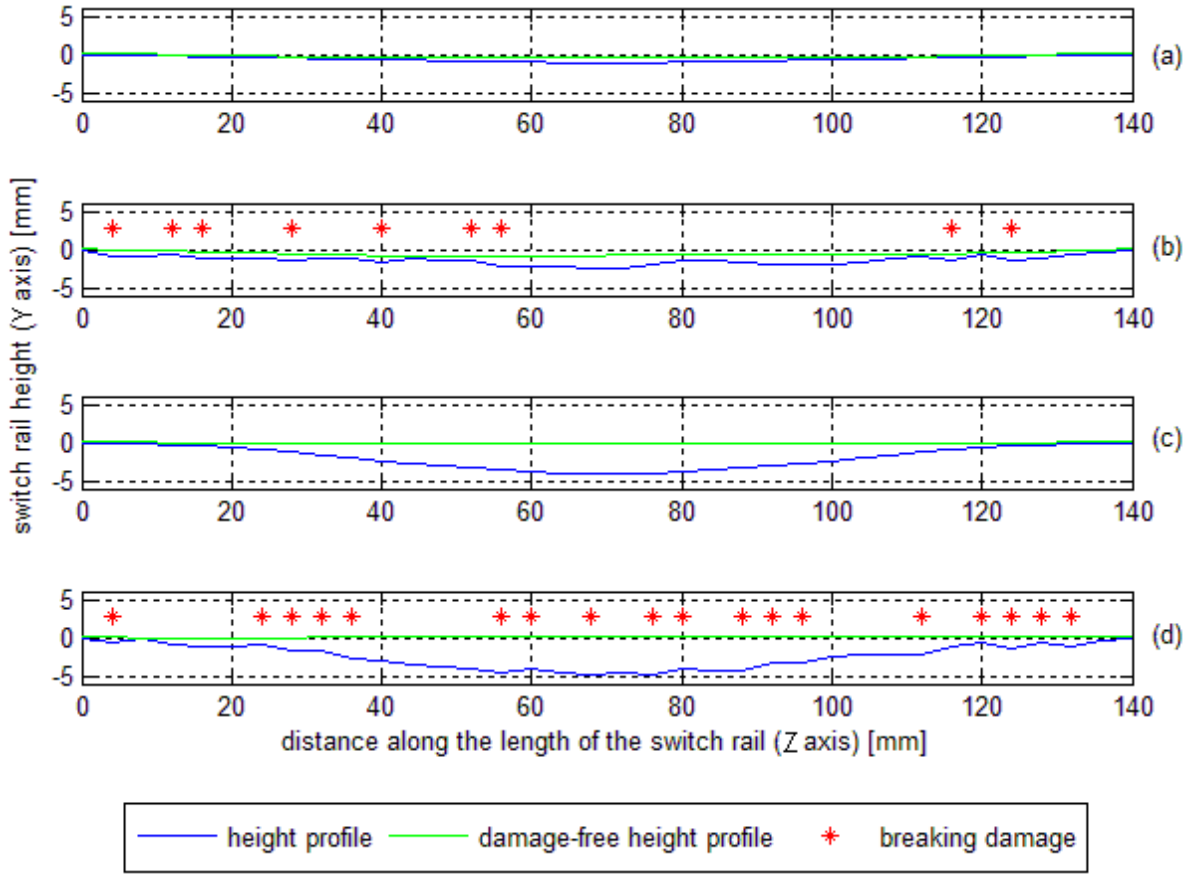

Figure 5-46 Identified damage defects in four hypothetical scenarios (1:1 scale)

In Figure 5-46 the red stars show where the second derivative of *potential damage* exceeded 40 µm/mm^2. Using this method, both small damage defects of just 1 mm (Figure 5-46, plot (b)) and large *gradient defects* (Figure 5-46, plot (c)) are correctly classified. In this example, the second derivative of *potential damage* in plot (c) was 8 times smaller than the threshold value.

Where no more than one or two damaged points are identified, the length of the damage is considered the same as the distance between the two consecutive 2D profiles (4 mm in this case). Where several damaged points are identified, the damage length is considered the same as the length of the *potential damage* (which is the case of Figure 5-46, plots (b) and (d)).

The *potential damage* also estimates the depth of the damage.

Automatic inspection of switch rail damage on a measured switch

As switches are immediately repaired or taken out of service once a derailment hazard is identified, the number of switches on the rail network which show a derailment hazard 4 is very is low. Moreover, due to health and safety requirements, it also very difficult to access a switch for research purposes on a live part of the NR infrastructure. Thus, due to this

combined difficulty, the measured S&Cs are limited in their diversity of faults. Figure 5-47 shows a photo of one of the switches that was inspected that had the greatest amount of damage, 13 PTS.

Figure 5-47 Photo of a measured switch (13 PTS, Whitemoor Rail Recycling Centre, photo 1)

Although the switch rail is overall in a poor condition, it does not present a derailment hazard 4. In plot (a) of Figure 5-48, the *damage-free height profile* correctly follows the shape of the *height profile* (abbreviated h.p. in Figure 5-48) where the gradients are small, but also identified a defect where the gradient changed abruptly.

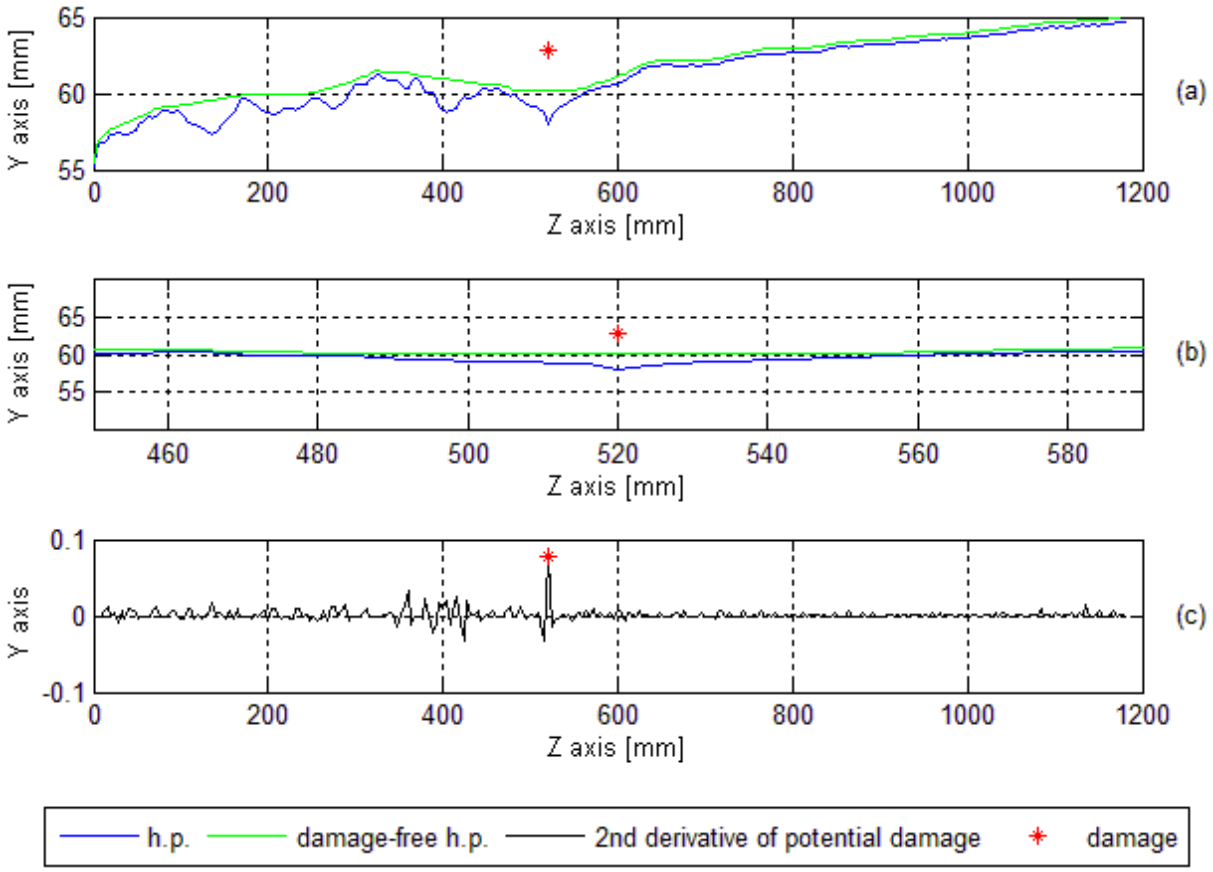

Figure 5-48 Switch rail damage analysis (plot b to scale 1:1)

A damage point was identified at 520 mm along the length of the switch. The location is shown in Figure 5-49 and its profile in plot (b) of Figure 5-48.

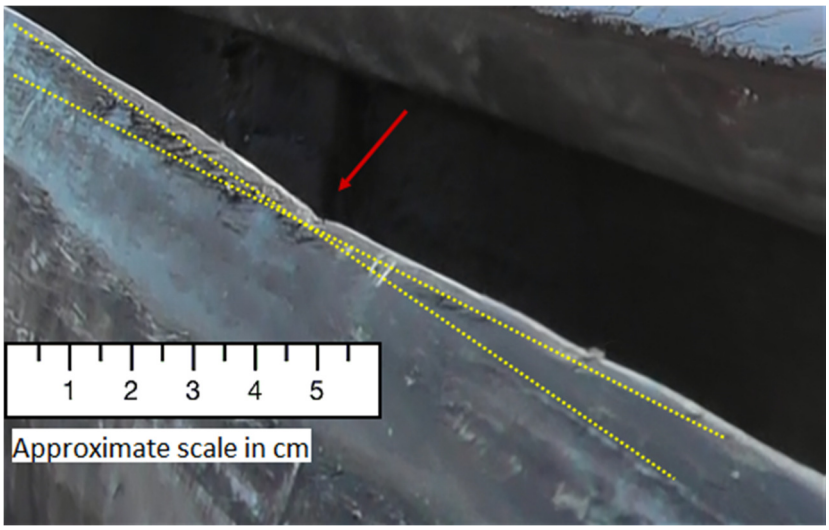

Figure 5-49 Photo of a measured switch (13 PTS, Whitemoor Rail Recycling Centre, photo 2)

The result is considered good as it reflects the outcome of an inspection as specified by the NR/L2/TRK/0053 inspection standard. As the length of the damage was identified at 4 mm (equal with the sampling period), the switch passes the derailment hazard 4 inspection.

5.1.7 Derailment hazard 5

The last derailment hazard within the NR/L2/TRK/0053 standard is concerned with the possibility of flange climb due to a sharp gauge corner profile. As explained in the standard, sharp gauge corners, which resemble the corners of a 20p coin, may provide an edge that can cut into the wheel and form a ledge to climb. The derailment risk is present in the case of austenitic manganese steel (AMS) switches only.

The manual inspection against sharp gauge corners is carried out using a small gauge, switch rail radius gauge, the size of a one pound coin.

Inspection procedure

Figure 5-50 shows three examples of correct inspection as published in the NR/L2/TRK/0053 inspection standard.

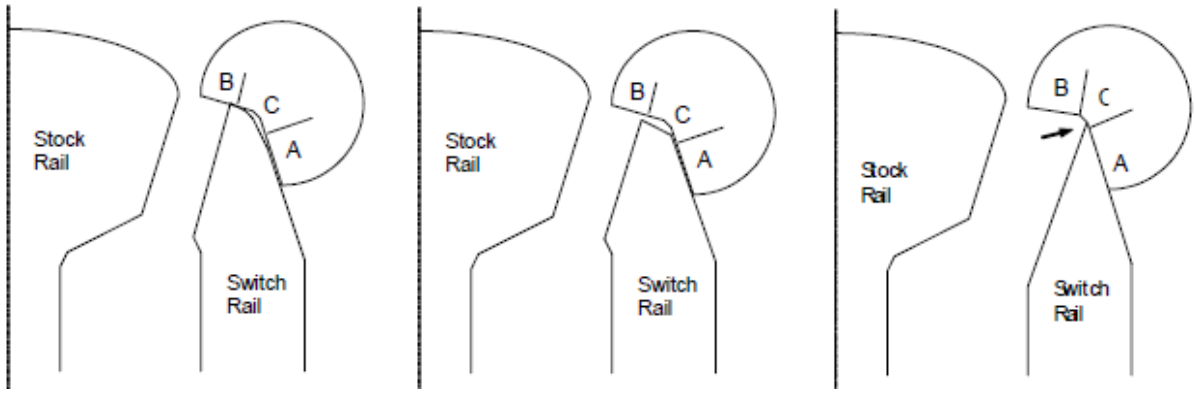

Figure 5-50 Exemplification of the usage of switch rail radius gauge
Courtesy and Copyright Network Rail

The following is a summary of the five inspection rules as stated in NR/L2/TRK/0053 [15]:

1. Face *A* of the switch rail radius gauge must be fitted flush to the rail; in Figure 5-50 all diagrams are considered to follow this rule although the left diagram can arguably be a good example;
2. If the switch rail is of "sufficient thickness" and there is no contact in face *B*, it fails the switch rail radius gauge inspection (e.g. Figure 5-50, centre diagram);

3. If the switch rail is so thin that the top of the switch rail falls within face *C*, it has to make contact at the top of face *A* in order to pass the switch rail radius gauge inspection (e.g. Figure 5-50, right diagram);
4. If the switch rail touches faces *A* and *B* and leaves a gap at *C* it passes the switch rail radius gauge inspection (e.g. Figure 5-50, left diagram), and;
5. Visual or tactile evidence of a sharp gauge corner fails the switch rail even if it passed the switch rail radius gauge inspection.

The above five rules form the basis for passing or failing a switch rail assessed for sharp gauge corners. In this section, each of the above rule is referred to as the n^{th} rule (e.g. 1^{st} rule through 5^{th} rule).

The 5^{th} rule implies that the inspection of the switch rails against derailment hazard 5 cannot be carried out by using only the switch rail radius gauge and that visual or tactile evidence can fail the switch rail irrespective of the inspection outcome of the gauge.

As the gauge has an arc circle cutting of 60 degrees with a radius of 6 mm, it fails any switch which has a radius gauge corner of less than 6 mm over at least 60 degrees (application of 2^{nd} rule).

Potential issues relating to the correct application and usage of switch rail radius gauge

The majority of switches (>95%) on the rail network can be confidently assessed based solely on the inspection standard. However, some switch rails may have a profile for which the correct inspection is not apparent in the inspection standard. In other words, the information provided by the inspection standard is not sufficient to always provide a confident and objective inspection result. Because of this, the use of the gauge can be subjective and may require a judgement call. Thus, through several meetings it was rapidly said that the gauge can be sometimes used in a subjective manner.

To develop a good understanding, a set of various switches was inspected, which included many non AMS (austenitic manganese steel) ones. Hypothetical situations were also considered. The following is a summary of the concerns raised relating to the inspection of switches using the switch rail radius gauge:

1. The size of the features that must be observed can sometimes be less than a millimetre. This makes it difficult to achieve precise and accurate inspections.

2. The phrase “thin such that the top surface of the switch rail falls within face *C* of the gauge” can lead to subjective use of the gauge. It is possible that for a given switch rail one person would class it as thin enough, apply the 3rd rule and pass it if contact is made at the top of face *A* and another would class the same switch rail as not thin enough to apply the 3rd rule and apply the 2nd rule and fail it.

3. Correct usage of the gauge implies that face ‘A’ is fitted flush to the rail. This is not always possible as the switch rail may have a concave or convex surface which face ‘A’ should be in contact with. The inspection standard does not define how the inspection should be carried out in such situations. Possible causes of concave and convex switch rail gauge faces are: damage, deformation, lipping and poor grinding. For slightly convex surfaces the gauge can usually be positioned in slightly different wrong positions. The more convex the face is, the greater the range of possible incorrect positions. This can lead to both pass and fail results on a single switch rail.

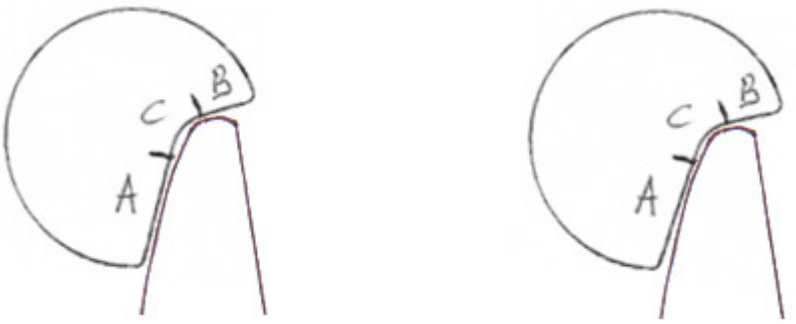

Figure 5-51 Example of how rocking of switch rail radius gauge may lead to different inspection results (left: pass example; right: fail example)

In Figure 5-51, the two rails have the same shape. The gauge is positioned differently by rocking it clockwise and anticlockwise. The left diagram shows the gauge fitted so that the lower part of the *A* face conforms better than the upper part. This can lead to the application of the 4th rule as the switch rail makes contact at *B* and has a gap at *C*, therefore passing it. Similarly, the right diagram shows the gauge fitted to better conform to the higher part of the *A* face. This can lead to the application of the 2nd rule, as the switch may seem thick enough and it does not make contact at *B*, therefore failing it.

4. Two specific situations can make it difficult to achieve an accurate and precise reading using the switch rail radius gauge. Considering a switch rail which conforms well on all three faces of the gauge (e.g. left diagram in Figure 5-52), it is difficult to accurately and

precisely identify if there is a small gap or a contact at face *C*. Similarly, considering a situation where the gauge may be in a small contact with the rail at the boundary between face *B* and *C* (e.g. red circle in Figure 5-52), it is difficult to objectively identify whether or not the contact is in face *B* or face *C*. Furthermore, by rocking the gauge clockwise and anticlockwise, the small contact can be slightly moved into face *B* or face *C,* which can change the outcome of the inspection (2nd rule and 4th rule).

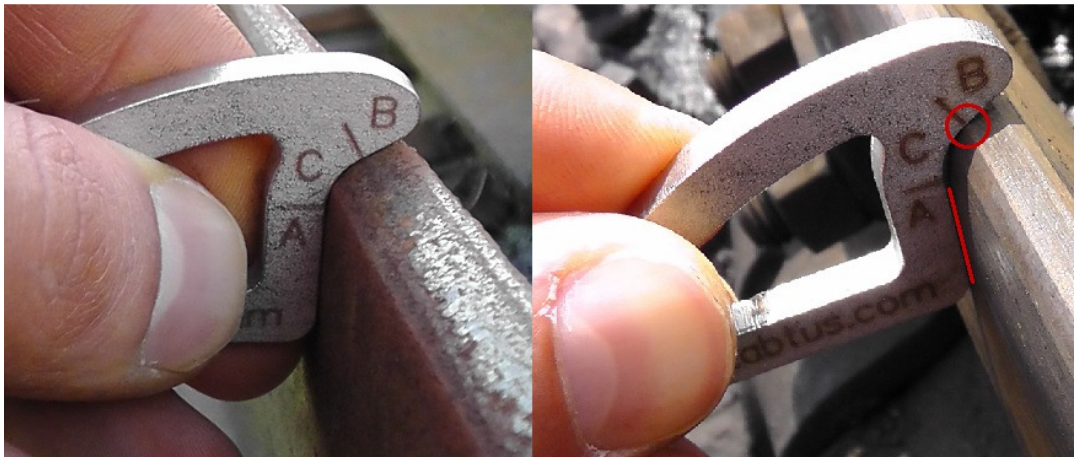

Figure 5-52 Two specific cases where it is difficult to accurately and precisely inspect switch rails using the switch rail radius gauge

5. In some situations, the use of the switch rail radius gauge can pass a switch rail that has a sharp gauge corner. In Figure 5-53, the 4th rule passes the switch rail in the left diagram and the 3rd rule passes the switch rail in the right diagram. Both switch rails have a sharp gauge corner.

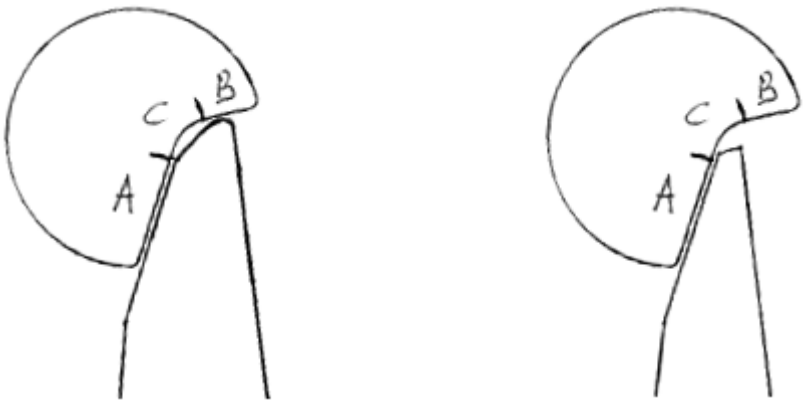

Figure 5-53 Diagram of two theoretical sharp switch rails that pass the switch rail radius gauge

The switch rail radius gauge can also fail to identify the sharp corners of the British 20 pence and 50 pence coins. Accepting that the *A* face cannot entirely be fitted flush, the application of the 4th rule passes both situations shown in Figure 5-54.

Figure 5-54 Switch rail radius gauge applied on a 20 pence and 50 pence coin

Thus, the switch rail radius gauge cannot reliably be used to meet the aim of derailment hazard 5 as stated by the inspection standard, which is to identify rails with pronounced edges "like a 20p coin" [15].

In a report written by Zarembski [61], an expert panel concluded: "This gauge [switch rail radius gauge] was judged to be inconclusive. The difference between compliance and non-compliance was determined to be very small, and it was not clear where non-compliance represented a dangerous condition."

The challenges of replicating derailment hazard 5 inspections as required by NR/L2/TRK/0053 inspection standard

It has been concluded that, accepting the inherent reliability limitations of the switch rail radius gauge, the research and design of an automatic inspection algorithm to replicate the derailment hazard 5 inspection requirements would require: (1) the development of a clear and concise set of rules that can define the correct application of the gauge on any piece of rail, (2) the research and development of an algorithm that can be assured to reliably carry out the fitting process based on the identified rules and (3) the research and development of an automatic inspection algorithm that can carry out the inspection task of visually and tactilely checking for signs of a sharp gauge corner. The third inspection task is difficult to automate due to its weak and loose definition, as the inspection task is not defined in a complete, objective and measurable manner.

Thus, due to the following reasons, the development of an algorithm for automatic inspection of switch rails against derailment hazard 5 is difficult to research and develop:

1. the switch rail radius gauge has, to some extent, inherent reliability issues;
2. is it difficult to accurately establish the correct use of the gauge for any rail shape, and;
3. it is difficult to accurately establish what tactile and visual evidence of a sharp switch rail is.

As a result, the author considers that the development of an alternative method for automatic inspection of switch rail sharpness is the best way to proceed. By considering an alternative approach:

1. the issues related to the correct usage of the gauge, the automatic fitting process, the gauge's inherent limitations and the automatic inspection of visually and tactilely inspecting the switch rail can all be avoided, and;
2. a more scientific approach can be developed resulting in higher reliability and safety assurance.

It must be noted that the development of an alternative method for the inspection of switch rails against sharp corners implies that the automatic inspection results are no longer fully comparable with manual inspection results.

The requirements and challenges of inspecting switch rails for sharp corners

The first question that needs to be answered is what rail property should be measured. Sharp corners can be well defined by two parameters: (1) the amount of angle change along the surface of the rail and (2) the distance along the surface of the rail over which the angle change takes place. However, the ratio between angle change and distance may not be sufficient if adequate values for angle change or distance are not considered. In order to establish meaningful limits, the following criteria are considered:

1. the rail shape must show an angle change greater than a certain limit in order to consider it a potential sharp corner; thus, the angle change is considered a qualifying parameter which has to reach certain levels, and;
2. a corner has to change its angle over a distance less than a certain limit in order to be a sharp one; thus, the distance parameter is considered a severity measurement

parameter which has to be below a certain level to consider the edge a severe one (failure).

Both parameters have to fulfil certain limits for a switch to be positively identified. Figure 5-55 shows the adopted limits for the identification of sharp switch rail corners.

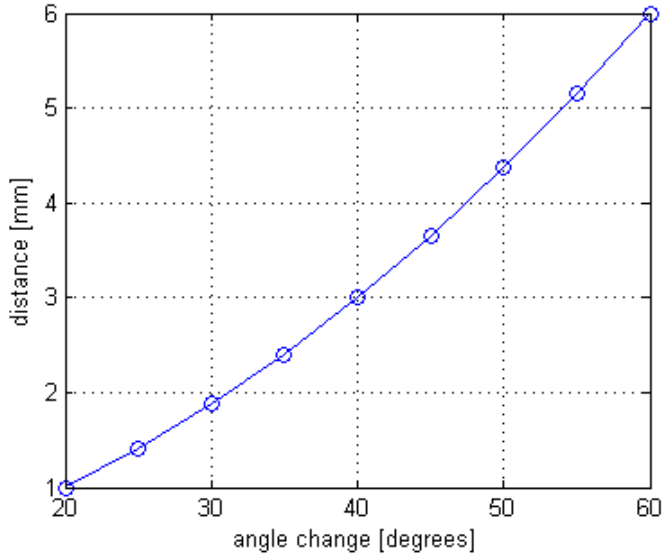

Figure 5-55 Limits for the identification of sharp switch rail corners

As there is no standard for identifying such limits, the limits used in this work have been established empirically through observation of various switch rails with and without sharp corners. Angle changes of less than 20 degrees are not considered a hazard even if the distance is as low as zero. Angle changes of 20 degrees are still considered too small to pose a derailment hazard 5, but are identified anyway. Angle changes of 25 to 35 degrees are considered to reflect the commonly sharp corners found on the railway network which pose a derailment hazard 5.

The design of the switch rail radius gauge features a corner of 60 degrees over a distance of 6.28 mm. Therefore, the gauge would fail any switch which shows a distance of less than 6.28 mm over an angle change of 60 degrees. This gauge behaviour was adopted in the new method by setting a limit of 6 mm for an angle change of 60 degree. However, most faults are expected to show an angle change of around 25 to 30 degrees.

Switch rails are positively identified if the distances along the angle changes of 20, 25, 30, 35 and 40 are: 1, 1.4, 1.9, 2.4 and 3 mm.

Considering two points in a two dimensional coordinate system defined by $P_1 = \{x_1, y_1\}$ and $P_2 = \{x_2, y_2\}$, the angle of the line that passes through the two points can be calculated using the following formulas:

$$m = \frac{y_2 - y_1}{x_2 - x_1}$$

$$\propto = \arctan(m)$$

where α is the angle. However the simple calculation of angle on a measured profile generally leads to poor results. Figure 5-56 shows a measured rail profile. Although the rail profile did not show any sharp corners, the use of the above formulas leads to noisy measurements of the rail angle, as shown in the lower plot of Figure 5-56.

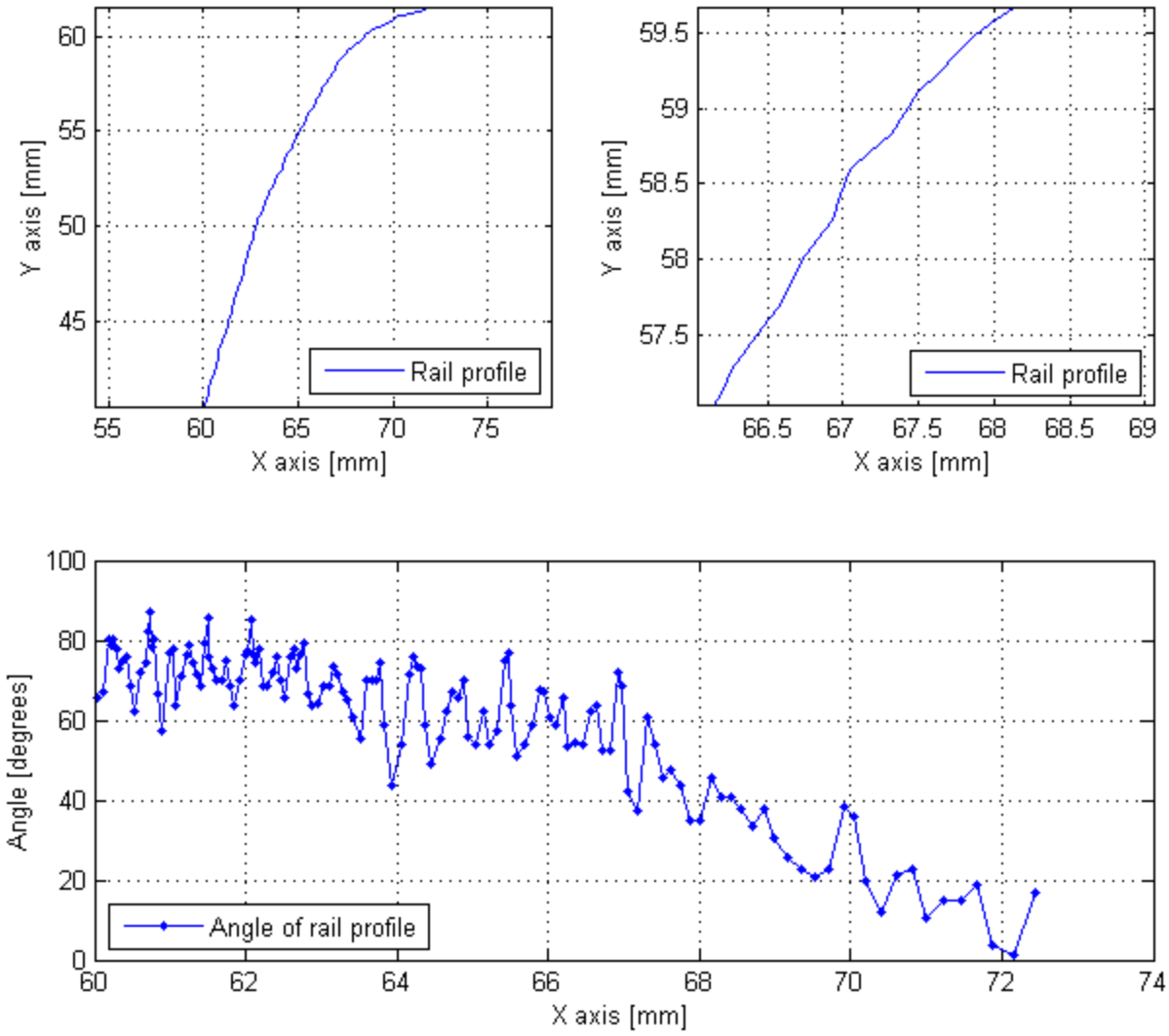

Figure 5-56 A switch rail profile and its angle along its surface

The difficulty in measuring the angle comes from the fact that the angle of the raw data shows high noise levels of up to ±15 degrees (as shown in the lower plot of Figure 5-56) although the surface can be considered to be relatively round (as shown in the upper left plot of Figure 5-56). As a result, the identification of 20 degrees corners is not immediately possible due to the high noise level. Ideally, the noise level should be at least four times lower than the useful value (e.g. less than ±5 degrees). Furthermore, the distance over which the angle change should be measured is just 1 mm, meaning that it could be defined by as few as just four 2D points.

In general, angle measurement methods which use very few points around the point where the angle is to be calculated result in noisy measurements, while methods which have a more holistic approach to the data (e.g. curve fitting) result in smoother measurements. The use of feature preserving filtering algorithms also presents a risk on both sides; they can over filter the data or accentuate the corners.

Another issue with the inspection of sharp corners is related to the overall shape of the rail and how it interacts with the train wheel. Due to the localized nature of the wheel-rail contact, a switch rail with a sharp surface may not pose a derailment hazard 5 if the sharp corner never comes in contact with any train wheels. Such a situation is shown in Figure 5-57.

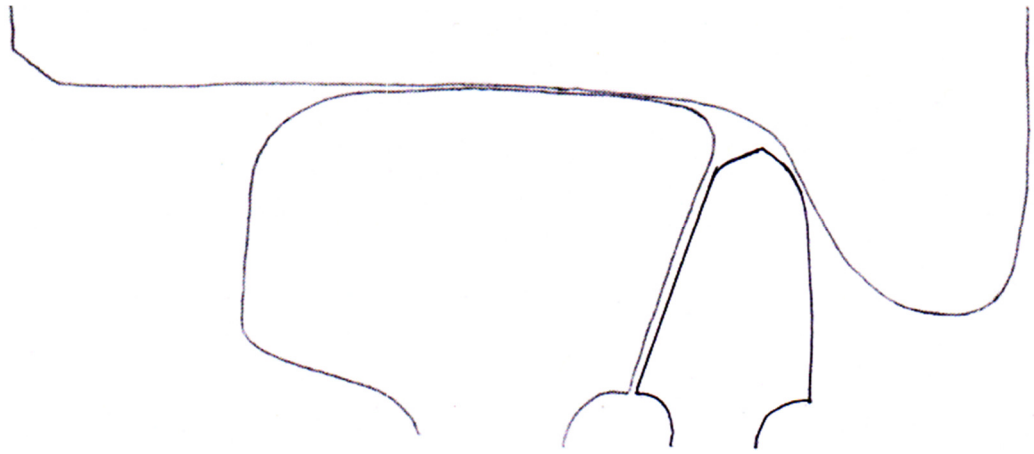

Figure 5-57 Sharp switch rail that does not pose a derailment hazard 5 (diagram 1)

Such situations should be identified in order to avoid the expenditure of unnecessary maintenance.

As the shape of the rail can change to an unknown shape through wear, damage and maintenance, very little information can be inferred about the rail which can be used for the

task of assessing its sharpness. For example, in many situations (as in Figure 5-57) sharp corners with angles close to horizontal do not come in contact with the train wheel. However, it cannot be concluded that the above statement will apply to all inspected switch rails. For example, the switch rail shown in Figure 5-58 has a very similar shape but due to its very low height, it is likely to make contact with train wheels.

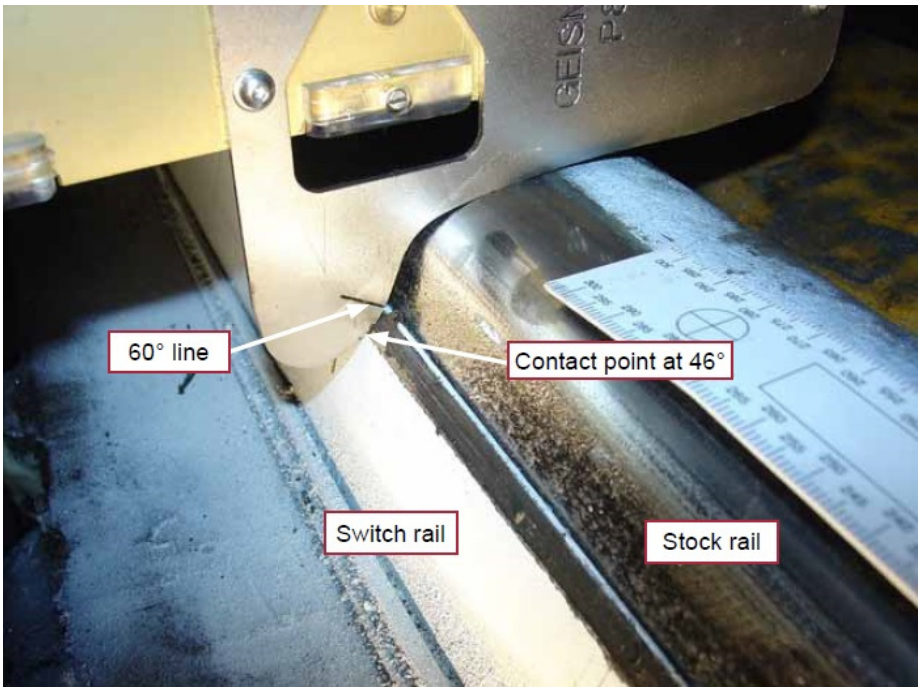

Figure 5-58 A switch rail with a sharp gauge corner
Courtesy and Crown Copyright RAIB

Thus, if anything is to be inferred about the impossibility of a sharp rail corner posing a derailment hazard 5, an approach must ensure that the statement is valid for all situations that can take place.

In order to identify if a sharp switch rail corner poses a derailment hazard 5, the wheel-rail interaction can be analysed. However, the analysis would reveal the answer only for the wheel profile used in the analysis. Analysis with a worse case wheel profile is not feasible, because in this context there is no wheel profile which can act as a worst case for all switch rails. This is because worst case is a case where the wheel profile is in contact with the largest possible area of the switch rail. This implies that the wheel-rail conformity is extremely good, which also implies that the wheel has a shape which is very similar to the combined shape of the stock rail and switch rail. The use of a set of wheel profiles in a wheel-rail analysis poses two other issues: (1) possible large computation time (as one accurate wheel-rail fitting can

take a few seconds to compute) and (2) the task of demonstrating that the selected set of wheel profiles is diverse enough to identify derailment hazard 5 for any switch rails.

Development of inspection algorithm

The first issue to be discussed here is the accuracy of the measured rail angle. Figure 5-59 shows the profile of a new P8 wheel and its corresponding angle.

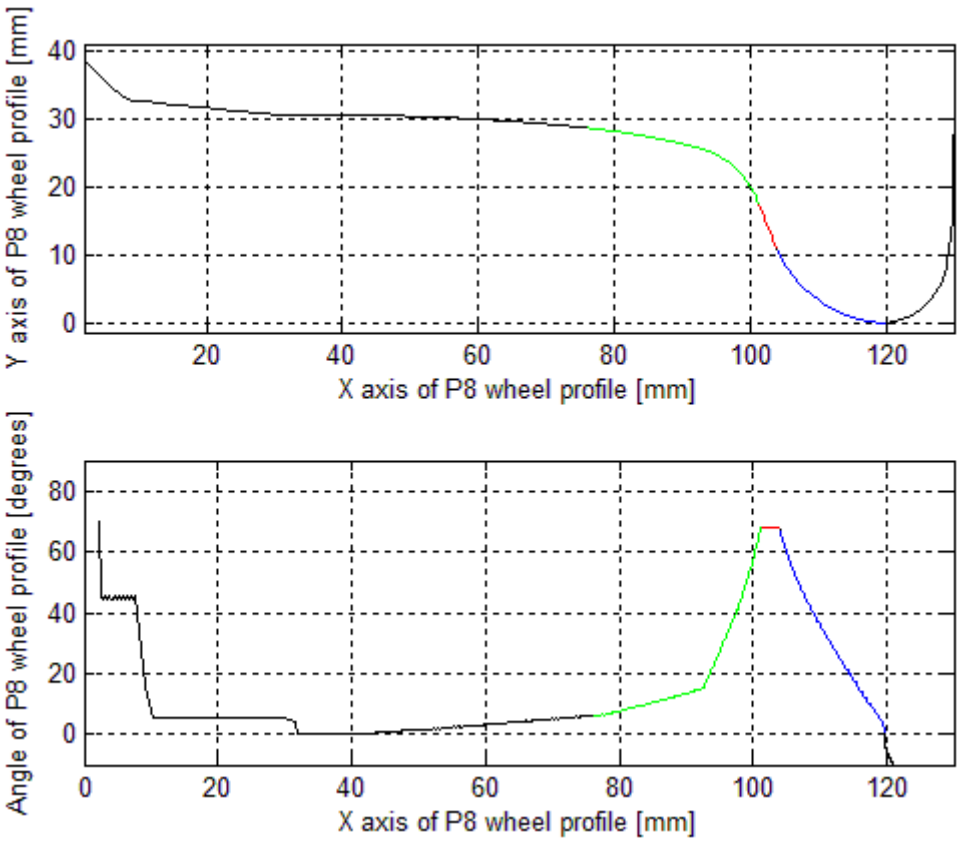

Figure 5-59 P8 wheel profile and its corresponding tangent

It can be observed that the angle of a new P8 profile (bottom plot of Figure 5-59) has three distinct sections: a green section where the angle is strictly increasing, a red section where the angle is constant, and a blue section where the angle is strictly decreasing. As the green and blue sections show strictly increasing and strictly decreasing angles, they are concave (green) and convex (blue) shapes. In all new and worn wheels, these sections always come as a whole and in the same order.

Figure 5-60 shows the profile and corresponding angle of two measured worn train wheels.

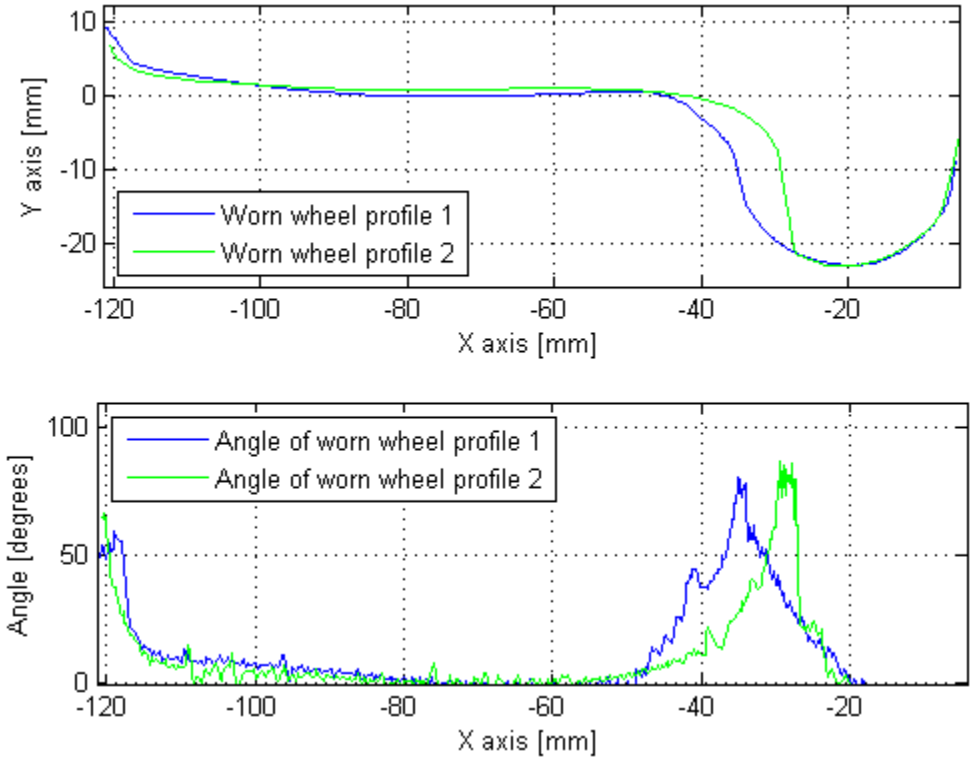

Figure 5-60 Two worn wheel profiles

Although the three sections in the two angle profiles shown in the bottom plot of Figure 5-60 are not strictly increasing, constant and strictly decreasing, the reason is considered to be primarily due to measurement errors and secondarily to very small wheel imperfections/defects. Thus, the wheel angle profiles are considered to be monotone.

When two objects are pushed against each other, any concave section of one object cannot come in contact with any concave section of the other object. In the context of wheel-rail interaction this means that any concave sections of the rail cannot come in contact with the concave section of the wheel. Because of this, considering just the concave and straight sections of the wheel, a wheel-rail fitting using the convex hull of a convex rail (instead of the actual rail) will result in the same contacts as when using the rail. Thus, the convex hull of the rail is used to improve the measurement of the rail angle.

Figure 5-61 shows that the convex hull is able to both (1) smooth out the measured angle and (2) have very little negative effect on the real corners which must be measured.

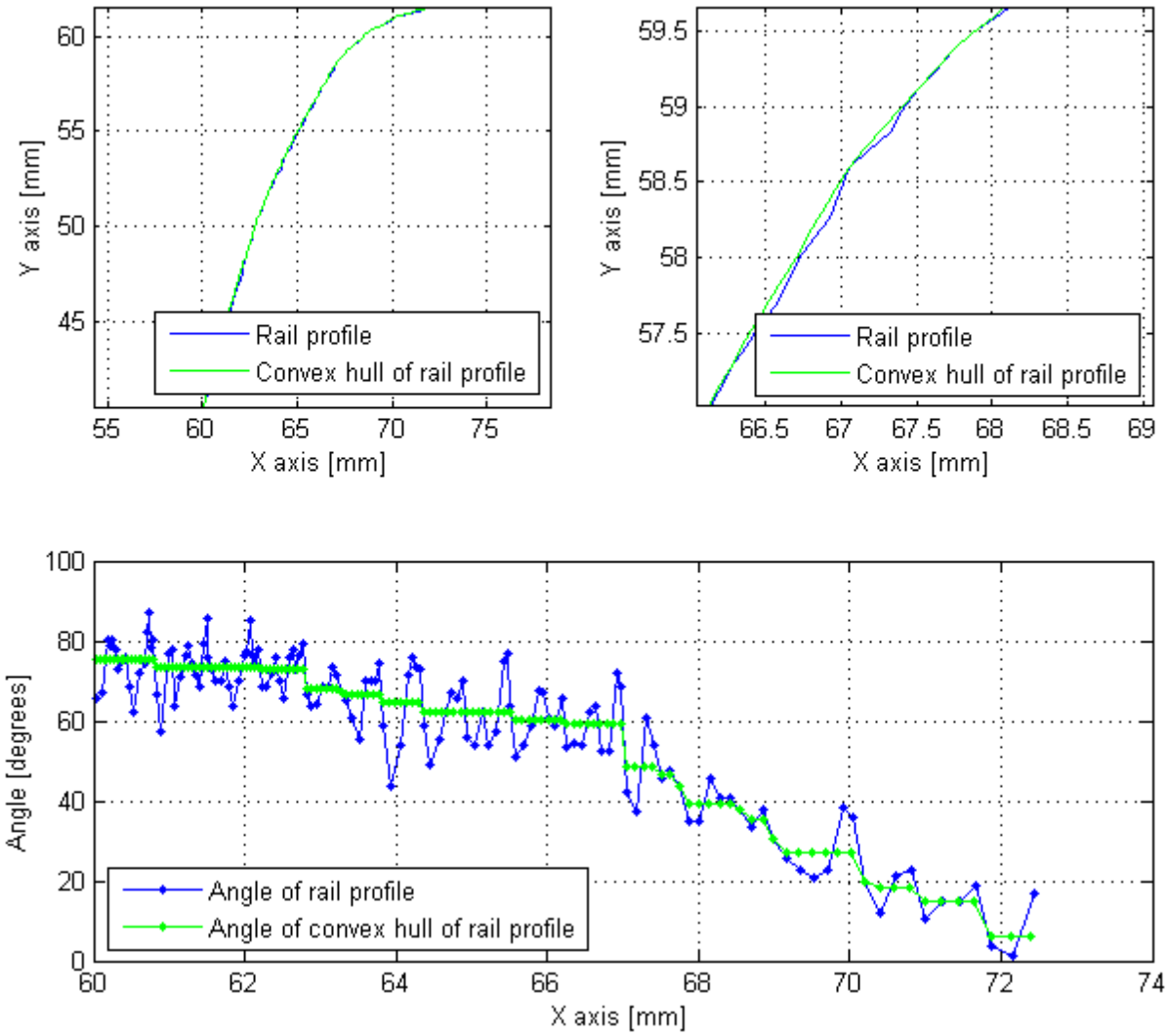

Figure 5-61 The angle of a measured rail profile and angle of convex hull of the same rail

For example, at 67 mm along the X axis, the rail has a small corner of approximately 10 degrees which is well preserved. Angle variations around that location do not pose a derailment hazard 5 as they do not come in contact with train wheels and are well filtered out.

The application of this method is of course limited to the convex parts of switch rails. However, as all switch rail profiles are designed and managed to a convex shape, the author identified just one case where corners can lead to concave areas in switch rails. This is generally at the lower end of the profile and is due to wear and/or metal migration.

The pronounced sharp corners on the lower part of the rail (as shown in Figure 5-62) are unlikely to appear on AMS switches (due to material hardness) and if any such corners form they do not present a derailment hazard 5.

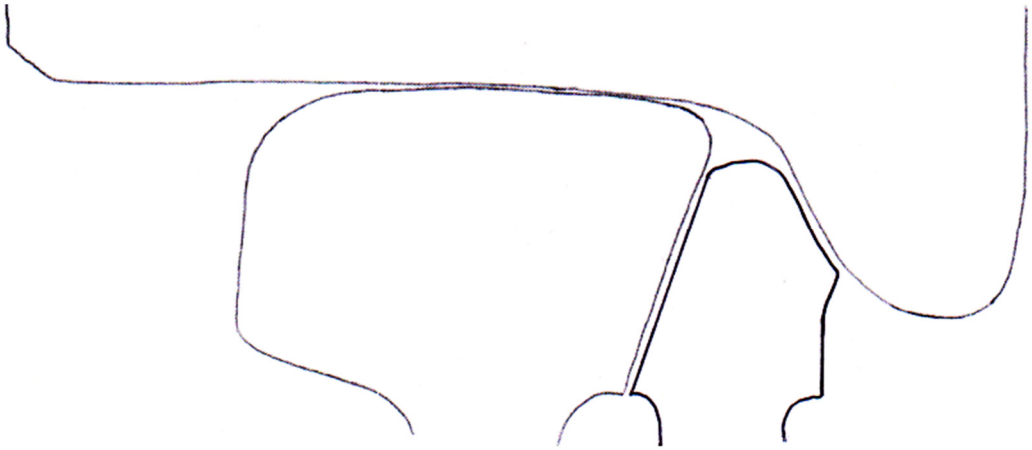

Figure 5-62 Sharp switch rail that does not pose a derailment hazard 5 (diagram 2)

The second issue discussed here is the elimination of sharp corners which do not come in contact with the wheel and hence do not pose a derailment hazard 5. This is achieved by calculating the convex hull of the stock rail and switch rail pair and identifying sharp switch rail corners which cannot come in contact with train wheels. Figure 5-63 shows an example.

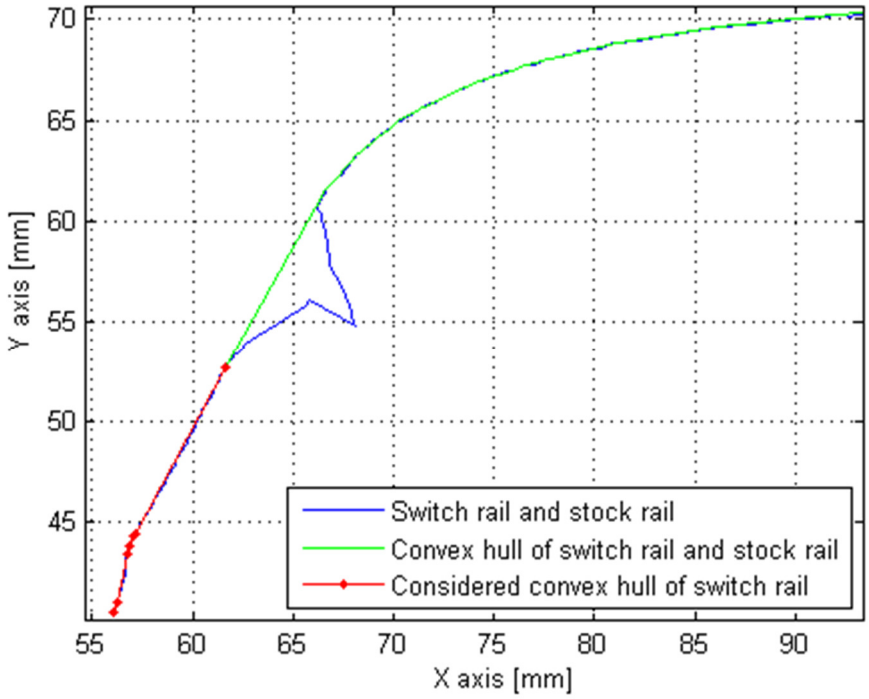

Figure 5-63 The use of convex hull to identify areas in the switch rail which cannot come in contact with any train wheel

For clarity the purpose of the two convex hulls which are carried out is summarized. The first one is applied only on the switch rail and its purpose is to filter the concave corners which

cannot come into contact with the concave areas of train wheels. The second one is applied over both the stock rail and switch rail and its purpose is to filter convex corners (although as a side effect it filters concave ones as well) of the switch rail which cannot come into contact with the concave areas of train wheels due to the presence of the stock rail.

Thus, only the red area is considered for evaluation against sharp corners. The pronounced sharp corner of the switch rail (around 65 mm on the X axis) is dismissed.

The measurement algorithm is as follows:

1. Calculation of convex hull over both the switch rail and stock rail

As shown in Figure 5-63 and explained above, this step identifies the switch rail area which cannot come in contact with any train wheel.

2. Expansion of considered area

As shown in Figure 5-64, switch rails can show sharp corners in the immediate vicinity of the convex hull. Thus, the considered area is expanded to account for possible wheel and rail deformations. Points forming the convex hull of the switch rail are added to the considered area until a minimum length of 0.7 mm is added.

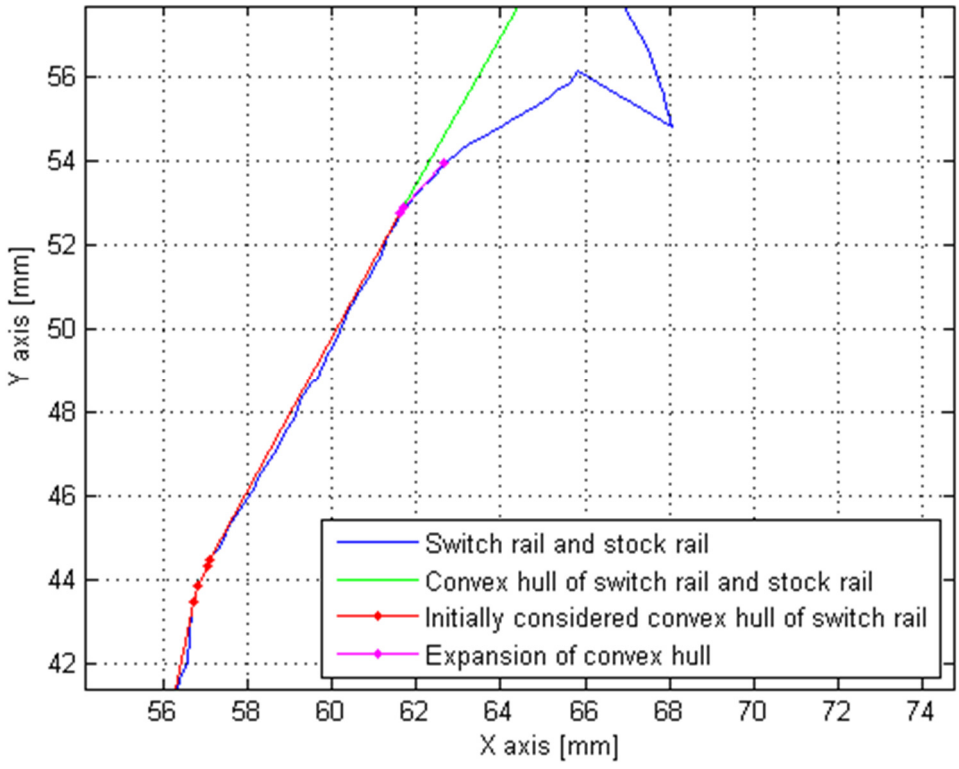

Figure 5-64 Expansion of considered area

The process is exemplified in Figure 5-64 where the expanded area is shown in pink.

3. Elimination of concave areas within the switch rail

In some situations, due to wear and metal migration, the switch rail can show concave areas. These areas are eliminated. This is achieved by calculating the convex hull of the switch rail and eliminating the lowest points in the switch rail until the maximum distance between the convex hull and the switch rail is less than 0.5 mm.

4. Elimination of switch rail points which are 30 mm below the top of the switch rail

Considering the design specification of the P8 wheel and worst case scenarios, the lowest wheel-rail contact point is never more than 30 mm below the top of the stock rail (or tread of the wheel).

5. Calculation of angles and distances

The shortest distance for angle changes of 20, 25, 30, 35, 40, 45, 50, 55 and 60 degrees is calculated and compared with the thresholds shown in Figure 5-55.

This particular example has two small corners with an angle change of around 15 degrees and thus no faults are identified.

Discussion of algorithm

The presented method provides good results as it is able to both filter the point cloud data and achieve accurate measurements of corners which come in contact with train wheels. For the measurement of sharp corners, the use of the convex hull is also a good substitute for worst case wheel-rail analysis, as it can help to identify all sharp corners which may come in contact with any train wheel.

5.1.8 Further possible improvements in the area of inspection and maintenance of S&Cs outside the current Network Rail standards (NR/L2/TRK/0053 and NR/L2/TRK/1054)

Sections 5.1.3 to 5.1.7 analysed the current inspection methods, outlined potential limitations in reliability (both due to method and human errors) and proposed new methods which replicate the current standards but without being affected by human errors.

As the title suggests, this section outlines possible improvements in the area of S&C inspection which builds up on the top the current NR/L2/TRK/0053 and NR/L2/TRK/1054

inspection standards. Some improvements are alterations to current inspection procedures while others are completely new practices.

Considering a laser-based approach to the inspection and maintenance of S&C, the following improvements are suggested:

1. The P8 contact angle measurement should at least be carried out using a set of 3 or 4 wheel profiles instead of a single P8 profile. In the future, the calculation of the P8 contact angle should be changed to measure the lowest possible contact angle for any worn train wheel. This would likely be achieved by analysing the rail profile without fitting any train wheels. This would increase the level of safety as the current TGP8 gauge measures the contact angle for a brand new P8 profile which is likely to be higher than the actual contact angle for certain worn P8 profiles.
2. The P8 contact angle could also be calculated while virtually wearing the rail profile. This would allow the amount of useful material remaining to be measured and would enable the prediction of future P8 derailment hazards. This would be beneficial towards asset management and maintenance planning.
3. Wheel-rail fitting can be used to measure the lateral position of the wheel set under flange contact conditions as it enters the switch. A large lateral displacement at the switch toe can identify the risk of striking the top of the switch rail. This was the cause of a tram derailment at Birmingham Snow Hill station [78], as shown in Figure 5-65.

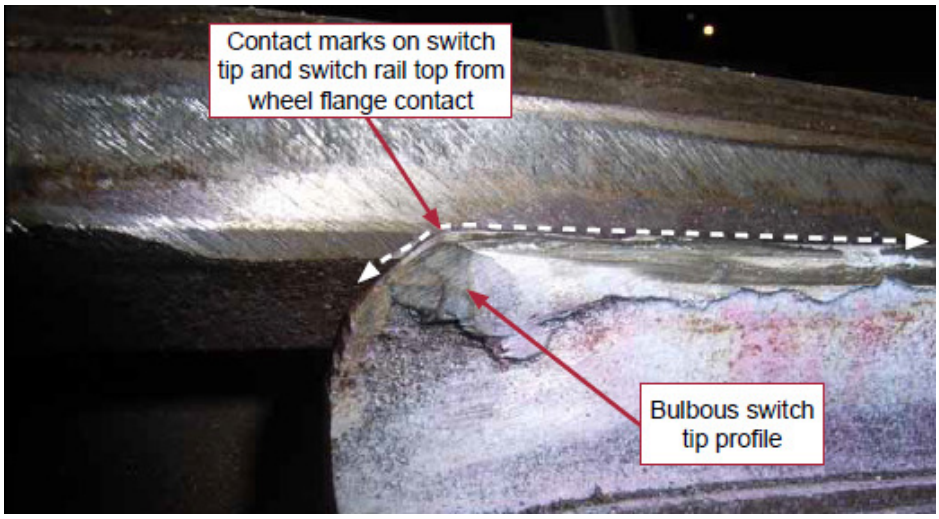

Figure 5-65 A switch rail which caused a tram to derail at Birmingham Snow Hill station
Courtesy and Crown Copyright RAIB

This derailment hazard is generally managed by periodically carrying out derailment hazard 1 inspections which aim to identify whether or not the maximum height of the switch rail is above the lowest point in the sidewear scar. However, it is likely that this inspection is not sufficient to identify the risk of striking the top of the switch rail when a square flange in being used. There is also no evidence to say that the tip of a switch rail which passes derailment hazard 1 cannot be struck by train wheels showing new and worn P8 profiles.

Figure 5-66 shows the lateral position of a simulated new P8 wheel profile on a measured switch rail which failed derailment hazard 1. The lateral position has been measured relative to the field point (14 mm below the top of the rail) of the measured stock rail just in front of the switch toe.

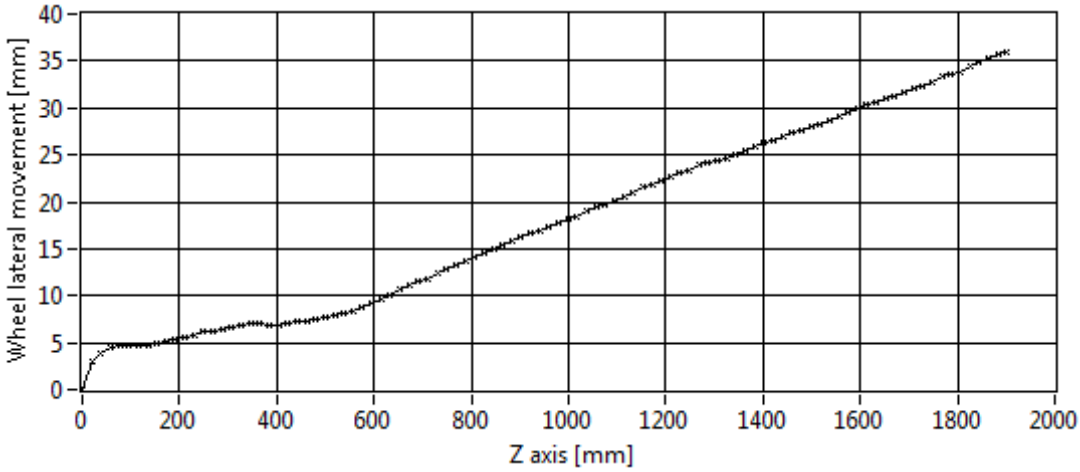

Figure 5-66 The lateral movement of a simulated P8 train wheel in flange contact with a measured switch rail that failed derailment hazard 1

The risk of striking the top of the switch rail is very evident, as Figure 5-66 shows a lateral movement of 3 mm in the first 25 mm of the switch and 5 mm in the first 70 mm of the switch. The figure also shows that the switch rail could be ground to a condition where the lateral movement would be smooth and start from zero. By simulating the lateral movement of train wheels, one can precisely identify whether or not the tip of a switch rail could be struck by train wheels (this analysis considers worst case for switch geometry where the wheel is always in flange contact with the rail). This could help achieve better safety as well as help to scope and plan the S&C repair work.

4. The *height profile* of the switch rail can be used to identify gradient defects.

   Figure 5-67 shows the *height profile* of a switch rail located in the area of Princes Street Gardens close to Edinburgh Waverley station, immediately following a derailment. RAIB concluded that "There is an apparent risk of a ramp being created where a switch rail that is failing gauge 2 in the first metre increases in height and is introduced between the stock rail and wheel flange from below, particularly where there is flange contact between the train wheels and the stock rail". Using an S&C laser-based trolley such conditions can be easily identified, which would help to scope the grind and weld repair.

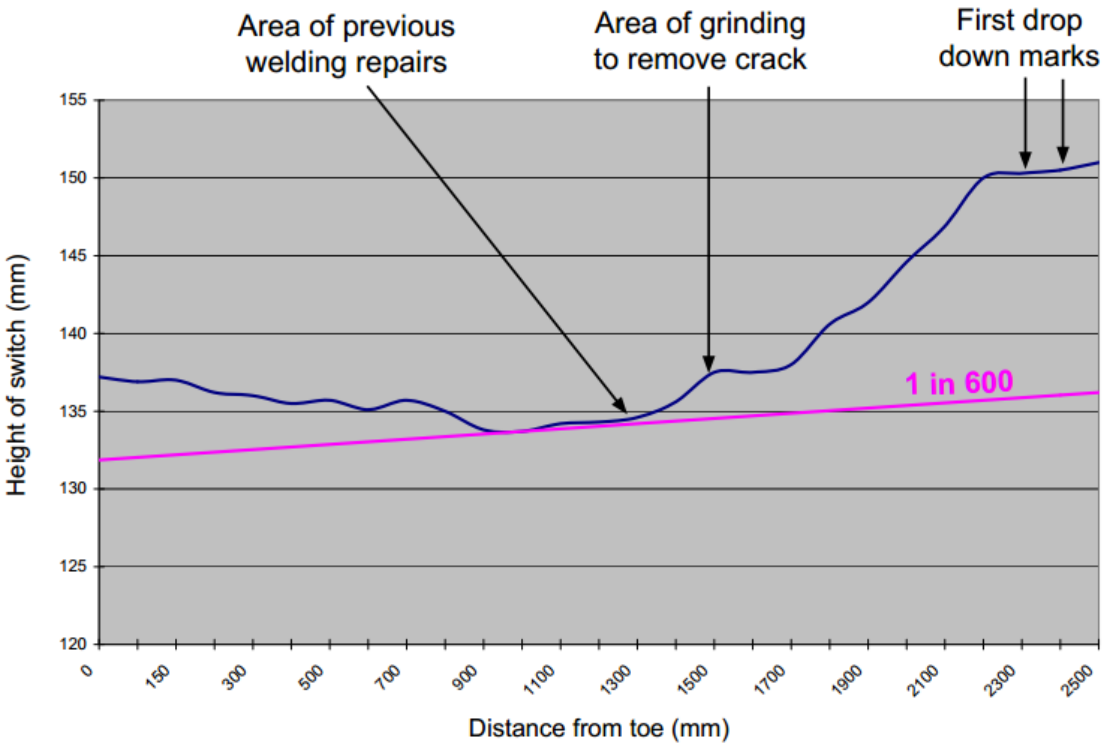

Figure 5-67 A switch rail height profile as measured by RAIB
Courtesy and Crown Copyright RAIB

5. When carrying out weld and grind repairs on switches, the repair actions could be used to simulate the shape of the switch after the planned repair work. Often, the switch repair work consists in grinding the switch rail. This process removes a defect but can introduce another. This is what happened in 2007 [11] when workers introduced a "derailment hazard 2" while repairing "derailment hazard 1". Similarly, a grind repair created the condition shown in Figure 5-67. Most switch rail grid repairs can be generally described by three vectors: angle of grinding, amount of grinding,

and distance. By simulating the proposed grind repair on the switch rail, one can recalculate the result of the five derailment hazards and identify whether or not the repair work can lead to another derailment hazard or other faults such as the one shown in Figure 5-67. This could be used as a powerful tool for improving the quality of switch rail repairs.

The above five improvements, together with the automatic inspection of the five derailment hazards, if used as part of a laser-based S&C inspection strategy could improve both the safety and quality of maintenance of S&Cs which in turn may also improve the life cycle cost (LCC). Chapter 7 discusses the advantages and disadvantages of the use of laser-based inspection of S&Cs under five different technical solutions: dedicated measurement trains, in-service trains, inspection wagons, road-rail vehicles, on-site robots, rail trolleys, and laser-based hand gauges.

6 INSPECTION OF RAILWAY CROSSING PROFILE

The profile of railway crossings are managed by Network Rail through period manual inspection as described in the NR/L2/TRK/1054 inspection standard. Depending on the type of the crossing, the standard specifies the use of a one-metre or two-metre straight edge in conjunction with a stepped gauge. When carrying out the inspection, the straight edge is placed on the crossing in seven positions (procedure also known as "7-point check"). However, three positions are very similar with other three positions, the difference being just the path for which the wear is inspected, straight path or diverging path. The seventh position is along the centre of the crossing, middle way between the straight path and the diverging path. Thus, the inspection standard specifies in total four methods for the inspection of crossing profile. These methods are discussed in separate sections from section 6.1.3 to section 6.1.6. The objectives of each of the mentioned sections are, as set out in section 1.4:

- to identify whether or not the use of current crossing profile inspection methods, as defined by the NR/L2/TRK/1054 inspection standard, can lead to considerable measurement errors and the source of those errors;
- to identify if possible and to develop alternative automatic inspection methods can be used to replicate the current crossing profile inspection tasks as defined by the NR/L2/TRK/1054 inspection standard whilst eliminating human errors;
- to identify whether or not improvements on the developed crossing profile inspection methods could reduce the systematic errors of inspecting crossings.

As the straight edge inspection method requires that the measured crossing profile is accurate along the length of the crossing, a method for registering the crossing profiles was developed and is described in section 6.1.1. Finally, section 6.1.7 presents a number of conclusions.

6.1.1 An approach for the registration of railway crossing point cloud data

As shown in section 4.3, the S&C inspection trolley was designed to minimise unwanted movement across the six degrees of freedom. The design of the trolley constrains its movement such that the acquired data can be used to accurately carry out a NR/L2/TRK/0053 inspection; however, this is not sufficient for the inspection of crossings in accordance with

the NR/L2/TRK/0054 inspection standard. The longitudinal height profile of the crossing, if unaccounted for, leads to unwanted roll of the measurement trolley which generates unacceptable measurement errors within the 3D model. As the height profile of the opposite rail is reasonably straight in comparison with the height profile of crossings, in the context of crossing inspection, the height profile of the opposite rail is considered straight. Thus the height profile of the crossing is accounted for by measuring the roll of the trolley.

Figure 6-1 The developed S&C laser-based trolley on a measured railway crossing

As the accuracy of inclinometers is greatly affected by accelerations (they are accurate only when stationary), a gyroscope is used to measure the roll angular speed which is defined by:

$$\omega = \frac{d\psi}{dt}$$

where ψ is the absolute roll angle.

The measurement of angular speed using gyroscopes has several disadvantages and limitations. They are summarised as follows:

1. The measurement is affected by the earth's rotation. Note that this is a disadvantage purely in the context of the presented work. Under worst case conditions, when the measurement axis of the gyroscope is parallel to the rotational axis of the earth, the complete angular speed is measured, which is 360 degrees per 24 hours. This equates to 4.16×10^{-3} degrees per second. As the distance between the trolley wheels along the X axis is approximately 1500 mm, the height profile of the crossing can be affected

by a maximum of $1500\sin(4.16\times10^{-3}) = 0.11$ mm per second. Thus, if measuring 30 seconds, the maximum error becomes 3.3 mm which is unacceptable. Depending on the location of the trolley (equator or poles) as well as its orientation (N-S or W-E), the absolute error varies between 0.11 mm per second and 0 mm per second.

2. Gyroscope measurements suffer from a constant bias [83]. As a result, the measured angular speed is not zero when the gyroscope is stationary. Due to this, the integrated angular speed is unbounded. In addition to the gyroscope bias, the input bias of the measurement device used to measure the output (generally voltage) of the gyroscope also contributes to measurement errors.
3. Most gyroscopes suffer from bias instability [83]. As a result, the bias is not constant over time. Most gyroscopes present a bias which is temperature dependent.
4. Other errors can occur, such as output linearity errors and random walk [83].

Figure 6-2 shows the measured height profile difference six times using a stationary CRS-09 gyroscope.

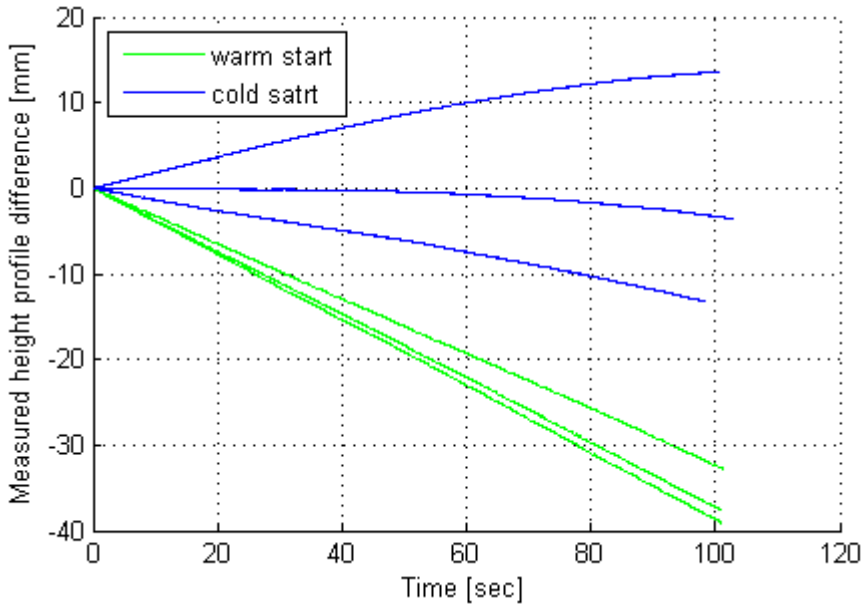

Figure 6-2 Measured height profile difference using a stationary CRS-09 gyroscope

The blue plots show three measurements where the gyroscope was powered off for at least 60 seconds prior to acquiring the data and the green plots show three measurements where the gyroscope was powered on for at least 5 minutes prior to acquiring the data. In practice, the bias drift is generally stabilised by keeping the gyroscope powered prior to taking measurements. However, in the context of an S&C laser based trolley this is not ideal, as it

requires significant overhead time. In railway geometry measurement applications both the constant bias and varying bias (due to bias instability) are easily compensated by high pass filtering. However, crossings generally show a dip in the middle, which when measured at walking speed produces an angular velocity that has the same appearance as a bias drift (in the blue plots of Figure 6-3 the effect of bias drift during cold start is very visible). For this reason, low pass filtering cannot be used.

Another approach is to eliminate just the DC component in the angular speed prior to integration. The results of this approach are shown in Figure 6-3.

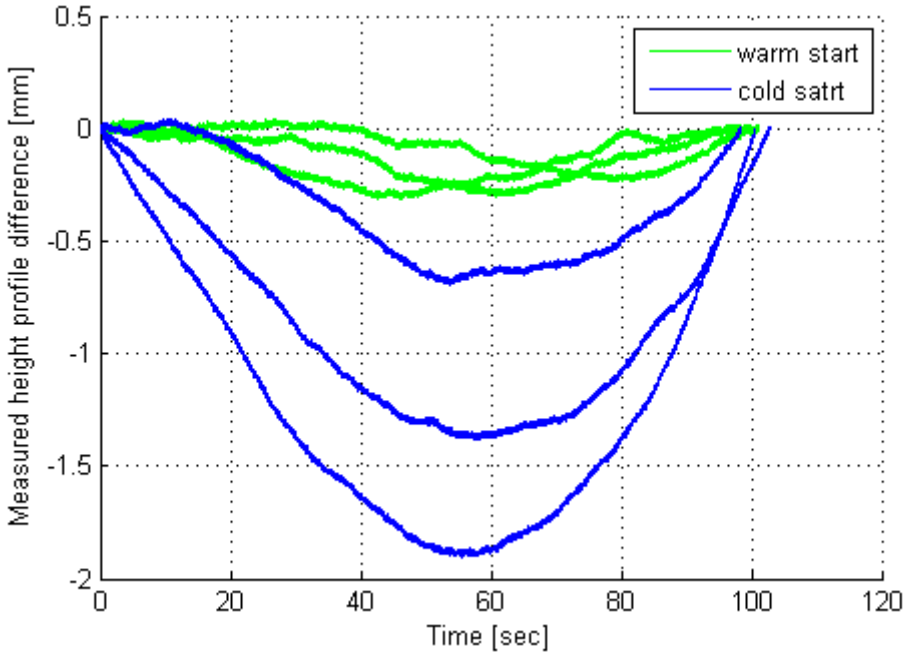

Figure 6-3 Measured height profile difference using a stationary CRS-09 gyroscope with the elimination of DC component prior to integration

This approach eliminates mean bias error but does not compensate for bias instability. As shown in Figure 6-3, the approach can lead to large errors of up to -2 mm when the signal is acquired for 100 seconds under cold start conditions. The acquisition of short data (less than 20 seconds) can reduce the maximum absolute error to about 0.2 mm. However, as shown in Figure 6-3, using this approach the end of the height profile is always measured at 0 mm. In the context of crossing inspection this is not acceptable, as one end of the crossing may be higher or lower than the other end.

Thus, a new approach is proposed which aims to measure the height profile of the crossing more accurately. For this reason, the output signal of the gyroscope during a finite amount of time is approximated to a function of the following four terms:

$$angular\ speed(t) = a\frac{t_{end} - t}{t_{end}} + b\frac{t}{t_{end}} + c \cdot \sin\left(\frac{t}{t_{end}} \cdot \pi\right) + d(t),$$

where a is the bias at the beginning of the measurement (including the bias of the voltage measurement device and the measurement of the earth's rotation), b is the bias at the end of the measurement, c is a factor proportional with the non-linearity of the varying bias and d is the real angular speed affected by all other gyroscope errors such as non-linearity errors, noise and random walk. As railway crossings are reasonably straight sections of the railway, the orientation of the gyroscope relative to the rotational axis of the earth can be considered constant. Hence, the effect of the earth's rotation is accounted for as a static bias.

The angular speed was measured following a series of steps as follows. The trolley was initially stationary for 10 seconds. In this time, knowing that the angular speed of the trolley relative to the rails was zero, the acquired data was used to estimate the initial bias, marked a in the previous formula. The trolley was pushed over the crossing and then pushed again back to its initial position (the trolley incremental encoder can be used to advise on its current position). The trolley was left stationary a second time for about 10 seconds, during which time the acquired data was used to estimate the bias at the end of the acquisition, marked b in the previous formula. The two estimated parameters were used to generate a compensation vector with linearly distributed values. The compensated angular speed was integrated in order to obtain the absolute roll value. The angular speed was compensated a second time by subtracting:

$$c \cdot \sin\left(\frac{t}{t_{end}} \cdot \pi\right),$$

where the c parameter is calculated so that the roll value at t_{end} is zero. This compensates the non-linear varying bias. The results of the proposed approach on the measured, stationary data are shown in Figure 6-4, where the absolute maximum error is approximately 0.2 mm.

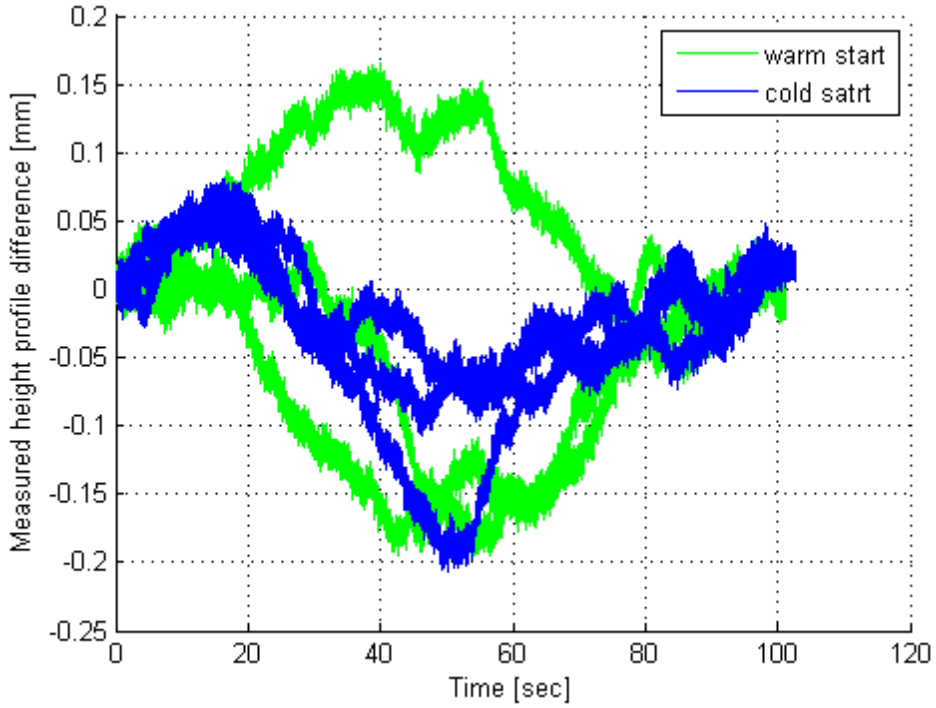

Figure 6-4 Measured height profile difference using a stationary CRS-09 gyroscope and the proposed method for improving the roll measurement

The approach was used to measure the height profile difference of 3 metres of rail over which a reference board with known dimensions was mounted. The reference board is shown in Figure 6-5.

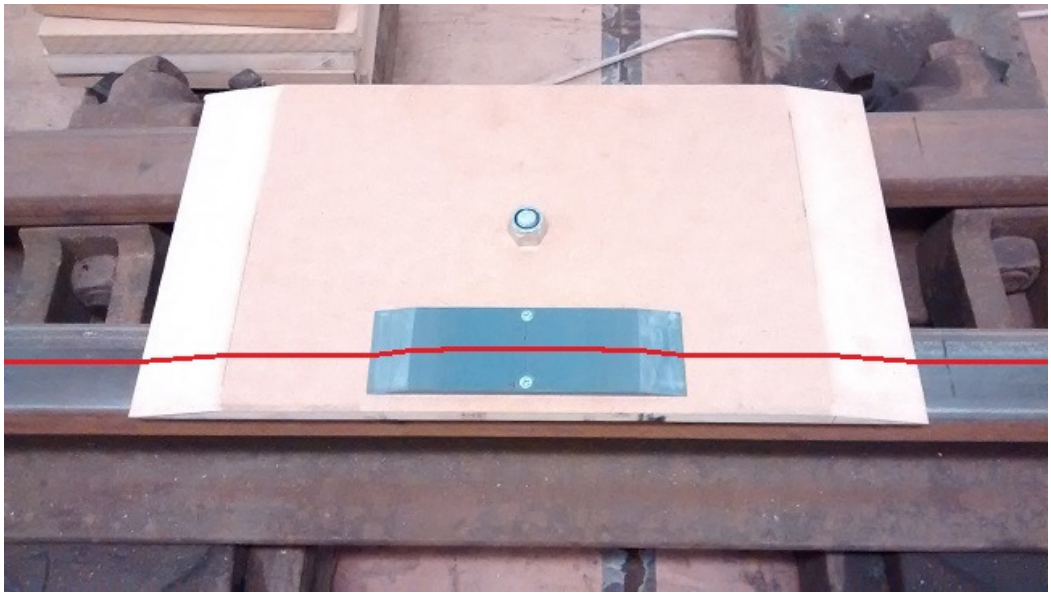

Figure 6-5 Reference board with known dimensions

The reference board had three progressive height steps of 13 mm, 5.7 mm and 0.3 mm as shown in Figure 6-6.

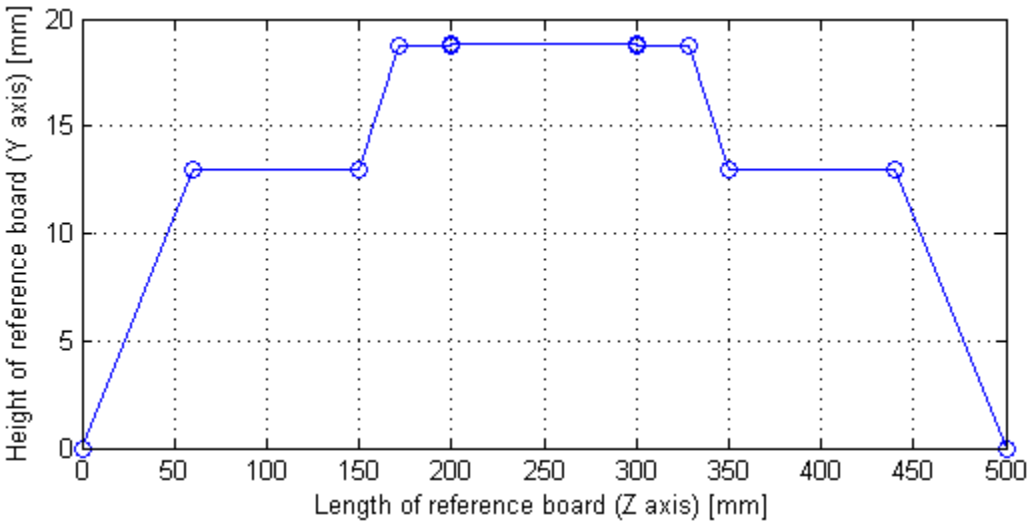

Figure 6-6 Dimensions of the reference board

The results of the proposed approach are shown in Figure 6-7 as nine plots, six cold start (blue) and three warm start (green).

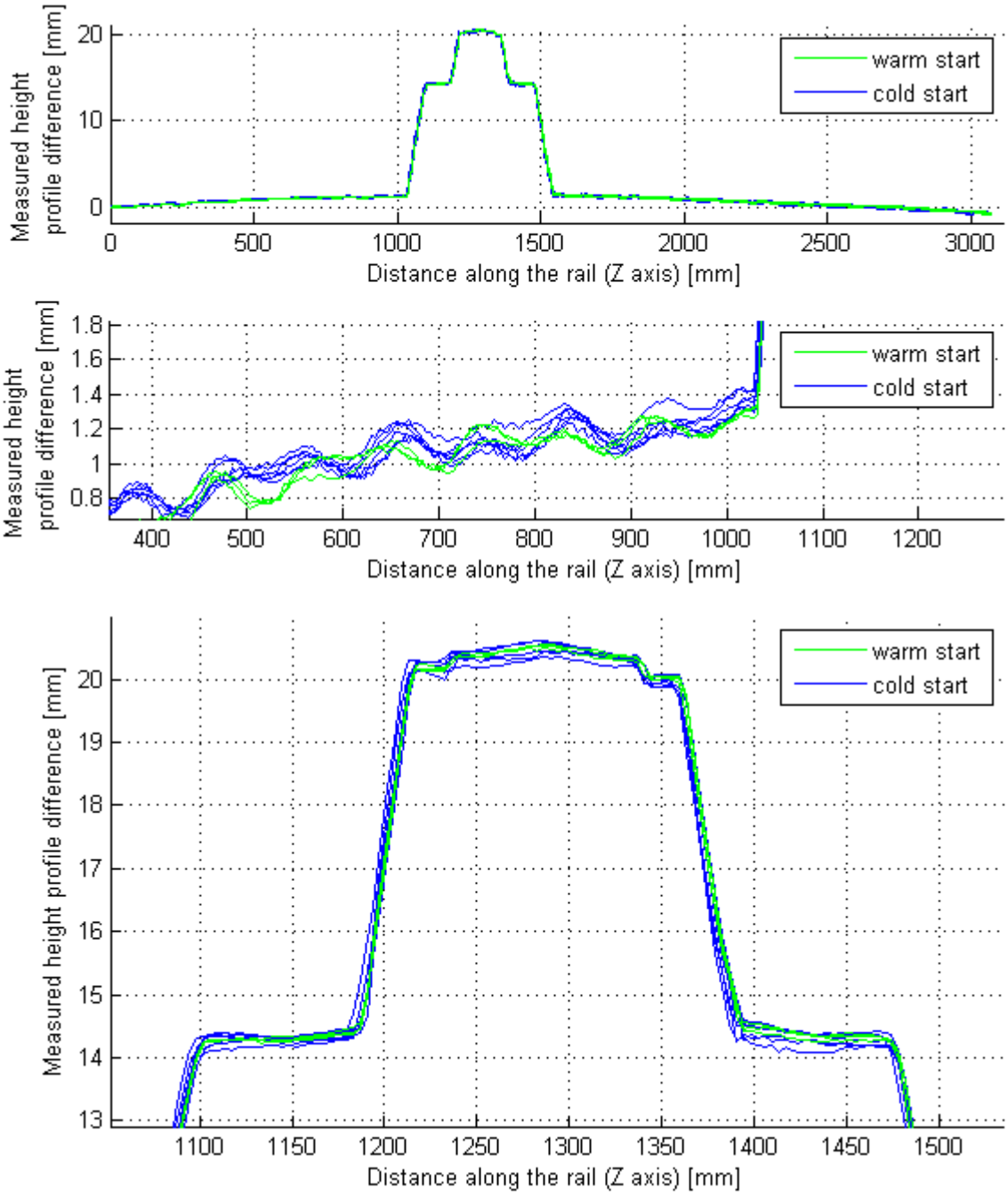

Figure 6-7 Measured height profile of height board using proposed approach

The three height steps of 13, 5.7 and 0.3 mm have been measured with good accuracy despite various measurement errors. One source of errors was wheel out of roundness, which is visible in the middle graph of Figure 6-7 as a 0.2 mm peak-to-peak variation. The trolley had two types of wheels, one of 30 mm in diameter and one of 50 mm in diameter. Each of the two types were subsequently replaced with ball units, which did not introduce out of roundness errors, and the diameter of the remaining wheel type matched the periodicity of the

measured height profile. This confirmed that the source of error was wheel out of roundness. However, in practice, the ball units have not been used on the trolley to measure S&Cs as they generated excessive noise and vibrations. Another source of errors was from the tilted wheel-rail contact as exemplified in Figure 6-8.

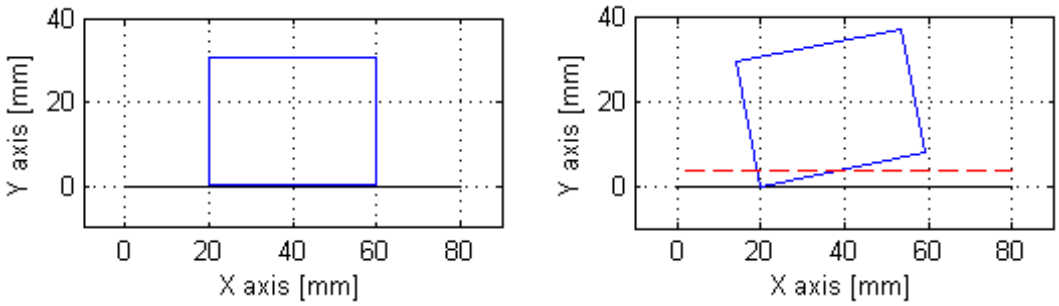

Figure 6-8 Example of wheel-rail contact measurement error

The height of the red dotted line in Figure 6-8 shows the measurement error when the wheel-rail contact point is considered to be horizontally in the middle of the wheel (at 40 mm along the X axis) but in reality is not (in the right plot of Figure 6-8 it is at 20 mm).

As the width of the wheels on the measurement side is 105 mm and the distance between the wheels across the width of the trolley (Y axis) is approximately 1500 mm, the assumption that the wheel-rail contact occurs in the middle of the wheel leads to a maximum measurement error of 105/2/1500=35 µm per millimetre of measured height. Thus, due to this error, a height measurement of 20 mm could be the result of measuring a true height of as low as 20-0.035×20=19.3 mm or as high as 20.7 mm. However, this would imply that the inspected track gauge is very different from the gauge of the trolley (e.g. track gauge of over 1490 mm for a designed gauge of 1435 mm) which is not the case in practise as the S&C would receive a ban on movements much before it could degrade to such a condition. Thus, such a worst case scenarios is not representative of real life situations.

The height of the rail relative to the opposite rail was not verified. This is due to the difficulty in carrying out such measurements. However, the ability of the algorithm to compensate for the earth's rotation, fixed bias and varying bias was demonstrated in Figure 6-4.

Conventionally, manual crossing measurements are carried out using 1 mm stepped gauges. Thus, manual measurements are limited to an accuracy of ±0.5 mm when all other errors are zero. However, when human errors are added, the measurement error can be in the range of millimetres, which is the reason why an automatic inspection system is desirable.

Measurement errors of up to ±0.5 mm are considered acceptable and thus the proposed approach is considered sufficiently accurate for the inspection of railway crossings.

6.1.2 Point cloud data preparation

Prior to analysing the profile of a measured crossing, the data is pre-processed, in seven steps, to achieve the following:

- registration of each 2D profile to ensure accuracy of 3D model;
- elimination of 3D points which are irrelevant towards profile inspection, and;
- separation of rails and identification of rail knuckle for easier analysis in the next sections.

The steps are as follows:

1. Calculation of roll angle with reference to time using the approach presented in section 6.1.1
2. Calculation of roll angle for each acquired 2D profile

An incremental encoder was used to know the position of the trolley along the Z axis. Every 4 mm the scanCONTROL lasers were triggered to acquire a 2D profile. Each 2D profile is time stamped when received by the computer. The beginning of the angular velocity measurement is also time stamped and added as an offset to the time axis of the roll angle waveform. The roll correction for each 2D profile is identified in the roll angle waveform at the moment in time defined by the timestamp of the 2D profile. Each 2D profile was rotated with the additive inverse of its corresponding roll angle. The middle of the contact points of the two top rollers sitting on the opposite rail was used for the axis origin of the rotation.

3. The point cloud data is reversed along the Z axis (if necessary) so that the stock rail is first followed by the crossing nose as distance increases along the Z axis

This was done so that the rest of the process is identical for the inspection of both diverging and straight routes (upper right plot in Figure 6-9). The point cloud data was decimated prior to plotting Figure 6-9 and Figure 6-10.

4. Elimination of unwanted wing rail

The flangeway gap which is always in excess of 30 mm was used to automatically identify the wing rail for elimination. The result is shown in the lower left plot of Figure 6-9.

5. Elimination of all points under 14 mm relative to the top of the rail

As all inspection tasks are carried out either at the top of rails or at 14 mm below the top of the rails, all points which are below this value are eliminated (lower right plot of Figure 6-9).

6. Separation of stock rail/wing rail and crossing nose

In order to ease the inspection process, the two components are separated. The flangeway gap, which is always in excess of 30 mm, was used to automatically classify the point cloud data (Figure 6-10).

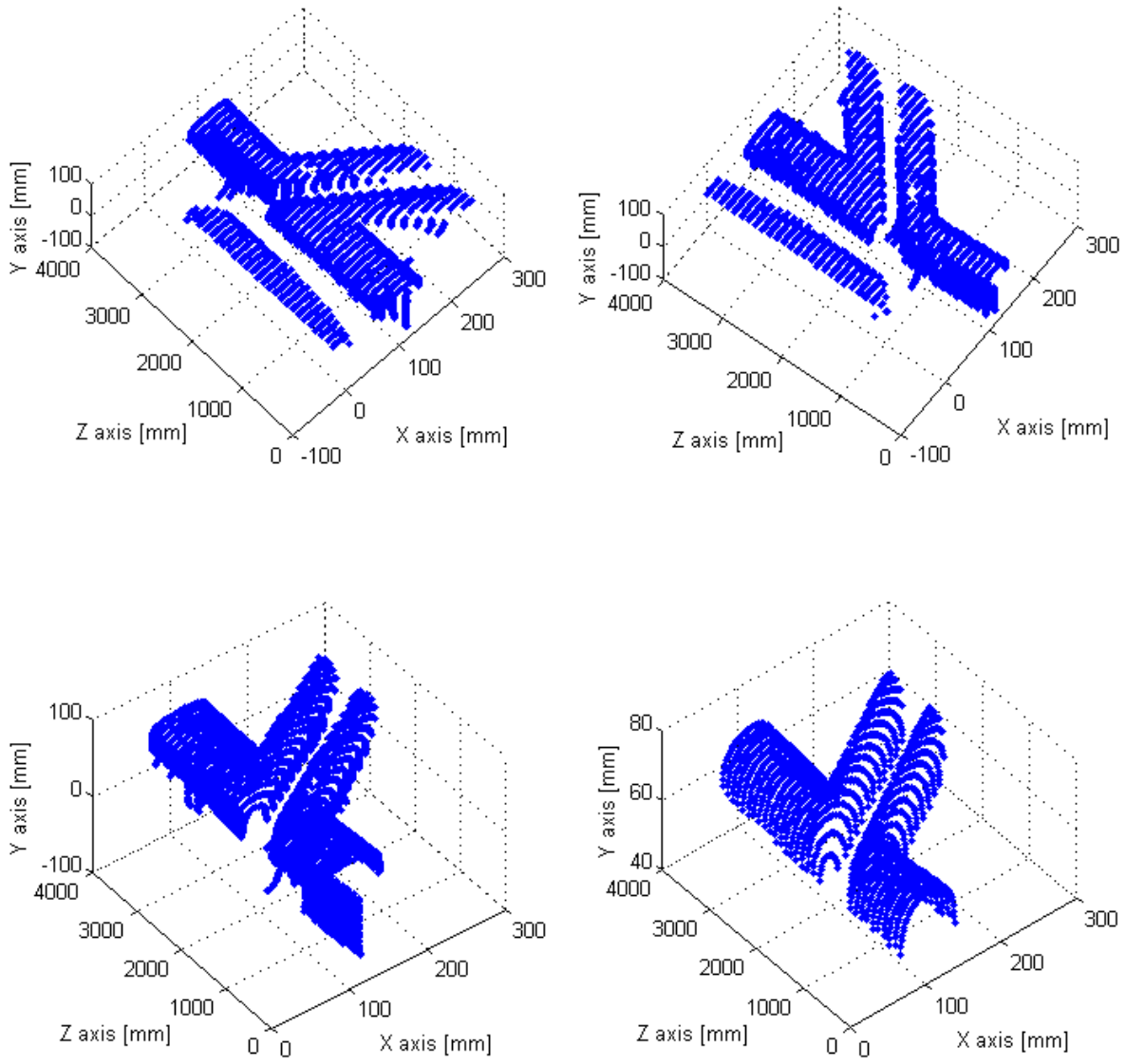

Figure 6-9 Results of preparation of crossing point cloud data; upper right: after sorting; lower left: after elimination of wing rail; lower right: after elimination of points under 14 mm

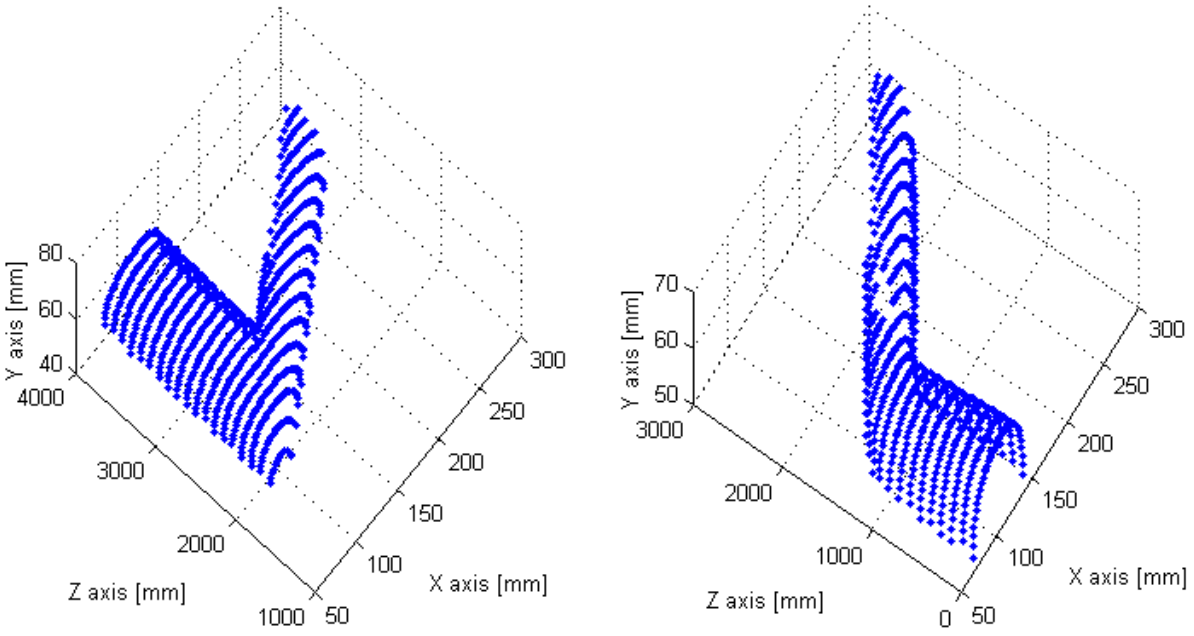

Figure 6-10 Results of separation; left: crossing nose; right: stock rail and wing rail

7. Identification of stock rail/wing rail knuckle

Prior to the identification of the stock rail/wing rail knuckle, the crossing angle was measured. All stock rail/wing rail gauge points that were on the X axis at least 30 mm away from the gauge point at the start of the stock rail were used to calculate a linear regression. The angle of the linear regression represents the crossing angle (in this example 1:8 or 7.2 degrees). A second regression was calculated using all the gauge points which were not used in the first linear regression and were at a distance of at least 30 mm from it. Considering the y values of the two linear regressions as null, the linear regressions intersect each other at the knuckle point.

6.1.3 Inspection of batter at the knuckle

For the inspection of batter at the rail knuckle, a straight edge is placed on top as shown in Figure 6-11. The right end of the edge is firmly pushed against the rail while the gap forming at the left end is measured using a stepped gauge.

The measurement algorithm is as follows:

1. Measurement of stock rail height profile (measured central to the width of the rail)
2. Selection of one metre of height profile starting from the knuckle point
3. Application of one-metre straight edge

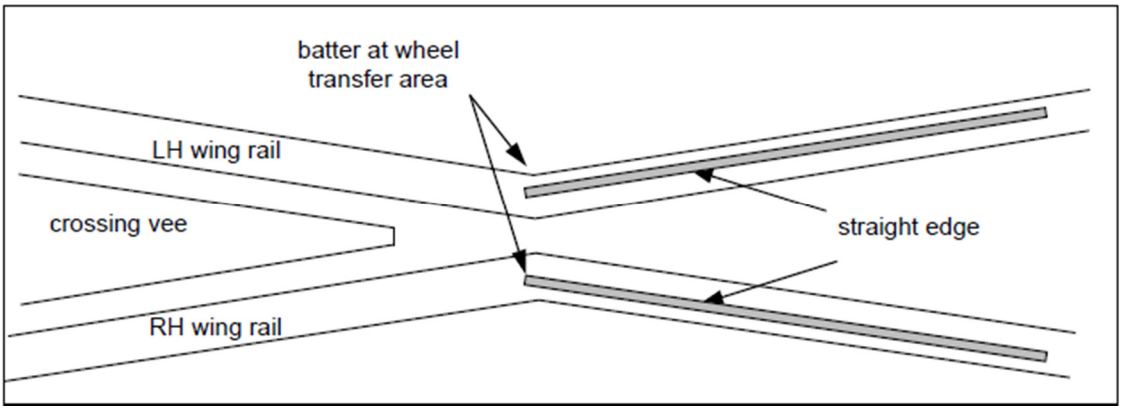

Figure 6-11 Inspection method of batter at the knuckle as defined in NR/L2/TRK/1054 Courtesy and Copyright Network Rail

The application of the straight edge was done so that the gap between the top of the stock rail and the right most 40 cm of the straight edge was minimal.

4. Calculation of stock rail top wear at knuckle

The wear was calculated as the maximum distance between the left most 20 cm of the straight edge and the corresponding stock rail height profile. All three inspected crossings presented minimal wear at the knuckle. Figure 6-12 and Figure 6-13 show two results of automatic inspection of batter at the rail knuckle ("13 PTS, diverging path" and "far end 1, diverging path").

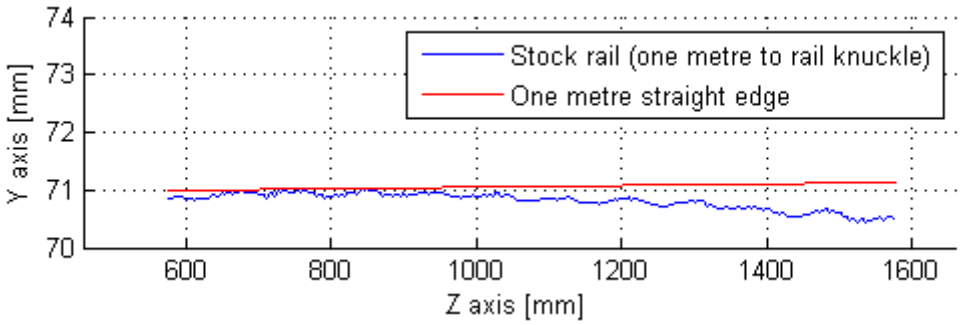

Figure 6-12 Inspection of batter at the knuckle (13 PTS, diverging path)

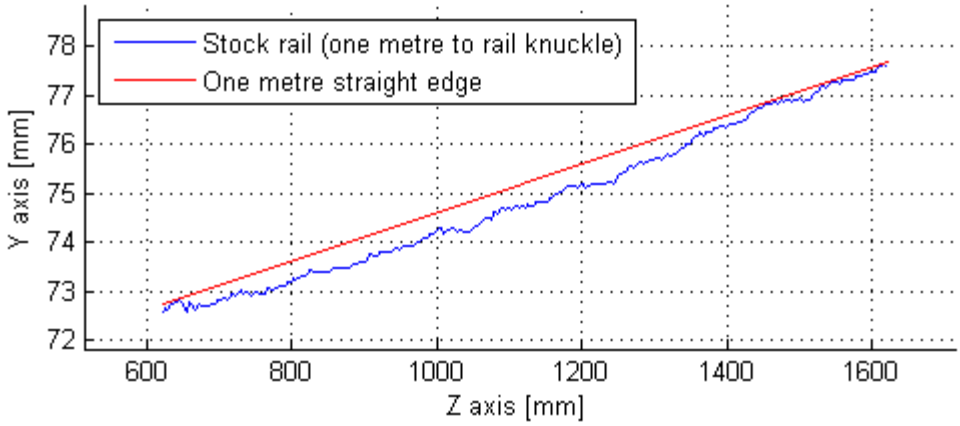

Figure 6-13 Inspection of batter at the knuckle (far end 1, diverging path)

Manual measurements did not identify any wear at the rail knuckle. The automatic measurements identified 0.7 mm and 0.2 mm of wear. If compensating the measurements for wheel out of roundness (as identified in section 6.1.1), then the measurements become approximately 0.5 to 0.6 mm and 0 to 0.1 mm respectively.

The automatic measurements also show the presence of twist, which is an important cause of rail derailments. This information can be used to better maintain the infrastructure. However, trolley based twist information should be treated with caution as the measurements are performed with the track unloaded.

6.1.4 Inspection of crossing sidewear

The inspection of crossing sidewear is accomplished by the application of a straight edge on the gauge side of the crossing 'vee' as shown in Figure 6-14.

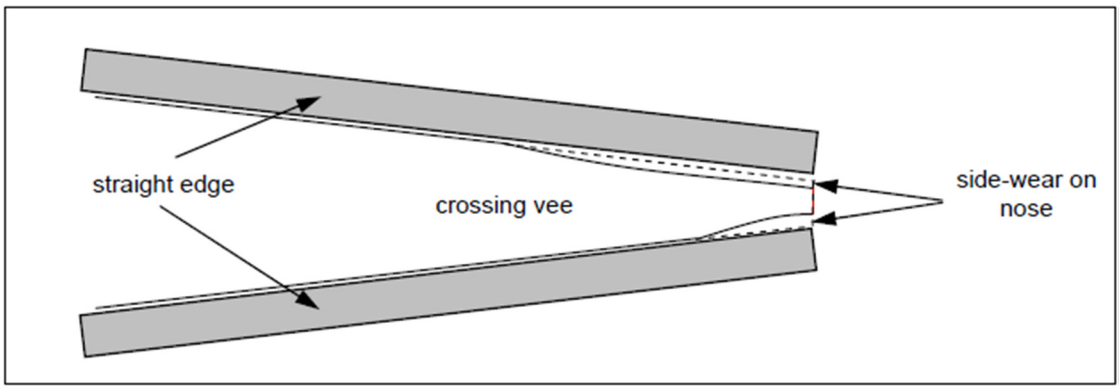

Figure 6-14 Inspection method of crossing sidewear as defined in NR/L2/TRK/1054
Courtesy and Copyright Network Rail

The straight edge has to be positioned approximately 14 mm below the top of the crossing and its left end (as pictured) has to be firmly fitted flush.

Manual inspections have been found to be difficult to carry out. The straight edge is wider than the flangeway gap and could not be fully inserted into the gap to achieve a firm horizontal position. Instead, the straight edge was introduced into the gap at an angle. Due to poor accessibility and the requirement to firmly fit the left side of the straight edge (as pictured in Figure 6-14) the gauge was often accidentally dropped in the flangeway gap before an accurate measurement was taken. Because of these difficulties, the measurement was carried out by two persons, one holding the straight edge and one inserting the stepped gauge.

Some crossings were difficult to measure as they did not show a long and straight surface to which the straight edge could be correctly fitted. Instead, pivoting points changed the amount of sidewear measured. The shape of the crossing could be a result of lipping and metal migration.

Another aspect is the height at which the measurement is taken. Although unspecified in the NR/L2/TRK/1054 standard, NR personnel carry out the inspection at 14 mm below the top of the crossing. The height of the crossing ‘vee’, as shown in Figure 6-20, has a designed height profile which shows a height difference of 7 mm at the tip. When worn, the difference further increases. It is unclear whether the whole straight edge should be placed horizontally at 14 mm below the highest part of the crossing, or if the edge should be placed at an incline, to reflect the height of the crossing profile.

The measurement algorithm is as follows:

1. Calculation of vertical position and pitch angle (rotation around the X axis) of straight edge

Two reference points are created. As it was not clear whether the orientation of the straight edge should be horizontal or inclined to reflect the height profile of the crossing, a calculation was carried out for each case. For both calculations, the gauge point at 1 metre away from the tip of the crossing ‘vee’ was used as the first reference point. For the first method, the gauge point of the stock rail knuckle was used as a second reference point. For the second method, the gauge point of the tip of the crossing ‘vee’ was used as a second reference point. The two

reference points are used to establish the Y axis position and pitch angle of the straight edge (i.e. constrains all Y coordinates of the straight edge).

2. Calculation of horizontal position and yaw angle (rotation around the Y axis) of straight edge

Due to various imperfections in the crossings, lipping and metal migration, it became evident that in some cases more accurate measurements can be obtained by aligning the straight edge parallel with the opposite stock rail rather than with the crossing nose (see Figure 6-15). After constraining the yaw angle, the straight edge was horizontally shifted until it intersected the crossing.

3. Calculation of sidewear

The sidewear is calculated by subtracting the x coordinates of the straight edge from the x coordinates of the crossing points that are at the same height (or the closest) as the straight edge.

Figure 6-15 shows a graphical result of both methods when used to measure the crossing sidewear of a 16 PTS crossing (straight path). The two methods did not produce the same results. The measurements differ the most at the tip of the crossing 'vee' where the measured sidewear was 1.85 mm and 1.15 mm. This shows that the vertical position of the second reference, and as a consequence the pitch angle of the straight edge, can change the amount of measured sidewear. Thus the question arose as to which approach is correct. As the crossing had very few unworn parts, the comparison with the profile of a new crossing would have been potentially inaccurate. Thus, a different approach was used.

The crossing sidewear is relevant only to the passing of train wheels. As a conclusion, the wheel-rail interaction was considered. The sidewear can be measured at a height of 14 mm below the tread of the wheel, where the vertical position of the tread of the wheel is given by a wheel-rail simulation. Although a crossing wheel-rail simulation had not been carried out in this work, published wheel-rail simulations show that due to the dip present in crossings, train wheels experience a vertical displacement of 2 to 5 mm. Thus, considering that the sidewear should be measured at the height where the gauge contact normally occurs, the first method measures the sidewear at a height which is too high, overestimating it. Train wheels are partially supported by the wing rail as they engage with the tip of the crossing 'vee'. Thus, the second method measures the sidewear at a height which is too low, underestimating it.

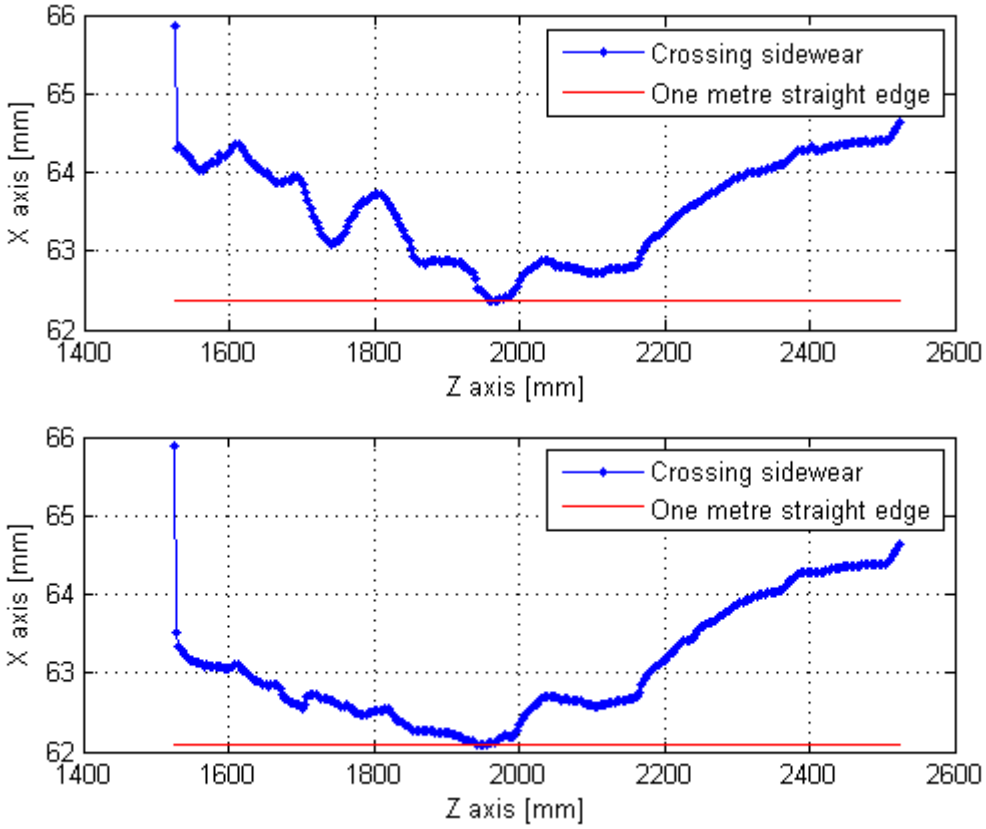

Figure 6-15 Crossing sidewear measurement example; top: stock rail knuckle used as second height reference; bottom: tip of crossing 'vee' used as second height reference (16 PTS, straight path)

According to published wheel-rail simulations, the second reference point should be in the range of 68.84-5 to 68.84-2 which comes out at 63.84 to 66.84 mm. As the vertical positions of the second reference point for the two methods were 62.95 mm and 68.84 mm respectively, this supports the conclusion that one method underestimates the sidewear and the other overestimates it.

As the vertical displacement of a train wheel running over crossings is generally not linear, but rather logarithmic, the author suggests that more accurate results should be obtained using a curved edge instead of a straight one, simulating the height of the wheel as is passes over the crossing.

The cosine like shape in the upper plot of Figure 6-15 was a result of localised deformation (similar to a score mark) on the side of the crossing. As a result, the author suggests that more accurate measurements could be possible if the sidewear measurement would be carried out at a range of depths instead of a fixed value (i.e. 10 to 14 mm).

Both methods show a high sidewear at 2500 mm along the Z axis, a location where the straight edge is expected to be fitted flush. The main reason for this result was a change in the shape of the crossing. Figure 6-16 shows two cross sections of the crossing nose, one at 1950 mm and one at 2500 mm. Note that unlike Figure 6-14 and Figure 6-15, these are not longitudinal sections (ZOX plane), but transverse ones (XOY plane).

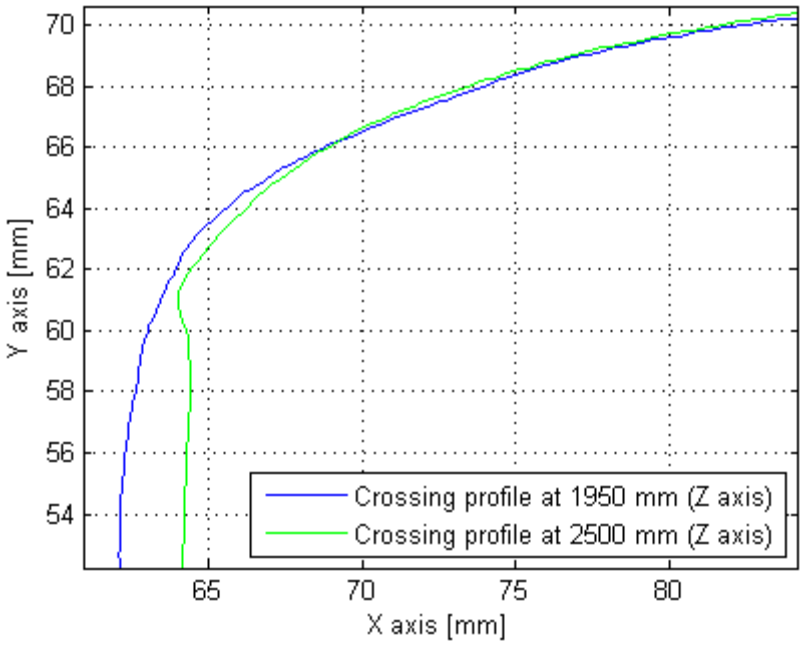

Figure 6-16 Two crossing profiles showing a change in shape (16 PTS, straight path, to scale)

The green plot was plotted with a vertical offset of 1 mm to vertically align the two plots. However, no offsets have been applied to the X axis. As the train wheels generally do not come in contact at angles shallower than 60 degrees, any wear below the point at 60 degrees does not matter from the wheel-rail interaction point of view. Thus, in the case of the green plot in Figure 6-16, the sidewear should be measured at a height of no less than 61 mm on the Y axis instead of 72-14=58 mm, as required by the standard 14 mm rule. If the straight edge is to be fitted flush at 14 mm below the top of the crossing considerable errors (2 mm) would affect the measurement at the crossing nose.

6.1.5 Inspection of wing rail top wear

The inspection of top wear on the wing rail is carried out by the application of a straight edge as shown in Figure 6-17. As the tread of train wheels is wider than the width of rails, the wheel-rail contact can occur anywhere within the two green lines. Railway crossings

generally suffer from excessive wear at the wheel-rail transfer area and the red spot shows an approximate location where the wing rail is likely to be most affected by top wear.

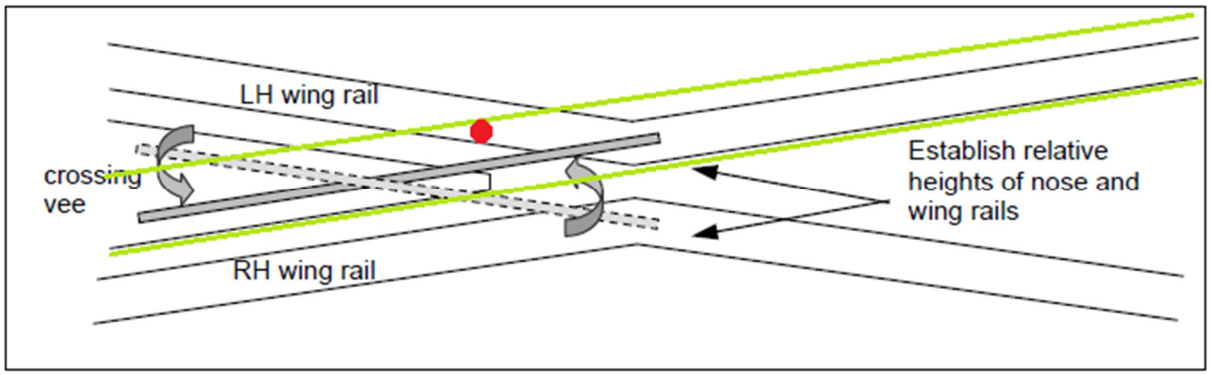

Figure 6-17 Inspection method of top wear of wing rail as defined in NR/L2/TRK/1054 adapted from NR/L2/TRK/1054; Courtesy and Copyright Network Rail

Manual measurements have been found to be very difficult to carry out. As the straight edge and the red spot are not vertically on top of each other, the application of the stepped gauge can be easily tilted, giving erroneous readings. It is difficult to know the correct orientation of the stepped gauge. Changing the position of the straight edge towards the wing rail underestimated the amount of wear, compromising the measurement.

The measurement algorithm is as follows:

1. Calculation of the straight edge position along the Z axis

The position of the straight edge along the Z axis was calculated as starting from the stock rail knuckle one metre towards and over the crossing 'vee'.

2. Calculation of the straight edge position along the X axis

The width of the stock rail at the knuckle is calculated and halved to find the horizontal middle of the rail. This distance is in the range of 34 to 37 mm relative to the gauge point. Both ends of the straight edge were positioned at the mentioned distance from the gauge point.

3. Calculation of height profile based on x and z coordinates
4. Application of the straight edge over the calculated height profile
5. Calculation of the stock rail/wing rail height profile

The height profile of the stock rail/wing rail must be calculated close enough to the gauge point so that the largest amount of wear can be measured, but at the same time, far enough

from the gauge point so that the naturally occurring corner of the rail is not mistakenly measured as top wear. As a compromise, the height profile was calculated at 10 mm from the gauge point.

6. Calculation of top wear

The top wear was calculated by subtracting the stock rail/wing rail height profile from the height of the straight edge.

Figure 6-18 shows the results of automatically inspecting the straight path of a 16 PTS crossing.

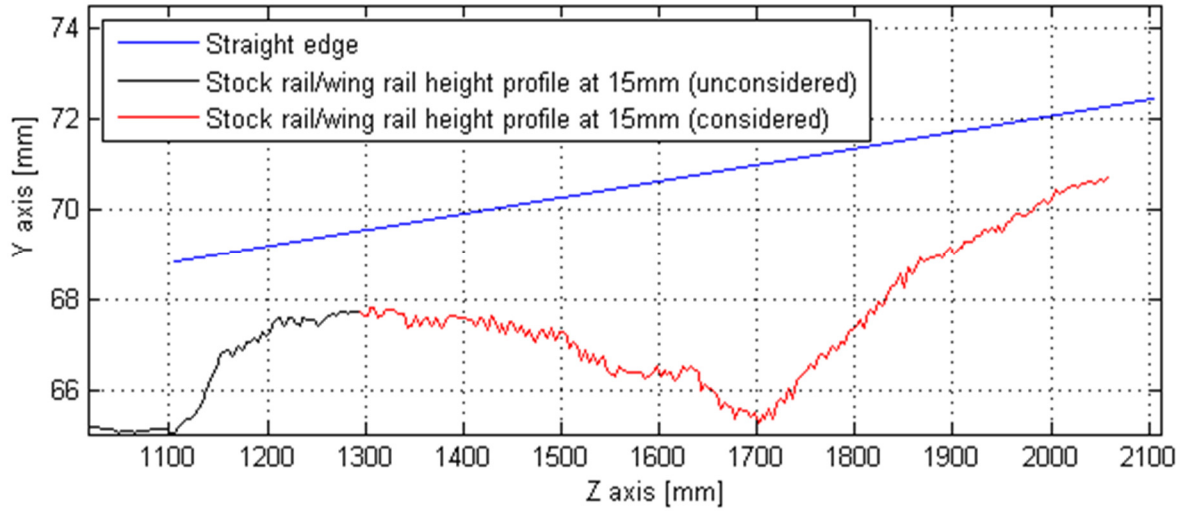

Figure 6-18 Wing rail top wear measurement example (16 PTS, straight path)

The significant difference of over 3 mm at the left end of the straight edge is due to the relatively round shape of the rail. Starting with the rail knuckle, the rail is chamfered, giving it a more square shape. However, even at approximately 1200 mm along the Z axis, the round shape of the rail results in measuring a two millimetre height difference between the height at the middle of the rail and the height at 10 mm from the gauge point. The author suggests that, at 1700 mm along the Z axis where the top wear of the wing rail is largest (5.5 mm relative to straight edge), a wear allowance should be considered to account for the slightly round design of the rail head.

The location of the highest wear, as marked by a red circle in Figure 6-17, was identified at around 1700 mm in the case of the straight path of 16 PTS. Figure 6-19 shows the wing rail profile at the mentioned location.

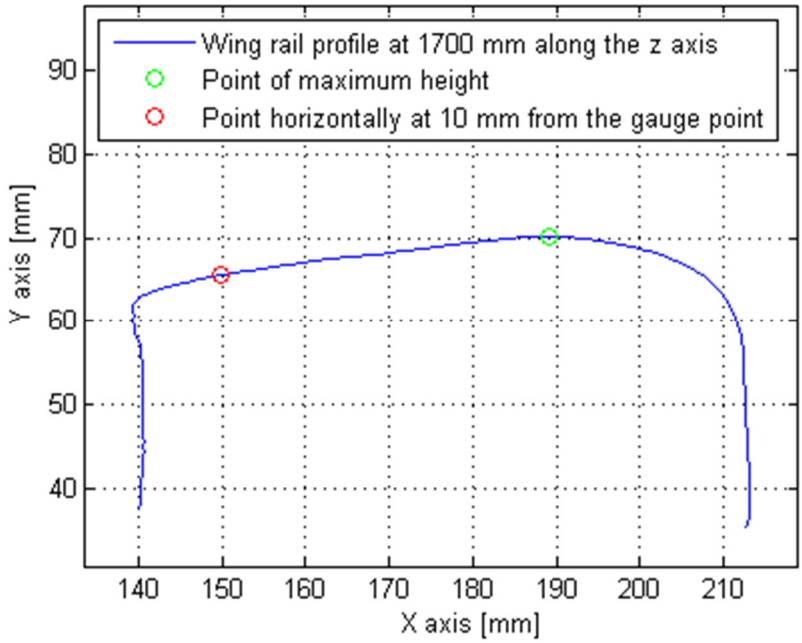

Figure 6-19 Wing rail profile at 1700 mm along the Z axis (16 PTS, straight path, to scale)

As the tread of the wheel starts to leave the wing rail, the right part of the rail has very little wear and the left part has developed excessive wear (green circle versus red circle in Figure 6-19). Because of this height difference (4.6 mm in this example) it was very difficult to measure the relative height of the red circle (in Figure 6-19) referenced to the straight edge (as shown in Figure 6-17). Depending on how the stepped gauge was handled, the readings changed by 2 to 3 mm. This measurement was found to be the most difficult and potentially the most inaccurate.

6.1.6 Inspection of crossing top wear

The inspection of top wear on the crossing is carried out by the application of a straight edge as shown in Figure 6-20.

Due to some crossing 'vees' having a dip in the middle, the manual inspection was found to be slightly inaccurate if the straight edge was fitted flush in the middle of the crossing (see Figure 6-21).

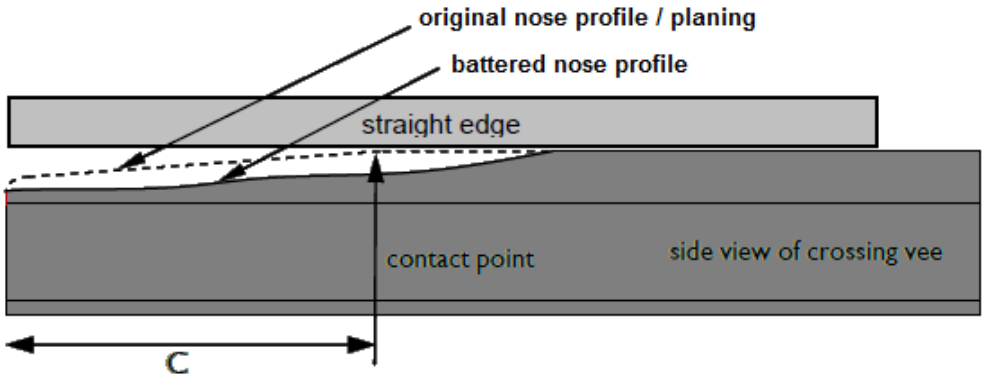

Figure 6-20 Inspection method of crossing top wear as defined by NR/L2/TRK/1054 Courtesy and Copyright Network Rail

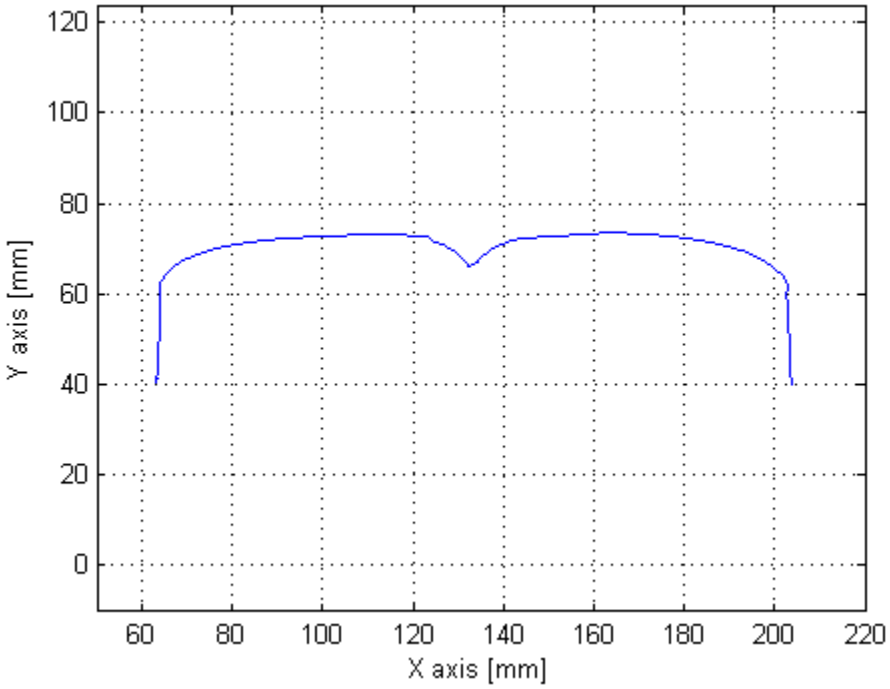

Figure 6-21 Crossing profile at 850 mm from the tip of the crossing 'vee' (16 PTS, straight path, to scale)

The measurement algorithm is as follows:

1. Calculation of crossing 'vee' height profile

In order to compensate for the dip as shown in Figure 6-21, the maximum height of the crossing was used to calculate the height profile of the crossing.

2. Application of straight edge over the calculated height profile

The straight edge was applied to the height profile so that a best fit was obtained for the right most 40 cm of the straight edge (as shown in Figure 6-20).

3. Calculation of top wear

The top wear was calculated by subtracting the crossing height profile from the height of the straight edge.

Figure 6-22 shows a measurement example of the same crossing, 16 PTS, straight path.

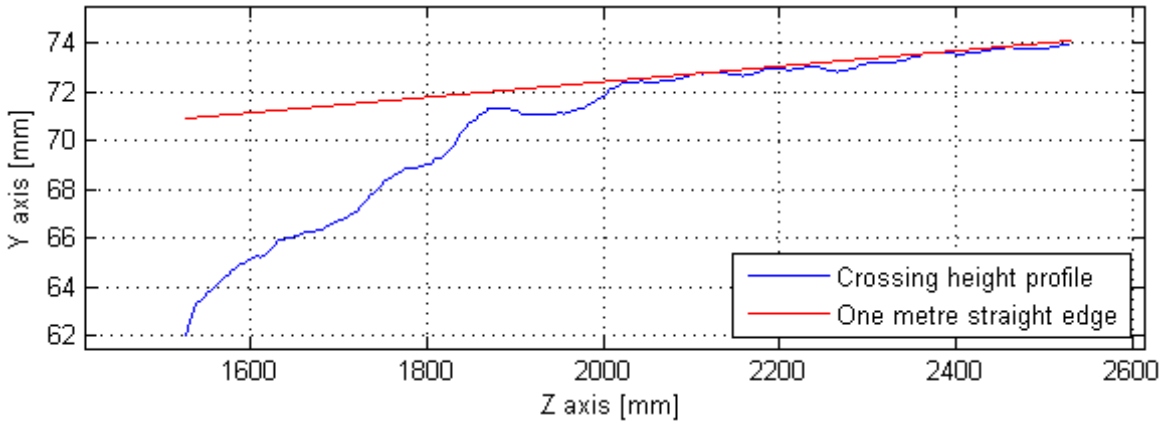

Figure 6-22 Crossing top wear measurement example (16 PTS, straight path)

Some crossings develop a distinct batter at the point where the train wheel loses contact with the wing rail. In Figure 6-22, such a batter is visible from 1900 to 2000 mm. In Figure 6-18 from the previous section, if a two millimetre allowance is given to account for the slightly rounded design shape of the rail, it can be observed that the wing rail wear starts at 1350 mm and ends around 2000 mm (the area where the red plot is more than 2 mm below the blue plot). The location of the batter on the crossing matches the location on the wing rail where the wear ends. This supports the hypothesis that the batter on the crossing nose is a result of the weight of the train wheel being moved onto the crossing nose.

Figure 6-23 shows the transverse profile of the wing rail (XOY plane) at two different locations, 1800 mm and 1950 mm. As part of the blue plot is vertically below the green plot it can be concluded that the blue plot shows more head wear than the green plot. The scale has different values for the X axis and Y axis respectively, as it is easier to observe the wear on the rail head. The wear on the blue plot can be observed as a slightly flat area. The green plot however does not show any flat area meaning that the wear on the wing rail at 1950 mm along the crossing is likely to be insignificant. The rail profile at the two locations of

1800 mm and 1950 mm in Figure 6-23 also supports the hypothesis that the batter on the crossing nose is a result of the weight of the train wheel being moved onto the crossing nose.

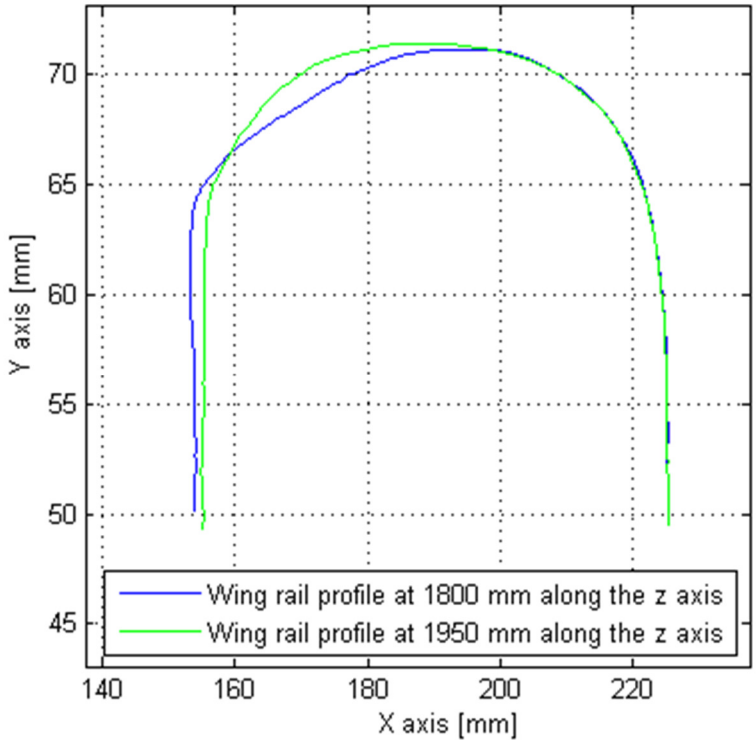

Figure 6-23 Wing rail profile (16 PTS, straight path, not to scale)

The batter on the crossing nose is a frequent crossing defect in the UK which is difficult to measure and size using current techniques. However, using automatic crossing measurements, the profile of the crossing and wing rail could be analysed in more detail to measure and quantify the wear, identify the presence of failure modes/wear mechanisms (such as the batter on the crossing nose) and even calculate wear rates. Such measurements could help towards asset management as well as aiding the weld and grind repair team with valuable information.

6.1.7 Conclusions

Straight edge analysis of railway crossing as sub millimetre accuracy is possible using measurement lasers. However, the straight edge methodology has inherent issues which can affect the accuracy of the measurements and the results provide limited information regarding the failure modes affecting the asset.

In the case of measuring crossing sidewear (i.e. see Figure 6-14), pivoting points resulted from lipping, metal migration and breakings can result in accurate measurements; more

accurate measurements should be possible if the sidewear would be measured above the area where lipping and breaking of the gauge corner occurs. Thus, the author proposes that the measurement would be carried out at a higher level such as 10 mm instead of 14 mm, or where the angle of the gauge corner is no greater than 60 degrees. Considering perfect shape conformity between the a new P8 wheel and the measured rail, the measurement would then take place somewhere between 95 mm and 100 mm on the horizontal axis of Figure 5-59, instead of over 100 mm, in the red area, where metal lipping and breakings are far more likely. The proposed method would also greatly minimize or eliminate the errors introduced by the changing shape of the crossing as shown in Figure 6-16. In this case the sidewear would be measured at a height of around 61 to 62 mm instead of 58 mm if the 14 mm rule would be applied. The chosen inclination of the straight edge can also affect the measurement and thus, should also be considered.

The inspection of wing rail top wear (Figure 6-17) is potentially the most inaccurate one when carried out manual using a straight edge. The reason for this is because the straight edge is not vertically above the area with the highest wear (red spot in Figure 6-17). As the straight edge is placed centrally on the head of the rail and the sidewear is cheeked closer to the gauge corner of the wing rail, the author suggests that due to the round shape of the gauge corner, an allowance should be given when measuring the wear. The amount depends on the design specification of the crossing. In the case of the straight path of crossing 16 PTS it is likely to be around 2 mm.

The use of non-contact automatic profile measurement systems could also be used to automatically identify wear related issues and occurring failure modes. For example, Figure 6-22 shows early sings of battering at the crossing nose as the weight of the train wheel is being moved onto the crossing nose.

It must be reminded that with the presented methodology, the measured height profile of the crossing is affected by the height profile of the opposite stock rail. However, the height profile of opposite stock rail can be considered straight when compared with crossings and any irregularities on the stock rail are attenuated due to the large distance of 1 m between the wheels that sit on the stock rail.

7 CURRENT AND POTENTIALLY IMPROVED MAINTENANCE REGIMES

This section considers the advantages and disadvantages of adapting and using the proposed S&C inspection system on a measurement train, an in-service train, a road-rail vehicle, a rail robot, as a trolley and as a laser-based hand gauge as part of the NR inspection regime for S&C profiles.

It must be noted that trains record the data while the track is loaded while lightweight robots (<300 kg), trolleys and handheld inspection devices record the data while the track is not loaded. Depending on the track loading, some measurements such as track gauge can differ substantially. In general, there is an interest in measuring the track parameters in both loaded and unloaded conditions. Thus, in the following section, the loading/unloading of the track is considered neither an advantage nor a disadvantage.

In this chapter, the term “possession” is often used. This term has a specific meaning when used by Network Rail and railway maintenance contractors and it is with the same meaning being used in this work. Under this meaning, trains which are scheduled in the train timetable do not take track possession regardless of whether the train is a passenger or a dedicated measurement train.

7.1.1 Current NR inspection regime of S&C profile

The current maintenance regime used by NR for the management of rail profiles in S&Cs throughout Britain is condition-based maintenance where the profile of S&C is repaired when it fails the periodic inspection. Furthermore, the periodic inspection is carried out at variable intervals. The interval between two consecutive inspections is determined based on various factors which include: track category, S&C type, S&C history, outcome of the last inspection and whether or not it is a recent installation. Thus, each S&C has a unique due by date for the next periodic inspection. Depending on the due date, schedule of the maintenance team, available possessions (if required) and other factors, a suitable date is arranged for the next inspection for each S&C. Typically, an S&C maintenance team visits two sites per day and inspect one or two switches and/or crossings per site (e.g. two switches at one site and a crossing at a different site).

7.1.2 Alternative profile inspection strategies for S&Cs

S&C inspection using dedicated measurement trains

Dedicated measurement trains can accurately inspect various track parameters at high speeds. These trains are generally expensive to maintain and run. In Britain, the New Measurement Train (NMT) is used to inspect medium and heavily used paths. Generally a path is inspected between once a month and every few months.

Advantages:

- Ability to automatically inspect a considerable numbers of S&Cs without requiring track possession

Disadvantages:

- Poor correlation between the automatically inspected S&Cs and the S&Cs requiring inspection
- Very poor S&C coverage in large stations (i.e. station with over 50 S&Cs)
- Inability to record both paths of an S&C in the same run
- S&Cs need to be clear of dirt and grease
- If the profile of the rails are not measured close to where the train wheel sits on the rail, the recorded height of the switch rail relative to the stock rail may be different than the one in practice when the switch rail is loaded; in this case the, in order to assure accurate inspections, the hogging of the switch rail should be measured automatically by the measurement train at the same time of measuring the rail profile (this may be very difficult to achieve on dirty switch rails)

S&C inspection using in-service trains

Small measurement equipment can be installed on in-service trains to inspect various track parameters [7,46]. In-service trains generally run on the same route several times a day.

Advantages:

- Ability to automatically inspect some S&Cs without requiring track possession
- Repeated measurements at fine time intervals
- Low running costs

Disadvantages:

- All disadvantages already mentioned re dedicated measurement trains

- Very low S&C coverage in the case of equipment permanently mounted on the train (because service trains generally run on the same routes)

S&C inspection using dedicated inspection wagons

An inspection wagon can be used to automatically inspect a considerable number of S&Cs within a large station.

Advantages:

- Ability to automatically inspect many S&Cs without requiring track possession
- Ability to automatically inspect many S&Cs within large stations

Disadvantages:

- Potentially high equipment cost
- Inspects all S&C in the same day (incompatible with current "due date" practice)
- S&Cs need to be clear of dirt and grease (could be overcome if cleaning is scheduled before inspection and lubrication afterwards)
- Similar to the dedicated measurement trains and in-service trains, switch rail hogging may need to be measured automatically and this may not be possible on dirty switch rails

S&C inspection using road-rail vehicles

Road-rail vehicles can be used to drive on both road and rail. They can be fitted with relatively large inspection equipment and can be used to drive to the inspection site. Once mounted on rails they can be used to inspect long track sections.

Advantages:

- Ability to measure specific S&Cs requiring inspection
- Potential to inspect a considerable number of S&Cs in a single site visit (provided they are all in the same area and can be easily thrown on demand)

Disadvantages:

- Potentially high equipment cost
- Requires track possession
- Difficult to use where level crossings are not present
- Difficult to move between specific S&Cs in large stations (> 50 S&Cs)

- Potentially low productivity if few (1 to 3) S&Cs are inspected per site visit

S&C inspection using on-site robots

Rail robots can be used to autonomously measure and inspect track parameters in various locations within a railway site. In the context of S&C inspection, their use is more beneficial in large stations where many S&Cs could be measured in one site visit.

Advantages:

- Ability to measure specific S&Cs requiring inspection
- Potential to inspect a considerable number of S&Cs in a single site visit (provided they are all in the same area and can be easily thrown on demand)

Disadvantages:

- Potentially high equipment cost
- Requires track possession
- Difficult to carry to and from inspection site (considering a weight of 150 kg)
- Difficult to move between specific S&Cs in large stations (> 50 S&Cs)
- Potentially low productivity if few (1 to 3) S&Cs are inspected per site visit

S&C inspection using rail trolleys

Measurement trolleys can be a relatively lightweight (20-40 kg) piece of equipment that can be used to inspect various track parameters.

Advantages:

- Ability to measure specific S&Cs requiring inspection
- Potential to inspect a considerable number of S&Cs in a single site visit (provided they are all in the same area)
- Easier to handle than road-rail vehicles and rail robots (due to size and weight)

Disadvantage:

- Very likely to require track possession
- Potentially low productivity if few (1 to 2) S&Cs are inspected per site visit

S&C inspection using laser-based hand gauges

Hand gauges (< 10 kg) are common in the rail industry and have the advantage of portability. Thus, they can be used on live tracks in Britain without the need to arrange a possession as workers can pick them up and leave the track when a train is approaching.

Advantages:

- Ability to measure specific S&Cs requiring inspection
- Easier to handle than road-rail vehicles, rail robots and rail trolleys (due to size and weight)
- No possession required
- Lower equipment cost compared with any other solution

Disadvantages:

- Less productive if needing to carry out many inspections in different locations of the same S&C

7.1.3 Conclusions

Each inspection method has its own advantages and the efficiency of each method depends on how these advantages are used in the implementation of the whole maintenance regime (in this context efficiency refers to the amount of money spent and time needed to routinely inspect all S&Cs in a network).

Referring strictly to train based inspection methods, the in-service train with permanently mounted inspection equipment provides the smallest throughput in terms of unique inspected S&Cs/month. The NMT is scheduled to run various train paths so that track sections are inspected periodically. It could be used to periodically inspect a relatively large amount of S&Cs in the rail network. This may also be achieved with an add-on system such as the RILA (compact measurement system that can be easily attached to the end of passenger trains) if its schedule is well planned. Although there is no correlation between the S&C requiring inspection and those inspected, due to the large number of inspected S&Cs, it is expected that it would significantly reduce the number of manual S&C profile inspections required.

Wagon based inspection systems such as the SIM (Switch Inspection and Measurement) could be used efficiently in large stations, as up to 100 S&Cs could be inspected in a few hours during the weekend night break.

However, the use and accuracy of these systems greatly depends on the cleanliness of the rails. It is very likely that the properties of lubricants would have to be improved and even then a case study would be needed to identify the safety risks involved with the automatic inspection of greasy and dirty switch rails. Moreover, the hogging of switch rails has to automatically be measured.

In the case of on-site inspection of S&Cs, an S&C inspection solution should ideally: (1) be easy to set-up and clean-up (mounting, dismounting, carrying), (2) be rapid to use and (3) not require track possession.

A laser-based hand gauge would be easy to carry around and use and it would not require track possession. However, these gauges are relatively slow to use as many individual measurements need to be carried out. As a conclusion, a laser-based hand gauge is efficient in the context of the current maintenance regime where many workers are required to visit a site to inspect a single S&C (or two, but at a distance apart) and do it without track possession.

The use of larger equipment for the inspection of a single S&C per site visit would not increase the inspection efficiency, as the time saved when carrying out the actual inspection is easily lost in the more time-consuming process of set-up and clean-up.

The efficiency of using rail trolleys, rail robots and road-rail vehicles is dependent on many factors. The most important factor is the number of S&Cs that are to be inspected per site visit. Other factors include: the ease with which points can be thrown on demand, the railway layout, the location of S&Cs requiring inspection and site access facilities. Thus, it can be difficult to accurately establish the efficiency of these methods, however, all three solutions have the potential to increase the inspection efficiency in large stations.

In comparison with rail robots and road-rail vehicles, rail trolleys have the advantage of being easier to set-up and clean-up, which means they can also be used by weld and grind teams when repairing an S&C. The benefits of using a laser-based S&C measurement trolley are: (a) a better and more comprehensive understanding of the condition of the S&C, (b) advice with regards to repair (i.e. the switch that derailed a train at Princes Street Gardens [12] was beyond repair when a repair was attempted; the inspection trolley could identify situations where repair by grinding would introduce more derailment risks), (c) re-inspect the S&C after completion of weld and grind work to assure the switch is safe for traffic. Table 7

summarises several advantages and disadvantages of the discussed current and potential S&C profile inspection systems.

Table 7 Summary comparison between various current and potential S&C profile inspection systems

Inspection system / Consideration	Dedicated measurement train	In service train with		Dedicated inspection wagon	Road-rail vehicle	On site robot	Rail trolley	Laser-based hand gauges
		permanently fixed equipment	detachable equipment (e.g. RILA)					
Throughput	Relatively high			High in large stations	Medium to high in large stations		Low to medium in large stations	Low
Correlation between inspected S&Cs and S&Cs that required inspection	Low to medium	Very low	Low to medium		Low to medium in large stations		Medium to high	High
Rail cleaning method and switch rail hogging measurement method	No documented methods				Potentially manual cleaning of rails and manual measurement of switch rail hogging		Manual cleaning of rails and manual measurement of switch rail hogging	
Track access method	Train timetabling	No access method needed as the in-service trains are already timetabled		Train timetabling	Track possession		Track possession or working on a line that is open to traffic	

8 CONCLUSIONS

8.1 Summary and findings

8.1.1 Stage one

As railway usage is set to increase, even less time will be available for the maintenance of railway assets. As a result the railway will need to continue to improve through more reliable infrastructure and better maintenance practices. S&Cs are a considerable cost driver of any complex railway and thus much attention is given, and will continue to be given, to both reducing maintenance costs and increasing availability of these assets.

S&Cs require a wide range of inspection tasks which have been reviewed and classified into the six key inspection groups:

1. Visual inspection tasks;
2. Inspection of shape, size and position of switch rails, stock rails, crossing, wing rails and check rails;
3. Geometry measurements (gauge, cant, twist, alignment and levelling);
4. Measurement of cracks in rails and crossing;
5. Tightness checks, and;
6. Point machine inspections.

The biggest challenge towards a “self-inspecting switch” is non-destructive testing for cracks, as, due to the non standard shape of rails, fast and accurate measurement cannot be foreseen in the near future. However, it has been concluded that, with the exception of crack measurement, the majority of S&C inspection tasks could soon be automated (in 5 to 10 years) by using a combination of proven technologies and research/prototype level advancements.

One key point is that if automatic inspection of S&C is to be introduced, S&C will have to be kept clean, as it is very unlikely that any advances in sensing and measurement technologies would be able to overcome this shortcoming. This is likely to be achieved through the use of better lubricants and better switch sliding mechanisms (e.g. switch rollers, dry slide chairs, etc).

Although in recent years, research on railway condition monitoring has rapidly increased and condition monitoring techniques have been successfully used to reduce maintenance costs and increase safety, these techniques have not been found to be useful in working towards the elimination of manual S&C inspection tasks. This is in part due to the type of inspections that are generally required by the inspection standards and in part due to the high inspection integrity required as a result of S&C being safety-critical assets.

Network Rail S&C inspection requirements were identified and categorised in sections 2.1 and 2.2. Relevant commercial and research solutions for the automatic inspection of S&Cs were also identified and classified in sections 2.3 and 2.4. The relevant solutions were compared against the identified inspection requirements and necessary advances and future challenges required to achieve a "self-inspecting" S&C have been identified and discussed in section 2.5. Thus, the first aim of this work was satisfied in Chapter 2.

8.1.2 Stage two

The activities undertaken in the second stage of this research, together with some of the outcomes, are summarised in the following bullet point list:

- Identified important accuracy requirements for the automatic inspection of switch rails against derailment hazards: the high importance of point cloud accuracy for the automatic inspection of TGP8 (sections 4.2 and 4.2.2 in particular);
- Identified causes for inaccurate manual inspection of switch rails (random errors): a 1 degree rotation of the NR4 gauge can change the measurement result by a full unit on the sidewear scale (section 4.2.2); slight changes in the positioning of the switch rail radius gauge can change the outcome of the inspection (section 5.1.7);
- Identified inherent issues relating to the switch inspection gauges (systematic errors): TGP8 gauge measurements can be inaccurate due to the poor conformity between the gauge and the inspected rail (section 5.1.4); the switch rail radius gauge is not able to identify all cases of sharp switch rails (section 5.1.7); the NR4 gauge measurements can be inaccurate when the field side of the inspected rail is not in a good condition (section 5.1.3);
- Developed accurate automatic inspection algorithms for each of the five derailment hazards (section 5);
- Developed an effective filtering algorithm (applicable only on convex data), which smooths the data while preserving the corners (section 5.1.2);

- Developed a method for accurately measuring the roll angle of the trolley when measuring railway crossings (section 6.1.1);
- Identified causes of inaccurate manual inspection of railway crossings: pivot points and localised wear can reduce the accuracy of the sidewear measurement by several millimetres (section 6.1.4); the height profile of the straight edge for the measurement of sidewear does not follow the vertical trajectory of the train wheel, reducing the accuracy further by up to a millimetre (section 6.1.4); due to several reasons which were identified, the measurement of top wear on the wing rail can be inaccurate by several millimetres (section 6.1.5); the measurement of top wear on the crossing nose can be inaccurate by several millimetres if the straight edge is placed in the developing gap of the crossing (section 6.1.6);
- Proposed several improvements to increase the accuracy of the automatic inspection of railway crossings from millimetres to sub-millimetre (sections 6.1.4 and 6.1.5);
- Developed automatic inspection algorithms for the inspection of railway crossings (sections 6.1.1 to 6.1.6), and;
- Developed a prototype trolley and carried out field trials for the inspection of S&Cs.

In sections 5.1.3 to 5.1.7 several issues relating to the manual profile inspection of switches were identified, alternative switch inspection methods with considerably reduced human error were developed tested and improvements to reduce systematic errors were proposed.

Similarly, in sections 6.1.3 to 6.1.6 issues relating to the manual profile inspection of crossings were identified, alternative crossing inspection methods with considerably reduced human error were developed and tested and improvements to reduce the systematic errors were proposed.

Thus, the second aim of this work was satisfied in chapters 3 to 6.

8.2 Limitations and future work

As the purpose of the research was to develop an automatic method for carrying out the S&C inspection tasks as they are set out in the NR/L2/TRK/0053 and NR/L2/TRK/1054 inspection standards (for compatibility with current practice), the performance of the method is affected by the inherent limitations of the manual gauges. The methods can be improved at the price of losing (to a certain extent) compatibility with current manual practices. However, the

author believes that as newer and improved methods are demonstrated to have a high integrity level, it is expected that the inspection standards are updated.

The automatic NR4 measurement could be replaced with an alternative measuring process which provides greater accuracy. The measurement result could then be converted to the NR4 sidewear scale to maintain compatibility.

The TGP8 measurement has serious limitations as, due to poor TGP8-rail conformity, the measurements are rarely accurate to +/-2 degrees. However, an alternative, accurate to within +/-2 degrees would fail many S&Cs which currently pass the TGP8 gauge. Thus, to maintain the same level of safety, the intervention limit would likely have to be reduced from the current threshold of 60 degrees.

Automatic inspection against sharp switch rails can provide reliable results; however, the calculation considers a worst case wheel profile for each analysed rail profile. Actual wheel profiles may be better than the worst case, leading to a conservative inspection. The algorithm could be improved by establishing limits to worst case wheel profiles. However, the undermining of the worst case wheel profile could lead to false negatives, making the task difficult.

The algorithms were tested on a limited number of S&Cs. Thus, prior to using these algorithms in a commercial product, they should be peer-reviewed and tested on a larger number of S&Cs.

Grease and dirt can render optical inspections useless and thus are an issue in the automatic inspection of S&Cs. The use of grease on rails has been proven to reduce the wear rate and it is therefore unlikely that NR will stop using grease on switch rails. Moreover, grease is also used by NR to mitigate the derailment risk. Thus, the research and development of better lubricants could play a significant role in the automation of S&C inspection. Desirable properties for a grease that is to be used on optically inspected S&C are: (a) reduced thickness to minimise optical measurement errors, and (b) less sticky to avoid attracting dirt and debris.

Portable laser based S&C inspection systems could potentially also be used to assist S&C repair works. New algorithms could be developed to simulate the condition of a switch blade after an intended set of repair actions (e.g. grind a certain amount at a certain angle). The algorithm could then alert the user if the intended repair can lead to the creation of a

derailment hazard. If such a system would have been used, the derailment in Glasgow [11] may have not happened (the repair work introduced a derailment hazard 2 while removing a derailment hazard 1).

Repeated profile measurements on the same S&Cs using in-service trains could be used to carry out trend analysis and failure prognosis. Such information could prove very valuable when used to improve the planning of S&C maintenance and renewals.

9 REFERENCES

1. McNulty SR. Realising the potential of GB rail, Final Independent Report of the Rail Value for Money Study, Detailed Report [Internet]. Department for Transport; 2011. Available from: https://www.gov.uk/government/uploads/system/uploads/attachment_data/file/4204/realising-the-potential-of-gb-rail.pdf
2. Department for Transport. National Policy Statement for National Networks [Internet]. 2014. Available from: https://www.gov.uk/government/uploads/system/uploads/attachment_data/file/387223/npsnn-web.pdf
3. Office of Rail and Road. Requirements for Network Rail's January 2013 Strategic Business Plan [Internet]. 2012. Available from: http://orr.gov.uk/__data/assets/pdf_file/0010/1243/network-rail-2013-sbp-requirements.pdf
4. The Future Railway. The Industry's Rail Technical Strategy 2012, Supporting Railway and Businesses [Internet]. 2012. Available from: http://www.futurerailway.org/Documents/RTS 2012 The Future Railway.pdf
5. McNulty SR. Realising the potential of GB rail, Report of the Rail Value for Money Study, Summary Report [Internet]. Department for Transport; 2011. Available from: https://www.gov.uk/government/uploads/system/uploads/attachment_data/file/4203/realising-the-potential-of-gb-rail-summary.pdf
6. Moubray J. Reliability-centred Maintenance, Second edition. Butterworth-Heinemann; 1997.
7. Nissen A, Colina J, Eiby JU, Taymans M, Lundgreen SO, Kiss C, et al. Inspection of Switches & Crossings, State of the Art Report. 2011.
8. Health and Safety Commission. Train derailment at Potters Bar 10 May 2002, A progress report by the HSE investigation board [Internet]. 2003. Available from: http://www.railwaysarchive.co.uk/documents/HSE_PottersRep052003.pdf
9. Rail Accident Investigation Branch. Derailment at Grayrigg, 23 February 2007 [Internet]. 2011. Available from: http://www.raib.gov.uk/cms_resources.cfm?file=/081023_R202008_Grayrigg_v5.pdf
10. Rail Accident Investigation Branch. Derailments at London Waterloo 11 September and 24 October 2006 [Internet]. 2007. Available from: http://www.raib.gov.uk/cms_resources.cfm?file=/071218_R442007_Waterloo.pdf
11. Rail Accident Investigation Branch. Derailment near Exhibition Centre station, Glasgow, 3 September 2007 [Internet]. 2009. Available from: http://www.raib.gov.uk/cms_resources.cfm?file=/090212_R042009_Glasgow.pdf
12. Rail Accident Investigation Branch. Derailment at Princes Street Gardens, Edinburgh 27 July 2011 [Internet]. 2012. Available from:

http://www.raib.gov.uk/cms_resources.cfm?file=/120830_R182012_Princes_St_Gardens.pdf

13. Rail Accident Investigation Branch. Derailment of a freight train at Shrewsbury station, 7 July 2012 [Internet]. 2012. Available from: http://www.raib.gov.uk/cms_resources/130722_R082013_Shrewsbury.pdf
14. Rail Accident Investigation Branch. Derailment at Archway, 2 June 2006 [Internet]. 2006. Available from: http://www.raib.gov.uk/cms_resources.cfm?file=/061211_R242006_Archway.pdf
15. Network Rail. Inspection and repair to reduce risk of derailment at switches (NR/L2/TRK/0053). 2008;(5):48.
16. Network Rail. Inspection, maintenance and repairs procedures for cast, welded and fabricated crossings in the track (NR/L2/TRK/1054). 2012;(4):34.
17. Network Rail. Catalogue of Network Rail Standards. 2015;(95):242. Available from: https://www.networkrail.co.uk/Catalogue-of-Network-Rail-Standards.pdf
18. Roberts C, Bouch C. A methodology for creating engineering models to help assess the cost impact of new railway technologies. Proceedings of the International Transport Economics Conference. Minnesota, USA; 2009.
19. Network Rail. Inspection and Maintenance of Permanent Way. 2009;(4):4.
20. Network Rail. Inspection and maintenance of permanent way – Inspection. 2009;(4):82.
21. Network Rail. Inspection and maintenance of permanent way – Rail management. 2009;(4):86.
22. Network Rail. Inspection and maintenance of permanent way – Geometry and gauge clearance. 2009;(4):28.
23. Network Rail. Inspection and maintenance of permanent way – Specific requirements for switches and crossings. 2009;(4):23.
24. Network Rail. Inspection and maintenance of permanent way – Installation requirements, maintenance limits and intervention limits. 2009;(4):41.
25. Network Rail. Signal Maintenance Specifications.
26. Network Rail. Point Inspection. 2010;(7):3.
27. Network Rail. Clamp Lock Hydraulic Points. 2009;(5):12.
28. Network Rail. Point Machine HW Style. 2009;(3):16.
29. Network Rail. Point Fittings. 2010;(7):19.
30. Network Rail. Mechanical Supplementary Drives. 2009;(6):3.
31. Network Rail. Point Fittings: Switch Rollers. 2009;(2):1.
32. DB Netz AG. Regelwerk Oberbau; Richtlinienfamilie 821 “Oberbau inspizieren.” 2009;(11).
33. Brouwer G. Questionnaire - Maintenance Specifications S&C. 2008.

34. Rail Accident Investigation Branch. Derailment at Primrose Hill / Camden Road, West Junction, 15 October 2013 [Internet]. 2014. Available from: http://www.raib.gov.uk/cms_resources.cfm?file=/141014_R212014_Camden_Road_West_Jn.pdf

35. Whalen MW, Heimdahl MPE. On the Requirements of High-Integrity Code Generation. High-Assurance Systems Engineering, 1999 Proceedings 4th IEEE International Symposium on 17-19 Nov 1999. 1999. p. 217–24.

36. Groom S. Can We Measure Our Way Out Of Trouble? The Truth Behind Condition Monitoring. The 6th IET call-for-papers conference on Railway Condition Monitoring. Birmingham; 2014.

37. Jardine KSA, Lin D, Banjevic D. A review on machinery diagnostics and prognostics implementing condition-based maintenance. Mech Syst Signal Process. 2006;20(7):1483–510.

38. An D, Kim NH, Choi J-H. Practical options for selecting data-driven or physics-based prognostics algorithms with reviews. Reliab Eng Syst Saf [Internet]. 2015;133(0):223–36. Available from: http://www.sciencedirect.com/science/article/pii/S0951832014002245

39. García FP, Tobias AM, Pinar JM, Papaelias M. Condition monitoring of wind turbines: Techniques and methods. Renew Energy [Internet]. 2012;46(0):169–78. Available from: http://www.sciencedirect.com/science/article/pii/S0960148112001899

40. Tran VT, Yang B-S. An intelligent condition-based maintenance platform for rotating machinery. Expert Syst Appl [Internet]. 2012;39(3):2977–88. Available from: http://www.sciencedirect.com/science/article/pii/S0957417411012905

41. Liu J, Wang W, Golnaraghi F. An Enhanced Diagnostic Scheme for Bearing Condition Monitoring. Ieee Trans Instrum Meas [Internet]. 2010;59(2):309–21. Available from: <Go to ISI>://WOS:000273565700007

42. Asada T, Roberts C, Koseki T. An algorithm for improved performance of railway condition monitoring equipment: Alternating-current point machine case study. Transp Res Part C Emerg Technol [Internet]. 2013;30(0):81–92. Available from: http://www.sciencedirect.com/science/article/pii/S0968090X1300020X

43. EURAILSCOUT. Switch Inspection & Measurement fact sheet [Internet]. 2014. Available from: http://www.eurailscout.com/1-switch-inspection-measurement-sim-features-and-arguments_en.html

44. Ji Z, Leu MC. Design of optical triangulation devices. Opt Laser Technol [Internet]. 1989;21(5):339–41. Available from: http://www.sciencedirect.com/science/article/pii/0030399289900686

45. Roberts C, Kent S, Rusu M, Larsson D, Huguet S, den Decker J, et al. Augmented Usage of Track by Optimisation of Maintenance, Allocation and Inspection of Railway Networks; Task 3.2: Modular, Self-Inspecting Infrastructure; Deliverable Report D3.2 [Internet]. 2014. Available from: http://www.automain.eu/IMG/pdf/d3.2._rev_version.pdf

46. Fugro. News Release: Guaging the distance [Internet]. 2013. Available from: http://fugro-aperio.com/new/files/Guaging_the_distance.pdf

47. Zarembski A, Palese J, Euston T, Scheiring W. Development and Implementation of Automated Switch Inspection Vehicle . 2011. Available from: https://www.arema.org/files/library/2011_Conference_Proceedings/Development_and_Implementation_of_Automated_Switch_Inspection_Vehicle.pdf

48. KLD Labs. Rail Profile Measurement [Internet]. 2014. Available from: http://www.kldlabs.com/track-assessment/rail-wear-measurement

49. Loccioni. Felix, the robot for railroad switch dimensional measurement [Internet]. 2013. Available from: http://research.loccioni.com/wp-content/uploads/2013/11/Felix_web1.pdf

50. Redeker R. Automain: the Self Inspecting Switch - The Strukton Approach . 2012.

51. Silmon JA. Operational industrial fault detection and diagnosis: Railway actuator case studies [PhD Thesis]. [Birmingham]: University of Birmingham; 2009.

52. Salas S. Vossloh's sensor experience for turnout monitoring system. Vossloh Cogifer SA; 2008.

53. Research Councils UK. Energy Harvesting for a Smart Washer [Internet]. 2014. Available from: http://gtr.rcuk.ac.uk/project/1AF18B99-51F6-4D8A-A606-6010B8DAECA6

54. RotaBolt. RotaBolt-TD system [Internet]. Available from: http://www.rotabolt.co.uk/td/

55. Asplund M, Larsson D, Rantatalo M, Nissen A, Kumar U. Inspection of railway turnouts using camera. World Congress on Railway Research. Sydney, Australia; 2013.

56. Tinsley Bridge Group. Rail Stretcher Bars – World Class Quality [Internet]. 2014. Available from: http://www.tinsleybridge.co.uk/2014/06/rail-stretcher-bars-world-class-quality/

57. Hsu SS. An Update on Common Crossings. 2014.

58. Molina LF, Resendiz E, Edwards JR, Hart JM, Barkan CPL, Ahuja N. Condition Monitoring of Railway Turnouts and Other Track Components Using Machine Vision. Proceedings of the Transportation Research Board 90th Annual Meeting. 2010.

59. Lewis SR, Lewis R, Evans G, Buckley-Johnstone LE. Assessment of railway curve lubricant performance using a twin-disc tester. Wear [Internet]. 2014;314(1-2):205–12. Available from: <Go to ISI>://WOS:000337018100027

60. Chen H, Fukagai S, Sone Y, Ban T, Namura A. Assessment of lubricant applied to wheel/rail interface in curves. Wear [Internet]. 2014;314(1-2):228–35. Available from: <Go to ISI>://WOS:000337018100030

61. Zarembski A. Reducing Wheel Climb at Switch Points to Reduce Derailments. 2014.

62. Interflon. Interflon Products [Internet]. Available from: http://www.directtracksolutions.co.uk/mar2011/Interflon Products sheets.pdf

63. Papaelias MP, Roberts C, Davis CL. A review on non-destructive evaluation of rails: state-of-the-art and future development. Proc Inst Mech Eng Part F-Journal Rail Rapid Transit [Internet]. 2008;222(4):367–84. Available from: <Go to

ISI>://WOS:000261435000006

64. Bombardier. Installation and Service Manual EBI Switch 2000; A Sleeper Integrated Point Machine. 2011.

65. IAD Rail Systems. High Performance Switch [Internet]. Available from: http://www.iadrailsystems.com/HPSS Overview - Standard.pdf

66. Silmon J, Roberts C. Using functional analysis to determine the requirements for changes to critical systems: Railway level crossing case study. Reliab Eng Syst Saf [Internet]. 2010;95(3):216–25. Available from: <Go to ISI>://WOS:000274590900008

67. Office of Rail Regulation. ORR response to "Derailment at Princes Street Gardens, Edinburgh" [Internet]. 2013. Available from: http://orr.gov.uk/__data/assets/pdf_file/0014/1607/raib-princes-st-gdn-2013-08-05.pdf

68. Wan C, Markine VL, Shevtsov IY. Improvement of vehicle-turnout interaction by optimising the shape of crossing nose. Veh Syst Dyn [Internet]. 2014;52(11):1517–40. Available from: <Go to ISI>://WOS:000345074800008

69. Department of Defence Systems Management College. Systems Engineering Fundamentals [Internet]. Defense Acquisition University Press; 2001. Available from: http://ocw.mit.edu/courses/aeronautics-and-astronautics/16-885j-aircraft-systems-engineering-fall-2005/readings/sefguide_01_01.pdf

70. Zarembski A, Palese J, Euston T. Automated Turnout Inspection. US: Harsco Corporation; 2013.

71. Curless B. From range scans to 3D models. SIGGRAPH Comput Graph. 1999;33(4):38–41.

72. Glaus R. The Swiss Trolley – A Modular System for Track Surveying. 2006.

73. PCL. About PCL [Internet]. Available from: http://pointclouds.org/about/

74. Volodine T. Point cloud processing using linear algebra and graph theory [PhD Thesis]. [Leuven]: Katholieke Universiteit Leuven; 2007.

75. Joseph O. Computational geometry in C. 2nd ed. Cambridge: The press syndicate of the University of Cambridge; 1998.

76. Kroon D-J. Iterative Closest Point using finite difference optimization to register 3D point clouds affine. 2009.

77. Wilm J. An implementation of various ICP (iterative closest point) features. 2010.

78. Rail Accident Investigation Branch. Derailment at Birmingham Snow Hill, Midland Metro, 29 January 2007 [Internet]. 2007. Available from: http://www.raib.gov.uk/cms_resources/071024_R382007_Snow_Hill.pdf

79. Felix S. Best Practice in Wheel-Rail Interface Management for Mixed Traffic railways. First. Birmingham; 2010.

80. Marquis B, Greif R. Application of Nadal limit in the prediction of wheel climb derailment. Proceedings of the Asme/Asce/Ieee Joint Rail Conference [Internet]. New York: Amer Soc Mechanical Engineers; 2012. p. 273–80. Available from: <Go to ISI>://WOS:000322053400031

81. Kester WA. Data Conversion Handbook [Internet]. Elsevier; 2005. Available from: http://books.google.co.uk/books?id=0aeBS6SgtR4C

82. Euston TL, Zarembski AM, Hartsough CM, Palese JW. Analysis of Wheel-Rail Contact Stresses Through a Turnout [Internet]. 2012 Joint Rail Conference. Philadelphia, Pennsylvania, USA; 2012. p. pp. 1–8. Available from: http://proceedings.asmedigitalcollection.asme.org/proceeding.aspx?articleid=1716260

83. Woodman O. An introduction to inertial navigation [Internet]. University of Cambridge; 2007. 37 p. Available from: https://www.cl.cam.ac.uk/techreports/UCAM-CL-TR-696.pdf

APPENDIX A: PUBLISHED PAPERS

During the course of the PhD, the following papers have been published:

1. The use of laser based trolley for railway switch and crossing inspection, Proceedings of the 2nd International Workshop & Congress on eMaintenance: trends in technologies and methodologies, challenges, possibilities and applications, December 2012, Luleå, Sweden (ISBN 978-91-7439-539-6).
2. The use of laser based trolley for railway switch and crossing inspection, International Journal of Condition Monitoring and Diagnostic Engineering Management, October 2013 (VOL. 16 NO. 4, ISSN 1363 - 7681).

APPENDIX B: LEADS TABLES

Table 8 NR/L2/TRK/001/D01 leads table

Leads to:	Relevancy:
GE/RT8000, Rule Book.	NA
NR/L2/TRK/001/A01, Inspection and maintenance of permanent way – Inspection.	R
NR/L2/TRK/001/B01, Inspection and maintenance of permanent way – Rail management.	NA
NR/L2/TRK/001/C01, Inspection and maintenance of permanent way – Geometry and gauging.	R
NR/L2/TRK/001/E01, Inspection and maintenance of permanent way - Installation requirements, maintenance limits and intervention limits.	R
NR/L2/TRK/0053, Inspection and repair procedures to reduce the risk of derailment at switches.	L
NR/L2/TRK/3011, Continuous welded rail (CWR) track.	NA
NR/L2/TRK/2049, Track design handbook.	NA
NR/L3/TRK/1202, S&C systems – Flat bottom full depth switches – Management of fixed stretcher bar assemblies, lock stretcher bar assemblies, fastenings and associated defects.	NA
NR/L3/TRK/1202/A, Action Tables.	NA
NR/L3/TRK/1202/B, Patrollers Action Table.	NA
NR/L3/TRK/3001, Ordering of switch and crossing components.	NA
RT/CE/S/037, Requirements for maintenance of trackwork in depots by Depot Facility Operators.	NA

RT/CE/S/054, Inspection of cast crossings and cast vees in the track.	L
NR/L3/TRK/003, Index to track engineering forms.	NA

Table 9 RT/CE/S/054 leads table

Leads to:	Relevancy:
RT/CE/S/056 Rail testing: non-ultrasonic procedures	NA
RT/CE/S/057 Rail Failure Handbook	NA
RT/CE/S/103 Track inspection requirements	D

Table 10 NR/L2/TRK/0053 leads table

Leads to:	Relevancy:
NR/SP/TRK/001 Inspection and maintenance of permanent way	D
NR/SP/TRK/0132 Maintenance arc welding of plain rails and switches and crossings	NA
NR/WI/TRK/001 Track Inspection Handbook	D
NR/SP/CTM/011 Competence and training in track engineering	NA
TEF/3008 Welders work return – switch repairs	NA
TEF/3029 Detailed switch inspection report (053)	NA
TEF/3042 Hand grinding record form (HG1)	NA
TEF/3054 Switches and crossings welding assessment / replacement form	NA
UIC Leaflet 716R Maximum permissible wear profiles for switches	NA

APPENDIX C: SWITCH INSPETION REQUIREMENTS

Please turn to next page.

Category			Countries that apply to	Inspection task	Type of inspection				
					visual inspecion	laser measuremen t	crack checks	switch rail fittings	point machine
Switch and crossing inspections	Visual inspections	Switch rail inspections	UK, DE	**Switch Rails** - check for broken, cracked, defective, worn, sideworn, affected by lipping or sharp gauge switch rails (UK); loose, not tight, periodical indentation, single indentation, black/brown spots, brocken, rupture, corrugation, lipping (measured in mm), head-checks, sheeling, spalling, wheel burns, clay pumping (DE)	X				
			UK, NL	**Flangeways** - obstructions in switches and flangeways or evidence of wheels striking the back of the open switch rail (check for scar signs that prove flange back contact) (UK); obstructions between the two rails (NL)	X				
		Stock rail inspections	UK, NL, DE	**Stock rail checks** - sideworn stock rail towards heel or at switch tips (UK); check for rolling contact fatigue condition (NL); rigidly fixed, broken, rupture, head-checks, corrugation, wheel burns, shelling, black or brown spots, indentations AND if closure rail, then also: defects in rail foot, short/long waves, baseplates pushed down into sleepers (DE)	X				
			UK, DE	**Stock rail lipping** - check for the presence of lipping on the stock rail throughout the movable part of the switch rail (UK); measured in mm (DE)	X				
			NL	**Heel baseplates**	X				
		Crossing inspection	UK, NL, DE	**Crossing check** - for broken, cracked, defective or worn, especially nose battering or wheel strikes damage (UK); for flaws, cracks or sinking of it (NL); for exfoliation, head checks, wheel burns, periodical indent, single indent, shelling, spalling, lipping, black/brown spots and condition of frog holes (DE)	X				
			DE	**Frog bolting mechanism** - check for missing, broken or not tight	X				
			NL	**Swing nose obstruction** - check for obstructions between the wing rail and the swing nose	X				
			NL	**Swing nose crossings slide chairs/plates and movable point** - visual check	X				
		Wing and check rails inspections	NL	**Check rail chairs** - visual inspection	X				
			DE	**Check rail** - loose, not tight	X				
			DE	**Wing rail** - loose, broken, torn, bent, squashed, lipping, black/brown spots	X				

Switch and crossing inspections	Visual inspections	Switch rail fittings inspections	UK	**Stretcher bars, lock stretcher bars and its associated brackets** - broken, loose, missing (bolts), distorted stretcher bar/brackets or dagamed	X				
			UK, DE	**Slide chairs and baseplates** - check for cleanliness and lubrication (UK); check for broken, bent or squashed (DE)	X				
			UK, NL, DE	**Rolling area of switch blade** - check for adequate lubrication; lubricate if necessary (UK); lubrication and roller systems (NL); check for missing, broken, loose or dirty (DE)	X				
		Track fittings inspection	UK	**Soleplate** - damaged, cracked or broken soleplate gauge stock block weld	X				
			UK, NL, DE	**Bolts** - for loose, broken or missing (UK); loose or missing (NL); broken, missing, worn, force fit and if the foot is grooved (DE)	X				
			DE	**Rail clips** - missing or broken	X				
			UK, NL	**Blocks** - missing, cracked or broken blocks (UK); distance blocks (NL)	X				
			NL	**Baseplates** - visual check	X				
			NL, DE	**Anti-creep device** - for missing or loose (DE)	X				
		Other inspections	NL	**Switch point heating**	X				
			NL	**ALL fasteners** - in switch, crossing, closure panel and tranzition zones	X				
			DE	**Horizontal screews** - tight enough	X				
			NL, DE	**Welds** - visual deformation of welds (NL); exfoliation, loose, broken, rupture, lipping, longitudinal cracks, lateral cracks (DE)	X				
			DE	**Rail joint** - check for brocken, loose, black/brown spots and measured in mm: lipping, material migration and hoist	X				
			DE	**Fishplate of rail joints** - check for loose or brocken fishplate, missing or not tight bolts and measured in mm: bent, deformed, hoist and material migration	X				
			NL	**Cables** - check for cables to be fastened	X				
			NL, DE	**Ballast, gravel** - check the condition and the profile of the ballast (at least 55cm outside sleeper) (NL); check to see if it is too much or too less (DE)	X				
			DE	**Sleepers** - many visual checks including some measured gauge checks	X				
			NL, DE	**Drainage** - check for good functioning of drainage (NL); check for vegetation,	X				
			DE	**Walking path** - check for vegetation or if too small	X				

Switch and crossing inspections	Measured inspections	Gauge, geometry and other plain line measurements	UK, NL	**Track gauge** measurement in front of the switch, at switch drivers, at the fixed heel blocks, acroos the moving areas of the switch and at the flangeways at the wing and check rails of crossings (UK)		X			
			UK, NL	**Check gauge** measurement at crossings fitted with a check rail (measurements done against the check rail) (UK); measurement is taken at both the entry of the check rail and the middle of it (NL)		X			
			DE	**Gauge** - not clear what kind of measurements are done		X			
			NL	**Free wheel passage** - measurement of free wheel passage at the switch rails		X			
			NL	**Cant, twist, leveling, alignment** - done with a measuring car (NL)					
			NL	**Vertical deflection** - measurement of vertical deflection (dynamic)					
		Switch rail inspections	UK	**Toe openings** in switches		X			
			UK	**Flangeway gap** measurement through the moving parts of switches		X			
			UK, NL, DE	**Switch toes position** - measurement of the position of switch toes (UK, NL); longitudinal height error (DE)		X			
			UK, NL	**Rail damage** - check to determine whether or not any damage or chipping of the running surface to the switch rail is safe or otherwise (with gauge)	X	X			
			UK, NL	**Rail profile** - check to see if the profile of switch rail tip with gauge (UK); horizontal and side wear measurement with gauge (NL)		X			
			DE	**Top and side wear** - top and side wear of the switch blade		X			
			DE	**Twist** - of switch rail					
			NL	**Cracks** - check for cracks in the switch rail			X		
		Stock rail inspections	UK, NL, DE	**Side wear** - measurement of plain rail side wear using NR4 gauge (NR); only in closure panel and transition zones (NL); measured in mm (DE)		X			
			NL, DE	**Top wear** - meausrement of plain line top wear in closure panel and tranzition zones (NL); measured in mm (DE)		X			
			NL	**Cracks** - check for cracks in the stock rail			X		
		Both switch and stock rail inspection	UK	**Profile** - check for wheel flange contact below 60º within the first 4000 mm of the switch rail using a P8 wheel profile		X			
			UK, DE	**Rail heights** - check to determine whether or not the tip of the switch rail is at least 15 mm below the top surface of the stock rail.* (UK); relative height between stock rail and switch rail (DE)		X			
			UK, NL	**Residual switch opening**		X			
			UK	**Stock rail side worn** - check if the tip of the switch rail projects above the bottom of the stock rail side wear.		X			
			UK	**False Flange Damage** check on stock rails and crossings	X				

Switch and crossing inspections	Measured inspections	Standard crossing inspection (inspections that apply for all crossings)	NL, DE	**Horizontal wear and vertical wear** - horizontal and vertical wear of the crossing (NL); is measured in mm and applies on movable nose as well (DE)		X			
			DE	**Flangeway gap in frog**		X			
			UK	**Crossing profile** - measurement of the crossing profile to judge in what way must weld repairs be carried out		X			
			UK	**AMS cracks** - Check for cracks in Austenitic Manganese Steel crossings			X		
			UK, NL	**Bainitic steel cracks** - Check for cracks in bainitic steel crossings			X		
		Swing nose specific inspections	NL	**Actuation, lockign and detection** - check correct functionality of actuation, locking and detection mecanisms					
			NL	**Swing nose heating** - check correct functionality of point heating for the swing nose (visual inspection)	X				
		Wing and check rails inspections	UK, NL	**Flangeway Gap** - measurement at the check rail and wing rail in crossings (UK); check rail flangeway gap only (NL)		X			
			DE, NL	**Check rail** - horizontal wear of the check rail		X			
			DE	**Wing rail** - horizontal wear and vertical wear (in mm)		X			
			UK	**Wing rail profile** - measurement of the wing rail profile to judge in what way must weld repairs be carried out		X			
		Track fittings inspection	UK	**Bolts and Other Fastenings** - check for correct torque, integrity and any signs of weakening					
		Other inspections	UK	**Ballast check** - voiding measurements to determine if or not it exceeds 7 mm					
			NL	**Insulation joints (glued)** - Measurement of the joint width, vertical wear, lipping and resistance at 100Khz					
			DE	**Insulation** - measure in mm wear of insulation bracket					

Point inspections	Generic point inspection	UK	**Visual checks**: obstructions, correct fitting of the switch rail against the stock rail, stretcher bar and brackets distortion and functionality of the point heating equipment	X				
	Point machine inspections	UK, NL	**Regular tests** - Facing point lock test, fluid level and RKB 222 padlock; lock doesn't engage for a 3,5mm gauge and it enagges for a 1,5mm gauge (UK); actuation, locking and detection equipment is checked (NL)					X
		UK	**Service A** - a detailed inspection that is specific to the type of point machine					X
		UK	**Service B** - a detailed inspection that is specific to the type of point machine					X
		NL	**Vibration** - vibration at the driving by passing train (visual inspection; checking the amount of movement)					X
	Point fittings inspections	UK	Various inspections are carried out to ensure that **insulations, nuts, bolts, lock nuts, brackets, bars, bracket fasteners, bolt holes, drilled holes, lock stretcher bars, adjustable stretcher bars, welds and brushes** are, if applicable, **in place, securely fitted, tight, properly adjusted, doesn't have signs of cracking or surface deterioration, not bent and have adequate clearances**.				X	
	Mechanical supplementary drive inspection	UK	Various inspections are carried out to ensure that **crank bases, cranks, sleeve on cranks, cotter pins, rodding, roller assemblies, drive pin and lock nuts** are, if applicable, **in place, securely fitted, tight, and they are not worn, seized, loose, bent or broken**.				X	
		UK	**Functional test** to see correct movement of the switch rails.					
	Switch rollers inspections	UK	Inspections to ensure that all the parts are secure and don't have signs of damage. Other visual checks are carried out to ensure that the switch rails are moving properly over the switch rollers.				X	

APPENDIX D: LASER SCANNER "SENSOR ACCEPTANCE REPORT"

Please turn to next page.

Sensor acceptance report

MICRO-EPSILON

Sensor type: scanCONTROL 2700-100(500) v31-08 S/N 113030003
Standard measuring range: 100 mm (z-axis) 00-0C-12-01-0E-41

Report version: 1.53 (4.1)

Calibration target: MICRO-EPSILON Optronic standard matt metal
Calibration equipm.: PM0269
Shutter time: automatically regulated
Ambient temperature: 20 +/-1 Degrees Celsius

Total measured points: 397521
Measured points inside standard measuring range: 121103

Measuring field width in the standard measuring range

Position	Distance (z)	Width (x)	
		Standard	Extended
Start (MBA)	350.0mm	93.2mm	93.2mm
Centre (MBM)	400.0mm	105.7mm	105.7mm
End (MBE)	450.0mm	118.1mm	118.1mm

The distances (z) in the standard measuring range are specified according to the data sheet.

Linearity

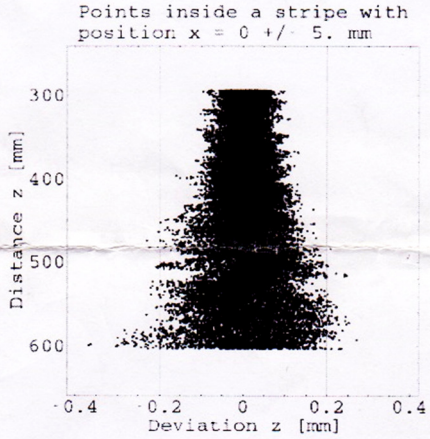

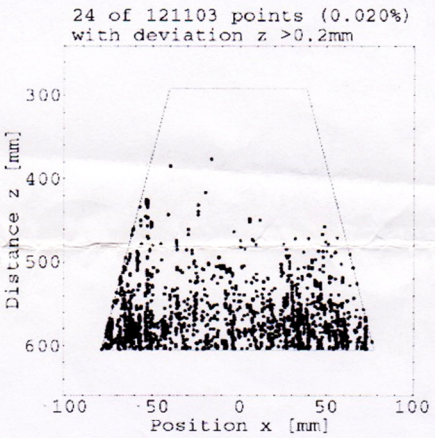

Top left:
Deviation z of all measured points
inside a stripe along the x axis

Top right:
All measured points with a deviation z
greater than 0.2 mm, point count
is inside standard measuring range

Right:
Deviation z of all measuring points
inside a stripe along the MBM

Table:
Statistics standard measuring range

Averaged points along the profile	w/o	160	640
Standard deviation 3*sigma/micrometer	137.5	19.2	11.8

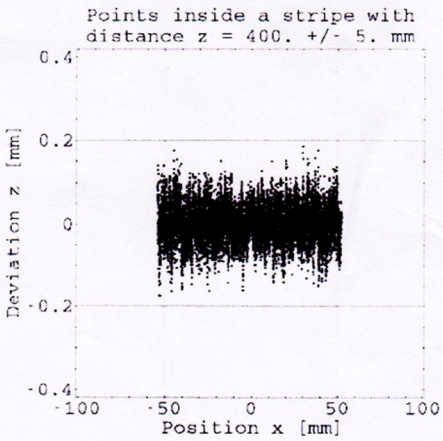

Notes
Differences from these data can occur due to target material and surface, target geometry, sensor mounting, temperature fluctuations during the measurement and strong circulation of warm air between sensor and target. The information in the data sheet and the operating instructions also apply.

Measurement of: 27 Mar. 2013 09:55:47 Tested by: AMO
Report of: 27 Mar. 2013 10:02:01 Report file: 113030003mes.pdf

Sensor acceptance report

MICRO-EPSILON

Sensor type: scanCONTROL 2700-100(500) v30-07 S/N 112090003
Standard measuring range: 100 mm (z-axis) 00-0C-12-01-08-EC

Report version: 1.53 (4.1)

Calibration target: MICRO-EPSILON Optronic standard matt metal
Calibration equipm.: PM0269
Shutter time: automatically regulated
Ambient temperature: 20 +/-1 Degrees Celsius

Total measured points: 402634
Measured points inside standard measuring range: 121099

Measuring field width in the standard measuring range

Position	Distance (z)	Width (x)	
		Standard	Extended
Start (MBA)	350.0mm	93.1mm	93.1mm
Centre (MBM)	400.0mm	105.6mm	105.6mm
End (MBE)	450.0mm	118.1mm	118.1mm

The distances (z) in the standard measuring range are specified according to the data sheet.

Linearity

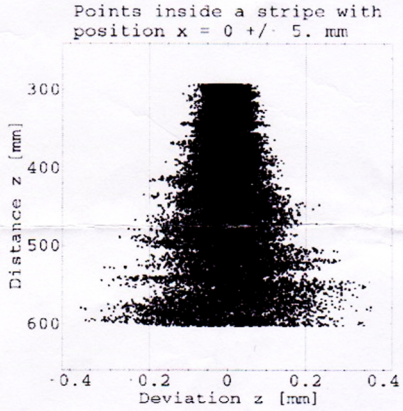

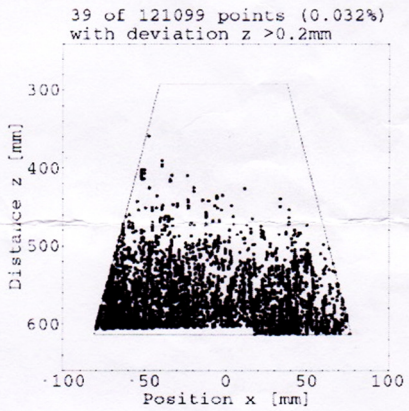

Top left:
Deviation z of all measured points
inside a stripe along the x axis

Top right:
All measured points with a deviation z
greater than 0.2 mm, point count
is inside standard measuring range

Right:
Deviation z of all measuring points
inside a stripe along the MBM

Table:
Statistics standard measuring range

Averaged points along the profile	w/o	160	640
Standard deviation 3*sigma/micrometer	147.1	19.9	10.3

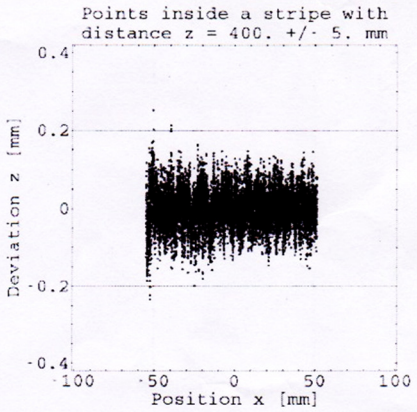

Notes
Differences from these data can occur due to target material and surface, target geometry, sensor mounting, temperature fluctuations during the measurement and strong circulation of warm air between sensor and target. The information in the data sheet and the operating instructions also apply.

Measurement of: 14 Sept. 2012 10:02:38 Tested by: AMO
Report of: 14 Sept. 2012 10:09:00 Report file: 112090003mes.pdf